UNIVERSITÀ DEGLI STUDI DI MILANO

Dipartimento di Scienze Farmaceutiche

Doctorate School in Chemical Sciences and Technologies

Curriculum

Chemical Sciences – XXVII Cycle

Preparation of bicyclic nitrogen intermediates as useful scaffolds for the synthesis of new biologically active compounds

PhD Thesis of

Matteo Salvi (R09768)

Supervisors

Prof.ssa Elisabetta Rossi; Dott. Roberto Artusi.

Coordinator

Prof.ssa Emanuela Licandro

Academic Year 2013/2014

The research presented in this PhD thesis is the result of the collaboration between the Dipartimento di Scienze Farmaceutiche (DISFARM, *Sezione di Chimica Generale e Organica "A. Marchesini"*) of the Università degli Studi di Milano and the *Rottapharm Biotech srl*, via Valosa di Sopra, 9 - 20052 Monza – Italy.

UNIVERSITÀ DEGLI STUDI DI MILANO

Acknowledgements

I want express a special thank to:

Prof.ssa Elisabetta Rossi and Dott. Roberto Artusi;

The researchers of Rottapharm Biotech srl, in particular the Medicinal Chemistry Department where I spent my PhD period;

Prof. Alessandro Contini for the computational support.

Thank you to my parents, my brother Edoardo and Simona that always supported me for the realization of this project.

Thank you to my friends and the people that supported me in these years.

Thank you to all my colleagues at Rottapharm Biotech srl and at Università degli Studi di Milano.

Index of contents

Chapter 1. The orexin system, general overview and aim of the project

1.1 The Orexin System Pharmacology

1.1.1 Introduction

The orexins (also called hypocretins) are neuropeptides that were first discovered in 1998 by two independent research groups, utilizing different methodologies. *Sakurai et al.* named these peptides orexin-A and -B because they were originally thought to promote feeding (the term orexin comes from the Greek word *orexis* that means appetite).[1] The team led by *de Lecea et al.* named the peptides hypocretin-1 and hypocretin-2 because they are produced in the hypothalamus and have some similarities to the incretin family of peptides.[2]

The *Sakurai et al.* research team reported the identification of orexins by "reverse pharmacological" approach. Most neuropeptides work though G Protein-Coupled Receptors (GPCRs) and there are many "orphan" GPCR genes in the human genome (the related ligands for these receptors molecules have not been identified yet). *Sakurai et al.* team transfected cells with orphan GPCR genes in order to obtain their expression. These transfected cells were subsequently used as reporter systems in order to detect endogenous ligands in tissue extracts. In this process orexin A and orexin B were identified as endogenous peptidic ligands for two orphan GPCRs: orexin receptor 1 (OX1R) and orexin receptor 2 (OX2R).[1]

The group of de Lecea *et al.* utilized a technique based on subtractive-PCR to identify transcripts that are specifically expressed in the hypothalamus.[2] Previously, they had obtained a library of cDNAs corresponding to a number of mRNA sequences selectively expressed in this region of the brain.[3] From this library, they subsequently identified one cDNA sequence that contains the entire coding region of a putative secretory protein of 131 amino acids. They predicted that this protein gives rise to two novel peptide products that are structurally related to each other (hypocretin-1 and -2).

These findings led to establish that the orexin system is composed of two endogenous peptides (Orexin A and Orexin B), that mediate their actions via interactions with two closely related GPCRs (OXR1 and OXR2). The orexins are produced by specialized neurons in the hypothalamus, which project to many different regions of the brain.[4]

Physiological studies over the last decade showed that orexin signalling plays a key role in a variety of important biological processes, including feeding, sleep-wake cycle, energy homeostasis,

---

[1] T. Sakurai, A. Amemiya, M. Ishii, I. Matsuzaki, R. M. Chemelli, H. Tanaka, S. C. Williams, J. A. Richardson, G. P. Kozlowski, S. Wilson, J. R. Arch, R. E. Buckingham, A. C. Haynes, S. A. Carr, R. S. Annan, D. E. McNulty, W. S. Liu, J. A. Terrett, N. Elshourbagy, A. D. J. Bergsma, M. Yanagisawa *Cell* **1998**, *92*, 73-85.

[2] L. de Lecea, T. S. Kilduff, C. Peyron, X. Gao, P. E. Foye, P. E. Danielson, C. Fukuhara, E. L. Battenberg, V. T. Gautvik, F. S. Bartlett, 2nd, W. N. Frankel, A. N. van den Pol, F. E. Bloom, K. M. Gautvik, J. G. Sutcliffe *Proc. Natl. Acad. Sci. USA* **1998**, *95*, 322-327.

[3] K. M. Gautvik, l. de Lecea, V. T. Gautvik, P. E. Danielson, P. Tranque, a. Dopazo, F. E. Bloom, J. G. Sutcliffe *Proc. Natl. Acad. Sci. USA* **1996,** *93,* 8733-8738.

[4] a) T. Nambu, T. Sakurai, K. Mizukami, Y. Hosoya, M. Yanagisawa and K. Goto, *Brain Res.* **1999**, *827*, 243-260; b) S. Muroya, H. Funahashi, A. Yamanaka, D. Kohno, K. Uramura, T. Nambu, M. Shibahara, M. Kuramochi, M. Takigawa, M. Yanagisawa, T. Sakurai, S. Shioda, T. Yada *Eur. J. Neurosci.* **2004**, *19*, 1524-1534.

addiction and reward seeking, amongst others.[5] In fact, there is clear evidence for defects in orexin signalling being involved in diet-induced obesity and diabetes,[6] narcolepsy,[7] panic anxiety disorder,[8] drug addiction[9] and Alzheimer's Disease.[10] These evidences justify the considerable efforts of pharmaceutical industries to develop new potent compounds active on the orexinergic system.

In particular, it has become clear that the effects of orexin peptides on arousal and sleep are profound. In fact, narcolepsy, one of the most common causes of sleepiness, is caused by a loss of the orexin-producing neurons. This consideration has fueled a strong interest in developing orexin antagonists as a novel approach for promoting sleep and treating insomnia.

Almost all hypnotics used so far in the clinic enhance γ-aminobutyric acid (*GABA*) signaling or alter monoamine signaling. Unfortunately these neurotransmitters affect numerous brain functions, and therefore these drugs can cause several side effects, such as unsteady gait and confusion. In contrast, orexin antagonists are expected to promote sleep with fewer side effects, and recent, large clinical studies look so promising that the first OX1R/OX2R antagonist *Suvorexant* has been recently approved for insomnia in USA (Aug 2014).

Another important evidence is the role of the orexins in mediating the effects of several drugs of abuse, such as cocaine, morphine and alcohol via projections to key brain regions. So at present, there are several orexin-based pharmacotherapies under development for the treatment of addiction.

1.1.2 Overview of orexin signaling

Orexin Peptides

As previously stated, molecular cloning studies showed that orexin A and orexin B are derived from a common precursor peptide, prepro-orexin encoded by the hypocretin gene (Human: HCRT; Rat/Mouse: Hcrt) located on chromosome *17q21*, Figure 1.

[5] J. T. Willie, R. M. Chemelli, C. M. Sinton, M. Yanagisawa *Annu. Rev. Neurosci.* **2001**, *24*, 429-458.

[6] a) H. Tsuneki, S. Murata, Y. Anzawa, Y. Soeda, E. Tokai, T. Wada, I. Kimura, M. Yanagisawa, T. Sakurai, T. Sasaoka *Diabetologia* **2008**, *51*, 657-667; b) H. Funato, A. L. Tsai, J. T. Willie, Y. Kisanuki, S. C. Williams, T. Sakurai, M. Yanagisawa *Cell Metab.* **2009**, *9*, 64-76.

[7] a) R. Chemeilli, J. T. Willie, C. M. Sinton, J. K. Elmquist, T. Scammell, C. Lee, J. A. Richardson, S. Clay Williams, Y. Xiong, Y. Kisanuki, T. E. Fitch, M. Nakazato, R. E. Hammer, C. B. Saper, M. Yanagisawa *Cell*, **1999**, *98*, 437-451; b) L. Lin, J. Faraco, R. Li, H. Kadotani, W. Rogers, X. Lin, X. Qiu, P. J. de Jong, S. Nishino, E. Mignot *Cell*, **1999**, *98*, 365-376.

[8] P. L. Johnson, W. Truitt, S. D. Fitz, P. E. Minick, A. Dietrich, S. Sanghani, L. Traskman-Bendz, A. W. Goddard, L. Brundin, A. Shekhar *Nat. Med.* **2009**, *16*, 111-115.

[9] J. A. Hollander, Q. Lu, M. D. Cameron, T. M. Kamenecka, P. J. Kenny *Proc. Natl. Acad. Sci. USA* **2008**, *105*, 19480-19485.

[10] J. E. Kang, M. M. Lim, R. J. Bateman, J. J. Lee, L. P. Smyth, J. R. Cirrito, N. Fujiki, S. Nishino, D. M. Holtzman *Science*, **2009**, *326*, 1005-1007.
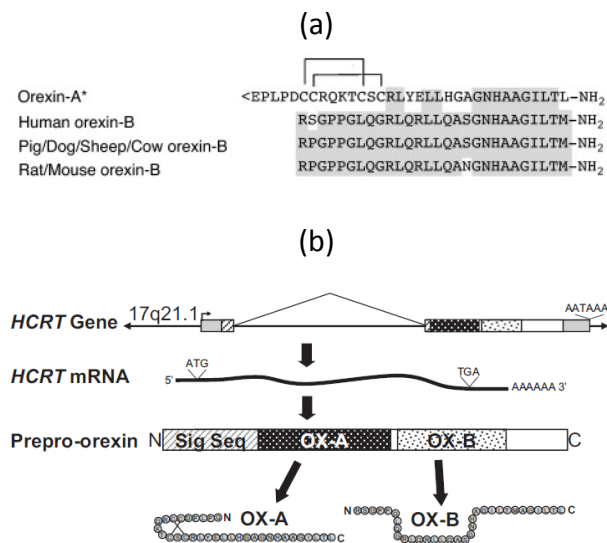
Figure 1. Orexins and orexin receptors. **(a)** Sequences of orexin A (identical in all studied mammalian species) and of orexin B in various species. The topology of the two intrachain disulfide bonds of orexin A is indicated above the sequence. Shadows indicate amino acid identity. (the picture is taken from *TRENDS in Pharmacological Sciences* 2011, note the pyroglutamic N-terminal, whereas usually the structure is reported with the unmodified *N*-terminal Gln residue, see for instance panel b and Figure 2). **(b)** OX-A and OX-B are encoded by the *HCRT* gene. Structures of the human gene [from UCSB genome browser (http://genome.ucsc.edu); intronic sequence is shown at 1/10th scale of exon sequence], mRNA, and protein gene products shown (picture elaboration from *Pharmacol Rev* 64:389–420, 2012).

The structure and organization of the hypocretin gene has been largely conserved through evolution. In all vertebrates examined, the gene is composed of two exons with the intron splice falling within the early portion of the open reading frame encoding the secretory signal sequence. The *HCTR* gene is expressed in the hypothalamus, where the mRNA is translated to the prepro-orexin precursor peptide (131-amino acid for human prepro-orexin peptide) that is proteolytically processed to give rise to orexin A (OX-A; 33 amino acids; 3562 Da) and Orexin B (OX-B; 28 amino acids; 2937 Da).

Structures of orexins were chemically determined by biochemical purification and sequence analysis by Edman sequencing and mass spectrometry.[1]

In mammals, the sequence of the mature OX-A ligand is entirely conserved among all species examined and contains two disulphide bonds, formed by [Cys^6-Cys^{12}, Cys^7-Cys^{14}]. Mature OX-A is further post-translationally modified with an *N*-terminal pyroglutamic acid.[1]

Mammalian OX-B sequences, on the other hand, are also very well conserved but are not identical across the species. In fact, in dogs, cows, sheeps, and pigs a proline residue substitutes for the serine residue present in humans in the second amino acid position. Moreover, in rodents besides this variation, another residue differs from the human sequence (asparagine 18, for serine 18).

It is interesting to notice that there is some sequence similarity between OX-A and OX-B, this homology could explain the relative overlapping of their pharmacological functions, i.e. their ability to serve as ligands for both OX1 and OX2 receptors, albeit with differing affinities.

Indeed, it should be emphasized that mammalian OX-A and OX-B sequences are identical in the C-terminal portion of the mature peptides, including the peptidic sequence *Gly-Asn-His-Ala-Ala-Gly-*

Ile-Leu-Thr. They also share the sequence *Arg-Leu-X-X-Leu-Leu* (X= non-conserved amino acids) spaced three amino acids *N*-terminal of the conserved peptidic sequence mentioned above. This evidence suggests that these residues may exist at one surface of an α-helical secondary structure.[1,11] Because both peptides have measurable affinities for each of the OX1 and OX2 receptors, these observations indicate that these residues are essential for orexin receptor interaction. This feature is shown in Figure 2 (http://www.rcsb.org/pdb/home/home.do).
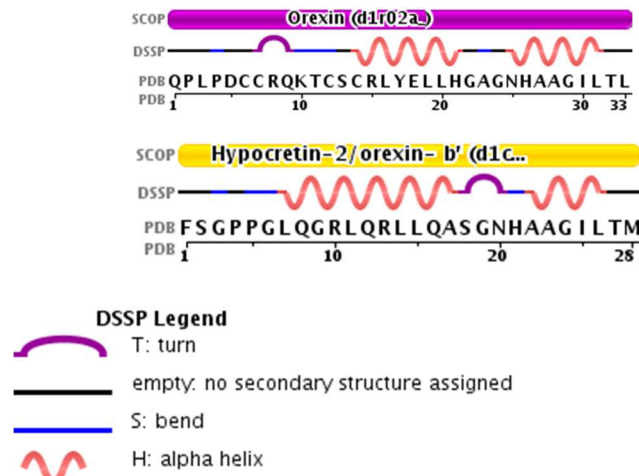
Figure 2. Representation of OXA and OxB peptidic sequences (From Protein Data Bank: http://www.rcsb.org/pdb/home/home.do; PDB ID: *1r02* and *1cq0*).

The x-ray structures of both orexin A and orexin B peptides were resolved (*Protein Data Bank*). A graphic representation of the PDB files of orexin peptides as cartoon was performed using *PyMol*™ program, Figure 3.

---

[11] K. K. Y. Wong, S. Y. L. Ng, L. T. O. Lee, H. K. H. Ng, B. K. C. Chow *Gen. Comp. End*. **2011**, *171*, 124-130.

(a)

(b)
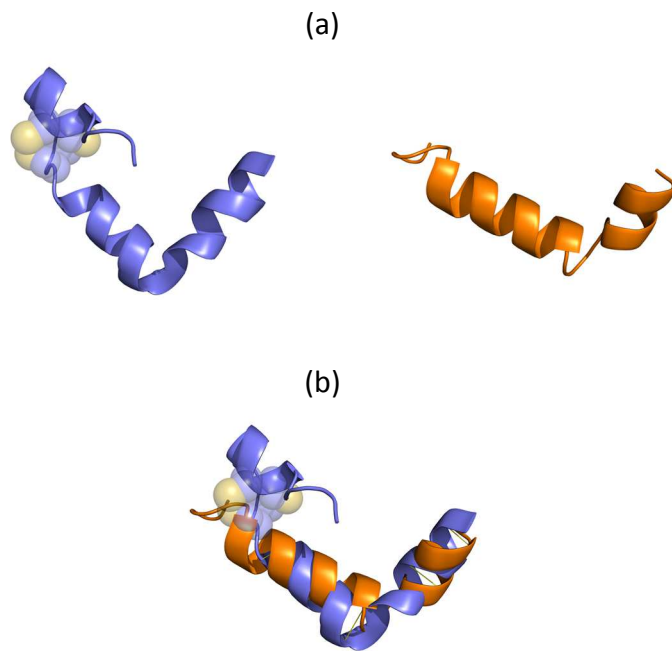
Figure 3. **(a)** OXA (blue) and OXB (orange) peptides. (**b**) *OxA/OXB Alignment.* The peptidic sequences are shown as cartoon and disulphide bonds in Orexin A as spheres. *PDB files (1r02* and *1cq0)* elaboration with *PyMol™ 1.5.0.3* program*.*

Orexin Receptors

The orexin peptides bind selectively to the OX1 and OX2 receptors (OX1R and OX2R, also known as *HCRTR1* and *HCRTR2*).[1] As already mentioned, these are GPCRs having, as usual for this class of receptors, 7-transmembrane domains and some similarity to other neuropeptide receptors (see below). All pharmacological actions of orexins seem to be mediated by these two receptors.

Among various classes of GPCRs, OX1R is structurally more similar to certain neuropeptide receptors, in particular to the Y2 Neuropeptide Y (NPY) receptor (26% similarity), followed by the thyrotropin-releasing hormone (TRH) receptor, cholesystokinin type-A receptor and NK2 neurokinin receptor.

In spite of these structural similarities to other neuropeptide receptors, neither OX1R nor OX2R has any significant affinity for neuropeptide Y, secretin, or similar peptides.[1,12]

The amino acid identity between the deduced full-length human OX1R and OX2R sequences is 64%. Thus, the similarity between the two orexin receptors is considerably higher than that with the other GPCRs listed above.[1] OX1R and OX2R are strongly conserved across mammals: amino acid identities between the human and rat homologues are 94% for OX1R and 95% for OX2R, Table 1 and Table 2.[1]

---

[12] T. Holmqvist, K. E. O. Akerman, J. P. Kukkonen *Neurosci Lett*. **2001**, *305*, 177-180.

Table1 and **Table2**. Mammalian Ox1R and OX2R protein homology (from *Pharmacol Rev* 64:389–420, 2012).

Mammalian OX₁ receptor protein homology

The indicated annotated protein sequences were compared with the human OX_1 receptor sequence using a BLASTP algorithm with default comparative parameters (http://blast.ncbi.nlm.nih.gov/Blast.cgi). Identity and similarity values are the percentage of identical or homologous amino acids shared with the core region of the human OX_1 receptor.

Protein	Identity	Similarity
	%	
OX₁ receptor		
Human	100	100
Rhesus	97	98
Chimp	94	96
Canine	93	95
Rabbit	93	95
Mouse	92	93
Rat	91	93
OX₂ receptor		
Human	69	80

Mammalian OX₂ receptor protein homology

The indicated annotated protein sequences were compared with the human OX_2 receptor sequence using a BLASTP algorithm with default comparative parameters (http://blast.ncbi.nlm.nih.gov/Blast.cgi). Identity and similarity values are the percentage of identical or homologous amino acids shared with the core region of the human OX_2 receptor.

Protein	Identity	Similarity
	%	
OX₂ receptor		
Human	100	100
Chimp	99	99
Rhesus	98	99
Canine	97	98
Rabbit	97	98
Mouse	94	96
Rat	94	96
OX₁ receptor		
Human	69	80

Human OXA has nearly equal activity on both orexin receptors, with ligand binding affinities (IC50) of 20 and 38 nM for OX1R and OX2R, respectively, and EC_{50} values of 30 and 34 nM in $[Ca^{2+}]_i$ mobilization assays of CHO cells transfected to express human OX1R and OX2R, respectively, Figure 4.[1] OX-B, however, has markedly less activity toward OX1R with an IC_{50} of 420 nM and an EC50 2500 nM. It is, therefore, somehow selective for OX2R, exhibiting an IC_{50} of 36 nM and EC50 of 60 nM.[1] This selectivity of OXB for OX2R has been used to interpret the relative roles of OX2R and OX1R in biological functions. Definitive receptor selective function, however, is demonstrated only with genetic and/or highly selective orexin receptor antagonist reagents.
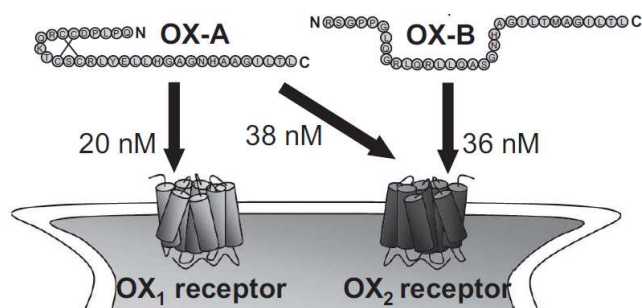
Figure 4. IC₅₀ values for radioligand binding by OX-A and OX-B are depicted with the exception of the affinity of OX-B for OX1R (420 nM, not shown), which is 10-fold less than for OX2R (36 nM) (Sakurai et al., 1998) (picture elaboration from *Pharmacol Rev* 64:389–420, 2012).

Further, recent studies showed molecular interactions and cross-talks between orexin receptors and other receptors. Hilairet et al. showed that when the cannabinoid receptor (CB1) and OX1R are co-expressed, there is a CB1-dependent enhancement of the orexin A potency to activate precise intracellular signal-transduction pathways. It was also shown that CB1 and OX1R are closely apposed at the plasma membrane to form heterodimers.[13] It was also showed that OX1R and OX2R are capable of forming a homo- or heterodimer.[14] These observations suggest complex signaling cascade might exist in the downstream of orexin receptors.

---

[13] S. Hilairet, M. Bouaboula, D. Carriere, G. Le Fur and P. Casellas *J. Biol. Chem.* **2003**, *278*, 23731-23737.
[14] M. B. Dalrymple, K. M. Kroeger, R. M. Seeber and K. A. Edine *85th Annual Endocrine Meeting* **2003**, P1-66.

Signal Transduction Systems of Orexin Receptors

Numerous studies have shown that orexins depolarize neurons and increase excitability and ignition rate for many minutes.[15] In general it is thought that OX1R couples to Gq, and OX2R can signal through Gq or Gi/Go, but coupling mechanisms seem to be different by cell type and have not been thoroughly examined in neurons, Figure 5.[16]
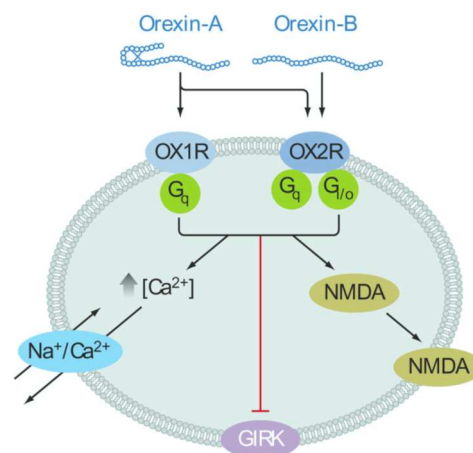
Figure 5. Orexin signaling mechanisms. Orexin-A signals through both OX1R and OX2R, whereas orexin-B signals mainly through OX2R. Intracellular cascades mediated by G proteins increase intracellular calcium and activate the Na+/Ca2+ exchanger, which depolarizes target neurons. These cascades also inactivate G protein–regulated inward rectifier (GIRK) channels. Increased expression of NMDA receptors on the cell surface produces long-lasting increases in neuronal excitability (picture from *Annu. Rev. Pharmacol. Toxicol. 2011* February 10; 51: 243–266).

Several ionic mechanisms mediate the acute effects of orexins. An inhibition of K-channels (including G protein-regulated inward rectifier -GIRK- channels) may make more excitable some neurons.[17] Further, the orexin receptor signalling can induce a sustained and fast intracellular Ca^{2+} gain by voltage-gated Ca-channels, by transient receptor potential channels or from intracellular stores.[1, 18]

Lastly, the Na^+/Ca^{2+} exchanger activation can contribute to the target neurons excitation.[19]

Further to these postsynaptic events, orexin can work at presinaptic level on nerve terminals to induce GABA or glutamate release. This generates more complex effects on downstream neurons.[16, 18a]

---

[15] a) J. J. Hagan, R. A. Leslie, S. Patel, M. L. Evans, T. A. Wattam *Proc. Natl. Acad. Sci. USA*. **1999**, *96*, 10911-10916; b) P. Bourgin, S. Huitron-Resendiz, A. D. Spier, V. Fabre, B. Morte *J. Neurosci*. **2000**, *20*, 7760-7765; c) R. J. Liu, A. N. van den Pol, G. K. Aghajanian *J. Neurosci.* **2002**, *22*, 9453-9464; d) E. Arrigoni, T. Mochizuki, T. E. Scammell *Acta Physiol.* **2010**, *198*, 223-235.

[16] T. E. Scammel, C. J. Winrow *Ann. Rev. Pharmacol. Toxicol. 2011*, *51*, 243-266.

[17] Q. V. Hoang, D. Bajic, M. Yanagisawa, S. Nakajim, Y. Nakajima *J. Neurophysiol*. **2003**, *90*, 693-702.

[18] a) A. N. van den Pol, X. B. Gao, K. Obrietan, T. S. Kilduff, A. B. Belousov *J. Neurosci.* **1998**, *18*, 7962-7971; b) K. A. Kohlmeier, T. Inoue, C. S. Leonard *J. Neurophysiol*. **2004**, *92*, 221-235; c). H. M. Peltonen, J. M. Magga, G. Bart, P. M. Turunen, M. S. Antikainen *Biochem. Biophys. Res. Commun.* **2009**, *385*, 408-412.

[19] a) D. Burdakov, B. Liss, F. M. Ashcroft *J. Neurosci.* **2003**, *23*, 4951-4957; b) C. Acuna-Goycolea, A. N. van den Pol *J. Neurosci*. **2009**, *29*, 1503-1513.

Orexin-mediated signalling can also give enduring increasing in neuronal excitability: in the ventral tegmental area (VTA), orexin increases the NMDA receptors numbers on the cell surface (neurons more reactive to the glutamate excitatory effect for hours).[20] Through this pathway, the orexins may generally excite neurons that promote arousal.

The neurons that release the orexin neurotransmitters also produce glutamate, dynorphin and other dynorphin-related neuropeptides.[21] These co-neurotransmitters may be physiologically remarkable, but less is known about their roles or conditions under which they are released.

---

[20] a) S. L. Borgland, S. A. Taha, F. Sarti, H. L. Fields, A. Bonci *Neuron*. **2006**, *49*, 589-601; b) S. L. Borgland, E. Storm, A. Bonci *Eur. J. Neurosci*. **2008**, *28*, 1545-1556.
[21] a) T. C. Chou, C. E. Lee, J. Lu, J. K. Elmquist, J. Hara *J. Neurosci*. **2001**; *21*, RC168 ; b) A. Crocker, R. A. España, M. Papadopoulou, C. B. Saper, J. Faraco *Neurology* **2005**, *65*, 1184-1188.

1.2 Medicinal Chemistry Approach

The great importance of the orexinergic system in the research projects aimed to find new drugs active on CNS is witnessed by the large number of medicinal chemistry projects in this field. For instance, the database Integrity (Thompson Reuters), consulted in November 2014, reports more than 200 leads.

The R&D activity on orexin antagonists involves either the big pharma companies and smaller biotech group. The following chart represents the major player found in an Integrity query on "Orexin".
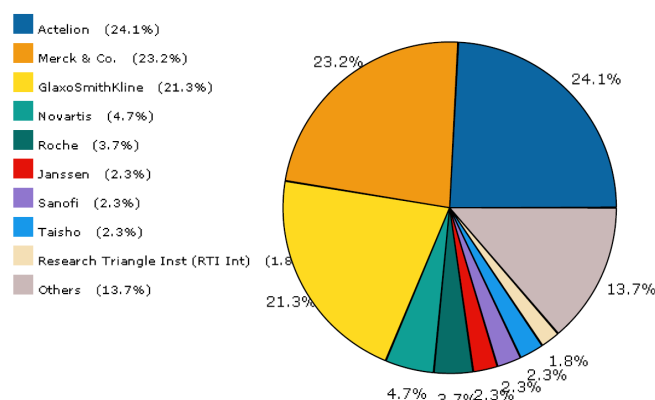
Figure 1. Pie Chart illustrating the competition in R&D development in orexin antagonists (Source: Thomson Reuters Integrity, Nov 2014).

As previously illustrated, while sleep disorders are the principal clinical field of investigation, the role of orexinergic system in controlling other aspects of behavior is mirrored by the following scheme, produced again by Integrity, illustrating the conditions targeted by the leads.
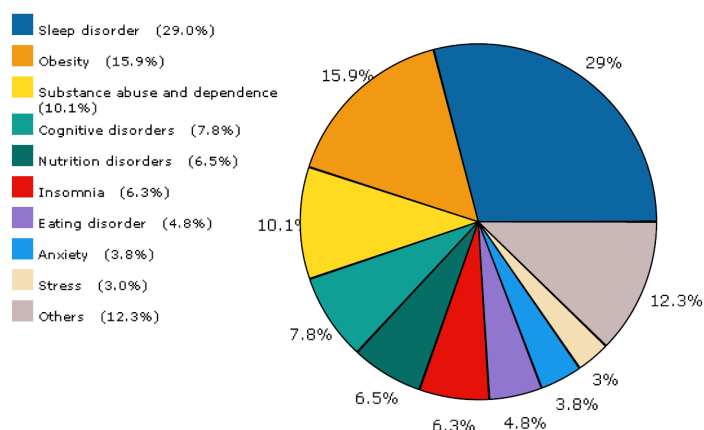
Figure 2. Pie Chart illustrating the major clinical conditions targeted by the orexin antagonists in development (Source: Thomson Reuters Integrity, Nov 2014).

Since the pharmacology of OX1R is not fully superimposable to that of OX2R (and the same is for OXA and OXB) - for instance, OX1Rs seem to have a predominant role in the control of anxiety, panic and addiction, while OX2Rs seem predominantly involved in sleep control – the R&D projects on these targets are almost evenly divided into three main classes, the dual orexin receptor antagonists (*DORAs*) representing approx. the 44% of the lead projects listed in Integrity, and the selective orexin receptor antagonists (*SORAs*) towards OX1R or OX2R, 26% and 30%, respectively. The scope of this thesis is on *DORAs*, since they are the most promising agents for treating insomnia. Indeed, *Suvorexant*, a DORA compound, is the first orexin antagonist approved for the market for treating sleep disorders (August 2014), and, therefore we tried to ameliorate some pharmacological features of *Suvorexan*t that emerged during its clinical development and that induced the FDA to lower its posology. Nevertheless, in a brief summary of the state of the art of orexinergic medicinal chemistry, it is worth to mention also the efforts made to obtain *SORAs* (mainly targeting OX2R) as hypnotic compounds devoid of the putative side effects of non-selective antagonists.

The following table,Table 1), taken from a recent paper by Khoo et al., summarizes very well the evolution of the research efforts in the orexinergic field.[1]

Table 1 taken from *Khoo et al, CNS Drugs (2014) 28, 713–730*

Table 1 Synthetic orexin ligands in preclinical and clinical development

Ligand	Company	Description
OXA (17-33)	SmithKline Beecham	Truncated orexin-A peptide with reduced potency but enhanced selectivity for the OX_1 receptor. Partial agonist
[Ala^{11},D-Leu^{15}]-Orexin B (SB-668875)	Banyu	Substituted orexin-B peptide with enhanced selectivity for the OX_2 receptor. Agonist
SB-334867	GlaxoSmithKline	SORA. MW 319.11. Research only. First selective OX_1 receptor antagonist
SB-408124	GlaxoSmithKline	SORA. MW 356.14. Research only. Selective OX_1 receptor antagonist
SB-674042	GlaxoSmithKline	SORA. MW 448.51. Research only. Selective OX_1 receptor antagonist
ACT-335827	Actelion	SORA. MW 518.64. Research only. Selective OX_1 receptor antagonist
TCS OX2 29	Banyu	SORA. MW 397.24. Research only. First small molecule selective OX_2 receptor antagonist
JNJ-10397049	Johnson and Johnson	SORA. MW 481.98. Research only. Selective OX_2 receptor antagonist
EMPA	Roche	SORA. MW 510.23. Research only. Selective OX_2 receptor antagonist
LSN2424100	Eli Lilly	SORA. MW 407.42. Research only. Selective OX_2 receptor antagonist
MK-1064	Merck	SORA. MW 461.85. Clinical candidate. Selective OX_2 receptor antagonist
Almorexant (ACT-078573)	Actelion and GlaxoSmithKline	DORA. MW 512.23. Treatment for insomnia. Reached Phase III trials before development was discontinued
SB-649868	GlaxoSmithKline	DORA. MW 477.15. Treatment for insomnia. Reached Phase II trials before development was discontinued
Filorexant (MK-6096)	Merck	DORA. MW 420.2. Treatment for insomnia. Currently under development (Phase II). No active clinical trials
Suvorexant (MK-4305)	Merck	DORA. MW 450.16. Treatment for insomnia. Phase III trials complete, awaiting FDA and PMDA approval. Proposed addition to Schedule IV by the United States Drug Enforcement Agency

MW molecular weight

---

[1] S. Y. Khoo, R. M. Brown *CNS Drugs*, **2014,** *28*, 713-730.

Being OXA and OXB neuropeptides, the first logical approaches towards new ligands acting at OX1R and/or OX2R as agonists or antagonists were with truncated and or modified orexin peptides.[2] These attempts gave origin to promising tools, such as OXA (17–33), which is a partial agonist at the OX1 receptor[3] and [Ala[11],D-Leu[15]]-Orexin B (SB-668875), in which the substitution of two residues in the orexin-B peptide produced, a potent agonist with increased selectivity for the OX2 receptor.[4]

However, the most important expansion of our knowledge of orexinergic pharmacology has been produced with small molecule antagonists.

The prototype was SB-334867 (developed by GlaxoSmithKline), a naphthyridine-substituted biarylurea with high affinity for the OX1 receptor (Selective Orexin Receptor 1 Anatgonist; *SORA 1*) without relevant cross-activity towards 50 other targets (GPCRs and ion channels).[5] However, its selectivity for OX1R is only approximately 50-fold higher than that for OX2R (Haynes et al., 2000; Porter et al., 2001), at higher doses, SB-334867 is likely to block both orexin receptors, moreover it has demonstrated binding activity with a number of other receptors and transporters, complicating its use as an orexin receptor probe [8b] s.[6] This Ox1R/OX2R selectivity is therefore, relatively modest compared to more recently developed antagonists. GlaxoSmithKline has developed further several commercially available small molecule OX1 receptor antagonists: in particular SB-408124 and SB-674042.[7] SB-408124 is urea-based small molecule, like SB-334867, that has a similar dissociation constant (Kb) for the OX1 receptor, 21.7 nM and 27.8 nM, respectively. SB-408124 Kb on OX2R is, on the other hand, 1410 nM. SB-674042, in contrast to the two ureas, has a proline-like core with two 5-membered heteroaromatic rings and two phenyl groups. It is significantly more potent than both SB-334867 and SB-408124, with a Kb of 1.1 nM for the OX1 receptor and 129 nM for the OX2 receptor: it is also a more selective OX1 receptor antagonist than either of its predecessors. More recently, Actelion Pharmaceuticals has reported a tetrahydropapaverine derivative OX1 receptor antagonist designated ACT-335827.[8] It is about 10 times more selective towards OX1R respect the OX2R, with Kb values of 41 and 560 nM respectively. It is orally bioavailable, able to cross the blood brain barrier (*BBB*).[9]

The structure of the selective orexin receptor 1 antagonists (*SORAs 1*) described above are reported in Figure 3.

[2] a) J. G. Darker, R. A. Porter, D. S. Eggleston, D. Smart, S. J. Brough, C. Sabido-David *Bioorg. Med. Chem. Lett.* **2001**, *11*, 737-740; b) M. Lang, R. M. Soll, F. Durrenberger, F. M. Dautzenberg, A. G. Beck- Sickinger *J. Med. Chem*. **2004**, *47*, 1153-1160.

[3] N. A German, A. M. Decker, B. P. Gilmour, B. F. Thomas, Y. Zhang *Med. Chem. Lett*. **2013**, *42,* 1224-1227.

[4] a) S. Asahi, S-I Egashira, M. Matsuda, H. Iwaasa, A. Kanatani, M. Ohkubo *Bioorg. Med. Chem. Lett*. **2003**, *13*, 111-113; b) J. Putula, P. M. Turunen, L. Johansson, J. Nasman, R. Ra, L. Korhonen *FEBS Lett*. **2011**, *585*, 1368-1374.

[5] R.A.Porter, W. N. Chan, S. Coulton, A. Johns, M. S. Hadley, K. Widdowson *Bioorg. Med. Chem. Lett.* **2001**, *11*, 1907-1910.

[6] C. J. Winrow, J. J. Renger *Br. J. Pharmacol*. **2014**, *171*, 283-293.

[7] C. J. Langmead, J. C. Jerman, S. J. Brough, C. Scott, R. A. Porter, H. J. Herdon Br. *J. Pharmacol*. **2004**, *141*, 340-346.

[8] M. A. Steiner, J. Gatfield, C. Brisbare-Roch, H. Dietrich, A. Treiber, F. Jenck *ChemMedChem*. **2013***, 8*, 898-903.

[9] M. A. Steiner, C. Sciarretta, A. Pasquali, F. Jenck *Front. Pharmacol*. **2013**, *4*.
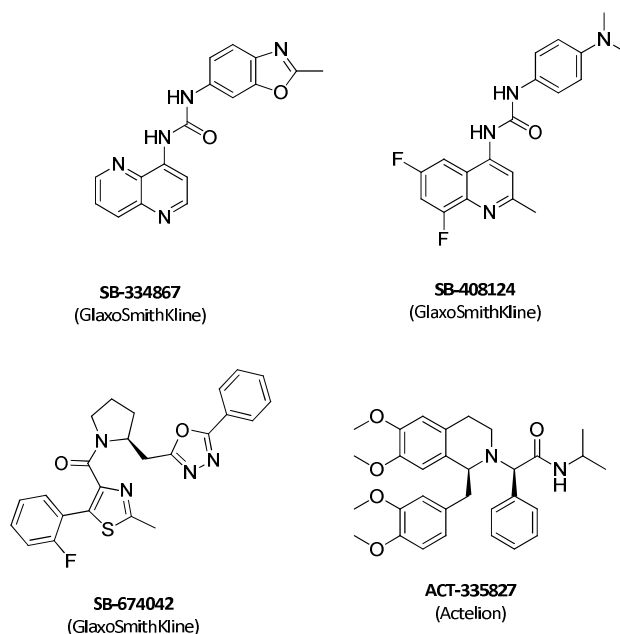
Figure 3. Selective Ox1 Receptor Antagonists (*SORAs 1*)

The small molecules selective OX2 receptor antagonists (*SORA-2*), in contrast, were developed by a different group of companies and have different structures. The first, TCS-OX2-29, is a tetrahydroisoquinoline reported in 2003 and developed by Banyu Pharmaceutical Co., a branch of Merck Sharpe & Dohme. It is highly selective for the OX2 receptor (IC$_{50}$ of 40 nM), while having no effect at the OX1 receptor (above µM range).[10] Subsequently was discovered JNJ-10397049 (Johnson&Johnson), a phenyl-dioxanyl urea compound with 600-fold selectivity for the OX2 receptor.[11]

In 2013 it was reported by literature EMPA (Hoffman-La Roche): it contain an acetamidic and sulfonamidic groups in a branched structure. It inhibits OX2 receptor in the nanomolar range, while inhibit OX1 receptor only over µM concentrations.[12] Furthermore, Eli Lilly developed LSN2424100, that present a sulfonamide as structural motif with aromatic/heteroaromatic substitutions.[13] LSN2424100 has highly activity towards the OX2R with a *Kb* of 0.44 nM, while show less activity for the OX1R with a Kb value of 90.3 nM (about 200-fold selective at OX2R). LSN2424100 had also shown antidepressant activity in mice and rats.

Merck has reported developing a *SORA 2* (MK- 1064) for insomnia, this product is reported in phase I clinical studies.[14]

The structure of the SORAs described were reported in Figure 4.

[10] M. Hirose, S-I Egashira, Y. Goto, T. Hashihayata, N. Ohtake, H. Iwaasa *Bioorg. Med. Chem. Lett.* **2003**, *13*, 4497-4499.

[11] L. C. McAtee, S. W. Sutton, D. A. Rudolph, X. Li, L. E. Aluisio, V. K. Phuong *Bioorg. Med. Chem. Lett.* **2004**, *14*, 4225-4229.

[12] P. Malherbe, E. Borroni, L. Gobbi, H. Knust, M. Nettekoven, E. Pinard *Br. J. Pharmacol.* **2009**, *156*, 1326-1341.

[13] T. E. Fitch, M. J. Benvenga, C. D. Jesudason, C. Zink, A. B. Vandergriff, M. Menezes *Front. Neurosci.* **2014**, *8*.

[14] A. J. Roecker, S. P. Mercer, J. D. Schreier, C. D. Cox, M. E. Fraley, J. T. Steen *ChemMedChem.* **2014**, *9*, 311-322.
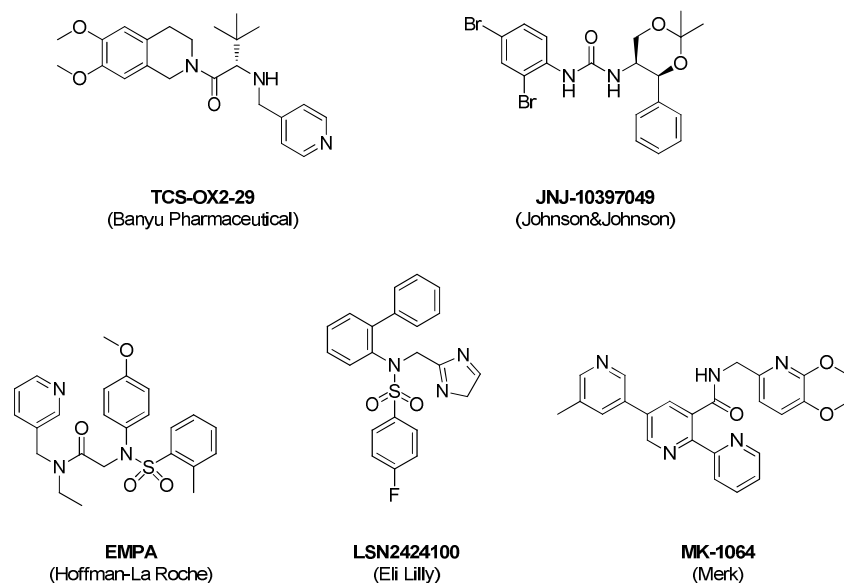
Figure 4. Selective Ox2 Receptor Antagonists (*SORAs 2*)

Several Dual Orexin Receptor Antagonist (*DORAs*, Figure 5), that bind both the orexin receptors, have entered in the clinical trials in the last years, mainly for the treatment of insomnia. The most representative are *Almorexant*, SB-649868 (GlaxoSmithKline), *Filorexant* and *Suvorexant* (Merk).

Almorexant is a tetrahydroisoquinoline, but presents additional substitutions respect TCS-OX2-29 (SORA-2) and it was developed for the treatment of insomnia.[15]

After in depth studies emerged that *Almorexant* may interact with the transmembrane domines 3 and 5-7 of both OXRs (is the same domain predicted to interact with the endogenous orexin peptides).[16] Almorexant completed Phase III clinical trials in 2009, however its development was stopped (by Actelion and GlaxoSmithKline) in 2011 due to the side effects profile.[17] Almorexant continued to be used in research as standard to development of new class of orexin antagonists.

GlaxoSmithKline also conduce independently the development of SB-649868 (Kb OX1R = 0.32 nM; Kb OX2R = 0.40 nM)

SB-649868 structure is based on a piperidine core functionalized by amidic bounds with heteroaromatic moieties.[18]

This compounds showed sleep-promoting effect in rats, good tolerability and half-life in clinical trials.[19] After the achievement of the Phase II clinical trials its development was stopped.[20]

---

[15] a) C. Brisbare-Roch, J. Dingemanse, R. Koberstein, P. Hoever, H. Aissaoui, S. Flores *Nat. Med*. **2007**, *13*, 150-155; b) P. Hoever, S. de Haas, J. Winkler, R. C. Schoemaker, E. Chiossi, J. van Gerven *Clin. Pharmacol. Ther*. **2010**, *87*, 593-600; c) P. Hoever, S. L. de Haas, G. Dorffner, E. Chiossi, J. M. van Gerven, J. Dingemanse *J. Psychopharmacol*. **2012**, *26*, 1071-1080; d) P. Hoever, G. Dorffner, H. Benes, T. Penzel, H. Danker-Hopfe, M. J. Barbanoj *Clin. Pharmacol. Ther*. **2012**, 91, 975-985.

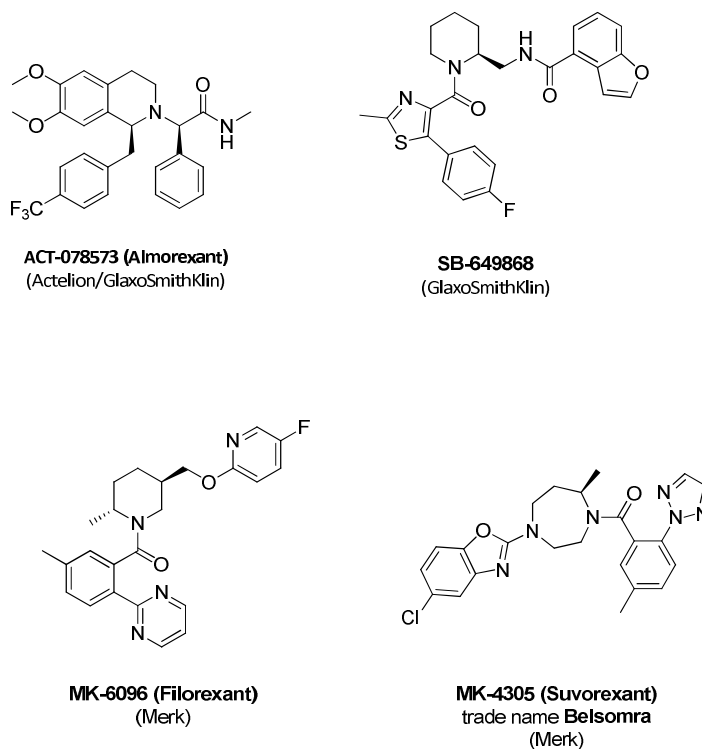[16] A. Heifetz, G. B. Morris, P. C. Biggin, O. Barker, T. Fryatt, J. Bentley *Biochemistry* **2012**, 51, 3178-3197.

[17] a) Actelion Pharmaceuticals, GlaxoSmithKline. Allschwil/ Basel, Switzerland and London. http://www.actelion.com; 2011. Accessed 21 Dec **2013**; b) H. G. Cruz, P. Hoever, B. Chakraborty, K. Schoedel, E. M. Sellers, J. Dingemanse *CNS Drugs* **2014**, *28*, 361-372; c) K. Shakeri-Nejad, M. Hoch, P. Hoever, J. Dingemanse *Eur. J. Pharm. Sci*. **2013**, *49*, 836-844.

[18] R. Di Fabio, A. Pellacani, S. Faedo, A. Roth, L. Piccoli, P. Gerrard *Bioorg. Med. Chem. Lett*. **2011**, *21*, 5562-5567.

[19] P. Bettica, G. Nucci, C. Pyke, L. Squassante, S. Zamuner, E. Ratti *J. Psychopharmacol*. **2012**, *26*, 1058-1070.

Filorexant and *Suvorexant* are two *DORAs* developed by Merck that have reached the clinical trails for the treatment of insomnia. *Filorexant* (MK-6096) is based on a 2-methyl-piperidine scaffold and showed to promoting sleep in rats, mice and dogs.[21] *Filorexant* was employed in clinical trials not only for the treatment of insomnia, but also to treat migraine, painful diabetic neuropathy and adjunctive therapy for depression.[22a-d]

The most important *DORA* developed from Merck is *Suvorexant*, a substituted diazepam, which has completed three Phase III clinical trials and was approved for sale (trade name *Belsomra*) by the U. S. Food & drug Administration in August 13th, 2014.[22e]

ACT-078573 (Almorexant)
(Actelion/GlaxoSmithKlin)

SB-649868
(GlaxoSmithKlin)

MK-6096 (Filorexant)
(Merk)

MK-4305 (Suvorexant)
trade name **Belsomra**
(Merk)

Figure 5. Dual Orexin Receptor Antagonists (*DORAs*)

[20] GlaxoSmithKline. clinicaltrials.gov. **2010**. clinicaltrials.gov/show/NCT00534872. Accessed 22 Dec **2013**.

[21] a) P. J. Coleman, J. D. Schreier, C. D. Cox, M. J. Breslin, D. B. Whitman, M. J. Bogusky *ChemMedChem*. **2012**, *7*, 415-424; b) C. J. Winrow, A. L. Gotter, C. D. Cox, P. L. Tannenbaum, S. L. Garson, S. M. Doran *Neuropharmacology* **2012**, *62*, 978-987.

[22] a) Merck Sharp & Dohme. clinicaltrials.gov. 2011. clinicaltrials.gov/show/NCT01021852. Accessed 19 Mar **2014**; b) Merck Sharp & Dohme. clinicaltrials.gov. 2012. clinicaltrials. gov/show/NCT01513291. Accessed 19 Mar **2014**; c) Merck Sharp & Dohme. clinicaltrials.gov. 2013. clinicaltrials.gov/show/NCT01564459. Accessed 19 Mar **2014**; d) Merck Sharp & Dohme. clinicaltrials.gov. 2013. clinicaltrials.gov/show/NCT01554176. Accessed 19 Mar **2014**; e) http://www.fda.gov/NewsEvents/Newsroom/PressAnnouncements/ucm409950.htm.

Chapter 2. Chemistry

2.1 Introduction

In this PhD project we concentrate our efforts in designing new DORAs compounds, trying to ameliorate some pharmacological features of *Suvorexant*, emerged during its clinical development, that induced the FDA to lower its posology.

Some of the orexin receptor antagonists known in literature, contain as a fundamental motif the ethylendiaminic sequence *NCCN*. For example, *Suvorexant* (developed by Merck) contains the methyl-diazepine core. SB-649868 developed by GlaxoSmithKline is based on the piperidin-2-ylmethanamine moiety and it has been evaluated in Phase II clinical trials for sleep disorders, Figure 1.

So, we planned to insert the *NCCN* motif in a bicyclic framework such as the norbornane in order to obtain a markedly rigid structure and to confer specific features to the final derivatives. Three distinct *NCCN*-containing scaffolds were proposed at the beginning of the Ph.D. project, namely the *TYPE I*, *TYPE II* and *TYPE III* scaffolds reported in Figure 1 and the chemical studies started with an accurate investigation of the literature concerning the synthesis of the three identified scaffolds.


Suvorexant (Belsomra)   SB-649868

TYPE I
2-azabicyclo[2.2.1]heptan-3-ylmethanamine

TYPE II
7-azabicyclo[2.2.1]heptan-2-amine

TYPE III
2-azabicyclo[2.2.1]heptan-6-amine
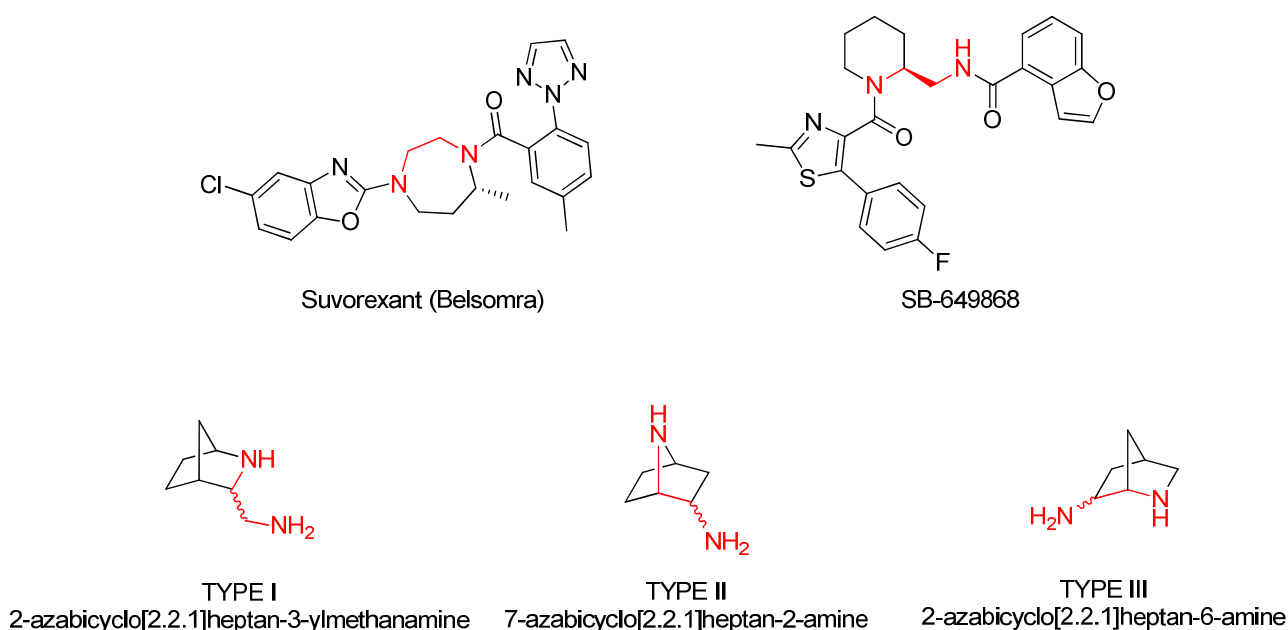
Figure 1

2.1.1 TYPE I scaffold (2-azabicyclo[2.2.1]heptan-3-ylmethanamine)

After a detailed research in the literature, we found that the *TYPE I* scaffold was already successfully employed for the preparation of several molecules with orexin antagonism activity by the Actelion Pharmaceuticals research group.[1] In particular, in a patent registered in 2009, the authors describe the synthesis and the biological properties of a series of compounds with the

---

[1] H. Aissaoui, C. Boss, R. Koberstein, T. Sifferlen, D. Trachsel. Actelion Pharmaceuticals LTD (CH). WO 2009104155A1.

general formula depicted in Figure 2. These compounds are in general substituted at the endocyclic nitrogen atom with aryl or heteroaryl (rings A and B, Figure 2), linked to the bicyclic core through an amide linkage. Beside, the exocyclic nitrogen bears heteroaryl substituents (ring R^1) that may be linked to the nitrogen atom directly or *via* an amide bond.


n = 0, 1
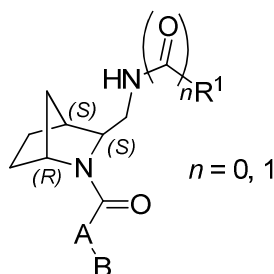
Figure 2

All synthesized compounds were tested as antagonists of human orexin-1 and orexin-2 receptors expressed by engineered cells. Best antagonistic activities (IC_{50} values) of tested compounds were 6 nM with respect to the OX1 receptor and 10 nM with respect to OX2 receptor.
Upon this finding, that increases the goodness of our working hypothesis, we decided to focus the research only on *TYPE II* and *TYPE III* scaffolds.

2.1.2 TYPE II scaffold (7-azabicyclo[2.2.1]heptan-2-amine)

The 7-azabicyclo[2.2.1]heptan-2-amine exists as a couple of diastereoisomers, namely compounds *endo* and *exo* in Figure 3, and each diastereoisomer as a couple of enantiomers.

(+/-)-endo-7-azabicyclo[2.2.1]heptan-2-amine

(1S,2S,4R)   (1R,2R,4S)

(+/-)-exo-7-azabicyclo[2.2.1]heptan-2-amine

(1S,2R,4R)   (1R,2S,4S)
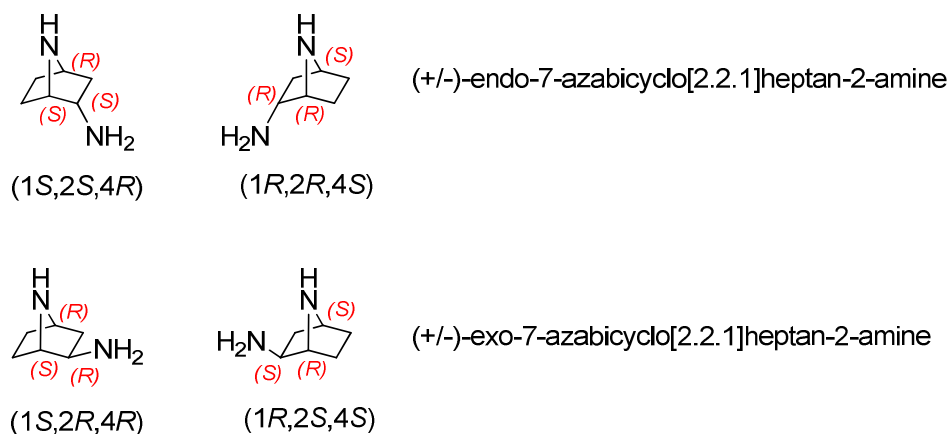
Figure 3

Thus, we started our investigation on *TYPE II* scaffold realizing the diastereoselective synthesis of both *endo* and *exo* compounds as racemic mixtures. The complete synthesis is reported in Scheme 1.[2]
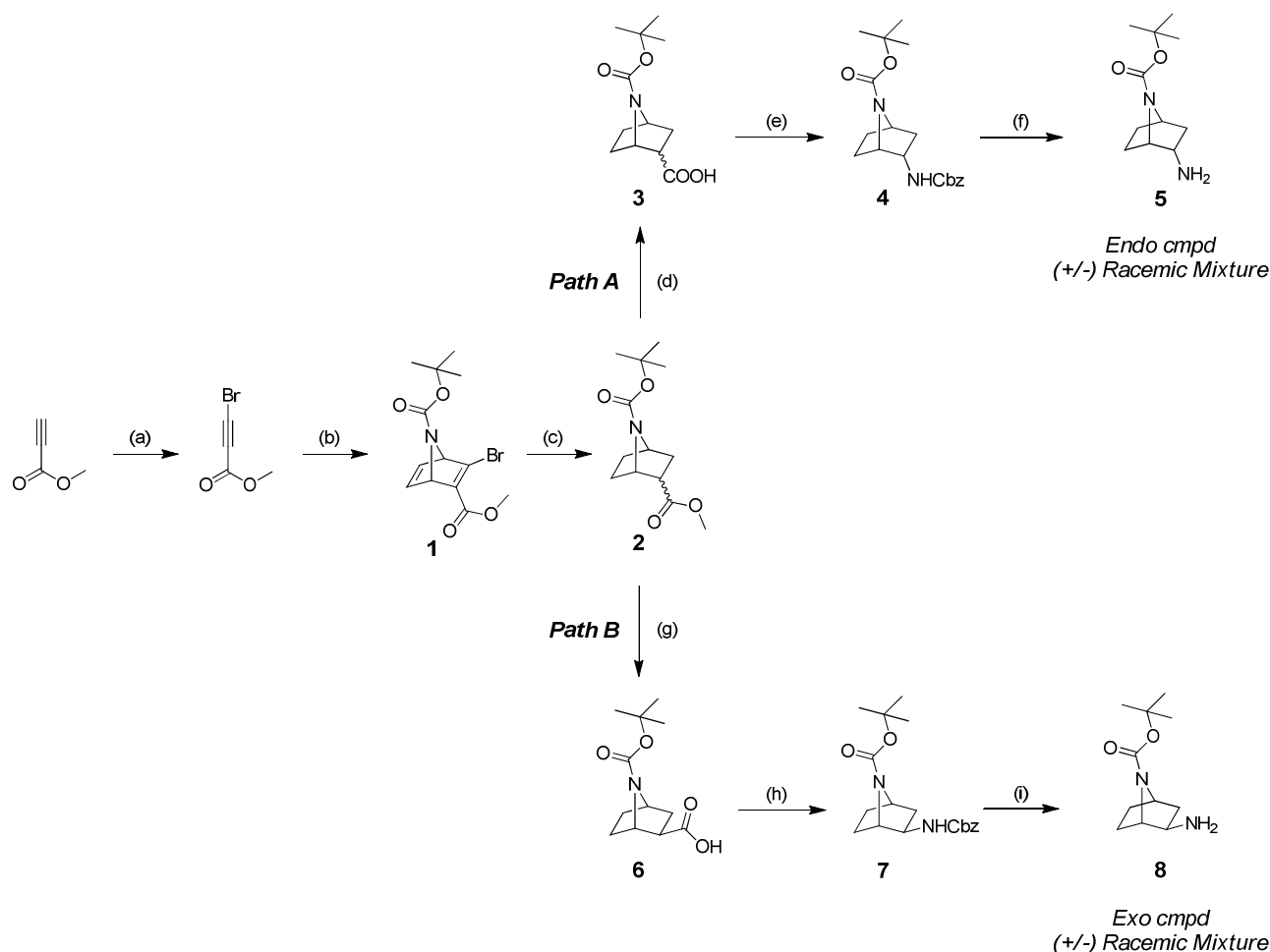
Reactants and conditions: (a) NBS, AgNO₃, Acetone, Rt, 85%; (b) *N-Boc*-Pyrrole, 90°C, 8-15%; (c) Pd/C 10%mol, H₂, MeOH, TEA, quant. **Path A**: (d) LiOH, THF/H₂O 3:1, Rt, quant. (e) TEA, diphenylphosphoryl azide, benzyl alcohol, toluene, 100°C, 80%; (f) Pd/C 1%mol, H₂ 50 psi, EtOH, quant. **Path B**: (g) NaOMe, MeOH, reflux then water/HCl, Rt, 53%; (h) diphenylphosphoryl azide, TEA, benzyl alcohol, toluene, 100°C, 57%; (i) Pd/C 2.5%mol, H₂ 50 psi, EtOH, Rt, quant.

Scheme 1

The synthetic route involved in the first step a thermal Diels-Alder reaction between methyl 3-bromopropiolate (obtained by bromuration of methyl propiolate with *N*-bromosuccinimide) and *tert*-butyl 1*H*-pyrrole-1-carboxylate, giving rise to the first key intermediate **1**. Hydrogenation of 1

---

[2] a) T. D. Ashton, K. M. Aumann, S. P. Baker,C. H. Schiesserb, P. Scammells *Bioorg. Med. Chem. Lett.* **2007**, *17*, 6779-6784; b) Walker, D. P.; Wishka, D. G.; Piotrowski, D. W.; Jia, S.; Reitz, S. C.; Yates, K. M.; Myers, J. K.; Vetman, T. N.; Margolis, B. J.; Jacobsen, E. J.; Acker, B. A.; Groppi, V. E.; Wolfe, M. L.; Thornburgh, B. A.; Tinholt, P. M.; Cortes-Burgos, L. A.; Walters, R. R.; Hester, M. R.; Seest, E. P.; Dolak, L. A.; Han, F.; Olson, B. A.; Fitzgerald, L.; Staton, B. A.; Raub, T. J.; Hajos, M.; Hoffmann, W. E.; Li, K. S.; Higton, N. R.; Wall, T. M.; Hurst, R. S.; Wong, E. H. F.; Rogers, B. N. *Bioorg. Med. Chem.* **2006**, *14*, 8219; c) Singh, S.; Basmadjan, G. P. *Tetrahedron Lett.* **1997**, *38*, 6829.

with hydrogen and palladium on carbon, in presence of triethylamine as base, gave the 7-*tert*-butyl 2-methyl 7-azabicyclo[2.2.1]heptane-2,7-dicarboxylate (**2**). Compound **2** was isolated as a racemic *endo*/*exo* mixture in about 88:12 ratio from ^{1}H NMR analysis and represents the common intermediate for the synthesis of both targeted compounds.

Thus, starting from intermediate **2** the *TYPE II* scaffold with the *endo*-stereochemistry was prepared following the synthetic route depicted in Scheme 1, path A. Hydrolysis of the methyl ester **2** with lithium hydroxide in THF/water at room temperature furnished quantitatively the free acid **3**. Compound **3** preserves the same *endo*/*exo* ratio of the starting material **2**. Then, in a one-pot reaction, the acid **3** was transformed firstly into the corresponding acylazide in the presence of diphenylphosphorylazide. In the second step of the one-pot reaction, thermal Curtius rearrangement of the acylazide, in the presence of benzyl alcohol as trapping reagent for the isocyanide intermediate, gave the *N-Cbz*-protected compound **4** in 80% yield. At this stage of the synthesis, flash chromatographic purification of the crude allowed for the isolation of pure **4** in *(+/-)-endo* configuration. A final hydrogenation step, performed with hydrogen at 50 psi, in ethanol at room temperature and in the presence of Pd/C (1%), provided the *Cbz* protecting group cleavage, giving rise to the *(+/-)-endo-tert*-butyl 2-amino-7-azabicyclo[2.2.1]heptane-7-carboxylate (**5**) in quantitative yield.

The adopted synthetic strategy to obtain the *exo-TYPE II* scaffold is depicted in Scheme 1, path B. Intermediate **2** in *(+/-)-endo*/*exo* mixture was subjected to complete inversion to *(+/-)-exo*-acid free acid derivative **6** by treatment with sodium methoxide in refluxing methanol at room temperature (yield 53%). Then, the *(+/-)-exo-tert*-butyl 2-amino-7-azabicyclo[2.2.1]heptane-7-carboxylate (**8**) was obtained following the same synthetic strategy described for the *endo* compound **5**.

The structures of the obtained compounds were assigned on the basis of combined 1D (^{1}H NMR, ^{13}C NMR) and 2D NMR (COSY, HSQC, NOESY) experiments. In particular, the analysis of 1D and 2D experiments allowed for the complete assignment of proton and carbon chemical shifts and coupling constants. The *endo*/*exo* stereochemistry at carbon 2 was assigned on the basis of coupling constant values. For illustration, for compounds **3** and **6** the relevant resonance assignments and measured coupling constants for ^{1}H NMR are reported in Figure 4.
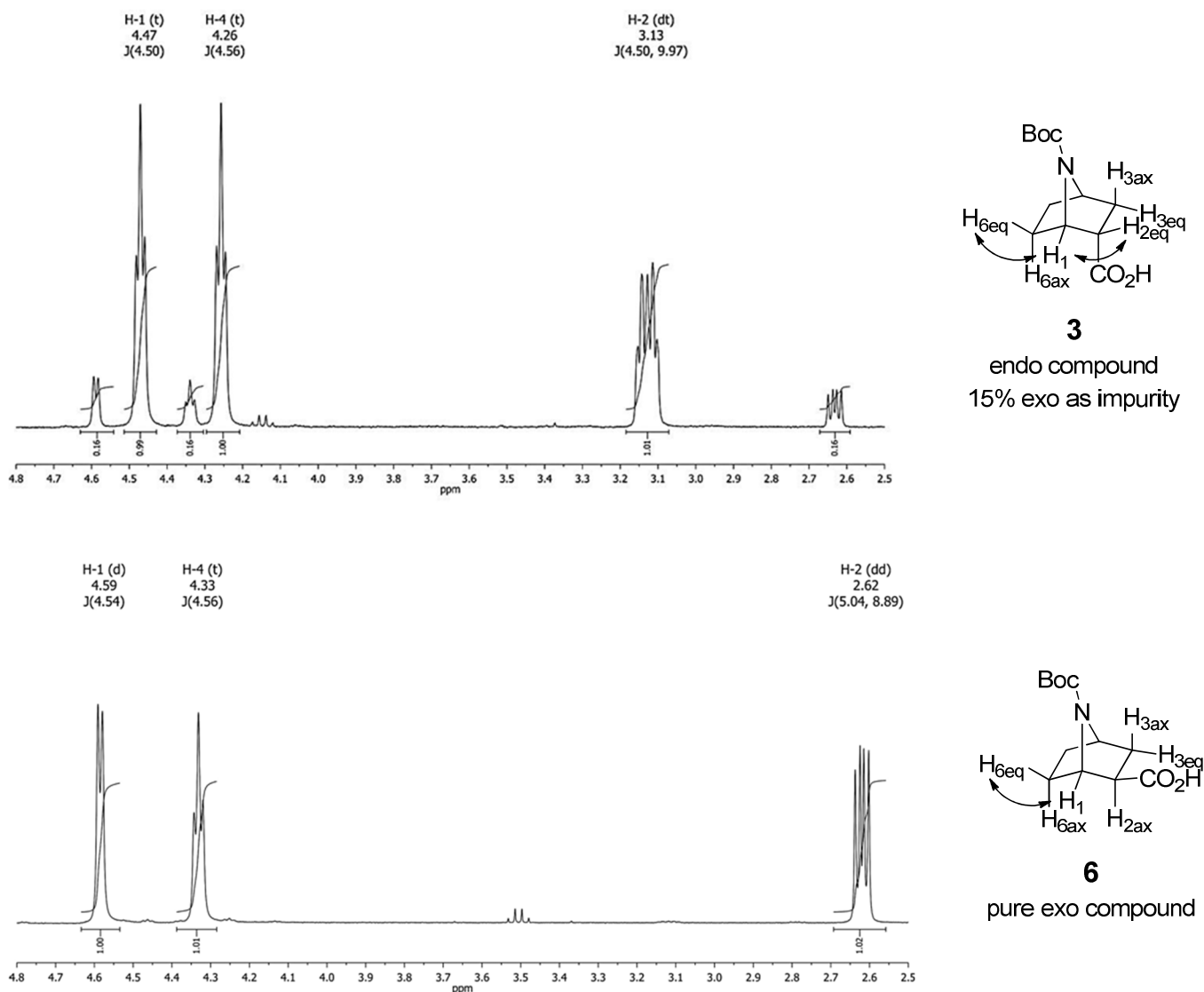
Figure 4

In compound **3** the angular hydrogen 1 appears as a triplet with a coupling constant of 4.5 Hertz with both equatorial hydrogens 2 and 6. The coupling constant of hydrogen 1 with axial hydrogen 6 is zero. The proton spectra of **3** shows as impurity a 15% of the corresponding *exo* compound **6**.

In compound **6** the angular hydrogen 1 appears as a doublet with a coupling constant of 4.5 Hertz with the equatorial hydrogen 6. The coupling constant of hydrogen 1 with both axial hydrogens 2 and 6 is zero. At the same time in compound **3** the signal of the hydrogen 2 is a double triplet and the same hydrogen in compound **6** is a double doublet with the coupling constant 2-1 equal to zero.

Measured ^3J coupling constants are in good agreement with calculated ^3J coupling constant ranges, achieved from dihedral angles values by Karplus equation, see Table 1.

Table 1. Measured ^{1}H–^{1}H coupling constant versus calculated ^{1}H–^{1}H coupling constant range (derived from dihedral angles).

	3 Φ	3 J (Hz) exp.	3 J (Hz) calc.	6 Φ	6 J (Hz) exp.	6 J (Hz) calc.
^3J H-1/H-2	41.1°	4.5	4.5-5.1	83.5°	0	0-1.0
^3J H-1/H-6ax	79.7°	0	0-1.0	80.3°	0	0-1.0
^3J H-1/H-6eq	48.3°	4.5	3.5-3.9	40.2°	4.5	4.7-5.3

2.1.3 Functionalization of TYPE II scaffold (7-azabicyclo[2.2.1]heptan-2-amine)

With both *endo* and *exo* compounds **5** and **8** in hand, we started the search for the more suitable substituents for both endocyclic and exocyclic nitrogen atoms.

On the basis of the rationale evaluation of the orexin antagonists known in literature, a "*template structure*" was adopted in order to carry out the *endo/exo TYPE II* scaffold rational exploration, Figure 5. The template bears a heteroaromatic ring (ring A in Figure 5) linked to the exocyclic nitrogen atom and a double aromatic/heteroaromatic system (rings B-C in Figure 5) linked through an amide bond to the endocyclic nitrogen atom of the scaffold.
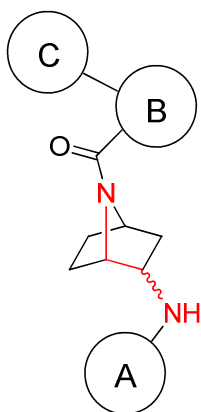
Figure 5

The functionalization of both nitrogen atoms of compounds **5** and **8** with aromatic and/or heteroaromatic rings allowed for the preparation of a small library of new compounds, Figure 6.

Each moiety, A or B-C, was analyzed and modified separately, fixing the other ring, in order to have a direct comparison with the compounds of the same series and a better understanding of the *SAR* (*Structure Activity Relationship*) after biological activity evaluation.

We started the synthetic work with the exploration of the *endo-TYPE II* scaffold **3**. The ring A was the first substituent analyzed, maintaining as B-C moiety the 2-methyl-5-phenylthiazole-4-carbonyl substituent. Five compounds (**9a-e**) with the ring A ri-elaboration were prepared, Figure 6a. Subsequently, we started with the B-C moiety rational investigation fixing as ring A the 5-(trifluoromethyl)pyridin-2-yl group and we synthesized six derivatives (**9f-k**), Figure 6b.
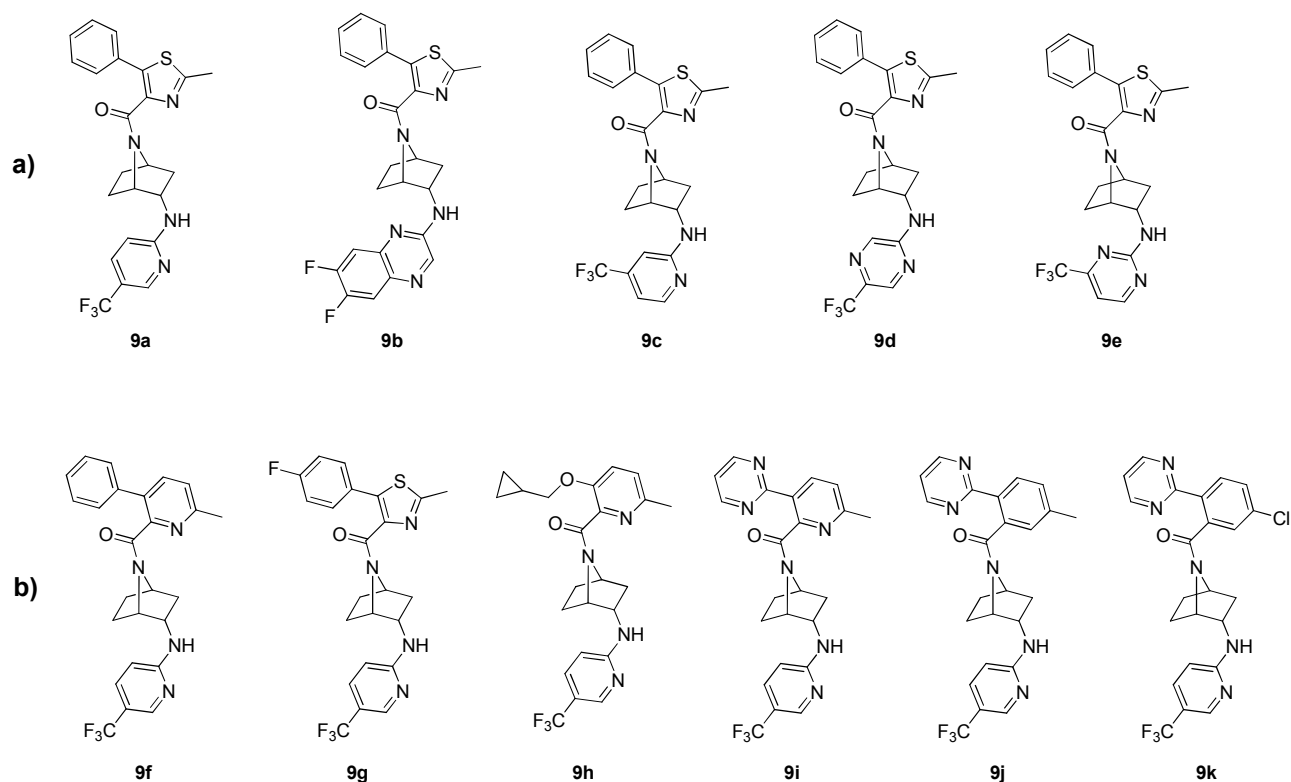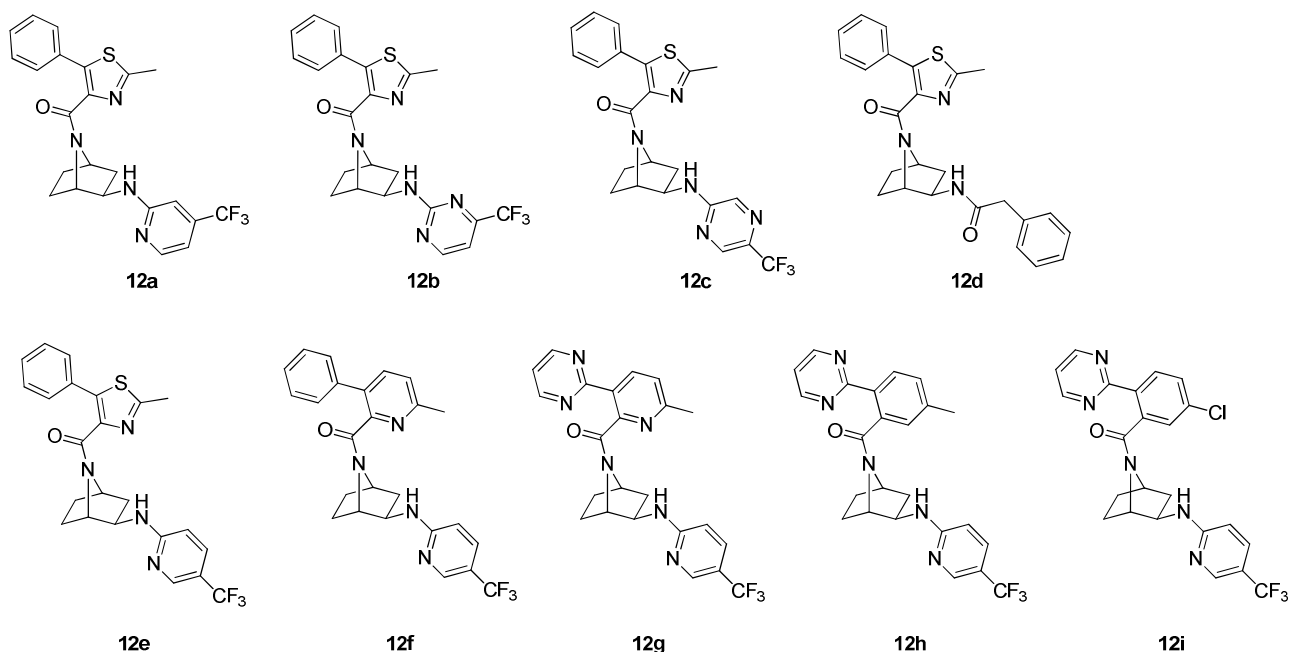
Figure 6

The adopted synthetic pathway is reported in Scheme 2 and consisted in the nucleophilic displacement of the appropriate heteroaryl halide (A-X, X = fluoride or chloride) with intermediate **5** in presence of a base (TEA or K₂CO₃) in dry DMF at 75-100°C affording compounds **10a-k** in 45-68% yields. After nearly quantitative *N-Boc* cleavage in the presence of TFA, the intermediates **11a-k** were reacted with the selected acids under classical amide coupling conditions in the presence of 2-chloro-4,6-dimethoxy-1,3,5-triazine as carboxylic activating agent. The eleven final products **9a-k** were obtained as *(+/-)-endo* racemic mixture in 55-83% yields.

5   **10a-k**   **11a-k**   **Compounds 9a-k**
(+/-)-endo Racemic Mixture
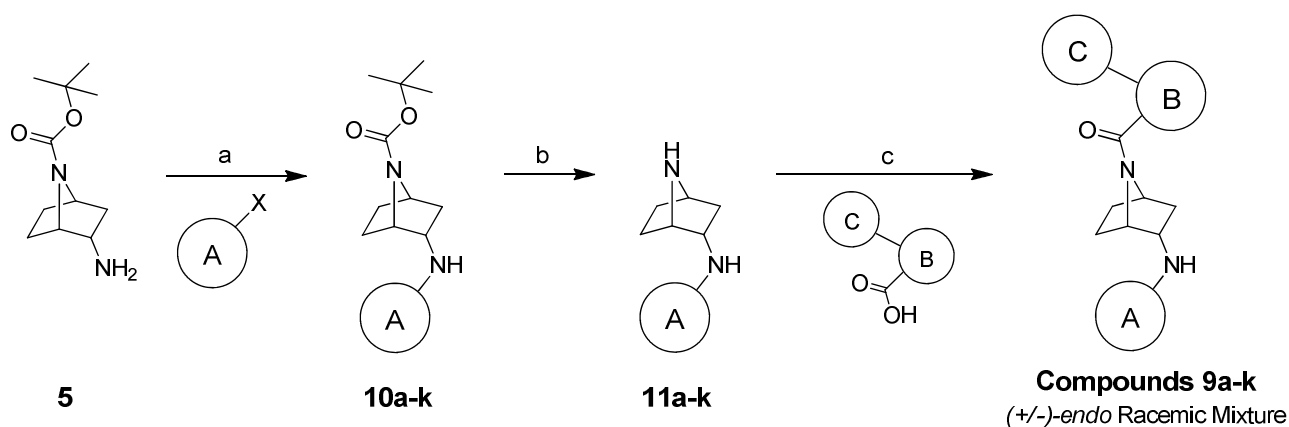
Reactants and conditions: (a) heteroaryl halides **A-X** (where **X**= F or Cl), TEA or K$_2$CO$_3$, DMF, 75-100°C, 44.5-68%; (b) DCM/TFA 4:1, Rt, 89-98%; (c) **C-B-COOH,** 2-chloro-4,6-dimethoxy-1,3,5-triazine, *N*-methylmorpholine, Rt then 100°C, 55-83%.

Scheme 2

Then we started the exploration of *(+/-)-exo-TYPE II* scaffold planning the synthesis of nine compounds (**12a-i**), Figure 7, and choosing the substituent at the nitrogen atoms with the same rationale adopted in the design of compounds **9a-k**.

12a   **12b**   **12c**   **12d**

12e   **12f**   **12g**   **12h**   **12i**

Figure 7

The synthetic pathway adopted for the synthesis of the *exo-TYPE II* derivatives was the same used for the *endo-TYPE II* analogues (reaction conditions and yields are reported in Scheme 3). The nine final products **12a-i** were obtained as *(+/-)-exo* racemic mixture.

a or b

c

d

C-B-COOH

8

13a-e

14a-e

Compounds 12a-i
(+/-)-exo Racemic Mixture
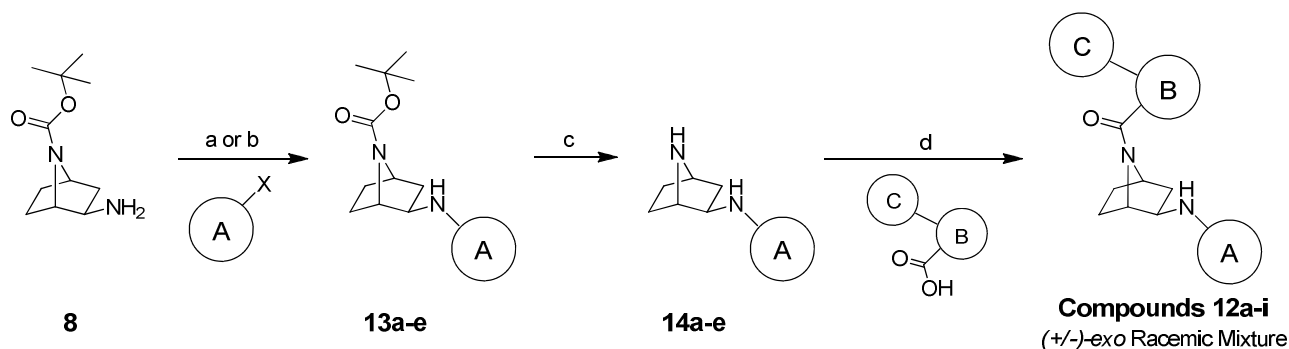
Reaction conditions: (a) heteroaryl halides **A-X** (where **X**= F or Cl), K_2CO_3, DMF dry, 85-100°C, 44-68%; (b) phenylacetyl-halide **A-X** (where X= Cl), pyridine, DCM, Rt, 73%; (c) DCM/TFA 4:1, Rt, 90-quant %; (d) **C-B-COOH**, 2-chloro-4,6-dimethoxy-1,3,5-triazine, *N*-methylmorpholine, Rt then 100°C, 72-88%.

Scheme 3

Compounds **9** and **12** are distereoisomers and their structures were assigned on the basis of combined 1D (^{1}H NMR, ^{13}C NMR) and 2D-NMR (COSY, HSQC, NOESY) experiments. The ^{1}H NMR analysis of compounds **9** and **12** reveals the existence in solution of two equilibrating species, two rotamers, for both series of compounds, in 1:1 ratio for **9** and 7:3 ratio for **12**. Rotamers are conformational isomers where interconversion by rotation around a single bond is restricted and an energy barrier has to be overcome in order to convert one conformer to another. When this rotation strain barrier is high enough to allow for the isolation of the conformers then the isomers become atropoisomers. The presence of two rotamers complicates the appearance of ^{1}H as well as ^{13}C NMR spectra and variable temperature (VT) NMR is the generally preferred method for studying the equilibration of the rotamers. In fact, at high temperature the two rotamers equilibrate and average simple spectra can be recorded at the coalescence temperature. Nevertheless, in our case working in DMSO-d_6 at 90 °C, the rotation barrier could not be overwhelmed. Recently, Ley and coworkers[3] reported a simple NMR experiment that permits to identify protons that are in mutual chemical exchange. The technique involves a 1D gradient NOE experiment in which a selected peak is irradiated during the experiment acquisition and looks like a negative peak (or a null peak depending on settled parameters) in the final spectrum. At the same time also those protons experiencing chemical exchange with the irradiated protons will appear as negative or null peaks in the final spectrum. This experiment is particularly useful also to distinguish between rotamers and diastereisomers. In our case the two species present in solution are undoubtedly rotamers because none of the frequency of **9** appear in the spectra of its diastereisomer **12**. Moreover, 1D gradient NOE experiment performed for compound **12e** (rotamers ratio 7:3) clearly show the existence of two species in chemical exchange process. In Figure 8 the chemical shifts of the protons irradiated in the 1D gradient NOE experiments are reported for both the rotamers.

[3] D. X. Hu, P. Grice, S. V. Ley *J. Org. Chem.* **2012**, *77*, 5198-5202.

Chemical shifts of diagnostic signals for major and minor* rotamers used in 1D gradient NOE experiments

4.08/4.71*H

2.13/1.91*

4.85/3.96*

12e
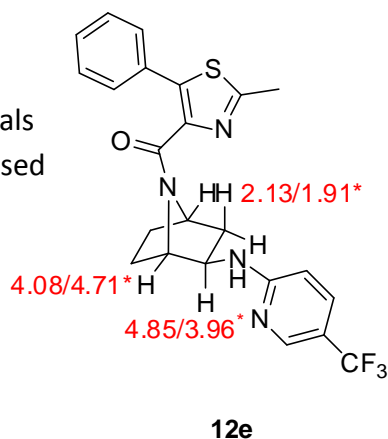
Figure 8

Moreover, as clearly shown in the picture in Figures 9, 10 and 11, saturation, respectively, of H-1, H-3$_{ax}$ and H-2 proton signals of the major rotamer result in the disappearance of the corresponding resonances of the minor rotamer. This demonstrates that the two detected species are in mutual chemical exchange.
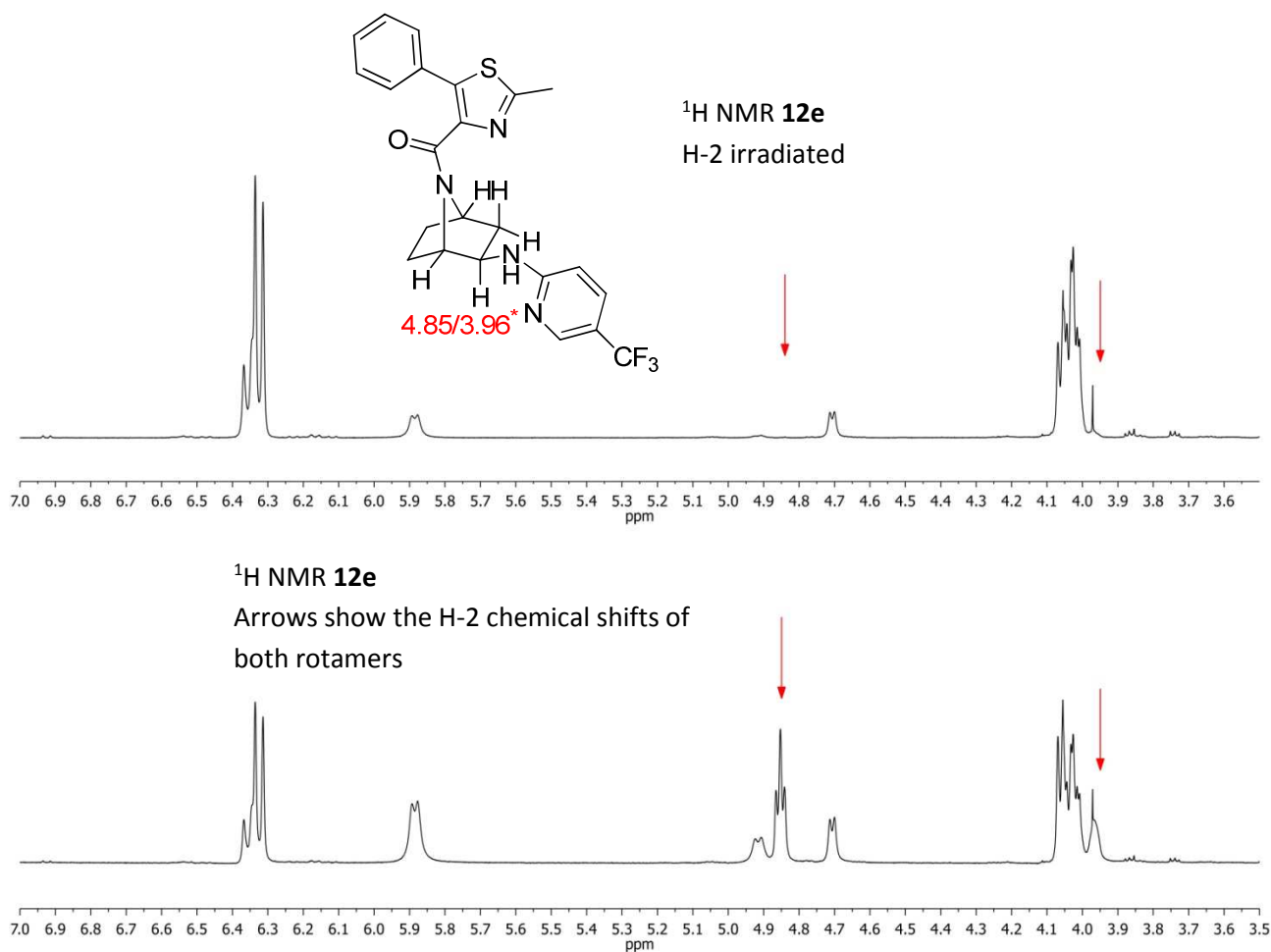

^{1}H NMR **12e**
H-1 irradiated

4.08/4.71*H
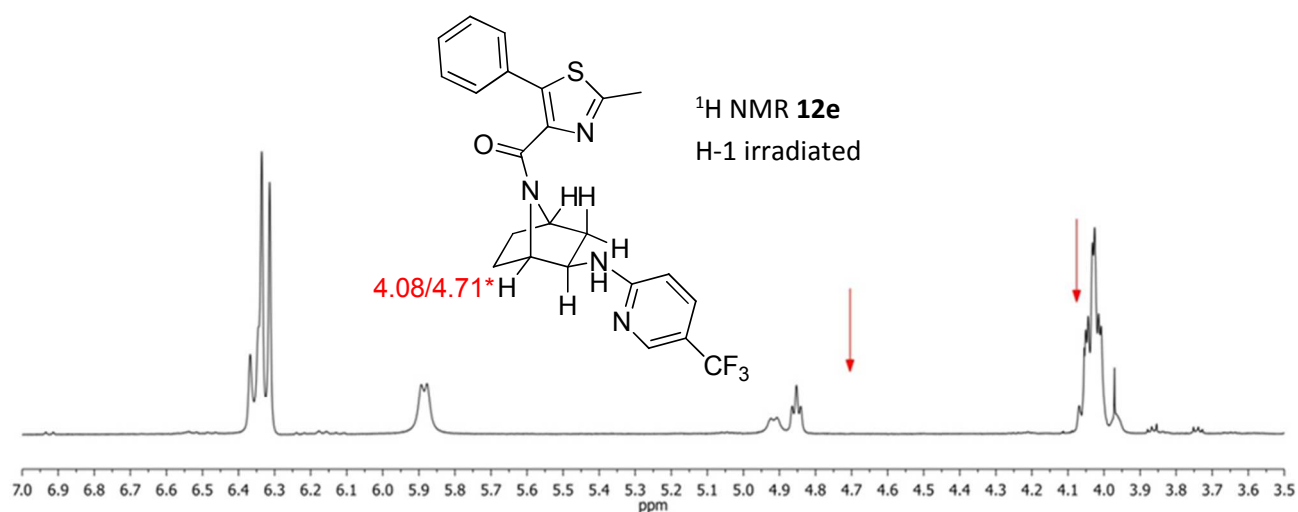
^{1}H NMR **12e**
Arrows show the H-1 chemical shifts of both rotamers
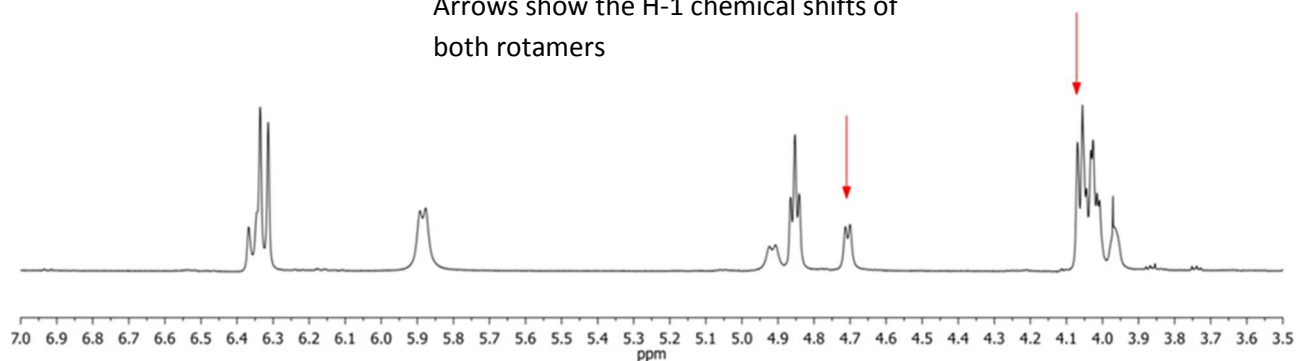
Figure 9
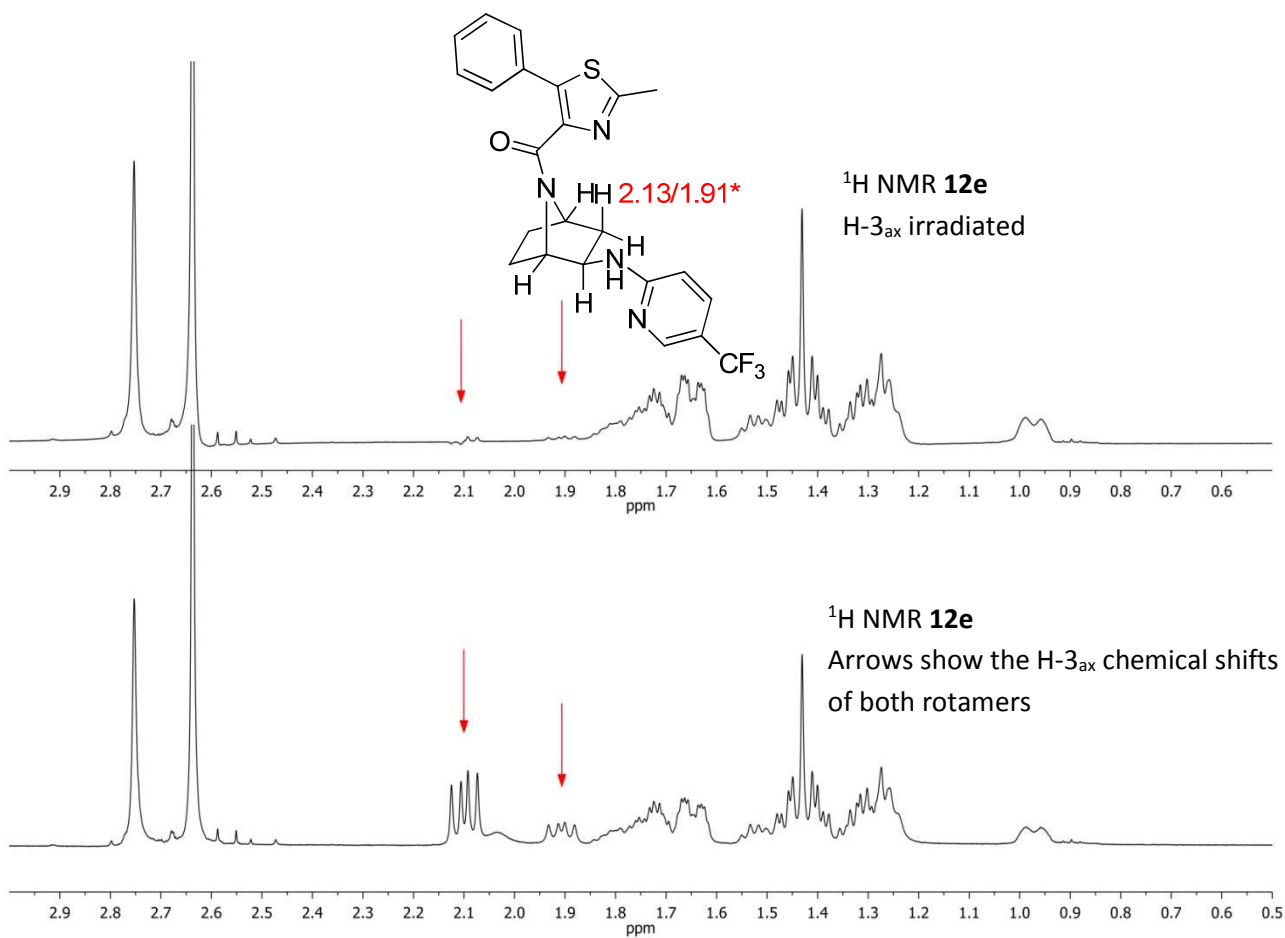
Figure 10

Figure 11

Moreover, the accurate analysis of 1D and 2D experiments allowed for the complete assignment of proton and carbon chemical shifts and coupling constants for both rotamers of the two series of synthesized compounds (**9** and **12**). The *endo/exo* stereochemistry at carbon 2 was assigned on the basis of coupling constant values. For illustration, for compounds **9k** and **12i** the relevant resonance assignments and measured coupling constants for ^{1}H NMR are reported in Figure 12.
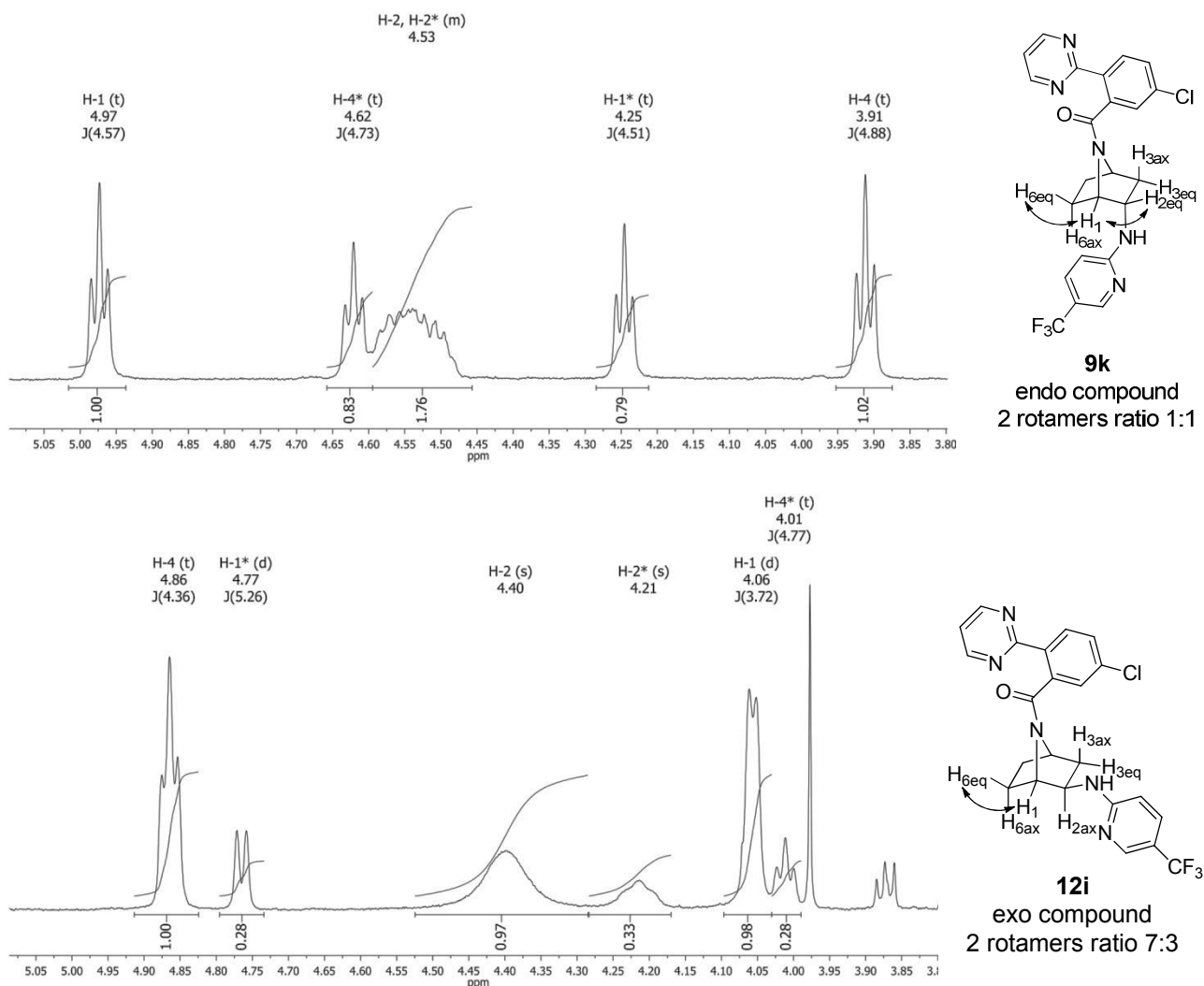
Figure 12

In Figure 12 the signals of one rotamer is normally numbered and the second one is marked with an asterisk. In compound **9k** the angular hydrogen 1 appears for both rotamers as a triplet with a coupling constant of 4.5 Hertz with both equatorial hydrogens 2 and 6 The coupling constant of hydrogen 1 with axial hydrogen 6 is zero.

In compound **12i** the angular hydrogen 1 appears as a doublet with a coupling constant of 4.5 Hertz with the equatorial hydrogen 6. The coupling constant of hydrogen 1 with both axial hydrogens 2 and 6 is zero. As already reported for compounds **3** and **6**, measured ^3J coupling constants are in good agreement with calculated ^3J coupling constant ranges, achieved from dihedral angles values by Karplus equation.

2.1.4 TYPE III scaffold (2-azabicyclo[2.2.1]heptan-6-amine)

Also the 2-azabicyclo[2.2.1]heptan-6-amine exists as a couple of diastereoisomers, namely compounds *exo* and *endo* in Figure 13, and each diastereoisomer as a couple of enantiomers.
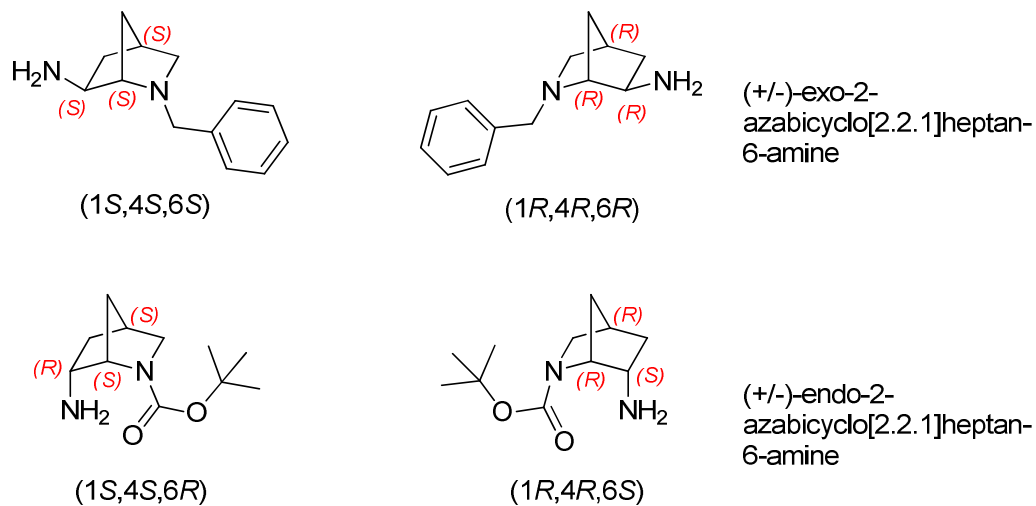
Figure 13

The complete synthesis of *TYPE III* scaffold in both *(+/-)-exo-* and *(+/-)-endo-* configurations is depicted in Scheme 4.
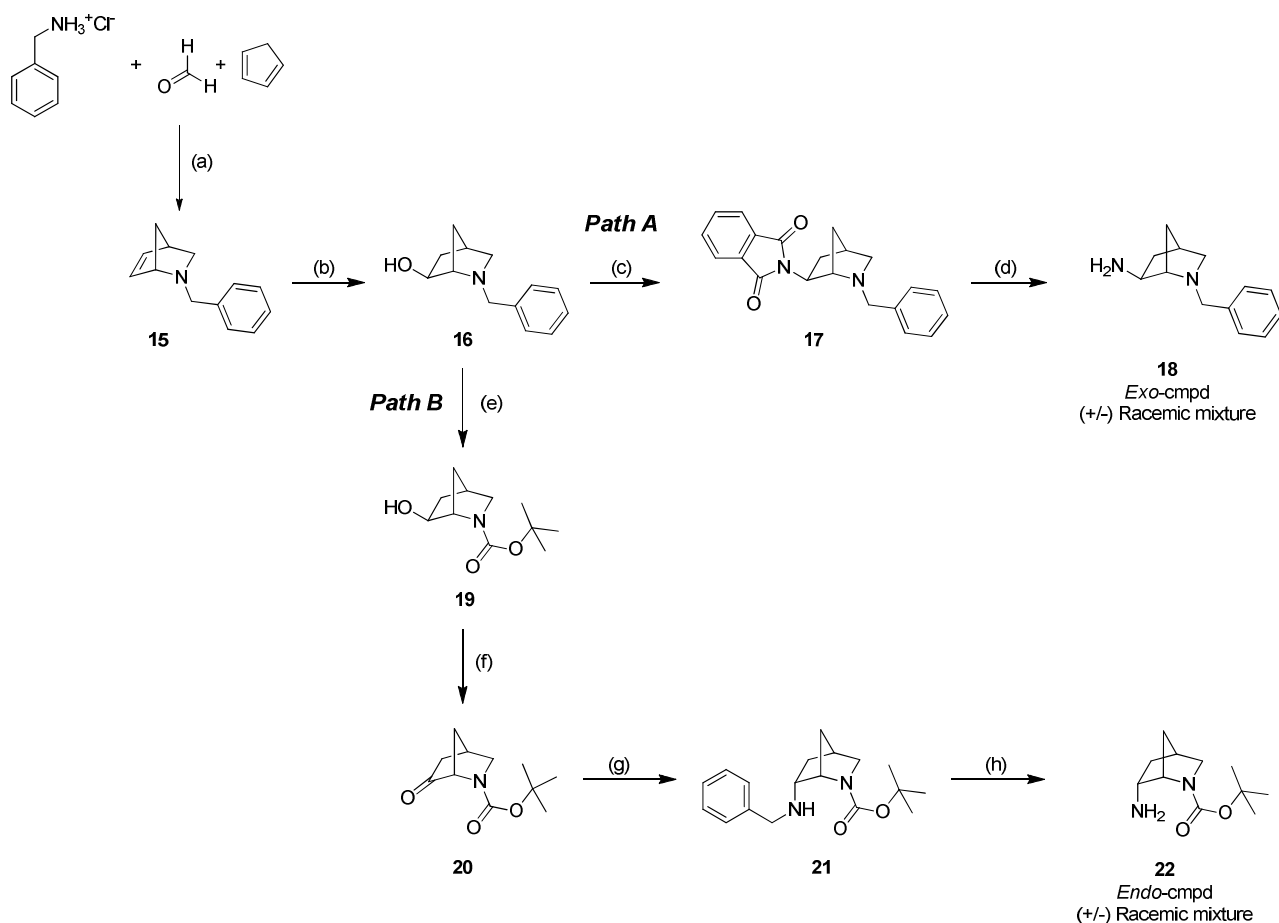
Reactants and conditions: (a) benzylamine hydrochloride, formaldehyde 37%Wt, then cyclopentadiene, water, Rt, 82%; (b) 1) borane-dimethylsulfide complex 2M in THF solution, THF, Rt, 2) NaOH/H₂O₂, THF/Water, 40°C, 49.5%. **Path A**: (c) phtalimide, triphenilphospine; 1,2-ethoxycarbonyl diazene 40% in Toluene, THF, 0°C then Rt, 72%; (d) hydrazine monohydrate, MeOH/THF 1:1, 65°C, 94%. **Path B**: (e) Pd-C/H₂, 30 psi, Boc₂O, EtOH, Rt, 87%; (f) oxalyl chloride, dimethylsulfoxide, TEA, DCM, -78 then Rt; 94%; (g) benzylamine, sodium triacetoxyhydroborate, 1,2-DCE; Rt; 94%; (h) Pd-C/H₂ 1atm, EtOH, Rt, 83%.

Scheme 4

The common intermediate for the synthesis of both desired compounds is the 2-benzyl-2-azabicyclo[2.2.1]heptan-6-ol **16** which was prepared in a two step sequence starting with the aza-Diels-Alder reaction in water, at room temperature between cyclopentadiene, formaldehyde and benzylamine hydrochloride giving rise to the azanorbornene **15** in 82% yield.[4] Subsequently, hybroboration of **15**, followed by a H₂O₂ oxidative workup give the corresponding alcohol **16** in 50% yield as a single regioisomer in *(+/-)-exo*-configuration, with only trace amounts of the *(+/-)-endo* alcohol derivative.[5]

Starting from compound **16**, the *exo-TYPE III* scaffold **18** was then prepared following the synthetic pathway depicted in Scheme 4, path A. The first step involves a Mitsunobu reaction with retention

---

[4] a) S. D. Larsen, P. A. Grieco *J. Am. Chem. Soc.* **1985**, *107*, 1769-1771. b) A. M. Bowser, J. S. Madalengoita, *Org. Lett.* **2004**, *6*, 309-3412.

[5] F. I. Carroll, P. Abraham, S. Chemburkar, X.-C. He, S. W. Mascarella, Y. W. Kwon, D. J. Triggle *J. Med. Chem.* **1992**, *35* 2184-2191.

of configuration giving rise to the *(+/-)-exo*-**17** in 72% yield.[4,6] The Mitsunobu reaction usually proceeds with inversion at the carbon atom of the reacting secondary alcohol. This inversion occurs in the final step of the reaction when the reacting nucleophile (in our case the imide nitrogen atom) attacks the key reactive intermediate oxyphosphonium ion, Scheme 5a.
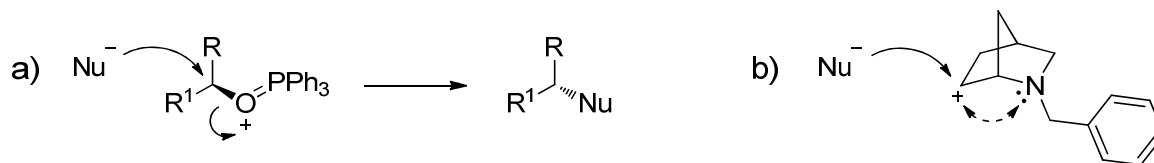
Scheme 5

However, as described by several authors the reaction can occur with complete racemization of the stereocenter through a mechanism involving a carbocationic intermediate instead of an oxyphosphonium ion. Moreover, the intramolecular stabilization of a real or incipient carbocation can influence the stereochemical outcome of the reaction. Probably, in our reaction, the formation of an incipient carbocation at C-6, stabilized by the adjacent nitrogen atom, is responsible for the formation of the observed product with retention of configuration, Scheme 5b.[4,5] The free amino group was finally obtained via phtalimide cleavage with hydrazine to give the desired (+/-)-e*xo*-**18** in 94% yield.

The adopted synthetic strategy to obtain the *endo-TYPE III* scaffold **22** is depicted in Scheme 4, path B. Starting from intermediate **16** one-pot nitrogen protecting group exchange from benzyl group to *Boc* group afforded the (+/-)-*exo*-compound **19** in 87% overall yield.[7] Then the hydroxyl group was converted to the corresponding ketone **20** in 94% yield by Swern oxidation. Finally, reductive amination with benzylamine in the presence of sodium triacetoxyhydroborate gave the derivative *(+/-)-endo*-**21** in 94% yield with excellent selectivity.[8] Reductive cleavage of the benzyl group with hydrogen (1 atm) and Pd/C afforded the final e*ndo*-compound **22** in 83% yield as *(+/-)-*racemic mixture.

Performing the synthesis of compounds **18** and **22** the appropriate choice of the protecting groups at the endocyclic nitrogen atoms is of outstanding importance in several steps. For instance, the regioselectivity in the oxidative hydroboration reaction is almost complete only using a benzyl residue as protecting group, changing from benzyl to *tert*-butoxy carbonyl group resulted in the isolation of 1:1 mixture of the two possible regioisomers. Moreover, the benzyl group is essential in the Mitsunobu reaction providing the correct electronic properties to the nitrogen atom stabilizing the incipient carbocation at C-6. On the other hand, for the synthesis of **22** starting from **16**, the presence of a benzyl group on *N*-1 would give, after Swern oxidation ad reductive amination with benzylamine (the better reactant for this reaction), an intermediate with the same protecting group at both nitrogens. On the contrary, mismatched substitution at the two nitrogen atoms is necessary to achieve selective deprotection to compound **22** for the subsequent

[6] C. F. Palmer, K. P. Parry, S. M. Roberts, V. Sik *J. Chem. Soc., Perkin Trans. 1* **1991**, 2051-2052.
[7] C. H. Mitch, S. J. Quimby, J. K. Reel, C. A. Whitesitt. Eli Lilly Co. WO1997040016 A1.
[8] J. W. Lampe, P. S. Watson, D. J. Slade US 20110144150 A1.

functionalization. For these reasons a protecting group exchange was realized as first step for the synthesis of **22** starting from **16**.

The structures of the obtained compounds were assigned on the basis of combined 1D (^{1}H NMR, ^{13}C NMR) and 2D NMR (COSY, HSQC, NOESY) experiments. In particular, the analysis of 1D and 2D experiments allowed for the complete assignment of proton and carbon chemical shifts and coupling constants. The *endo/exo* stereochemistry at carbon 2 was assigned on the basis of coupling constant values and NOE interactions. For illustration, for compounds **18** and **22** diagnostic NOE interactions and relevant coupling constant values are reported in Figure 14.
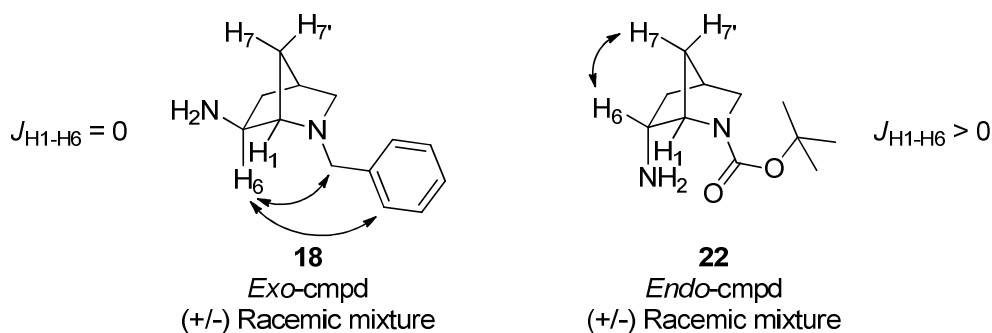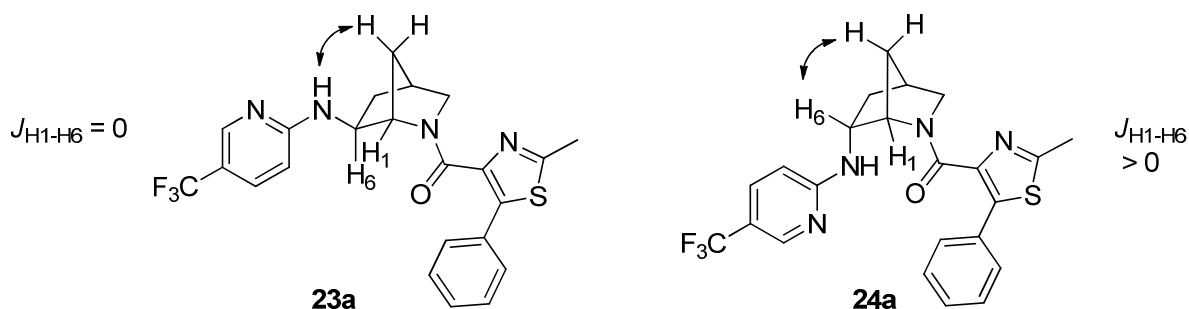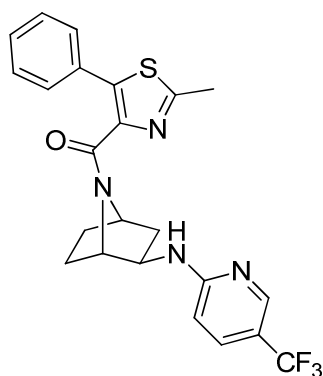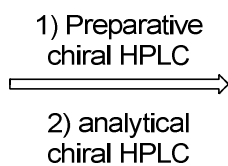

Figure 14

As already reported, the coupling constant between H-1 and H-6 is different from zero only in the *endo* compound **22**. Moreover, NOE interactions between H-6 and both benzylic and aromatic protons in **18** and between H-6 and H-7 in **22** allows for the discrimination of the two diastereoisomers.

2.1.5 Functionalization of TYPE III scaffold (2-azabicyclo[2.2.1]heptan-6-amine)

The functionalization of both nitrogen atoms of compounds **18** and **22** with aromatic and/or heteroaromatic rings was performed following the same template approach reported for *TYPE II* scaffolds, Figure 15. However in this case we prepared only two derivatives (**23a-b**) of the *exo*-**18** compound and five derivatives (**24a-e**) of the *endo*-**22** which would be the most active stereoisomer on the basis of computational studies performed in parallel with the synthetic work (see Chapter 3).
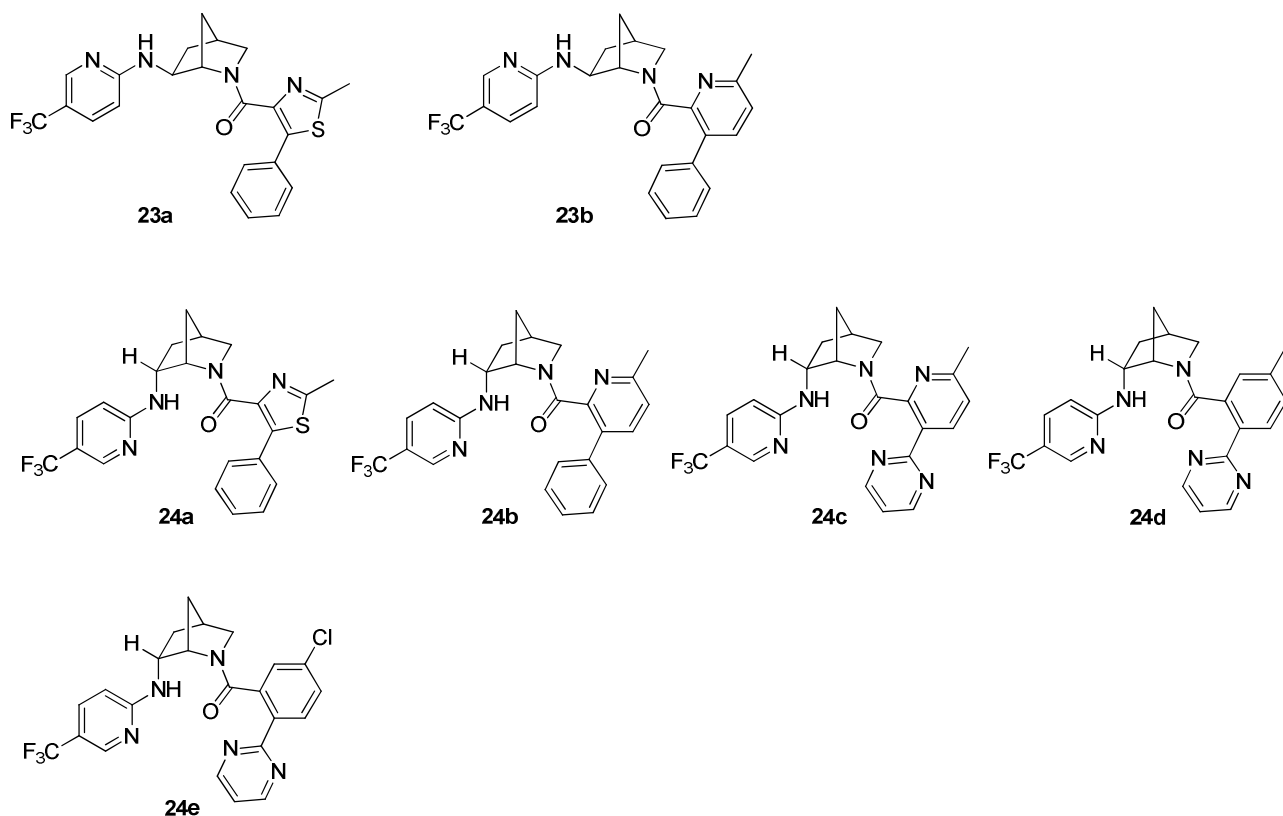
Figure 15

The synthetic pathways employed to obtain compounds **23a-b** and **24a-e** are summarized in Scheme 6 and parallel those reported for compounds **9** and **12**.
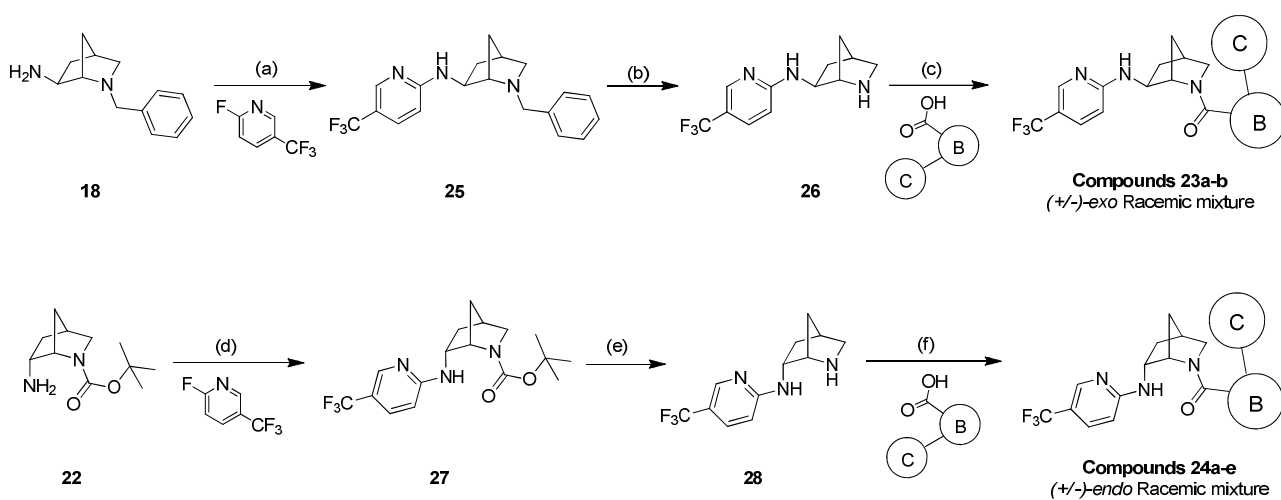
Reactants and conditions: (a) 2-fluoro-5-(trifluoromethyl)pyridine, K₂CO₃, DMF dry, 100°C, 75%; (b) Pd-C/H₂ 5 psi, EtOH, Rt, 89%; (c) **C-B-COOH,** 2-chloro-4,6-dimethoxy-1,3,5-triazine, *N*-methylmorpholine, Rt then 100°C, 65-76% ; (d) 2-fluoro-5-(trifluoromethyl)pyridine, K₂CO₃, DMF dry, 100°C, 88%; (e) DCM/TFA 4:1, Rt, quant; (f) **C-B-COOH,** 2-chloro-4,6-dimethoxy-1,3,5-triazine, *N*-methylmorpholine, Rt then 100°C, 34-79%.

Scheme 6

The structures of the obtained compounds were assigned on the basis of combined 1D (^{1}H NMR, ^{13}C NMR) and 2D-NMR (COSY, HSQC, NOESY) experiments. The ^{1}H NMR analysis of compounds **23** and **24** reveals the existence of two rotamers for both series of compounds, in 7:3 ratio for **23** and in ratios ranging from 97:3 to 80:20 for **24**. In particular, the analysis of 1D and 2D experiments allowed for the complete assignment of proton and carbon chemical shifts and coupling constants. The *endo/exo* stereochemistry at carbon 2 was assigned on the basis of coupling constant values and nOe interactions. For illustration, for compounds **23a** and **24a** diagnostic NOE interactions and relevant coupling constant values are reported in Figure 16.

Figure 16

2.1.6 Preparative chiral HPLC separation

After biological evaluation assays (see Chapter 4) the most active compounds resulted to pertain, respectively, to the *exo-TYPE II* and *endo-TYPE III* series. In particular, in the first series compound **12a** and in the second series compound **24b** resulted to be the best candidates and were subjected to chiral preparative HPLC separation in order to evaluate the activity of the two enantiomers, Figure 14. The preparative chromatography was performed for both **12a** and **24b** on a Chiralpak ADH column (25x2cm, 5µm), eluent heptane (10%) and ethanol (90%) added with dihethylamine (0.1%), flow rate 10 mL/min. The collected fractions were analyzed by chiral analytical HPLC on a ADH column (250x4.6mm, 5µm), eluent heptane (10%) and ethanol (90%) added with dihethylamine (0.1%), flow rate 5 mL/min, giving rise to the result summarized in Figure 17.
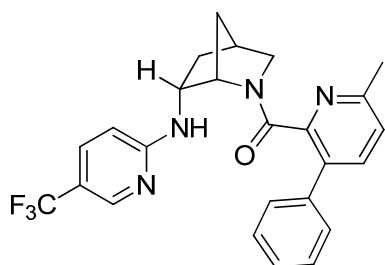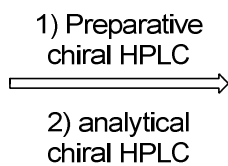
12e
(+/-)-exo Racemic Mixture

1) Preparative
chiral HPLC

2) analytical
chiral HPLC

Compound 12e/E1
rt 11.5', optical purity 100%
[α]$_D$ = + 49.4

Compound 12e/E2
rt 13.3', optical purity 98.6%
[α]$_D$ = - 47.6

24b
(+/-)-endo Racemic Mixture

1) Preparative
chiral HPLC

2) analytical
chiral HPLC

Compound 24b/E1
rt 7.5', optical purity 100%
[α]$_D$ = - 98.6

Compound 24b/E2
rt 11.4', optical purity 97.3%
[α]$_D$ = + 96.3

Figure 17

38

2.2 General Methods

All the reactions, that involve the use of reagents sensitive to oxygen or hydrolysis, were carried out under inert atmosphere. The glassware was previously dried in an oven at 110 °C and set with cycles of vacuum and nitrogen. Also syringes, used to transfer reagents and solvents, were previously set under nitrogen atmosphere.

When the purity of the obtained product is not indicated means purity >95% (purity determined by 1HNMR and UPLC-Uv detector).

The aromatic and/or heteroaromatic substituents (moieties A and B-C) not commercially available employed for the *TYPE II* and *TYPE III* scaffolds functionalization are all note in literature. Their synthesis and characterization are not reported.

Reagents and solvents

Unless otherwise state reagents, solvents and dry solvents were purchased from commercial suppliers and used as received.

Chromatography/purification of compounds

The chromatographic column separations were conducted by automated flash technique, using Isolera-One Biotage apparatus with Bitage HP-SI or KP-NH columns for direct phase separation or RediSep Rf Gold AqC18 columns for reverse phase separations.

For the basic compounds extraction was employed Biotage ISOLUTE SCX columns.

For thin-layer chromatography (TLC), Biotage KP-SIL TLC plates or KP-NH TLC Plates were employed and the detection was performed by irradiation with UV light (λ = 254 nm), by basic solution of KMnO4 (3.0 g $KMnO_4$, 20.0 g K_2CO_3 and 0.3 g KOH in 300 mL of H_2O), ninhydrin, Pancaldi solution or with iodine vapours.

NMR spectroscopy

^{1}H NMR analyses were performed with a Varian-Gemini 200 or with Bruker 300, 400 or 500 Avance spectrometers at room temperature, respectively at 200, 300, 400 or 500 MHz. The coupling constants (*J*) are expressed in Hertz (Hz), the chemical shifts (δ) in ppm. The multiplicities of the proton spectra were described by the following abbreviations: s (singlet), d (doublet), t (triplet), q (quartet), m (multiplet), dd (double doublet), dq (double quartet), dt (double triplet), td (triple doublet), ddd (double double doublet).

^{13}C NMR analyses were performed with the same instruments at 50.3, 75.45, 100 and 125.75 MHz; APT sequences were used to distinguish the methine and methyl carbon signals from those arising

from methylene and quaternary carbon atoms. DEPT sequences were adopted for the same purpose.

Mass spectrometry

Low resolution MS spectra were recorded by an Acquity UPLC – Waters appartus with ESI source, with automated sampling system. The values are expressed as mass-charge ratio and the relative intensities of the most significant peaks are shown in brackets.

HPLC analysis

The HPLC analysis and the chiral resolution of selected compounds were performed with an Agilent 1200 HPLC and a Shimadzu LC8A assembled HPLC.

Polarimetry

Perkin Elmer 342 plus was employed for the analysis of optically active compounds.

Abbreviations

Ac	Acetyl
AcOEt	Ethyl Acetate
Alk	Alkyl
APT	Attached Proton Test
Ar	Aryl
Boc	*t*-Butyloxycarbonyl
brs	Broad signal
Bu	Butyl
°C	Celsius degree
CDMT	2-chloro-4,6-dimethoxy-1,3,5-triazine
COSY	Correlation spectrometry
cm	Centimetre
Cy	Cyclohexyl
CyHex	Cyclohexane
δ	Chemical shift
d	Doublet
DA	Diels-Alder
dd	Double doublet
d.e.	Diastereomeric excess
DEPT	Distortionless Enhancement by Polarization Transfer
ddd	Double double doublet
DME	1,2-Dimethoxyethan
DCM	Dichloromethane
DMF	Dimethylformamide
dt	Double triplet
ED	Electron-donating
EI	Electron collision ionization

eq   Equivalents
ESI   Electronspray ionization
Et   Ethyl
eV   Electronvolt
EW   Electron-withdrawing
g   Gram
h   hours
Hex   Hexyl
HP-SI   High performance silica gel
Hz   Hertz
IR   Infrared spectrometry
i-Pr   *iso*-Propyl
J   Coupling constant
L   Ligand
LA   Lewis Acid
m   Multiplet
m-   meta
M   Molar
[M+]   Molecular ion peak
Me   Methyl
MeOH   Methanol
mg   Milligram
MHz   Megahertz
min   Minutes
mL   Millilitre
mmol   Millimol
m.p.   Melting point
MS   Mass spectrometry
m/z   Mass / Load
NMM   N-methylmorpholine
N   Normal
NMR   Nuclear magnetic resonance
NOE(SY)   Nuclear Overhauser Effect
o-   ortho
p-   para
Pent   Pentyl
Ph   Phenyl
PMB   *p*-methoxybenzyl
ppm   parts per million
PPTS   Pyridinium *p*-toluensulphonate
Pr   Propyl
Py   Pyridine
p-Tol   *p*-Tolyl
q   Quartet
rt   room temperature
s   Singlet
sat. sol.   Saturated solution
SI   Silica gel

T	Temperature
t	Triplet
t	Time
td	Triple doublet
tert	tertiary
t-Bu	*tert*-Butyl
THF	Tetrahydrofuran
TFA	Trifluoroacetic acid
TLC	Thin layer chromatography
Wt	Weight

2.3 Synthesis of (+/-)-endo- and (+/-)-exo-7-azabicyclo[2.2.1]heptan-2-amine (5 and 8), experimental data

(+/-)-7-*tert*-butyl 2-methyl 3-bromo-7-azabicyclo[2.2.1]hepta-2,5-diene-2,7-dicarboxylate (1)
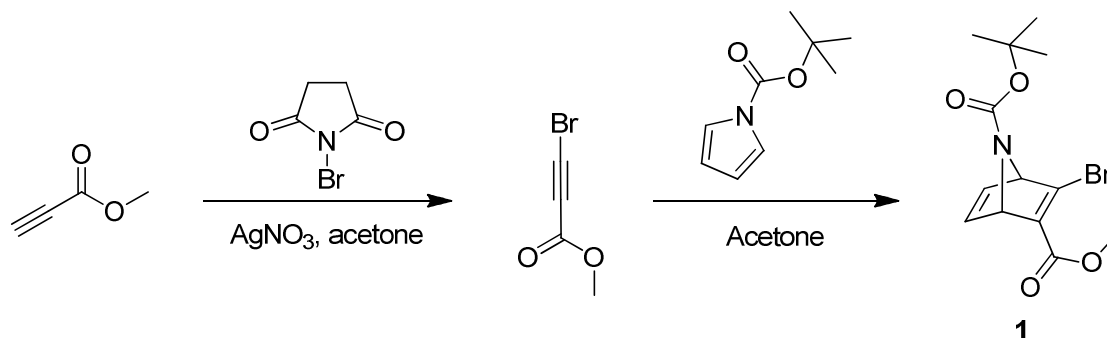
Step 1: To a stirred solution of methyl propiolate (7.57 mL, 85 mmol) in acetone (50 mL), cooled at 0°C, silver nitrate (1.445 g, 8.50 mmol) and then NBS (18.16 g, 102 mmol) were added. The reaction mixture was stirred at 0 °C for 10 min and then at room temperature for 1 h. The reaction was monitored by ^{1}HNMR analysis (the disappearance of the acetylenic proton was checked, 2.70 δ in CDCl$_3$). The sample was filtered before the NMR analysis.

Then the reaction mixture was filtered over a celite pad, washing with acetone (20 mL), and the filtrate was concentered under reduced pressure at room temperature to obtain a final concentration of about 15% Wt (70 mL).

The final concentration of the solution was determined *via* [1]H MNR analysis.

Methyl 3-bromopropiolate= 28.58% Wt, 13.33%mol.

Grams of the solution = 48.83 g.

Grams of methyl 3-bromopropiolate= 13.96 g (theoretical amount = 13.85 g).

^{1}H NMR (400 MHz, CDCl$_3$) δ = 3.71 (s, 3 H).

Step 2: To the previously obtained solution of methyl 3-bromopropiolate, *tert*-butyl pyrrol-1-carboxylate (30 mL, 179 mmol) was added. The reaction mixture was stirred at 90 °C, under N$_2$ atmosphere, for 24 h. The reaction was monitored by SI-TLC (CyHex/AcOEt 8:2; I$_2$ as resolving agent). Then the reaction mixture was concentrated under reduced pressure and loaded on a silica gel column for purification.

Purification: Isolera-One Biotage, Snap 340g HP-SI Column, sample dissolved in CyHex, eluent: from CyHex/AcOEt 100:0 to 80:20 in gradient.

The containing product fractions were collected and the solvent eliminated under reduced pressure to give **1** as yellow oil (4.31 g, purity 90%, 11.75 mmol, 13.8%).

ANALYSIS
Formula: C$_{13}$H$_{16}$BrNO$_4$
Mol. Weight: 330.17 g/mol

¹H NMR (400 MHz, CDCl₃) δ = 7.15 (brs, 2 H); 5.51 (brs, 1 H); 5.16 (brs., 1 H); 3.82 (s, 3 H); 1.44 (s, 9 H).

MS (ESI+) m/z (%) = 276 (100) [M-56H]⁺.

(+/-)-*endo*/(+/-)-*exo*-7-*tert*-butyl 2-methyl 7-azabicyclo[2.2.1]heptane-2,7-dicarboxylate (2)

1   **2**
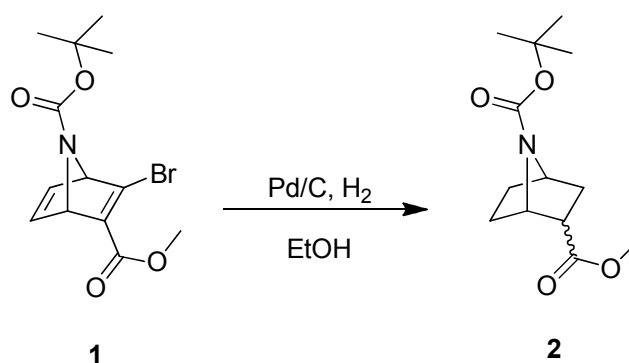
Palladium 10% on activated carbon (1.354 g, 1.272 mmol) was suspended in water (2 mL) and EtOH (10 mL). This mixture was added to a solution of compound **1** (4.20 g, 12.72 mmol) and TEA (3.55 mL, 25.4 mmol) in EtOH (40 mL). The reaction was performed in a hydrogenation apparatus. The reaction mixture was subject to four N_2/vacuum cycles and then to four H_2/vacuum cycles. Then the mixture was stirred at room temperature under H_2 atmosphere (1.1 atm) for 16 h.

Then the reaction mixture was filtered through a Celite pad (2 cm height; 9.5 cm diameter) washing with EtOH/MeOH 9:1 (150 mL). The filtrate was concentrated under reduced pressure to give a white solid. The obtained solid was taken up in DCM (50 mL) and the organic layer was washed with water (2x50 mL), dried over anhydrous Na_2SO_4, filtered and the solvent eliminated under reduced pressure. Compound **2** was isolated as yellow oil (3.07 g, 12.02 mmol, 95%)

ANALYSIS

Note: Compound **2** was isolated as (+/-)-*endo*/(+/-)-*exo* mixture of diastereoisomers in about 88:12 ratio from ^{1}H NMR analysis. Chemical shifts of the major diasteoisomer are reported.

Formula: $C_{13}H_{21}NO_4$

Mol. Weight: 255.31 g/mol

^{1}H NMR (400 MHz, CDCl₃) (*endo* diastereoisomer) δ = 4.41 (t, *J*=4.4 Hz, 1 H); 4.23 (t, *J*=4.4 Hz, 1 H); 3.72 (s, 3 H); 3.02 - 3.11 (m, 1 H); 1.93 - 2.05 (m, 1 H); 1.84 - 1.93 (m, 1 H); 1.77 - 1.84 (m, 1 H); 1.66 - 1.77 (m, 1 H); 1.48 - 1.52 (m, 2 H); 1.47 (s, 9 H).

MS (ESI+) m/z (%) = 199 (100%) [M-56H]⁺.

(+/-)-endo/exo-7-(tert-butoxycarbonyl)-7-azabicyclo[2.2.1]heptane-2-carboxylic acid (3)

2   **3**
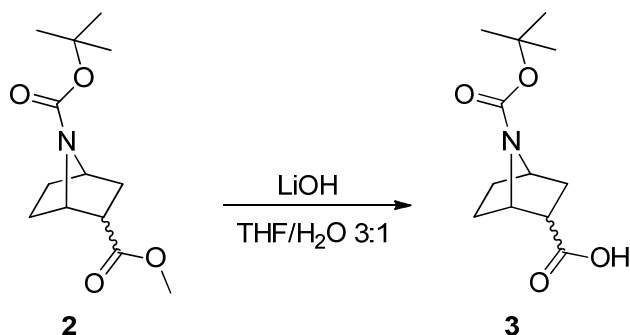
To a stirred solution of compound **2** (1.695 g, 6.64 mmol) in THF/water (33 mL, 3:1), cooled at 0 °C, a solution of lithium hydroxide in water (0.352 g, 8.39 mmol) was added. The mixture was stirred at room temperature for 17 h.

Then the solvent was evaporated under reduced pressure and the residue taken up in water (10 mL) and the pH adjusted to a value of 2 with HCl 2N (4.5 mL) . The aqueous phase was then extracted with AcOEt (3x50 mL) and the combined organic layers were dried over anhydrous Na_2SO_4, filtered and the solvent eliminated under reduced pressure to give **3** as an amber oil (1.616 g, 6.70 mmol, quantitative).

ANALYSIS

Note: Compound **3** was isolated as *endo/exo* mixture in about 87:13 ratio from ^{1}H NMR analysis. Chemical shifts of the major diasteoisomer are reported.

Formula: $C_{12}H_{19}NO_4$

Mol. Weight: 241.28 g/mol

^{1}H NMR (400 MHz, CDCl$_3$) (*endo* diasteroisomer) δ = 4.47 (t, *J*=4.4 Hz, 1 H); 4.26 (t, *J*=4.6 Hz, 1 H); 3.09 - 3.17 (m, 1 H); 1.97 - 2.07 (m, 1 H); 1.72 - 1.90 (m, 3 H); 1.61 - 1.69 (m, 1 H); 1.52 (dd, *J*=11.0, 3.7 Hz, 1 H); 1.48 (s, 9 H).

MS (ESI+) m/z (%) = 185 (100%) [M-56H]$^+$.

(+/-)-*endo*-*tert*-butyl 2-(((benzyloxy)carbonyl)amino)-7-azabicyclo[2.2.1]heptane-7-carboxylate (4)
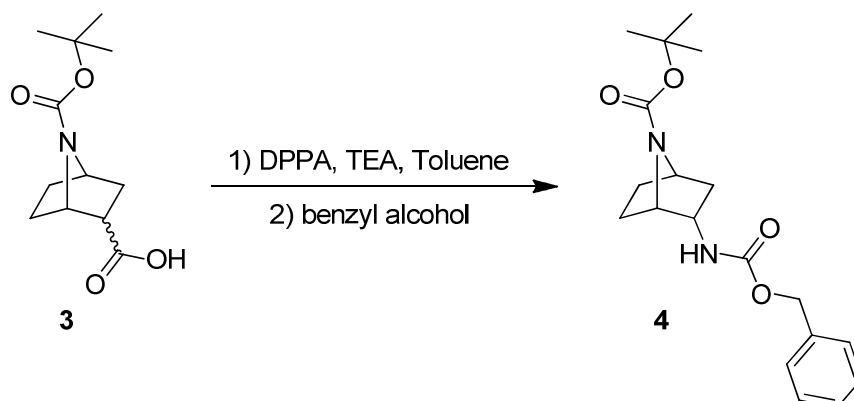
To a nitrogen flushed solution of **3** (1.60 g, 6.63 mmol) and TEA (1.1 mL, 7.89 mmol) in dry toluene (25 mL) diphenyl phosphoryl azide (1.5 mL, 7.88 mmol) was added under stirring. After complete addition, the mixture was slowly warmed to 90 °C over 30 min and then stirred at 90 °C for 1h. Then the reaction mixture was cooled at room temperature, benzyl alcohol (1.034 mL, 9.95 mmol) was added and the resulting mixture was further heated at 90 °C for 18 h.

The reaction mixture was cooled at room temperature and then extracted successively with citric acid 5% wt (2x40 mL), water (2x40 mL), NaHCO$_3$ sat. sol. (2x40 mL) and brine (2x20 mL). The organic layer was dried over anhydrous Na$_2$SO$_4$, filtered and the solvent eliminated under reduced pressure.

Purification: Isolera-One Biotage, Snap 100g HP-SI Column, sample dissolved in DCM, eluent: from CyHex/AcOEt 100:0 to 50:50 in gradient.

The containing product fractions were collected and the solvent was eliminated under reduced pressure to give **4** as white solid (2.175 g, purity 84%, 5.27 mmol, 80%).

ANALYSIS
Formula: C$_{19}$H$_{26}$N$_2$O$_4$
Mol. Weight: 346.42
Rf: Product: 0.76 (CyHex/AcOEt 5:5; SI-TLC).
^{1}H NMR (400 MHz, CDCl$_3$) δ = 7.43 - 7.30 (m, 5 H); 5.22 - 5.05 (m, 2 H); 4.82 (brs, 1 H); 4.39 (brs, 1 H); 4.20 (brs, 1 H); 4.16 - 3.99 (m, 1 H); 2.44 - 2.31 (m, 1 H); 1.89 - 1.75 (m, 2 H); 1.75 - 1.64 (m, 1 H); 1.47 (s, 9 H); 1.44 - 1.37 (m, 1 H); 0.91 (dd, J=12.7, 4.4 Hz, 1 H).
^{13}C NMR (APT) (50 MHz, CDCl$_3$) δ = 156.17 (C=O), 155.61 (C=O), 136.48 (C), 128.80 (2xCH), 128.47 (CH), 80.09 (C), 67.13 (CH$_2$), 59.11 (CH), 58.90 (CH), 51.88 (CH), 37.67 (CH$_2$), 29.92 (CH$_2$), 28.49 (3 x CH$_3$), 22.24 (CH$_2$).
MS (ESI+) m/z (%) = 347 (100%) [MH]$^+$.

(+/-)-endo-tert-butyl 2-amino-7-azabicyclo[2.2.1]heptane-7-carboxylate (5)
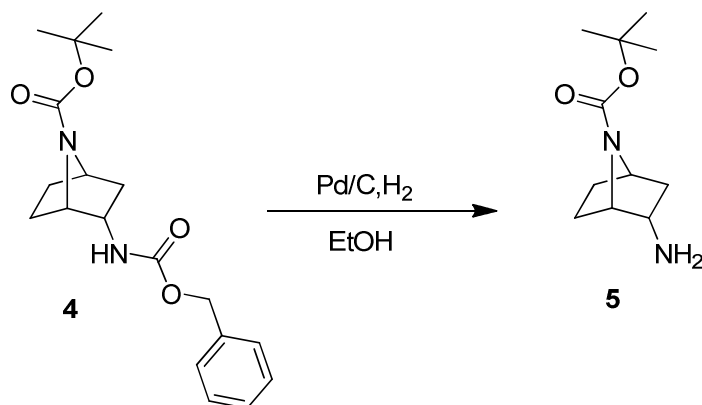
Palladium 5% on activated carbon, (0.230 g, 0.054 mmol) was suspended in EtOH (5 mL). This mixture was added to a solution of **4** (84%) (2.150 g, 5.21 mmol) in EtOH (20 mL). The reaction was conduced in a hydrogenation apparatus. The reaction mixture was subject to four H_2/vacuum cycles. Then the solution was stirred at room temperature under H_2 atmosphere (50 psi) for 16 h.

The reaction mixture was then filtered through a Celite pad washing with EtOH (30 mL) and MeOH (30 mL). The filtrate was concentrated under reduced pressure to give an oil which was purified by column chromatography.

Purification: Isolera-One Biotage, Snap 55g KP-NH Column, sample dissolved in DCM, eluent: DCM/MeOH 98:2 isocratic.

The containing product fractions were collected and the solvent was eliminated under reduced pressure to give **5** as clear oil (1.189 g, purity 90%, 5.04 mmol, 97%).

ANALYSIS

Formula: $C_{11}H_{20}N_2O_2$

Mol. Weight: 212.29 g/mol

Rf: 0.9 (DCM/MeOH 95:5; TLC KP-NH).

^{1}H NMR (400 MHz, $CDCl_3$) δ = 4.13 (brs, 1 H); 4.03 (brs, 1 H); 3.54 - 3.46 (m, 1 H); 2.31 - 2.21 (m, 1 H); 2.05 (ddd, J=12.9, 9.3, 4.4 Hz, 1 H); 1.86 - 1.75 (m, 1 H); 1.72 - 1.61 (m, 1 H); 1.53 - 1.47 (m, 4 H); 1.47 (s, 10 H); 0.84 (dd, J=12.2, 4.40 Hz, 1 H).

^{13}C NMR (APT) (50 MHz, $CDCl_3$) δ = 155.22 (C=O), 80.53 (C), 58.41 (CH), 57.28 (CH), 51.18 (CH), 35.91 (CH_2), 29.61 (CH_2), 28.45 (3 x CH_3), 22.79 (CH_2).

MS (ESI+) m/z (%) = 213 (100%) $[MH]^+$.

(+/-)-exo-7-(*tert*-butoxycarbonyl)-7-azabicyclo[2.2.1]heptane-2-carboxylic acid (6)

2 → (MeONa, MeOH) → **6**
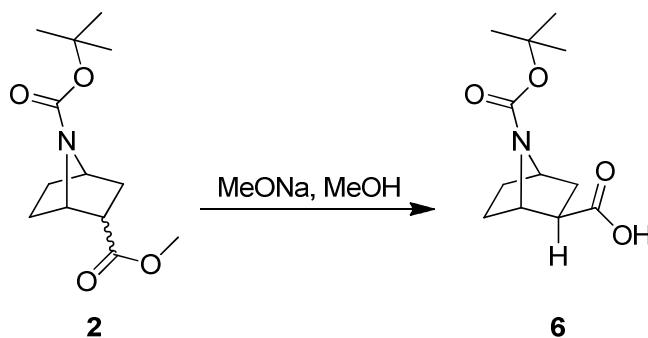
To a nitrogen flushed solution of **2** (250 mg, 0.979 mmol) in dry MeOH (5 mL) solid sodium methoxide (132 mg, 2.448 mmol) was added. The reaction mixture was stirred and heated at reflux (65 °C) for 24h. Then a second amount of sodium methoxide (397 mg, 7.34 mmol) was added and the reaction mixture was stirred at 65 °C for further 21h.

Then the mixture was cooled to room temperature, water (5 mL) was added and stirring was continued for 1h at room temperature. The mixture was concentrated in order to eliminate the MeOH and then the pH was adjusted to 4.5 with conc. HCl. The resulting precipitate was collected and dried *in vacuo*. The obtained solid was subsequently washed with Et_2O/CyHex 6:4 (10 mL) and dried *in vacuo* to afford compound **6** as off-white solid (125 mg, 0.518 mmol, 53%).

ANALYSIS

Formula: $C_{12}H_{19}NO_4$

Mol. Weight: 241.28 g/mol

^{1}H NMR (400 MHz, $CDCl_3$) δ = 4.59 (d, J=4.4 Hz, 1 H); 4.33 (t, J=4.6 Hz, 1 H); 2.62 (dd, J=9.0, 5.1 Hz, 1 H); 2.31 - 2.22 (m, 1 H); 1.92 - 1.75 (m, 2 H); 1.66 (dd, J=12.5, 9.0 Hz, 1 H); 1.56 - 1.46 (m, 2 H); 1.45 (s, 9 H).

^{13}C NMR (APT) (50 MHz, $CDCl_3$) δ = 178.23 (C=O), 155.18 (C=O), 80.22 (C), 59.50 (CH), 56.14 (CH), 47.50 (CH), 33.56 (CH_2), 29.71 (CH_2), 29.00 (CH_2), 28.39 (3 x CH_3).

MS (ESI+) m/z (%) = 186 (100%) [M-56H]$^+$.

(+/-)-exo-tert-butyl 2-(((benzyloxy)carbonyl)amino)-7-azabicyclo[2.2.1]heptane-7-carboxylate (7)

6

1) DPPA, TEA, Toluene

2) benzyl alcohol

7
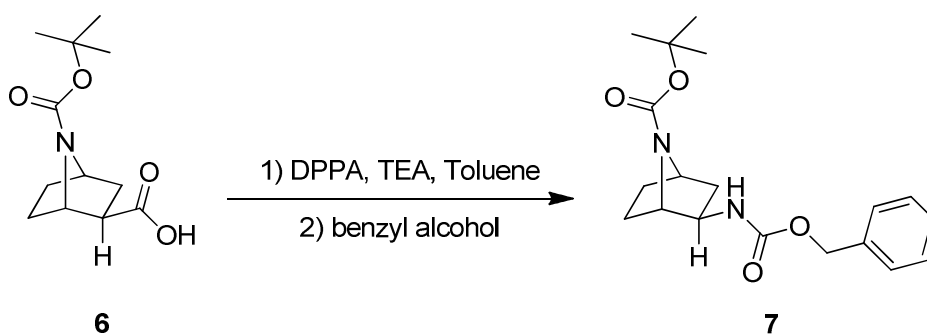
To a nitrogen flushed solution of **6** (110 mg, 0.456 mmol) and TEA (0.076 mL, 0.547 mmol) in dry toluene (2 mL) diphenyl phosphoryl azide (0.104 mL, 0.547 mmol) was added under stirring. After complete addition, the mixture was slowly warmed to 90 °C over 30 min and then stirred at 90 °C for 1h. Then the reaction mixture was cooled at room temperature, benzyl alcohol (0.071 mL, 0.684 mmol) was added and the resulting mixture was further heated at 90 °C for 18 h.

The reaction mixture was cooled at room temperature and then extracted successively with citric acid 5%Wt (2x10 mL), water (2x10 mL), NaHCO$_3$ sat. sol. (2x10 mL) and brine (2x10 mL). The organic layer was dried over anhydrous Na$_2$SO$_4$, filtered and the solvent eliminated under reduced pressure.

Purification: Isolera-One Biotage, Snap 25g HP-SI Column, sample dissolved in DCM, eluent: from CyHex/AcOEt 100: to 50:50 in gradient.

The containing product fractions were collected and the solvent was eliminated under reduced pressure to give compound **7** as colorless oil (124 mg, purity 90%, 0.322 mmol, 71%).

ANALYSIS
Formula: C$_{19}$H$_{26}$N$_2$O$_4$
Mol. Weight: 346.42 g/mol
¹H NMR (400 MHz, CDCl$_3$) δ = 7.42 - 7.30 (m, 5 H); 5.20 - 5.06 (m, 2 H); 4.99 (brs, 1 H); 4.25 (t, J=4.6 Hz, 1 H); 4.14 (d, J=4. 9 Hz, 1 H); 3.84 - 3.76 (m, 1 H); 1.96 (dd, J=13.0, 8.1 Hz, 1 H); 1.85 - 1.65 (m, 2 H); 1.56 - 1.49 (m, 1 H); 1.45 (s, 9 H); 1.43 - 1.31 (m, 2 H).
¹³C NMR (APT) (100 MHz, CDCl$_3$) δ = 156.14 (C=O), 155.56 (C=O), 136.48 (C), 128.50 (2xCH), 128.09 (CH), 80.00 (C), 66.66 (CH$_2$), 61.59 (CH), 55.61 (CH), 54.67 (CH), 40.27 (CH$_2$), 28.33 (CH$_2$), 28.23 (3 x CH$_3$), 25.82 (CH$_2$).
MS (ESI+) m/z (%) = 347 (100%) [MH]$^+$.

(+/-)-exo-tert-butyl 2-amino-7-azabicyclo[2.2.1]heptane-7-carboxylate (8)
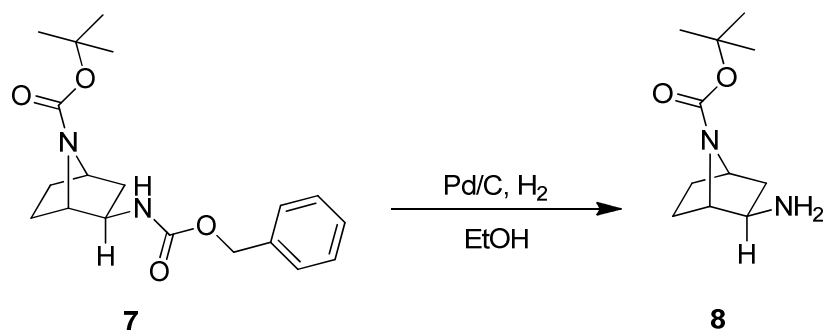
Palladium 5% on activated carbon (59.6 mg, 0.014 mmol) was suspended in EtOH (0.5 mL). This mixture was added to a solution of **7** (97 mg, 0.280 mmol) in EtOH (5 mL). The reaction was performed in a hydrogenation apparatus. The reaction mixture was subject to four H_2/vacum cycles and then stirred at room temperature under H_2 atmosphere (1.1 atm) for 16 h.

The reaction mixture was then filtered through a Celite pad washing with EtOH (10 mL) and MeOH (10 mL). The filtrate was concentrated under reduced pressure to give an oil which was purified by column chromatography.

Purification: Isolera-One Biotage, Snap 11g KP-NH Column, sample dissolved in DCM, eluent: DCM/MeOH 98:2 isocratic.

The containing product fractions were collected and the solvent was eliminated under reduced pressure to give **8** as a clear oil that solidify on standing to give a white solid (48 mg, purity 95%, 0.214 mmol, 76%).

ANALYSIS
Formula: $C_{11}H_{20}N_2O_2$
Mol. Weight: 212.29 g/mol
^{1}H NMR (400 MHz, CDCl$_3$) δ = 4.22 (brs, 1 H); 3.90 (brs, 1 H); 2.98 (dd, J=7.6, 3.2 Hz, 1 H); 1.83 (dd, J=12.7, 7.8 Hz, 1 H); 1.79 - 1.60 (m, 2 H); 1.48 (s, 9 H); 1.41 - 1.26 (m, 3 H).
^{13}C NMR (DEPT) (100 MHz, CDCl$_3$) δ = 156.49 (C=O), 79.59 (C), 64.43 (CH), 55.74 (CH), 55.46 (CH), 41.90 (CH$_2$), 28.31 (3 x CH$_3$), 28.22 (CH$_2$), 25.90 (CH$_2$).
MS (ESI+) m/z (%) = 213 (100%) [MH]$^+$.

2.4 Synthesis of endo-TYPE II derivatives 9a-k, experimental data

(+/-)-endo-tert-butyl 2-((5-(trifluoromethyl)pyridin-2-yl)amino)-7-azabicyclo[2.2.1]heptane-7-carboxylate (10a)
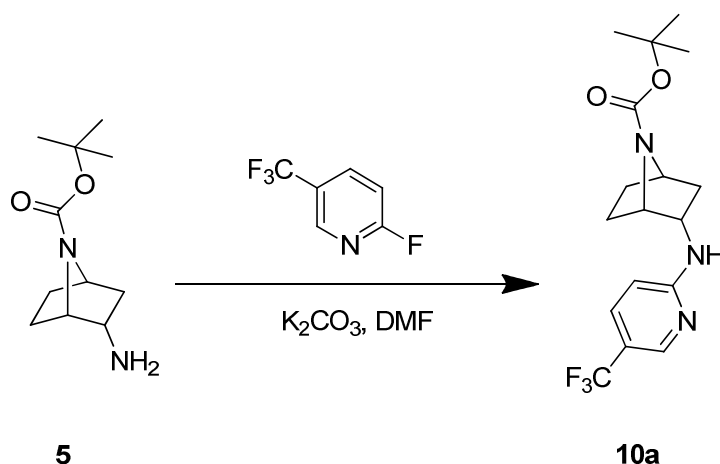
A mixture of **5** (100.6 mg, 0.474 mmol), 2-fluoro-5-(trifluoromethyl)pyridine (0.070 mL, 0.580 mmol) and K_2CO_3 (132.5 mg, 0.959 mmol) in DMF (1 mL) was stirred under N_2 atmosphere for 10 min. The reaction was then performed under microwave heating: 3 cycles at 100 °C for 20 min.

Then the solvent was evaporated under reduced pressure and the residue was taken up in $NaHCO_3$ sat. sol. (10 mL) and the mixture extracted with AcOEt (3x10 mL). The organic layers were collected, washed with water (30 mL), dried over anhydrous Na_2SO_4 and filtered. Then the solvent was evaporated under reduced pressure.

Purification: Isolera-One Biotage, Snap 10g HP-SI Column, sample dissolved in DCM, eluent: from CyHex 100% to CyHex/AcOEt 75:25 in gradient.

The containing product fractions were collected and the solvent was evaporated under reduced pressure to give **10a** as white solid (84.5 mg, purity 95%, 0.23 mmol, 47%).

ANALYSIS
Formula: $C_{17}H_{22}F_3N_3O_2$
Mol. Weight: 357.37 g/mol
Rf: 0.67 (CyHex/AcOEt 5:5; SI-TLC)
¹H NMR (400 MHz, CDCl₃) δ = 8.36 (s, 1 H); 7.65 (dd, J=8.8, 2.4 Hz, 1 H); 6.50 (d, J=8.8 Hz, 1 H); 5.16 (brs, 1 H); 4.49 (brs, 1 H); 4.25 (brs, 1 H); 4.17 - 4.07 (m, 1 H); 2.55 - 2.45 (m, 1 H); 1.92 - 1.81 (m, 2 H); 1.75 - 1.63 (m, 1 H); 1.56 - 1.51 (m, 1 H); 1.50 (s, 9 H); 1.05 (dd, J=12.7, 4.4 Hz, 1 H).
¹³C NMR (APT) (50 MHz, CDCl₃) δ = 160.13 (C=O), 155.75 (C), 146.39 (q, J = 4.4 Hz, CH), 134.91 (q, J = 3.2 Hz, CH), 124.67 (q, J = 270.3 Hz, CF₃), 116.38 (q, J = 33.0 Hz, C), 106.04 (CH), 80.19 (C), 58.52 (CH), 56.83 (CH), 52.94 (CH), 38.49 (CH₂), 30.20 (CH₂), 28.50 (3 x CH₃), 22.06 (CH₂).
MS (ESI+) m/z (%) = 358 (100) [MH]⁺.

(+/-)-endo-tert-butyl 2-((6,7-difluoroquinoxalin-2-yl)amino)-7-azabicyclo[2.2.1]heptane-7-carboxylate (10b)
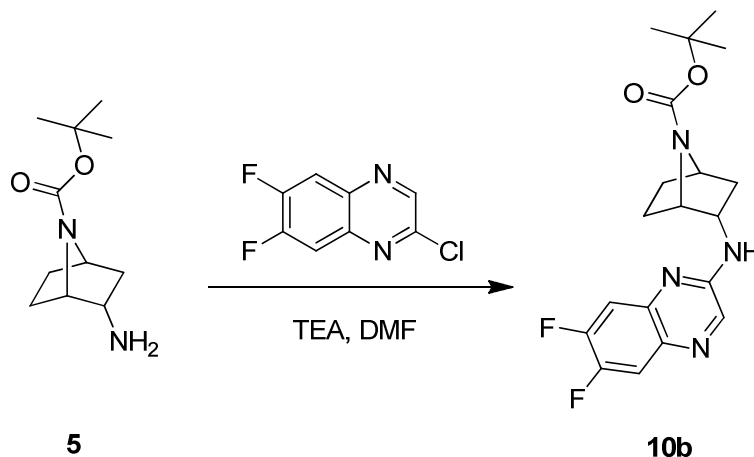
A mixture of **5** (100 mg, 0.471 mmol), 2-chloro-6,7-difluoroquinoxaline (97 mg, 0.485 mmol) and TEA (0.200 mL, 1.435 mmol) in DMF (1 mL) was stirred under N$_2$ atmosphere for 10 min. The reaction was then performed initiallt under microwave heating: 3 cycles at 75 °C for 1 h.

To promote the complete conversion of starting **5** further 2-chloro-6,7-difluoroquinoxaline (20 mg, 0.100 mmol) and TEA (0.050 mL, 0.359 mmol) were added. The reaction mixture was subjected to a further mw cycle at 75°C for 1 h.

The reaction mixture was subsequently further heated at 75 °C for 18h (thermal reaction).

Then the solvent was evaporated under reduced pressure and the residue taken up in NaHCO$_3$ sat. sol. (10 mL) and the mixture extracted with AcOEt (3x20 mL). The organic layers were collected, washed with water (50 mL), dried over anhydrous Na$_2$SO$_4$ and filtered. Then the solvent was evaporated under reduced pressure.

Purification: Isolera-One Biotage, Snap 25g HP-SI Column, sample dissolved in DCM, eluent: from DCM 100% to DCM/AcOEt 8:2 in gradient.

The containing product fractions were collected and the solvent was evaporated under reduced pressure to give **10b** as yellow solid (107.5 mg, 0.27 mmol, 61%).

ANALYSIS
Formula: C$_{19}$H$_{22}$F$_2$N$_4$O$_2$
Mol. Weight: 376.40 g/mol
Rf: 0.25 (DCM/AcOEt 8:2; SI-TLC)
^{1}H NMR (400 MHz, CDCl$_3$) δ = 8.22 (s, 1 H); 7.65 (dd, J=10.3, 8.2 Hz, 1 H); 7.46 (dd, J=11.2, 7.8 Hz, 1 H); 5.09 (brs, 1 H); 4.70 (brs, 1 H); 4.44 - 4.35 (m, 1 H); 4.29 (brs, 1 H); 2.61 - 2.48 (m, 1 H); 1.95 - 1.81 (m, 2 H); 1.77 - 1.66 (m, 1 H); 1.65 - 1.47 (m, 10 H); 1.09 (dd, J=12.5, 4.6 Hz, 1 H).
^{13}C NMR (APT) (50 MHz, CDCl$_3$) δ 155.79 (C=O), 152.64 (dd, J=253.4, 15.4, CF), 151,66 (C), 148.84 (dd, J=248.6, 15.6), 138.12 (d, J=3.8, CH), 133.38 (d, J=10, C), 115.13 (dd, J=17.3, 2.1, CH), 112.70 (d, J=17.5, CH), 80.22 (C), 58.73 (CH), 56.78 (CH), 52.49 (CH), 38.27 (CH$_2$), 30.20 (CH$_2$), 28.54 (3 x CH$_3$), 22.20 (CH$_2$).

MS (ESI+) m/z (%) = 377 (100) [MH]$^+$.

(+/-)-endo-tert-butyl 2-((4-(trifluoromethyl)pyridin-2-yl)amino)-7-azabicyclo[2.2.1]heptane-7-carboxylate (10c)
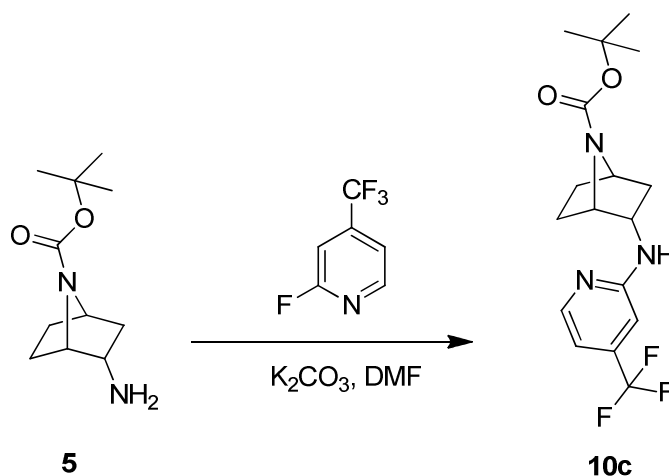
A mixture of **5** (100 mg, 0.471 mmol), 2-fluoro-4-trifluoromethyl-pyridine (93 mg, 0.565 mmol) and K_2CO_3 (130 mg, 0.942 mmol) in DMF (1 mL) was stirred under N_2 atmosphere for 10 min. The reaction mixture was heated at 100 °C for 22 h.

Then the solvent was evaporated under reduced pressure and the residue taken up in $NaHCO_3$ sat. sol. (10 mL) and the mixture extracted with AcOEt (3x20 mL). The organic layers were collected, washed with water (50 mL), dried over anhydrous Na_2SO_4 and filtered. Then the solvent was evaporated under reduced pressure.

Purification: Isolera-One Biotage, Snap 25g HP-SI Column, sample dissolved in DCM, eluent: from DCM 100% to DCM/AcOEt 8:2 in gradient.

The containing product fractions were collected and the solvent was evaporated under reduced pressure to give **10c** as white solid (114 mg, 0.32 mmol, 68%).

ANALYSIS
Formula: $C_{17}H_{22}F_3N_3O_2$
Mol. Weight: 357.37 g/mol
Rf: 0.65 (DCM/AcOEt 8:2; SI-TLC)
^{1}H NMR (400 MHz, CDCl$_3$) δ = 8.24 (d, J=5.4 Hz, 1 H); 6.81 (dd, J=5.4, 1.0 Hz, 1 H); 6.62 (s, 1 H) 4.96 (d, J=5.4 Hz, 1 H); 4.50 (brs, 1 H); 4.28 - 4.19 (m, 1 H); 4.16 - 4.07 (m, 1 H); 2.56 - 2.46 (m, 1 H); 1.94 - 1.81 (m, 2 H); 1.74 - 1.64 (m, 1 H); 1.57 - 1.46 (m, 10 H); 1.04 (dd, J=12.5, 4.6 Hz, 1 H).
^{13}C NMR (APT) (50 MHz, CDCl$_3$) δ = 158.68 (C=O), 155.75 (C), 149.75 (CH), 140.12 (q, J=33.4 Hz, C), 123.18 (q, J=273.1 Hz, CF$_3$), 108.88 (q, J=3.3 Hz, CH), 102.59 (q, J=4.1 Hz, CH), 80.15 (C), 58.57 (CH), 56.82 (CH), 53.02 (CH), 38.51 (CH$_2$), 30.21 (CH$_2$), 28.49 (3 x CH$_3$), 22.07 (CH$_2$).
MS (ESI+) m/z (%) = 358 (100) [MH]$^+$.

(+/-)-*endo*-*tert*-butyl 2-((5-(trifluoromethyl)pyrazin-2-yl)amino)-7-azabicyclo[2.2.1]heptane-7-carboxylate (10d)
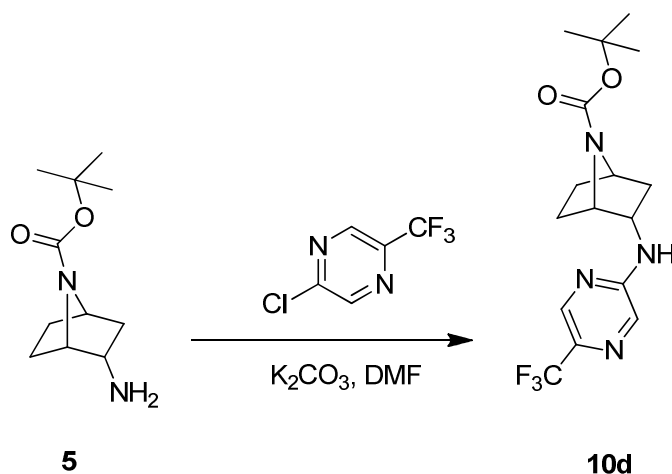
A mixture of **5** (100 mg, 0.471 mmol), 2-chloro-5-(trifluoromethyl)pyrazine (103 mg, 0.565 mmol) and K_2CO_3 (130 mg, 0.942 mmol) in DMF (1 mL) was stirred under N_2 atmosphere for 10 min. The reaction mixture was heated at 100 °C for 4 h, then 75 °C for 14 h.

Then the solvent was evaporated under reduced pressure and the residue taken up in $NaHCO_3$ sat. sol. (10 mL) and the mixture extracted with AcOEt (3x20 mL). The organic layers were collected, washed with water (50 mL), dried over anhydrous Na_2SO_4 and filtered. Then the solvent was evaporated under reduced pressure.

Purification: Isolera-One Biotage, Snap 25g HP-SI Column, sample dissolved in DCM, eluent: from DCM 100% to DCM/AcOEt 8:2 in gradient.

The containing product fractions were collected and the solvent was evaporated under reduced pressure to give **10d** as yellow solid (79 mg, purity 95%, 0.21 mmol, 44.5%).

ANALYSIS
Formula: $C_{16}H_{21}F_3N_4O_2$
Mol. Weight: 358.36 g/mol
Rf: 0.48 (DCM/AcOEt 8:2; SI-TLC)
¹H NMR (400 MHz, CDCl₃) δ = 8.38 (s, 1 H); 7.98 (s, 1 H); 5.16 (d, J=4.9 Hz, 1 H); 4.55 (brs, 1 H); 4.33 - 4.21 (m, 2 H); 2.58 - 2.47 (m, 1 H); 1.94 - 1.84 (m, 1 H); 1.84 - 1.78 (m, 1 H); 1.77 - 1.66 (m, 1 H); 1.56 - 1.47 (m, 10 H); 1.07 (dd, J=12.7, 4.4 Hz, 1 H).
¹³C-NMR (APT) (50 MHz, CDCl₃) δ = 155.64 (C=O), 155.33 (C), 140.10 (CH), 132.69 (q, J=35.1, C), 131.69 (CH), 122.4 (q, J=271.8, CF₃), 80.33 (C), 58.51 (CH), 56.78 (CH), 52.60 (CH), 38.34 (CH₂), 30.14 (CH₂), 28.50 (3 x CH₃), 22.18 (CH₂).
MS (ESI+) m/z (%) = 303 (100) [M-56H]⁺.

(+/-)-endo-tert-butyl 2-((4-(trifluoromethyl)pyrimidin-2-yl)amino)-7-azabicyclo[2.2.1]heptane-7-carboxylate (10e)
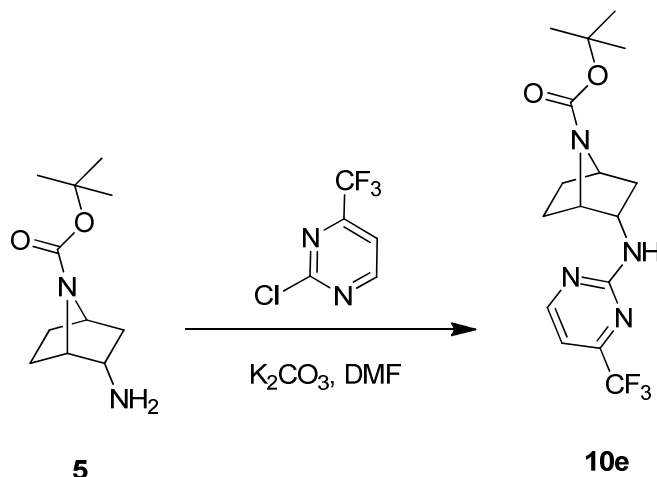
A mixture of **5** (100 mg, 0.471 mmol), 2-chloro-4-(trifluoromethyl)pyrimidine (103 mg, 0.565 mmol) and K_2CO_3 (130 mg, 0.942 mmol) in DMF (1 mL) was stirred under N_2 atmosphere for 10 min. The reaction mixture was heated at 100 °C for 4 h, then 75 °C for 14 h.

Then the solvent was evaporated under reduced pressure and the residue taken up in $NaHCO_3$ sat. sol. (10 mL) and the mixture extracted with AcOEt (3x10 mL). The organic layers were collected, washed with water (30 mL), dried over anhydrous Na_2SO_4 and filtered. Then the solvent was evaporated under reduced pressure.

Purification: Isolera-One Biotage, Snap 25g HP-SI Column, sample dissolved in DCM, eluent: from DCM 100% to DCM/AcOEt 8:2 in gradient.

The containing product fraction were collected and the solvent was evaporated under reduced pressure to give **10e** as white solid (139 mg, 039 mmol, 82%).

ANALYSIS
Formula: $C_{16}H_{21}F_3N_4O_2$
Mol. Weight: 358.36 g/mol
Rf: 0.63 (DCM/AcOEt 8:2; SI-TLC)
^{1}H NMR (400 MHz, CDCl$_3$) δ = 8.58 - 8.45 (m, 1 H); 6.89 (d, J=4.9 Hz, 1 H); 5.50 (brs, 1 H); 4.55 (brs, 1 H); 4.35 (dd, J=10.3, 5.4 Hz, 1 H); 4.25 (brs, 1 H); 2.54 - 2.43 (m, 1 H); 1.93 - 1.80 (m, 2 H); 1.75 - 1.66 (m, 1 H); 1.55 - 1.45 (m, 10 H); 1.05 (dd, J=12.5, 4.6 Hz, 1 H).
^{13}C-NMR (APT) (50 MHz, CDCl$_3$) δ = 162.20 (C=O), 160.51 (CH), 157.38 (q, J=38.4, C), 155.75 (C), 120.61 (q, J=275.1, CF$_3$), 106.39 (CH), 80.03 (C), 58.71 (CH), 56.77 (CH), 52.54 (CH), 37.97 (CH$_2$), 30.15 (CH$_2$), 28.46 (3 x CH$_3$), 22.26 (CH$_2$).
MS (ESI+) m/z (%) = 303 (100) [M-56H]$^+$.

General Procedure A: synthesis of *(+/-)-endo*-compounds 11a-e

Compound **10a-e** (1eq) was dissolved in a solution of DCM (Ratio: 4.0) and TFA (Ratio: 1.0; 30 eq) and then the mixture was stirred at room temperature for 1 h.

Then the solvent was evaporated under reduced pressure.

Purification: the residue was taken up in MeOH and loaded on SCX column; Eluent MeOH then Ammonia (2M in MeOH). The containing product fractions were collected and the solvent was eliminated under reduced pressure to give **11a-e**.

(+/-)-endo-N-(5-(trifluoromethyl)pyridin-2-yl)-7-azabicyclo[2.2.1]heptan-2-amine (11a)
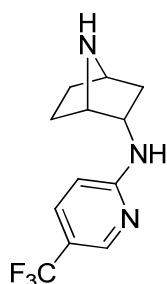
11a

General Procedure A was followed using **10a** (120 mg, 0.336 mmol) to give **11a** as white solid (66.5 mg, 0.26 mmol, 77%).

ANALYSIS

Formula: $C_{12}H_{14}F_3N_3$

Mol Weight: 257.25 g/mol

^{1}H NMR (400 MHz, Acetone-d_6) δ = 8.31 (s, 1 H); 7.61 (dd, J=8.8, 2.0 Hz, 1 H); 6.54 - 6.77 (m, 2 H); 4.16 (d, J=5.4 Hz, 1 H); 3.83 (t, J=4.6 Hz, 1 H); 3.47 - 3.58 (m, 1 H); 2.09 - 2.18 (m, 1 H); 1.83 (ddd, J=12.6, 8.4, 4.4 Hz, 1 H); 1.50 - 1.63 (m, 1 H); 1.41 - 1.50 (m, 1 H); 1.29 - 1.41 (m, 1 H); 1.05 - 1.14 (m, 1 H).

^{13}C-NMR (APT) (50 MHz, Acetone-d_6) δ = 161.31 (C=O), 145.93 (CH), 133.49 (CH), 125.48 (q, J=273.1 Hz, CF$_3$), 113.91 (q, J=30.3 Hz, C), 107.87 (CH), 58.64 (CH) , 56.79 (CH), 53.75 (CH), 37.38 (CH$_2$), 30.87 (CH$_2$), 22.91 (CH$_2$).

MS (ESI+) m/z (%) = 258 (100) [MH]$^+$.

N-((+/-)-endo-7-azabicyclo[2.2.1]heptan-2-yl)-6,7-difluoroquinoxalin-2-amine (11b)
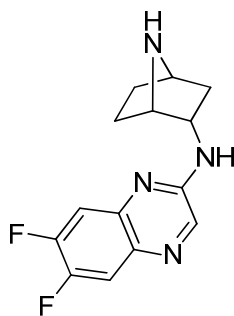
11b

General Procedure A was followed using **10b** (92 mg, 0.244 mmol) to give **11b** as clear-yellow solid (68.2 mg, purity 95%, 0.24 mmol, 96%).

ANALYSIS

Formula: $C_{14}H_{14}F_2N_4$

Mol. Weight: 276.28 g/mol

^{1}H NMR (400 MHz, CDCl$_3$) δ = 8.20 (s, 1 H); 7.63 (dd, J=10.8, 8.3 Hz, 1 H); 7.43 (dd, J=11.2, 8.3 Hz, 1 H); 5.06 (d, J=5.4 Hz, 1 H); 4.24 - 4.34 (m, 1 H); 4.08 (t, J=4.6 Hz, 1 H); 3.72 (t, J=4.9 Hz, 1 H); 2.36 (dddd, J=12.6, 11.17, 5.1, 2.9 Hz, 1 H); 1.77 - 1.86 (m, 1 H); 1.70 - 1.77 (m, 1 H); 1.46 - 1.59 (m, 2 H); 1.02 (dd, J=12.7, 4.4 Hz, 1 H).

^{13}C-NMR (APT) (50 MHz, CDCl$_3$) δ = 152.56 (dd, J=257.7, 15.3, CF), 152.09 (C), 148.66 (dd, J=247.9, 15.4, CF), 139.86 (d, J=14.0, C), 138.23 (CH), 133.78 (d, J=10.0, C), 115.09 (d, J=17.3, CH), 112.70 (d, J=17.7, CH), 58.92 (CH), 57.09 (CH), 53.78 (CH), 38.96 (CH$_2$), 31.25 (CH$_2$), 23.11 (CH$_2$).

MS (ESI+) m/z (%) = 278 (100) [MH]$^+$.

(+/-)-endo-N-(4-(trifluoromethyl)pyridin-2-yl)-7-azabicyclo[2.2.1]heptan-2-amine (11c)
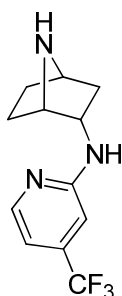
11c

General Procedure A was followed using **10c** (99 mg, 0.277 mmol) to give **11c** as white solid (69.0 mg, 0.27 mmol, 97%).

Formula: $C_{12}H_{14}F_3N_3$

Mol. Weight: 257.25 g/mol

¹H NMR (400 MHz, CDCl₃) δ = 8.23 (d, *J*=4.9 Hz, 1 H); 6.78 (dd, *J*=5.4, 0.9 Hz, 1 H); 6.60 (s, 1 H); 4.95 (d, *J*=5.4 Hz, 1 H); 3.96 - 4.06 (m, 1 H); 3.91 (t, *J*=4.4 Hz, 1 H); 3.70 (t, *J*=4.9 Hz, 1 H); 2.32 (dddd, *J*=12.5, 10.9, 5.4, 2.9 Hz, 1 H); 1.83 - 1.91 (m, 1 H); 1.62 - 1.75 (m, 1 H); 1.46 - 1.57 (m, 2 H); 0.97 (dd, *J*=12.7, 4.4 Hz, 1 H).

¹³C-NMR (APT) NMR (50 MHz, CDCl₃) δ = 159.10 (C), 149.81 (CH), 139.98 (q, J=33.1, C), 123.25 (q, J=273.0, CF₃), 102.55 (q, J=4.2, CH), 108.5 (q, J=3.1, CH), 58.89 (CH), 57.13 (CH), 54.27 (CH), 39.00 (CH₂), 31.24 (CH₂), 23.11 (CH₂).

MS (ESI+) m/z (%) = 259 (100) [MH]⁺.

(+/-)-*endo*-N-(5-(trifluoromethyl)pyrazin-2-yl)-7-azabicyclo[2.2.1]heptan-2-amine (11d)
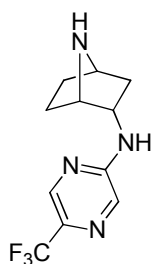
11d

General Procedure A was followed using **10d** (65 mg, 0.181 mmol) to give **11d** as clear-yellow solid (45.3 mg, 0.1 mmol, 94%).

Formula: $C_{11}H_{13}F_3N_4$

Mol. Weight: 258.24

¹H NMR (400 MHz, CDCl₃) δ = 8.36 (s, 1 H); 7.95 (d, *J*=1.0 Hz, 1 H); 5.15 (d, *J*=4.9 Hz, 1 H); 4.11 - 4.20 (m, 1 H); 3.97 (t, *J*=4.4 Hz, 1 H); 3.73 (t, *J*=4.9 Hz, 1 H); 2.30 - 2.40 (m, 1 H); 1.76 - 1.84 (m, 1 H); 1.67 - 1.76 (m, 1 H); 1.47 - 1.60 (m, 2 H); 1.01 (dd, *J*=12.5, 4.6 Hz, 1 H).

¹³C-NMR (APT) (50 MHz, CDCl₃) δ = 155.73 (C), 140.33 (q, J=3.5, CH), 132.32 (q, J=35.6, C), 131.45 (CH), 122.49 (q, J=271.8, CF₃), 58.80 (CH), 57.09 (CH), 53.89 (CH), 38.91 (CH₂), 31.22 (CH₂), 23.18 (CH₂).

MS (ESI+) m/z (%) = 260 (100) [MH]⁺.

(+/-)-*endo*-N-(4-(trifluoromethyl)pyrimidin-2-yl)-7-azabicyclo[2.2.1]heptan-2-amine (11e)
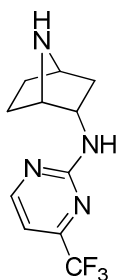
11e

General Procedure A was followed using **10e** (122 mg, 0.340 mmol) to give **11e** as white solid (86.0 mg, purity 90%, 0.30 mmol, 89%).

ANALYSIS

Formula: $C_{11}H_{13}F_3N_4$

Mol. Weight: 258.24 g/mol

^{1}H NMR (400 MHz, CDCl$_3$) δ = 8.50 (brs, 1 H); 6.86 (d, *J*=4.9 Hz, 1 H); 5.51 (brs, 1 H); 4.20 - 4.29 (m, 1 H); 3.95 (t, *J*=4.2 Hz, 1 H); 3.69 (t, *J*=4.9 Hz, 1 H); 2.29 (dddd, *J*=12.7, 11.2, 5.1, 3.2 Hz, 1 H); 1.79 - 1.88 (m, 1 H); 1.64 - 1.71 (m, 1 H); 1.43 - 1.57 (m, 2 H); 0.99 (dd, *J*=12.7, 4.9 Hz, 1 H).

^{13}C-NMR (APT) (50 MHz, CDCl$_3$) δ = 162.59 (C), 160.63 (CH), 156.19 (q, J=35.5, C), 120.68 (q, J=275.2, CF$_3$), 105.99 (CH), 58.93 (CH), 57.15 (CH), 53.80 (CH), 38.64 (CH$_2$), 31.05 (CH$_2$), 23.09 (CH$_2$).

MS (ESI+) m/z (%) = 260 (100) [MH]$^+$.

General Procedure B: synthesis of *(+/-)-endo*-compounds 9a-k

To a solution of the appropriate carboxylic acid (1.0 eq) in dioxane (1 mL) were added in sequence *N*-methylmorpholine (3 eq) and CDMT (1.5 eq) under N_2 atmosphere and the resultant solution was stirred for 30 min at room temperature. Then the amine **11a-e** (1.2 eq) pre-dissolved in dioxane (1.5 mL) was added and the mixture was stirred at 100 °C for 1 h.

The solvent was then evaporated under reduced pressure. The residue was taken up in AcOEt and washed in sequence with NH_4Cl sat.sol., $NaHCO_3$ sat. sol. and water. Then the organic layer was dried over anhydrous Na_2SO_4, filtered and the solvent was eliminated under reduced pressure.

Purification: Isolera-One Biotage, Flash chromatography by HP-SI Column or Reverse Phase Column.

The containing product fractions were collected and the solvent eliminated under reduced pressure to give the final compound **9a-e** as *(+/-)-endo*-racemic mixture.

Analysis of proton and carbon NMR spectra reveals for compounds **9a-k** the presence of two rotamers of the molecule in 1:1 ratio. In particular, in proton NMR spectra the two rotamers can be easily detected and described. On the contrary, carbon NMR spectra are complicated by the presence of signals splitted by the presence of C-F coupling and the C_{sp2} carbon atom signals are difficult to distinguish and assign. For these reasons in carbon NMR spectra only the chemical shifts of aliphatic carbons are reported for both rotamers of each compound.

(2-methyl-5-phenylthiazol-4-yl) *(+/-)-endo*-2-((5-(trifluoromethyl)pyridin-2-yl)amino)-7-azabicyclo[2.2.1]heptane-7-carboxylate (9a)

9a
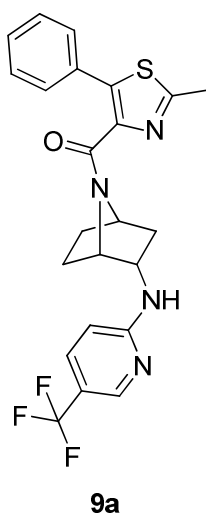
General Procedure B was followed using the 2-methyl-5-phenylthiazole-4-carboxylic acid (40.3 mg, 0.184 mmol), amine **11a** (43 mg, 0.167 mmol), NMM (0.055 mL, 0.501 mmol) and CDMT (44.0 mg, 0.251 mmol) in dioxane (2 mL). After purification (Snap 10g HP-SI Column, sample dissolved in DCM, eluent: from CyHex/AcOEt 100:0 to 0:100 in gradient) **9a** was obtained as a white solid (49.5 mg, 0.11 mmol, 65%).

Formula: $C_{23}H_{21}F_3N_4OS$

Mol. Weight: 458.50

Note: From NMR spectra were observed two signal patterns in about 1:1 ratio due to the two rotamers of the molecule. Chemical shifts of both rotamers are reported.

Rf: 0.08 (CyHex/AcOEt 5:5; SI-TLC).

^{1}H NMR (400 MHz, Acetone-d_6) δ = 8.39 (s, 1 H); 8.29 (s, 1 H); 7.68 - 7.58 (m, 6 H); 7.50 - 7.35 (m, 6 H); 6.78 (m, 2 H); 6.68 (d, J=8.8 Hz, 1 H); 6.59 (d, J=8.8 Hz, 1 H); 5.03 (t, J=4.9 Hz, 1 H); 4.63 (t, J= 4.9, 1 H,); 4.25 (m, 2 H); 3.98 (m, 2 H); 2.72 (s, 3 H); 2.76 (s, 3 H); 2.30 (m, 1 H); 1.94 (m, 2 H); 1.86 (m, 1 H); 1.74 (m, 1 H); 1.63 - 1.45 (m, 4 H); 1.32 (m, 2 H); 1.20 (m, 1 H).

^{13}C-NMR (APT) (MHz, Acetone-d_6) δ = 59.62 (CH), 57.97 (CH), 55.92 (CH), 54.01 (CH), 52.97 (CH), 51.94 (CH), 37.49 (CH_2), 36.04 (CH_2), 30.54 (CH_2), 22.62 (CH_2), 21.26 (CH_2), 18.38 (2 x CH_3), (one CH_2 signal obscured by acetone-d_6 signals).

MS (ESI+) m/z (%) = 460 (100) [MH]$^+$.

(2-methyl-5-phenylthiazol-4-yl) (+/-)-endo-2-((6,7-difluoroquinoxalin-2-yl)amino)-7-azabicyclo[2.2.1]heptane-7-carboxylate (9b)

9b
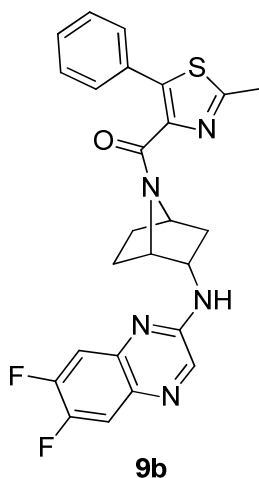
General Procedure B was followed using the 2-methyl-5-phenylthiazole-4-carboxylic acid (45.7 mg, 0.208 mmol), amine **11b** (50.5 mg, 0.174 mmol), NMM (0.057 mL, 0.521 mmol) and CDMT (45.7 mg, 0.260 mmol) in dioxane (2.5 mL). After purification (Snap 10g HP-SI Column, sample dissolved in DCM 100%, eluent: from DCM/MeOH 98:2 to 95:5 in gradient) **9b** was obtained as a white solid (32 mg, 0.07 mmol, 39%).

Formula: $C_{25}H_{21}F_2N_5OS$

Mol. Weight: 477.53 g/mol

Note: From NMR spectra were observed two signal patterns in about 1:1 ratio due to the two rotamers of the molecule. Chemical shifts of both rotamers are reported.

Rf: 0.35 (DCM/MeOH 95:5; SI-TLC).

¹H NMR (400 MHz, DMSO-d_6) δ = 8.33 (s, 1 H); 8.27 (s, 1 H); 8.01 (m, 2 H); 7.82 (m, 2 H); 7.65 (dd, J=11.9, 8.5 Hz, 1 H); 7.57 - 7.36 (m, 10 H); 7.31 (dd, J= 11.6, 8.3 Hz, 1H); 4.93 (t, J=4.4 Hz, 1 H); 4.59 (t, J=4.4 Hz, 1 H); 4.21 (t, J=4.4 Hz, 1 H); 4.14 (m, 1 H); 3.87 (t, J=4.4 Hz, 1 H); 3.81 (m, 1 H); 2.76 (s, 3 H); 2.71 (s, 3 H); 2.20 (m, 1 H); 1.86 – 1.65 (m, 4 H); 1.60 – 1.39 (m, 4 H); 1.35 – 1.12 (m, 3 H).

¹³C-NMR (APT) (75 MHz, Pyr-d_5) δ 60.20 (CH), 58.42 (CH), 56.54 (CH), 54.61 (CH), 53.13 (CH), 52.13 (CH), 37.72 (CH$_2$), 36.20 (CH$_2$), 31.17 (CH$_2$), 29.68 (CH$_2$), 23.49 (CH$_2$), 22.13 (CH$_2$), 19.17 (CH$_3$), 19.11 (CH$_3$).

MS (ESI+) m/z (%) = 479 (100) [MH]$^+$.

(2-methyl-5-phenylthiazol-4-yl) *(+/-)-endo*-2-((4-(trifluoromethyl)pyridin-2-yl)amino)-7-azabicyclo[2.2.1]heptane-7-carboxylate (9c)

9c
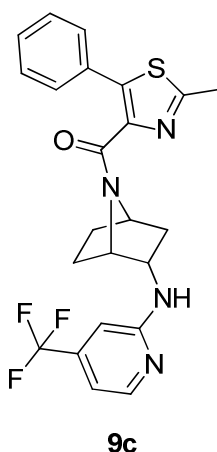
General Procedure B was followed using the 2-methyl-5-phenylthiazole-4-carboxylic acid (53.5 mg, 0.244 mmol), amine **11c** (52.3 mg, 0.203 mmol), NMM (0.067 mL, 0.610 mmol) and CDMT (53.5 mg, 0.305 mmol) in dioxane (2.5 mL). After purification (Snap 10g HP-SI Column, sample dissolved in DCM 100%, eluent: from DCM/MeOH 98:2 to 95:5 in gradient) **9c** was obtained as a white solid (62 mg, 0.13 mmol, 65%).

ANALYSIS

Formula: C$_{23}$H$_{21}$F$_3$N$_4$OS

Mol. Weight: 458.50 g/mol

Note: From NMR spectra were observed two signal patterns in about 1:1 ratio due to the two rotamers of the molecule. Chemical shifts of both rotamers are reported.

Rf: 0.37 (DCM/MeOH 95:5; SI-TLC).

¹H NMR (400 MHz, Acetone-d_6) δ = 8.29 (d, J=5.1 Hz, 1 H); 8.21 (d, J=5.2 Hz, 1 H); 7.61 (m, 4 H); 7.44 (m, 6 H); 7.57 - 7.64 (m, 2 H); 7.75 (m, 4 H); 7.59 (m, 2H); 5.04 (t, J=4.5 Hz, 1 H); 4.63 (t, J=4.9 Hz, 1 H); 4.26 (m, 1 H); 3.97 (m, 1 H); 2.76 (s, 3 H); 2.74 (s, 3 H); 2.31 (m, 1 H); 1.96 (m, 2 H); 1.88 (m, 1 H); 1.75 (m, 1 H); 1.63 - 1.44 (m, 4 H); 1.29 (m, 2 H); 1.16 (m, 1 H).

13C-NMR (APT) (50 MHz, Acetone-d_6) δ = 59.64 (CH), 57.91 (CH), 55.89 (CH), 53.92 (CH), 53.00 (CH), 51.97 (CH), 37.68 (CH$_2$), 36.27 (CH$_2$), 30.58 (CH$_2$), 22.57 (CH$_2$), 21.19 (CH$_2$), 18.37 (2 x CH$_3$), (one CH$_2$ signal obscured by acetone-d_6 signals).

MS (ESI+) m/z (%) = 479 (100) [MH]$^+$.

(2-methyl-5-phenylthiazol-4-yl) *(+/-)-endo*-2-((5-(trifluoromethyl)pyrazin-2-yl)amino)-7-azabicyclo[2.2.1]heptane-7-carboxylate (9d)
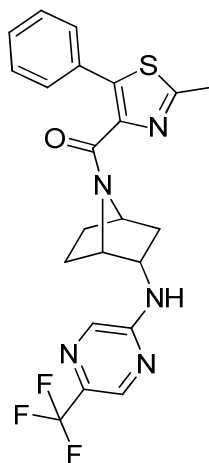
9d

General Procedure B was followed using the 2-methyl-5-phenylthiazole-4-carboxylic acid (34.1 mg, 0.156 mmol), amine **11d** (34.5 mg, 0.130 mmol), NMM (0.043 mL, 0.389 mmol) and CDMT (34.1 mg, 0.194 mmol) in dioxane (2.5 mL). After purification (Snap 10g HP-SI Column, sample dissolved in DCM 100%, eluent: from DCM/MeOH 100:0 to 95:5 in gradient) **9d** was obtained as a white solid (48 mg, 0.10 mmol, 80%).

ANALYSIS

Formula: C$_{22}$H$_{20}$F$_3$N$_5$OS

Mol. Weight: 459.49 g/mol

Note: From NMR spectra were observed two signal patterns in about 1:1 ratio due to the two rotamers of the molecule. Chemical shifts of both rotamers are reported.

Rf: 0.36 (DCM/MeOH 95:5; SI-TLC).

1H NMR (400 MHz, Acetone-d_6) δ = 8.43 (s, 1 H); 8.34 (s, 1 H); 8.04 (s, 1 H); 7.98 (s, 1 H); 7.61 (m, 4 H); 7.45 (m, 6 H); 7.31 (m; 2 H); 5.03 (t, J=4.0 Hz, 1 H); 4.65 (t, J=4.9 Hz, 1 H); 4.28 (m, 2 H); 4.00 (m, 2 H); 2.76 (s, 3 H); 2.74 (s, 3 H); 2.33 (m, 1 H); 1.97 (m, 2 H); 1.88 (m, 1 H); 1.77 (m, 1 H); 1.64 - 1.45 (m, 4 H); 1.34 (m, 2 H); 1.25 (m, 1 H).

13C-NMR (APT) (50 MHz, Acetone-d_6) δ = 59.38 (CH), 57.94 (CH), 55.61 (CH), 53.98 (CH), 52.64 (CH), 51.67 (CH), 37.36 (CH$_2$), 35.96 (CH$_2$), 30.52 (CH$_2$), 22.73 (CH$_2$), 21.33 (CH$_2$), 18.38 (2 x CH$_3$), (one CH$_2$ signal obscured by acetone-d_6 signals).

MS (ESI+) m/z (%) = 461 (100) [MH]$^+$.

(2-methyl-5-phenylthiazol-4-yl) *(+/-)-endo-***2-((4-(trifluoromethyl)pyrimidin-2-yl)amino)-7-azabicyclo[2.2.1]heptane-7-carboxylate (9e)**
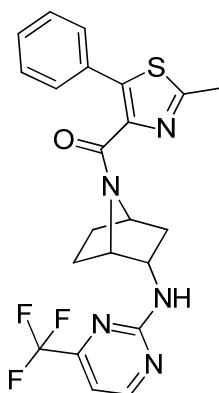
9e

General Procedure B was followed using the 2-methyl-5-phenylthiazole-4-carboxylic acid (60.5 mg, 0.276 mmol), amine **11e** (65.3 mg, 0.230 mmol), NMM (0.076 mL, 0.690 mmol) and CDMT (60.6 mg, 0.345 mmol) in dioxane (3 mL). After purification (Snap 25g HP-SI Column, sample dissolved in DCM 100%, eluent: from AcOEt/DCM/MeOH 90:10:0 to AcOEt/DCM/MeOH 60:37:3 in gradient) **9e** was obtained as a white solid (80.6 mg, 0.18 mmol, 76%).

ANALYSIS
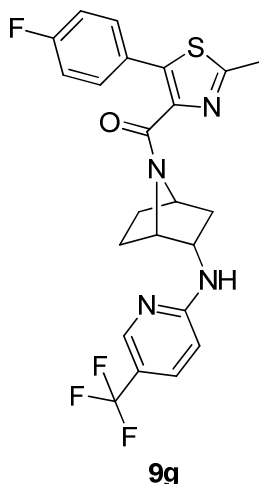**Formula**: $C_{22}H_{20}F_3N_5OS$
Mol. Weight: 459.49 g/mol
Note: From NMR spectra were observed two signal patterns in about 1:1 ratio due to the two rotamers of the molecule. Chemical shifts of both rotamers are reported.
Rf: 0.40 (DCM/MeOH 95:5; SI-TLC).
^{1}H NMR (400 MHz, Acetone-d_6) δ = 8.67 (brs, 1 H); 8.58 (brs, 1 H); 7.60 (m, 4 H); 7.43 (m, 6 H); 7.18 (m; 2 H); 7.02 (d, J=4.7, 1 H); 6.97 (d, J=4.7, 1 H); 4.99 (m, 1 H); 4.64 (m, 1 H); 4.27 (m, 2 H); 3.98 (m, 2 H); 2.80 (s, 3 H); 2.73 (s, 3 H); 2.28 (m, 1 H); 1.97 (m, 2 H); 1.84 (m, 1 H); 1.70 (m, 2 H); 1.73 - 1.46 (m, 4 H); 1.40 (m, 1 H); 1.25 (m, 1 H).
^{13}C-NMR (APT) (50 MHz, Acetone-d_6) δ = 59.52 (CH), 58.03 (CH), 55.76 (CH), 53.96 (CH), 53.08 (CH), 51.98 (CH), 36.88 (CH_2), 35.28 (CH_2), 30.40 (CH_2), 28.96 (CH_2), 22.67 (CH_2), 21.44 (CH_2), 18.33 (2 x CH_3).
MS (ESI+) m/z (%) = 461 (100) $[MH]^+$.

(6-methyl-3-phenylpyridin-2-yl) *(+/-)-endo*-2-((5-(trifluoromethyl)pyridin-2-yl)amino)-7-azabicyclo[2.2.1]heptane-7-carboxylate (9f)

9f
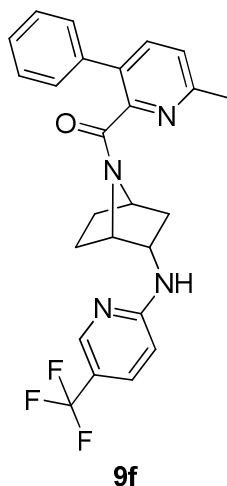
General Procedure B was followed using the 6-methyl-3-phenylpicolinic acid (64.7 mg, 0.303 mmol), amine **11a** (65 mg, 0.253 mmol), NMM (0.083 mL, 0.758 mmol) and CDMT (66.5 mg, 0.379 mmol) in dioxane (2.5 mL). After purification (Snap 10g HP-SI Column, sample dissolved in DCM 100%, eluent: from DCM/MeOH 100:0 to 95:5 in gradient) **9f** was obtained as a white solid (99 mg, purity 95% 0.21 mmol, 83%).

ANALYSIS

Formula: $C_{25}H_{23}F_3N_4O$
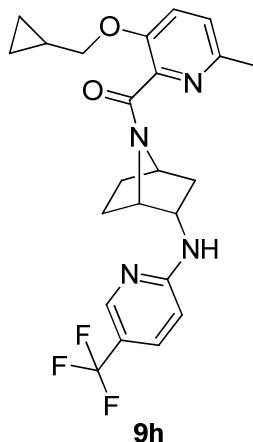
Mol. Weight: 452.47 g/mol

Note: From NMR spectra were observed two signal patterns in about 1:1 ratio due to the two rotamers of the molecule. Chemical shifts of both rotamers are reported.

^{1}H NMR (400 MHz, Acetone-d_6) δ = 8.38 (m, 1 H); 8.27 (m, 1 H); 7.80 (m, 2 H); 7.67 – 7.56 (m, 6 H); 7.49 – 7.35 (m, 8 H); 6.75 (m, 2 H); 6.66 (d, J=4.7, 1 H); 6.58 (d, J=4.7, 1 H); 4.97 (t, J=4.0 Hz, 1 H); 4.57 (t, J=4.9 Hz, 1 H); 4.10 (m, 1 H); 3.97 (m, 2 H); 3.61 (m, 1 H); 2.61 (s, 3 H); 2.57 (s, 3 H); 2.18 (m, 1 H); 1.93 – 1.75 (m, 3 H); 1.64 (m, 1 H); 1.56 (m, 1 H); 1.49 - 1.35 (m, 3 H); 1.31 - 1.20 (m, 2 H); 1.12 (m, 1 H).

^{13}C-NMR (APT) (50 MHz, Acetone-d_6) δ = 58.93 (CH), 57.17 (CH), 55.38 (CH), 53.46 (CH), 52.75 (CH), 52.04 (CH), 37.41 (CH_2), 36.15 (CH_2), 30.38 (CH_2), 29.26 (CH_2), 23.39 (2 x CH_3), 22.44 (CH_2), 21.41 (CH_2).

MS (ESI+) m/z (%) = 454 (100) [MH]$^+$.

(5-(4-fluorophenyl)-2-methylthiazol-4-yl) *(+/-)-endo*-2-((5-(trifluoromethyl)pyridin-2-yl)amino)-7-azabicyclo[2.2.1]heptane-7-carboxylate (9g)

9g

General Procedure B was followed using the 5-(4-fluorophenyl)-2-methylthiazole-4-carboxylic acid (71.9 mg, 0.303 mmol), amine **11a** (65 mg, 0.253 mmol), NMM (0.083 mL, 0.758 mmol) and CDMT (66.5 mg, 0.379 mmol) in dioxane (2.5 mL). After purification (Snap 10g HP-SI Column, sample dissolved in DCM 100%, eluent: from DCM/MeOH 100:0 to 95:5 in gradient) **9g** was obtained as a white solid (87 mg, 0.18 mmol, 70%).

ANALYSIS
Formula: $C_{23}H_{20}F_4N_4OS$
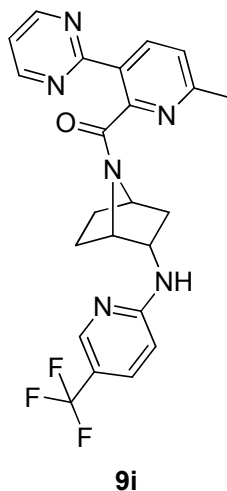**Mol. Weight**: 476.49 g/mol
Note: From NMR spectra were observed two signal patterns in about 1:1 ratio due to the two rotamers of the molecule. Chemical shifts of both rotamers are reported.
^{1}H NMR (400 MHz, Acetone-d_6) δ = 8.39 (s, 1 H); 8.31 (s, 1 H); 7.65 (m, 6 H); 7.23 (m, 4 H); 6.80 (m, 2 H); 6.68 (d, J=8.8 Hz, 1 H); 6.62 (d, J=8.9 Hz, 1 H); 5.02 (t, J=4.0 Hz, 1 H); 4.63 (t, J=5.0 Hz, 1 H); 4.34 (t, J=4.5 Hz, 1 H); 4.27 (m, 1 H); 4.02 (m, 2 H); 2.80 (s, 3 H); 2.76 (s, 3 H); 2.31 (m, 1 H); 2.09 (m, 1 H); 1.90 – 1.85 (m, 2 H); 1.76 (m, 1 H); 1.63 - 1.48 (m, 4 H); 1.41 – 1.29 (m, 2 H); 1.24 (m, 1 H).
^{13}C-NMR (APT) (75 MHz, Acetone-d_6) δ = 59.78 (CH), 58.14 (CH), 56.14 (CH), 54.22 (CH), 53.11 (CH), 52.06 (CH), 37.73 (CH$_2$), 36.14 (CH$_2$), 30.75 (CH$_2$), 29.24 (CH$_2$), 22.84 (CH$_2$), 21.39 (CH$_2$), 18.55 (2 x CH$_3$).
MS (ESI+) m/z (%) = 479 (100) [MH]$^+$.

(3-(cyclopropylmethoxy)-6-methylpyridin-2-yl) *(+/-)-endo*-**2-((5-(trifluoromethyl)pyridin-2-yl)amino)-7-azabicyclo[2.2.1]heptane-7-carboxylate (9h)**

9h

General Procedure B was followed using the 3-(cyclopropylmethoxy)-6-methylpicolinic acid (50 mg, 0.241 mmol), amine **11a** (51.7 mg, 0.201 mmol), NMM (0.066 mL, 0.603 mmol) and CDMT (53.0 mg, 0.302 mmol) in dioxane (2.5 mL). After purification (Snap 10g HP-SI Column, sample dissolved in DCM 100%, eluent: from DCM/MeOH 100:0 to 95:5 in gradient) **9h** was obtained as a white solid (70.4 mg, 0.16 mmol, 78%).

ANALYSIS

Formula: $C_{23}H_{25}F_3N_4O_2$
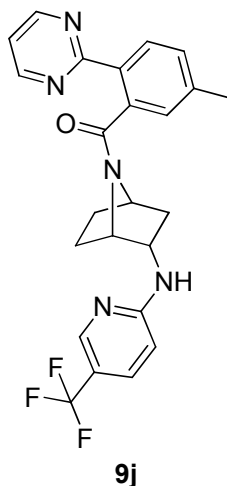
Mol. Weight: 446.47g/mol

Note: From NMR spectra were observed two signal patterns in about 1:1 ratio due to the two rotamers of the molecule. Chemical shifts of both rotamers are reported.

¹H NMR (400 MHz, Acetone-d_6) δ = 8.41 (s, 1 H); 8.22 (s, 1 H); 7.67 (dd, J=8.8, 2.3 Hz, 1 H); 7.60 (dd, J=8.8, 2.4 Hz, 1 H); 7.41 (t, J= 8.7 Hz, 2 H); 7.23 (dd, J= 8.2, 7.4 Hz, 2 H); 6.87 (m, 2 H); 6.73 (d, J=8.8 Hz, 1 H); 6.64 (d, J=8.8 Hz, 1 H); 5.08 (t, J=4.6 Hz, 1 H); 4.69 (t, J=4.9 Hz, 1 H); 4.57 (m, 1 H); 4.45 (m, 1 H); 4.04 (t, J=4.5 Hz, 1 H); 4.00 – 3.91 (m, 4 H); 3.73 (t, J=5.0 Hz, 1 H); 2.55 – 2.35 (m, 2 H); 2.46 (s, 3 H); 2.43 (s, 3 H); 2.10 – 1.80 (m, 4 H); 1.74 – 1.56 (m, 4 H); 1.41 – 1.21 (m, 4 H); 0.58 (m, 4 H); 0.37 (m, 4 H).

¹³C-NMR (APT) (50 MHz, Acetone-d_6) δ = 73.55 (CH₂), 59.13 (CH), 57.50 (CH), 55.70 (CH), 53.81 (CH), 52.99 (CH), 52.14 (CH), 37.63 (CH₂), 36.17 (CH₂), 30.74 (CH₂), 29.39 (CH₂), 22.75 (CH₂), 22.62 (CH), 21.50 (CH₂), 10.22 (CH), 2.86 (CH₂).

MS (ESI+) m/z (%) = 448 (100) [MH]⁺.

(6-methyl-3-(pyrimidin-2-yl)pyridin-2-yl) *(+/-)-endo*-2-((5-(trifluoromethyl)pyridin-2-yl)amino)-7-azabicyclo[2.2.1]heptane-7-carboxylate (9i)

9i

General Procedure B was followed using the 6-methyl-3-(pyrimidin-2-yl)picolinic acid (65.3 mg, 0.303 mmol), amine **11a** (65 mg, 0.253 mmol), NMM (0.083 mL, 0.758 mmol) and CDMT (66.5 mg, 0.379 mmol) in dioxane (2.5 mL). After purification (Snap 10g HP-SI Column, sample dissolved in DCM 100%, eluent: from DCM/MeOH 100:0 to 95:5 in gradient) **9i** was obtained as a white-pink solid (65.4 mg, 0.14 mmol, 56%).

ANALYSIS

Formula: $C_{23}H_{21}F_3N_6O$
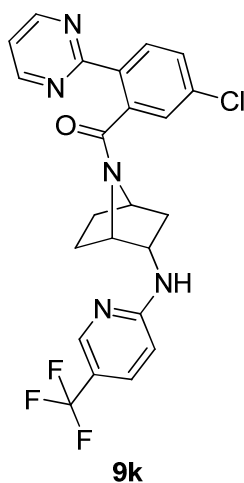
Mol. Weight: 454.45 g/mol

Note: From NMR spectra were observed two signal patterns in about 1:1 ratio due to the two rotamers of the molecule. Chemical shifts of both rotamers are reported.

^{1}H NMR (400 MHz, Acetone-d_6) δ = 8.88 (m, 4 H); 8.41 (m, 3H); 8.21 (m, 1 H); 7.67 (dd, J= 8.8, 2.4 Hz, 1 H); 7.59 (dd, J= 8.9, 2.4 Hz, 1 H); 7.49 - 7.38 (m, 4 H); 6.89 (m, 1H); 6.84 (m, 1H); 6.74 (d, J= 8.8 Hz, 1 H); 6.62 (d, J= 8.8 Hz, 1 H); 5.02 (t, J=4.6 Hz, 1 H); 4.66 (t, J=4.8 Hz, 1 H); 4.63 (m, 1 H); 4.33 (t, J=4.6 Hz, 1 H); 3.99 (t, J=4.7 Hz, 1 H); 2.64 – 2.49 (m, 2 H); 2.65 (s, 3 H); 2.61 (s, 3 H); 2.12 – 1.92 (m, 5 H); 1.86 – 1.75 (m, 2 H); 1.73 – 1.56 (m, 2 H); 1.45 – 1.39 (m, 1 H); 1.33 – 1.29 (m, 1 H).

^{13}C-NMR (APT) (50 MHz, Acetone-d_6) δ = 59.30 (CH), 57.64 (CH), 55.62 (CH), 53.64 (CH), 52.86 (CH), 52.10 (CH), 37.67 (CH$_2$), 36.57 (CH$_2$), 30.62 (CH$_2$), 29.42 (CH$_2$), 23.70 (2 x CH$_3$), 22.65 (CH$_2$), 21.64 (CH$_2$).

MS (ESI+) m/z (%) = 456 (100) [MH]$^+$.

(5-methyl-2-(pyrimidin-2-yl)phenyl) *(+/-)-endo-***2-((5-(trifluoromethyl)pyridin-2-yl)amino)-7-azabicyclo[2.2.1]heptane-7-carboxylate (9j)**

9j

General Procedure B was followed using the 5-methyl-2-(pyrimidin-2-yl)benzoic acid (65.0 mg, 0.303 mmol), amine **11a** (65 mg, 0.253 mmol), NMM (0.083 mL, 0.758 mmol) and CDMT (66.5 mg, 0.379 mmol) in dioxane (2.5 mL). After purification (Snap 10g HP-SI Column, sample dissolved in DCM 100%, eluent: from DCM/MeOH 100:0 to 95:5 in gradient) **9j** was obtained as a brown solid (74.7 mg, 0.16 mmol, 64.5%).

ANALYSIS
Formula: $C_{24}H_{22}F_3N_5O$
Mol. Weight: 453.46 g/mol
Note: From NMR spectra were observed two signal patterns in about 1:1 ratio due to the two rotamers of the molecule. Chemical shifts of both rotamers are reported.
^{1}H NMR (400 MHz, Acetone-d_6) δ = 8.85 (m, 4 H); 8.41 (m, 1H); 8.21 (m, 1 H); 8.07 (d, J= 7.9 Hz, 2 H); 7.67 (dd, J=8.8, 2.3 Hz, 1 H); 7.58 (dd, J=8.9, 2.3 Hz, 1 H); 7.38 (m, 6 H); 6.85 (m, 1H); 6.80 (m, 1H); 6.72 (d, J= 8.8 Hz, 1 H); 6.59 (d, J= 8.9 Hz, 1 H); 4.96 (t, J=4.6 Hz, 1 H); 4.61 (t, J=4.7 Hz, 1 H); 4.53 (m, 1 H); 4.23 (t, J=4.6 Hz, 1 H); 3.87 (t, J=4.9 Hz, 1 H); 2.54 – 2.45 (m, 3 H); 2.48 (s, 3 H); 2.46 (s, 3 H); 2.03 (m, 1 H); 1.93 (m, 3 H); 1.81 – 1.52 (m, 4 H); 1.37 (m, 1 H); 1.25 (m, 1 H).
^{13}C-NMR (APT) (50 MHz, CDCl$_3$) δ 59.90 (CH), 58.20 (CH), 55.47 (CH), 53.67 (CH), 53.11 (CH), 52.36 (CH), 39.18 (CH$_2$), 37.77 (CH$_2$), 31.00 (CH$_2$), 29.72 (CH$_2$), 22.70 (CH$_2$), 21.67 (CH$_2$), 21.46 (CH$_3$).
MS (ESI+) m/z (%) = 454 (100) [MH]$^+$.

(5-chloro-2-(pyrimidin-2-yl)phenyl) *(+/-)-endo*-**2-((5-(trifluoromethyl)pyridin-2-yl)amino)-7-azabicyclo[2.2.1]heptane-7-carboxylate (9k)**

9k

General Procedure B was followed using the 5-chloro-2-(pyrimidin-2-yl)benzoic acid (71.1 mg, 0.303 mmol), amine **11a** (65 mg, 0.253 mmol), NMM (0.083 mL, 0.758 mmol) and CDMT (66.5 mg, 0.379 mmol) in dioxane (2.5 mL). After purification (Snap 10g HP-SI Column, sample dissolved in DCM 100%, eluent: from DCM/MeOH 100:0 to 95:5 in gradient) **9k** was obtained as a white-purple solid (88.4 mg, 0.19 mmol, 73.8%).

ANALYSIS

Formula: $C_{23}H_{19}ClF_3N_5O$

Mol. Weight: 473.88 g/mol

Note: From NMR spectra were observed two signal patterns in about 1:1 ratio due to the two rotamers of the molecule. Chemical shifts of both rotamers are reported.

^{1}H NMR (400 MHz, Acetone-d_6) δ = 8.88 (m, 4 H); 8.41 (m, 1H); 8.20 (m, 3 H); 7.70 - 7.52 (m, 6 H); 7.46 (m, 2 H); 6.87 (m, 1H); 6.82 (m, 1H); 6.73 (d, J= 8.8 Hz, 1 H); 6.61 (d, J= 8.9 Hz, 1 H); 4.97 (t, J=4.6 Hz, 1 H); 4.62 (t, J=4.6 Hz, 1 H); 4.53 (m, 1 H); 4.25 (t, J=4.5 Hz, 1 H); 3.91 (t, J=4.9 Hz, 1 H); 2.57 – 2.47 (m, 2 H); 2.05 (m, 2 H); 1.95 (m, 3 H); 1.81 – 1.55 (m, 4 H); 1.39 (m, 1 H); 1.29 (m, 1 H).

^{13}C-NMR (APT) (75 MHz, Acetone-d_6) δ = 60.34 (CH), 58.67 (CH), 55.92 (CH), 53.99 (CH), 52.99 (CH), 52.01 (CH), 37.79 (CH$_2$), 36.45 (CH$_2$), 30.80 (CH$_2$), 22.74 (CH$_2$), 21.63 (CH$_2$), (one CH$_2$ signal obscured by acetone-d_6 signals).

MS (ESI+) m/z (%) = 474 (100) [MH]$^+$.

2.5 Synthesis of exo-TYPE II derivatives 12a-i, experimental data

(+/-)-*exo*-*tert*-butyl 2-((4-(trifluoromethyl)pyridin-2-yl)amino)-7-azabicyclo[2.2.1]heptane-7-carboxylate (13a)
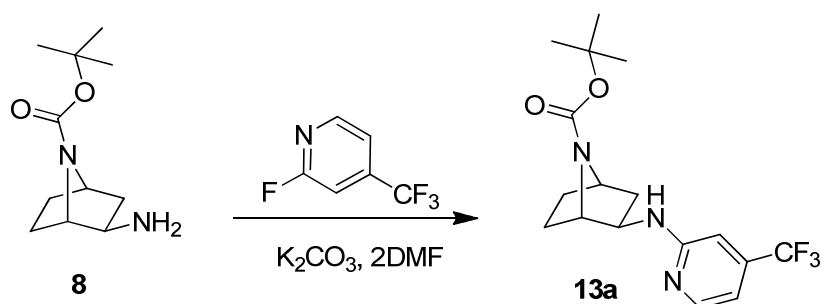
A mixture of **8** (90 mg, 0.339 mmol), 2-fluoro-4-trifluoromethyl-pyridine (85 mg, 0.515 mmol) and K_2CO_3 (120 mg, 0.868 mmol) in DMF (1 mL) was stirred under N_2 atmosphere for 10 min. The reaction mixture was heated at 100 °C for 13 h.

The solvent was then evaporated under reduced pressure and the residue taken up in $NaHCO_3$ sat. sol. (10 mL) and the mixture extracted with AcOEt (3x20 mL). The organic layers were collected, washed with water (50 mL), dried over anhydrous Na_2SO_4 and filtered. Then the solvent was evaporated under reduced pressure.

Purification: Isolera-One Biotage, Snap 10g HP-SI Column, sample dissolved in DCM/MeOH, adsorbed on silica gel and loaded dry on column, eluent: from CyHex/AcOEt 100:0 to 70:30 in gradient.

The containing product fractions were collected and the solvent was evaporated under reduced pressure to give **13a** as white solid (88.7 mg; purity 92%; 0.23 mmol; 67.3%).

ANALYSIS
Formula: $C_{17}H_{22}F_3N_3O_2$
Mol. Weight: 357.37 g/mol
Rf: 0.75 (CyHex/AcOEt 5:5; SI-TLC)
Note: From ^{1}H NMR analysis traces of *endo*-compound were observed (about 8%mol).
^{1}H NMR (400 MHz, CDCl$_3$) δ = 8.23 (d, J=5.3 Hz, 1 H); 6.76 (d, J=5.4 Hz, 1 H); 6.52 (s, 1 H); 4.93 (d, J=5.9 Hz, 1 H); 4.31 (brs, 1 H); 4.22 (d, J=4.9 Hz, 1 H); 3.97 (td, J=7.4, 3.0 Hz, 1 H); 2.05 (dd, J=13.0, 7.6 Hz, 1 H); 1.93 - 1.81 (m, 1 H); 1.81 - 1.70 (m, 1 H); 1.59 - 1.51 (m, 2 H); 1.45 (s, 9 H); 1.43 - 1.39 (m, 1 H).
^{13}C-NMR (DEPT) (100 MHz, CDCl$_3$) δ = 157.55 (C), 156.28 (C), 149.00 (CH), 139.63 (q, J=33.4, C), 122.93 (q, J=273.0, CF$_3$), 108.06 (CH), 103.95 (CH), 79.98 (C), 60.87 (CH), 55.73 (CH), 55.33 (CH), 40.62 (CH$_2$), 28.26 (CH$_2$), 28.22 (3 x CH$_3$), 25.94 (CH$_2$).
MS (ESI+) m/z (%) = 358 (100) [MH]$^+$.

(+/-)-*exo*-*tert*-butyl 2-((4-(trifluoromethyl)pyrimidin-2-yl)amino)-7-azabicyclo[2.2.1]heptane-7-carboxylate (13b)
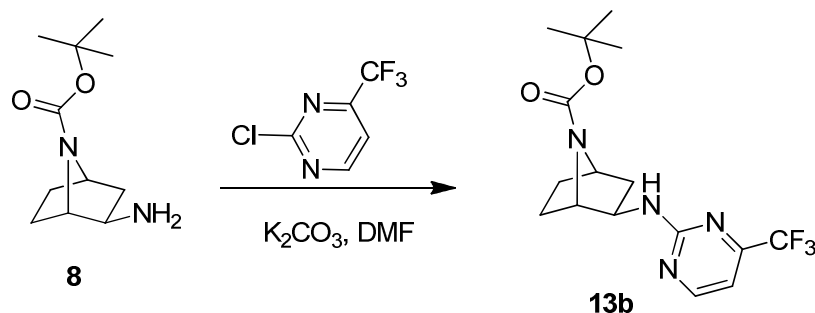
A mixture of **8** (90 mg, 0.339 mmol), 2-chloro-4-(trifluoromethyl)pyrimidine (95 mg, 0.520 mmol) and K_2CO_3 (115 mg, 0.832 mmol) in DMF (1 mL) was stirred under N_2 atmosphere for 10 min. The reaction mixture was heated at 100 °C for 13 h.

The solvent was then evaporated under reduced pressure and the residue taken up in $NaHCO_3$ sat. sol. (10 mL) and the mixture was extracted with AcOEt (3x10 mL). The organic layers were collected, washed with water (30 mL), dried over anhydrous Na_2SO_4 and filtered. Then the solvent was evaporated under reduced pressure.

Purification: Isolera-One Biotage, Snap 25g HP-SI Column, sample dissolved in DCM, eluent: from DCM/AcOEt 100:0 to 80:20 in gradient.

The containing product fractions were collected and the solvent was evaporated under reduced pressure to give **13b** as white solid (66.8 mg; purity 80%; 0.15 mmol; 44.0%).

*ANALYSIS*

Formula: $C_{16}H_{21}F_3N_4O_2$

Mol. Weight: 358.36 g/mol

Rf: 0.63 (CyHex/AcOEt 5:5; SI-TLC)

^{1}H NMR (400 MHz, CDCl$_3$) δ = 8.51 (d, *J*=4.9 Hz, 1 H); 6.85 (d, *J*=4.9 Hz, 1 H); 5.55 (brs, 1 H); 4.32 (brs, 1 H); 4.23 (d, *J*=4.9 Hz, 1 H); 4.08 (td, J=7.7, 3.2 Hz, 1 H); 2.05 (dd, J=13.0, 7.6 Hz, 1 H); 1.92 - 1.73 (m, 2 H); 1.65 - 1.59 (m, 1 H); 1.57 - 1.50 (m, 1 H); 1.45 (s, 9 H); 1.43 - 1.38 (m, 1 H).

^{13}C-NMR (DEPT) (100 MHz, CDCl$_3$) δ = 161.47 (C), 160.35 (CH), 156.07 (C), 155.81 (q, J=32.8, C), 120.44 (q, J=276.3, CF$_3$), 105.75 (CH), 79.95 (C), 61.01 (CH), 55.54 (CH), 55.01 (CH), 40.22 (CH$_2$), 28.48 (CH$_2$), 28.19 (3 x CH$_3$), 25.90 (CH$_2$).

MS (ESI+) m/z (%) = 304 (100) [M-56H]$^+$.

(+/-)-exo-tert-butyl 2-((5-(trifluoromethyl)pyrazin-2-yl)amino)-7-azabicyclo[2.2.1]heptane-7-carboxylate (13c)
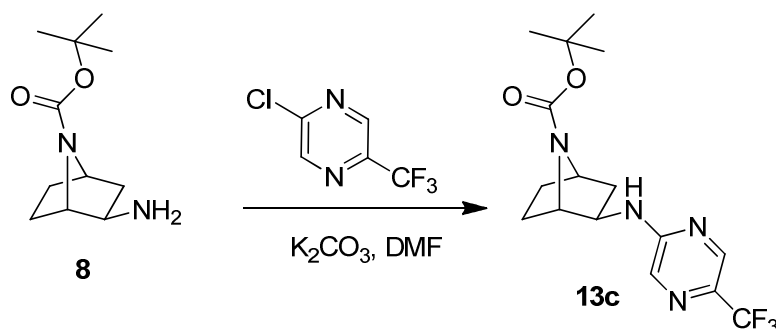
A mixture of **8** (90 mg, 0.339 mmol), 2-chloro-5-(trifluoromethyl)pyrazine (95 mg, 0.520 mmol) and K_2CO_3 (115 mg, 0.832 mmol) in DMF (1 mL) was stirred under N_2 atmosphere for 10 min. The reaction mixture was heated at 100 °C for 13 h.

The solvent was then evaporated under reduced pressure and the residue taken up in $NaHCO_3$ sat. sol. (10 mL) and the mixture extracted with AcOEt (3x20 mL). The organic layers were collected, washed with water (50 mL), dried over anhydrous Na_2SO_4 and filtered. Then the solvent was evaporated under reduced pressure.

Purification: Isolera-One Biotage, Snap 25g HP-SI Column, sample dissolved in DCM, eluent: from DCM/AcOEt 100:0% to 80:20 in gradient.

The containing product fractions were collected and the solvent was evaporated under reduced pressure to give **13c** as white-yellow solid (54.7 mg; 0.153 mmol; 45%).

ANALYSIS

Formula: $C_{16}H_{21}F_3N_4O_2$

Mol. Weight: 358.36 g/mol

¹H NMR (400 MHz, CDCl₃) δ = 8.34 (s, 1 H); 7.87 (d, J=1.0 Hz, 1 H); 5.36 (brs, 1 H); 4.33 (brs, 1 H); 4.24 (d, J=4.4 Hz, 1 H); 4.07 (td, J=7.3, 3.0 Hz, 1 H); 2.09 (dd, J=13.2, 7.8 Hz, 1 H); 1.93 - 1.83 (m, 1 H); 1.83 - 1.73 (m, 1 H); 1.58 - 1.48 (m, 2 H); 1.46 (s, 9 H); 1.43 (d, J=3.4 Hz, 1 H).

¹³C-NMR (DEPT) (100 MHz, CDCl₃) δ = 156.45 (C), 154.50 (C), 139.84 (CH), 132.45 (CH), 131.78 (q, J=35.1, C), 122.32 (q, J=271.7, CF_3), 80.27 (C), 60.85 (CH), 56.01 (CH), 54.86 (CH), 40.49 (CH_2), 28.54 (CH_2), 28.23 (3 x CH_3), 25.88 (CH_2).

MS (ESI+) m/z (%) = 359 (100) [MH]⁺.

(+/-)-exo-tert-butyl 2-(2-phenylacetamido)-7-azabicyclo[2.2.1]heptane-7-carboxylate (13d)
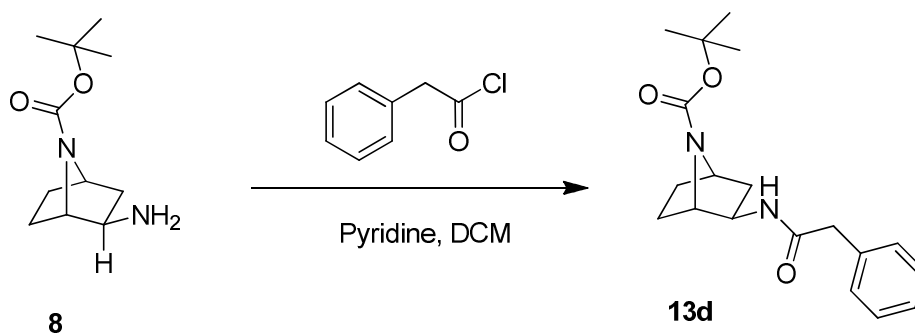
To **8** (70 mg, 0.330 mmol) in dry DCM (2 mL) was added pyridine (0.080 mL, 0.989 mmol) followed by phenacetyl chloride (0.052 mL, 0.396 mmol). The resulting mixture was left to stir for 18 hours at room temperature.

Then the reaction was quenched by addition of NaHCO$_3$ sat. sol. (10 mL) and DCM (10 mL). After brief mixing, the organic layer was separated, dried over anhydrous Na$_2$SO$_4$ and then the solvent was eliminated under reduced pressure.

Purification: Isolera-One Biotage, Snap 10g HP-SI Column, sample dissolved in DCM, eluent: from CyHex/AcOEt 100:0 to 50:50 in gradient.

The containing product fractions were collected and the solvent eliminated under reduced pressure to give **13d** as colorless oil (84 mg; purity 95%; 0.24 mmol; 73.2%).

ANALYSIS

Formula: C$_{19}$H$_{26}$N$_2$O$_3$

Mol. Weight: 330.42 g/mol

^{1}H NMR (400 MHz, CDCl$_3$) δ = 7.39 - 7.32 (m, 2 H); 7.32 - 7.29 (m, 1 H); 7.28 - 7.23 (m, 2 H); 5.74 (brs, 1 H); 4.20 (t, J=4.6 Hz, 1 H); 4.05 (d, J=5.4 Hz, 1 H); 4.03 – 3.98 (m, 1 H); 3.54 (s, 2 H); 1.94 (dd, J=13.2, 7.8 Hz, 1 H); 1.81 - 1.63 (m, 2 H); 1.48 (d, J=3.9 Hz, 1 H); 1.43 (s, 9 H); 1.41 - 1.30 (m, 2 H).

^{13}C-NMR (DEPT) (100 MHz, CDCl$_3$) δ = 170.30 (C), 156.05 (C), 134.73 (C), 129.23 (CH), 128.91 (CH), 127.24 (CH), 79.95 (C), 61.23 (CH), 55.76 (CH), 53.12 (CH), 43.72 (CH$_2$), 40.47 (CH$_2$), 28.30 (CH$_2$), 28.24 (3 x CH$_3$), 26.02 (CH$_2$).

MS (ESI+) m/z (%) = 331 (100) [M-56H]$^+$.

(+/-)-exo-tert-butyl 2-((5-(trifluoromethyl)pyridin-2-yl)amino)-7-azabicyclo[2.2.1]heptane-7-carboxylate (13e)

8   **13e**
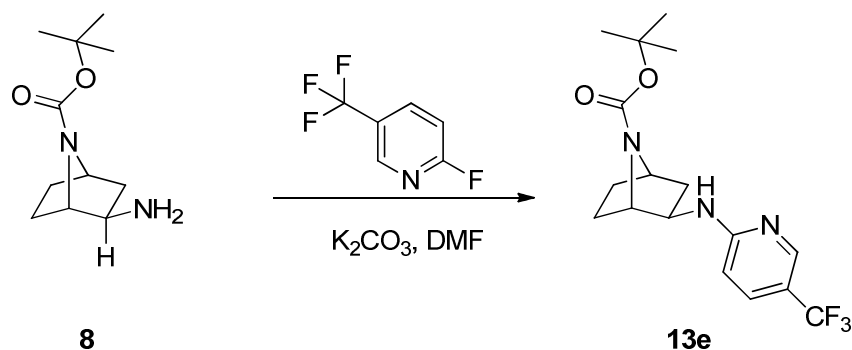
A mixture of **8** (300 mg, 1.131 mmol), 2-fluoro-5-(trifluoromethyl)pyridine (0.190 mL, 1.574 mmol) and potassium carbonate (360 mg, 2.60 mmol) in DMF (3 mL) was stirred under N_2 atmosphere for 10 min. The reaction mixture was heated at 100 °C for 2 h then at 85 °C for 18 h.

The solvent was then evaporated under reduced pressure and the residue taken up in $NaHCO_3$ sat. sol. (30 mL) and the mixture extracted with AcOEt (3x30 mL). The organic layers were collected, washed with water (50 mL), dried over anhydrous Na_2SO_4 and filtered. Then the solvent was evaporated under reduced pressure.

Purification: Isolera-One Biotage, Snap 50g HP-SI Column, sample dissolved in DCM/MeOH, adsorbed on silica gel and loaded dry on column, eluent: from CyHex/AcOEt 100:0 to 70:30 in gradient.

The containing product fractions were collected and the solvent was evaporated under reduced pressure to give **13e** as white solid (295 mg, purity 93%, 0.767 mmmol, 67.9%).

ANALYSIS
Formula: $C_{17}H_{22}F_3N_3O_2$
Mol. Weight: 357.37 g/mol
Rf: 0.70 CyHex/AcOEt 5:5 (TLC-SI)
^{1}H NMR (400 MHz, CDCl₃) δ = 8.35 (s, 1 H); 7.58 (dd, J=8.8, 2.4 Hz, 1 H); 6.38 (d, J=8.8 Hz, 1 H); 5.16 (brs, 1 H); 4.31 (brs, 1 H); 4.23 (d, J=4.9 Hz, 1 H); 4.00 (brs, 1 H); 2.07 (dd, J=13.0, 7.6 Hz, 1 H); 1.92 - 1.71 (m, 2 H); 1.62 - 1.47 (m, 3 H); 1.45 (s, 9 H); 1.44 - 1.38 (m, 1 H).
^{13}C-NMR (DEPT) NMR (100 MHz, CDCl₃) δ = 159.09 (C), 156.33 (C), 145.95 (CH), 134.11 (CH), 124.46 (q, J=270.2, CF₃), 115.59 (q, J=33.0, C), 107.35 (CH), 80.01 (C), 60.90 (CH), 55.80 (CH), 55.24 (CH), 40.55 (CH₂), 28.56 (CH₂), 28.22 (3 x CH₃), 25.95 (CH₂).
MS (ESI+) m/z (%) = 358 (100) [MH]⁺.

General Procedure C: synthesis of compounds 14a-e

Compound **13a-e** (1eq) was dissolved in a solution of DCM (Ratio: 4.0) and TFA (Ratio: 1.0; 30 eq) and then the mixture was stirred at room temperature for 1 h.

Then the solvent was evaporated under reduced pressure.

Purification: the residue was taken up in MeOH and loaded on SCX column, eluent MeOH then Ammonia (2M in MeOH). The containing product fractions were collected and the solvent was eliminated under reduced pressure to give **14a-e**.

(+/-)-exo-N-(4-(trifluoromethyl)pyridin-2-yl)-7-azabicyclo[2.2.1]heptan-2-amine (14a)
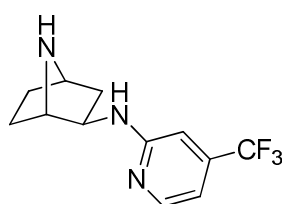
14a

General Procedure C was followed using **13a** (70 mg, 0.180 mmol) to give **14a** as white solid (46.5 mg; purity 90%; 0.163 mmol, 90%).

ANALYSIS

Formula: $C_{12}H_{14}F_3N_3$

Mol. Weight: 257.25 g/mol

^{1}H NMR (400 MHz, CDCl$_3$) δ = 8.23 (d, J=5.4 Hz, 1 H); 6.75 (d, J=5.4 Hz, 1 H); 6.53 (s, 1 H); 4.94 (d, J=6.4 Hz, 1 H); 3.82 (td, J=7.5, 3.2 Hz, 1 H); 3.73 (t, J=4.4 Hz, 1 H); 3.58 (d, J=4.9 Hz, 1 H); 1.98 (dd, J=12.7, 7.8 Hz, 1 H); 1.67 - 1.33 (m, 5 H).

^{13}C-NMR (DEPT) (100 MHz, CDCl$_3$) δ = 158.15 (C), 149.42 (CH), 139.40 (q, J=33.3, C), 123.03 (q, J=123.03, CF$_3$), 108.02 (CH), 103.65 (CH), 61.38(CH), 55.62 (CH), 54.71 (CH), 40.51 (CH$_2$), 29.47 (CH$_2$), 26.67 (CH$_2$).

MS (ESI+) m/z (%) = 258 (100) [MH]$^+$.

(+/-)-exo-N-(4-(trifluoromethyl)pyrimidin-2-yl)-7-azabicyclo[2.2.1]heptan-2-amine (14b)
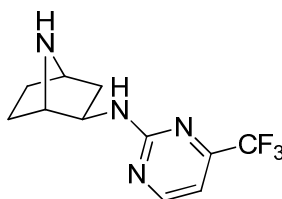
14b

General Procedure C was followed using **13b** (55 mg, 0.123 mmol) to give **14b** as white-yellow solid (40.0 mg; purity 80%; 0.124 mmol, quant).

ANALYSIS
Formula: $C_{11}H_{13}F_3N_4$
Mol. Weight: 258.24 g/mol
^{1}H NMR (400 MHz, CDCl$_3$) δ = 8.57 - 8.42 (m, 1 H); 6.83 (d, J=4.9 Hz, 1 H); 5.68 (brs, 1 H); 4.02 (td, J=7.7, 3.2 Hz, 1 H); 3.78 (t, J=4.4 Hz, 1 H); 3.66 (d, J=4.9 Hz, 1 H); 2.17 (brs, 1 H); 1.99 (dd, J=13.2, 7.8 Hz, 1 H); 1.78 - 1.36 (m, 5 H).
^{13}C-NMR (DEPT) (100 MHz, CDCl$_3$) δ = 161.67 (C), 160.33 (CH), 156.37 (q, J=33.6, C), 120.49 (q, J=275.02, CF$_3$), 105.52 (CH), 61.55 (CH), 55.65 (CH), 54.49 (CH), 40.28 (CH$_2$), 29.40 (CH$_2$), 26.71 (CH$_2$).
MS (ESI+) m/z (%) = 259 (100) [MH]$^+$.

(+/-)-*exo*-N-(5-(trifluoromethyl)pyrazin-2-yl)-7-azabicyclo[2.2.1]heptan-2-amine (14c)

14c
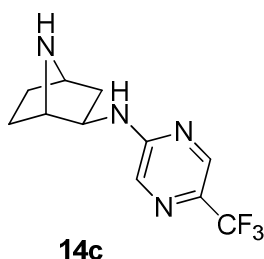
General Procedure C was followed using **13c** (50 mg, 0.140 mmol) to give **14c** as white solid (34.0 mg; 0.130 mmol, 93%).

ANALYSIS
Formula: $C_{11}H_{13}F_3N_4$
Mol. Weight: 258.24 g/mol
^{1}H NMR (400 MHz, CDCl$_3$) δ = 8.33 (s, 1 H); 7.88 (s, 1 H); 5.44 (d, J=7.3 Hz, 1 H); 4.01 (td, J=7.8, 2.9 Hz, 1 H); 3.81 (t, J=4.4 Hz, 1 H); 3.65 (d, J=4.9 Hz, 1 H); 2.38 (brs, 1 H); 2.00 (dd, J=12.7, 7.8 Hz, 1 H); 1.74 - 1.55 (m, 3 H); 1.55 - 1.44 (m, 2 H).
^{13}C-NMR (DEPT) (100 MHz, CDCl$_3$) δ = 154.76 (C), 139.86 (CH), 131.59 (q, J=35.1), 132.57 (CH), 122.36 (q, J=271.53, CF$_3$), 61.57 (CH), 55.75 (CH), 53.80 (CH), 39.83 (CH$_2$), 29.57 (CH$_2$), 26.72 (CH$_2$).
MS (ESI+) m/z (%) = 260 (100) [MH]$^+$.

N-((+/-)-exo-7-azabicyclo[2.2.1]heptan-2-yl)-2-phenylacetamide (14d)
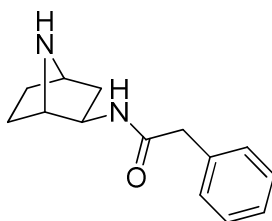
14d

General Procedure C was followed using **13d** (67 mg, 0.193 mmol) to give **14d** as white-yellow solid (46 mg; purity 90%; 0.180 mmol, 93%).
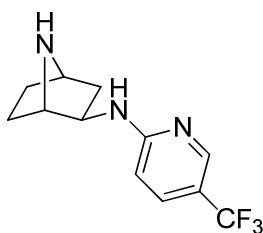
ANALYSIS
Formula: $C_{14}H_{18}N_2O$
Mol. Weight: 230.31 g/mol
^{1}H NMR (400 MHz, CDCl$_3$) δ = 7.39 - 7.32 (m, 2 H); 7.32 - 7.29 (m, 2 H); 7.27 (s, 1 H); 5.93 - 5.67 (m, 1 H); 3.93 (td, J=8.1, 2.9 Hz, 1 H); 3.68 - 3.63 (m, 1 H); 3.54 (s, 2 H); 3.47 (d, J=4.4 Hz, 1 H); 2.02 (brs, 1 H); 1.83 (dd, J=13.0, 8.1 Hz, 1 H); 1.61 - 1.42 (m, 3 H); 1.42 - 1.33 (m, 1 H); 1.30 - 1.21 (m, 1 H).
^{13}C-NMR (DEPT) (100 MHz, CDCl$_3$) δ = 170.31 (C), 135.08 (C), 129.25 (CH), 128.82 (CH), 127.11 (CH), 62.01 (CH), 55.51 (CH), 52.15 (CH), 43.79 (CH$_2$), 39.71 (CH$_2$), 29.54 (CH$_2$), 27.07 (CH$_2$).
MS (ESI+) m/z (%) = 232.1 (100) [MH]$^+$.

(+/-)-exo-N-(5-(trifluoromethyl)pyridin-2-yl)-7-azabicyclo[2.2.1]heptan-2-amine (14e)

14e

General Procedure C was followed using **13e** (275 mg, 0.770 mmol) to give **14e** as white solid (186 mg, 0.716 mmol, 93%).

ANALYSIS
Formula: $C_{12}H_{14}F_3N_3$
Mol. Weight: 257.25 g/mol
^{1}H NMR (400 MHz, CDCl$_3$) δ = 8.35 (s, 1 H); 7.56 (dd, J=8.8, 2.45 Hz, 1 H); 6.39 (d, J=8.8 Hz, 1 H); 5.10 (d, J=6.4 Hz, 1 H); 3.87 (td, J=7.5, 3.2 Hz, 1 H); 3.75 (t, J=4.4 Hz, 1 H); 3.60 (d, J=4.9 Hz, 1 H); 1.98 (dd, J=13.0, 7.6 Hz, 1 H); 1.68 - 1.38 (m, 5 H).

13C-NMR (DEPT) (100 MHz, CDCl$_3$) δ = 159.58 (C), 146.12 (CH), 134.07 (CH), 124.63 (q, J=270.2, CF$_3$), 115.36 (q, J=32.9, C), 106.93 (CH), 61.23(CH), 55.47 (CH), 54.75 (CH), 40.77 (CH$_2$), 29.77 (CH$_2$), 26.96 (CH$_2$).

MS (ESI+) m/z (%) = 258 (100) [MH]$^+$.

General Procedure D: synthesis of *(+/-)-exo*-compounds 12a-i

To a solution of the appropriate carboxylic acid (1.0 eq) in dioxane (1 mL) were added in sequence *N*-methylmorpholine (3 eq) and CDMT (1.5 eq) under N_2 atmosphere and the resultant solution was stirred for 30 min at room temperature. Then the amine **14a-e** was added (1.2 eq) pre-dissolved in dioxane (1 mL) and the mixture was stirred at 100 °C for 1 h.

The solvent was then evaporated under reduced pressure. The residue was taken up in AcOEt and washed in sequence with NH_4Cl sat. sol., $NaHCO_3$ sat. sol. and water. Then the organic layer was dried over anhydrous Na_2SO_4, filtered and the solvent was eliminated under reduced pressure.

Purification: Isolera-One Biotage, flash chromatography by HP-SI Column or Reverse Phase Column. The containing product fractions were collected and the solvent eliminated under reduced pressure to give the final compound **12a-i** as *(+/-)-exo*-racemic mixture.

Analysis of proton and carbon NMR spectra reveals for compounds **12a-i** the presence of two rotamers of the molecule in ratio ranging from 8:3 to 7:3. In particular, in proton NMR spectra the major rotamer can be easily detected and described. On the contrary, carbon NMR spectra are complicated by the presence of signals splitted by the presence of C-F coupling and the C_{sp2} carbon atom signals are difficult to distinguish and assign. For these reasons in carbon NMR spectra only the chemical shifts of aliphatic carbons are reported for both rotamers of each compound.

(2-methyl-5-phenylthiazol-4-yl) *(+/-)-exo*-2-((4-(trifluoromethyl)pyridin-2-yl)amino)-7-azabicyclo[2.2.1]heptane-7-carboxylate (12a)
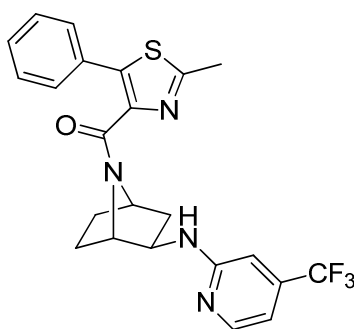
12a

General Procedure D was followed using the 2-methyl-5-phenylthiazole-4-carboxylic acid (35 mg, 0.160 mmol), amine **14a** (30 mg, 0.105 mmol), NMM (0.040 mL, 0.364 mmol) and CDMT (33 mg, 0.188 mmol) in dioxane (2 mL). After purification (Snap 10g HP-SI Column, sample dissolved in DCM 100%, eluent: from DCM/MeOH 100:0 to 95:5 in gradient) **12a** was obtained as white solid (43mg; 0.092 mmol; 88%).

ANALYSIS
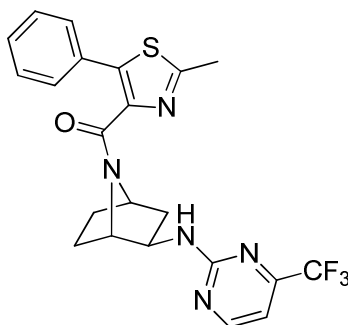**Formula**: $C_{23}H_{21}F_3N_4OS$

Mol. Weight: 458.50 g/mol

Note: From NMR spectra two signal patterns were observed (about 7:3 ratio in acetone-d_6) due to the two rotamers of the molecule. Chemical shifts of the major rotamer are reported.

¹H NMR (400 MHz, Acetone-d_6) (major rotamer) δ = 8.18 (d, J=5.2, 1H); 7.54 - 7.49 (m, 2H); 7.46 - 7.35 (m, 3H); 6.74 (d, J=5.4, 1H); 6.71 (s, 1H); 6.30 (brs, 1H); 4.69 (t, J=4.9, 1H); 4.12 (d, J=5.2, 1H); 3.96 (m, 1H); 2.50 (s, 3H); 2.10 (m, 1H); 1.78 – 1.26 (m, 5H).

¹³C-NMR (DEPT) (100 MHz, CDCl$_3$) (major rotamer) δ = 61.87 (CH), 58.28 (CH), 57.55 (CH), 55.15 (CH), 54.68 (CH), 53.08 (CH), 41.14 (CH$_2$), 39.70 (CH$_2$), 29.09 (CH$_2$), 28.14 (CH$_2$), 26.29 (CH$_2$), 25.27 (CH$_2$), 19.19 (CH$_3$), 18.81 (CH$_3$).

MS (ESI+) m/z (%) = (100) [MH]$^+$

(2-methyl-5-phenylthiazol-4-yl) *(+/-)-exo*-2-((4-(trifluoromethyl)pyrimidin-2-yl)amino)-7-azabicyclo[2.2.1]heptane-7-carboxylate (12b)

12b

General Procedure D was followed using 2-methyl-5-phenylthiazole-4-carboxylic acid (30 mg, 0.137 mmol), amine **14b** (25 mg, 0.097 mmol), NMM (0.032 mL, 0.290 mmol) and CDMT (30 mg, 0.171 mmol) in dioxane (2 mL). After purification (Snap 10g HP-SI Column, sample dissolved in DCM 100%, eluent: from DCM/MeOH 100:0 to 95:5 in gradient) **12b** was obtained as white solid (32mg; 0.070 mmol; 71.9%).

ANALYSIS

Formula: C$_{22}$H$_{20}$F$_3$N$_5$OS
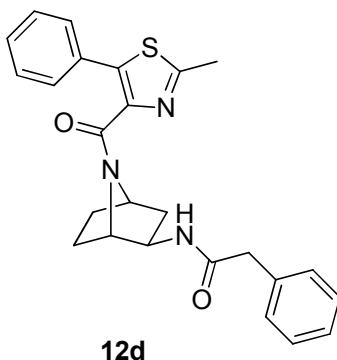
Mol. Weight: 459.49 g/mol

Note: From NMR spectra were observed two signal patterns (about 7:3 ratio in Acetone-d_6) due to the two rotamers of the molecule. Chemical shifts of the major rotamer are reported.

¹H NMR (400 MHz, Acetone-d_6) (major rotamer) δ = 8.59 (d, J=4.8, 1H); 7.61 - 7.55 (m, 2H); 7.46 - 7.37 (m, 3H); 6.97 (d, J=4.8, 1H); 6.44 (brs, 1H); 4.75 (t, J=4.7, 1H); 4.29 (m, 1H); 4.03 (m, 1H); 2.63 (s, 3H); 2.10 (m, 1H); 1.87 – 1.35 (m, 5H).

¹³C-NMR (DEPT) (100 MHz, CDCl$_3$) (major rotamer) δ = 61.46 (CH), 58.31 (CH), 57.28 (CH), 55.34 (CH), 54.31 (CH), 53.28 (CH), 40.71 (CH$_2$), 40.25 (CH$_2$), 29.35 (CH$_2$), 27.98 (CH$_2$), 27.4 (CH$_2$)1, 24.98 (CH$_2$), 19.15 (CH$_3$), 18.76 (CH$_3$).

MS (ESI+) m/z (%) = 461 (100) [MH]⁺.

(2-methyl-5-phenylthiazol-4-yl) *(+/-)-exo*-**2-((5-(trifluoromethyl)pyrazin-2-yl)amino)-7-azabicyclo[2.2.1]heptane-7-carboxylate (12c)**
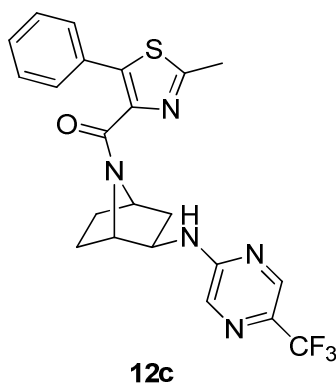
12c

General Procedure D was followed using the 2-methyl-5-phenylthiazole-4-carboxylic acid (30 mg, 0.137 mmol), amine **14c** (25 mg, 0.097 mmol), NMM (0.032 mL, 0.290 mmol) and CDMT (30 mg, 0.171 mmol) in dioxane (2 mL). After purification (Snap 10g HP-SI Column, sample dissolved in DCM 100%, eluent: from DCM/MeOH 100:0 to 95:5 in gradient) **12c** was obtained as white solid (36.0 mg; 0.078 mmol; 81%).

ANALYSIS
Formula: $C_{22}H_{20}F_3N_5OS$
Mol. Weight: 459.49 g/mol
Note: From NMR spectra in Acetone-d_6 there were two signal patterns in about 75:25 ratio due to the two rotamers of the molecule. Chemical shifts of the major rotamer are reported.
¹H NMR (400 MHz, Acetone-d_6) (major rotamer) δ = 8.30 (s, 1H); 7.99 (s, 1H); 7.52 - 7.48 (m, 2H); 7.45 - 7.39 (m, 3H); 7.10 (brs, 1H); 4.71 (t, J=4.8, 1H); 4.19 (d, J=5.3 Hz, 1H); 3.95 (m, 1H); 2.48 (s, 3H); 2.10 (m, 1H); 1.82 – 1.21 (m, 5H).
¹³C-NMR (DEPT) (100 MHz, CDCl₃) (major rotamer) δ = 61.10 (CH), 58.22 (CH), 57.67 (CH), 55.08 (CH), 54.42 (CH), 53.19 (CH), 41.01 (CH₂), 39.31 (CH₂), 29.10 (CH₂), 28.32 (CH₂), 26.14 (CH₂), 25.30 (CH₂), 18.79 (CH₃), 18.63 (CH₃).
MS (ESI+) m/z (%) = 461 (100) [MH]⁺.

N-((+/-)-*exo*-7-(2-methyl-5-phenylthiazole-4-carbonyl)-7-azabicyclo[2.2.1]heptan-2-yl)-2-phenylacetamide (12d)

12d

General Procedure D was followed using the 2-methyl-5-phenylthiazole-4-carboxylic acid (37.1 mg, 0.169 mmol), amine **14d** (30 mg, 0.130 mmol), NMM (0.043 mL, 0.391 mmol) and CDMT (36.6 mg, 0.208 mmol) in dioxane (2 mL). After purification (Snap 10g HP-SI Column, sample dissolved in DCM 100%, eluent: from DCM/MeOH 100:0 to 95:5 in gradient) **12d** was obtained as white-yellow solid (43.5 mg; 0.097 mmol; 74.3%).

ANALYSIS
Formula: $C_{25}H_{25}N_3O_2S$
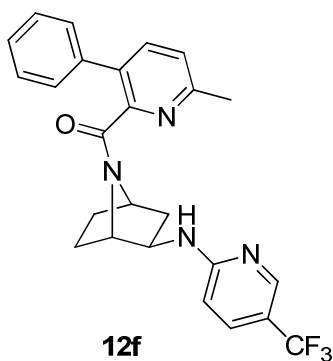**Mol. Weight**: 431.55 g/mol
Note: From NMR spectra were observed two signal patterns (about 7:3 ratio in Acetone-d_6) due to the two rotamers of the molecule. Chemical shifts of the major rotamer are reported.
^{1}H NMR (400 MHz, Acetone-d_6) (major rotamer) δ = 7.61 - 7.55 (m, 2H); 7.47 - 7.36 (m, 3H); 7.36 - 7.17 (m, 5H); 4.66 (t, J=4.8 Hz, 1H); 4.00 (d, J=5.1 Hz, 1H); 3.80 (m, 1H); 3.47 (d, J=14.5 Hz, 1H); 3.39 (d, J=14.5 Hz, 1H); 2.72 (s, 3H); 1.97 (m, 1H); 1.69 – 1.25 (m, 5H).
^{13}C-NMR (DEPT) (100 MHz, CDCl$_3$) (major rotamer) δ = 62.09 (CH), 58.94 (CH), 57.54 (CH), 53.68 (CH), 52.92 (CH), 52.62 (CH), 43.53 (CH$_2$), 43.29 (CH$_2$), 40.48 (CH$_2$), 39.63 (CH$_2$), 28.87 (CH$_2$), 28.01 (CH$_2$), 26.42 (CH$_2$), 25.33 (CH$_2$), 19.00 (2 x CH$_3$).
MS (ESI+) m/z (%) = 433.2 (100) [MH]$^+$.

(2-methyl-5-phenylthiazol-4-yl)(*(+/-)-exo*-2-((5-(trifluoromethyl)pyridin-2-yl)amino)-7-azabicyclo[2.2.1]heptan-7-yl)methanone (12e)
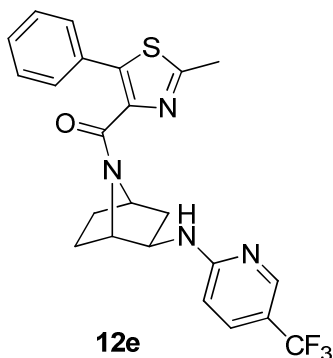
12e

General Procedure D was followed using the 2-methyl-5-phenylthiazole-4-carboxylic acid (35 mg, 0.160 mmol), amine **14e** (30 mg, 0.117 mmol), NMM (0.040 mL, 0.364 mmol) and CDMT (33 mg, 0.188 mmol) in dioxane (2 mL). After purification (Snap 10g HP-SI Column, sample dissolved in DCM 100%, eluent: from DCM/MeOH 100:0 to 95:5 in gradient) was obtained **12e** as white solid (46.5 mg, 0.100 mmol, 86%).

ANALYSIS

Formula: $C_{23}H_{21}F_3N_4OS$

Mol. Weight: 458.50 g/mol

Note: From NMR spectra were observed two signal patterns (about 7:3 ratio in CDCl$_3$) due to the two rotamers of the molecule. Chemical shifts of the major rotamer are reported.

^{1}H NMR (400 MHz, CDCl$_3$) (major rotamer) δ = 8.29 (s, 1H); 7.54 - 7.36 (m, 6H); 6.35 (d, J=8.8 Hz, 1H); 5.93 (brs, 1H); 4.86 (t, J=4.9, 1H); 4.06 (m, 2H); 2.64 (s, 3H); 2.12 (m, 1H); 1.85 – 1.20 (m, 5H).

^{13}C-NMR (DEPT) (1001 MHz, CDCl$_3$) (major rotamer) δ = 61.61 (CH), 55.13 (CH), 53.07 (CH), 39.99 (CH$_2$), 28.22 (CH$_2$), 26.42 (CH$_2$), 18.96 (CH$_3$).

MS (ESI+) m/z (%) = 460 (100) [MH]$^+$

(6-methyl-3-phenylpyridin-2-yl)(*(+/-)-exo*-2-((5-(trifluoromethyl)pyridin-2-yl)amino)-7-azabicyclo[2.2.1]heptan-7-yl)methanone (12f)

12f

General Procedure D was followed using the 6-methyl-3-phenylpicolinic acid (30 mg, 0.141 mmol), amine **14e** (30 mg, 0.117 mmol), NMM (0.040 mL, 0.364 mmol) and CDMT (31 mg, 0.177 mmol) in dioxane (2 mL). After purification (Snap 10g HP-SI Column, sample dissolved in DCM 100%, eluent: from DCM/MeOH 100:0 to 95:5 in gradient) **12f** was obtained as white solid (43 mg; 0.093 mmol; 80%).

ANALYSIS

**Formula**: $C_{25}H_{23}F_3N_4O$

Mol. Weight: 452.47 g/mol

Note: From NMR spectra analysis two signal patterns were observed (about 7:3 ratio in CDCl$_3$) due to the two rotamers of the molecule. Chemical shifts of the major rotamer are reported.

^{1}H NMR (400 MHz, CDCl$_3$) (major rotamer) δ = 8.25 (s, 1H); 7.67 (d, J=8.0 Hz, 1H); 7.52 - 7.39 (m, 6H); 7.22 (d, J=8 Hz, 1H); 6.45 (d, J=8.8 Hz, 1H); 6.33 (brs, 1H); 4.81 (t, J=4.9, 1H); 4.07 (m, 1H); 3.67 (d, J=5.3 Hz 1H); 2.62 (s, 3H); 2.07 (m, 1H); 1.88 – 1.10 (m, 5H).

^{13}C-NMR (DEPT) (100 MHz, CDCl3) (major rotamer) δ = 60.94 (CH), 58.06 (CH), 56.31 (CH), 55.07 (CH), 53.84 (CH), 52.51 (CH), 40.64 (CH$_2$), 40.27 (CH$_2$), 29.02 (CH$_2$), 28.39 (CH$_2$), 26.36 (CH$_2$), 25.3 (CH$_2$)7, 24.12 (CH$_3$), 23.97 (CH$_3$).

MS (ESI+) m/z (%) = 454 (100) [MH]$^+$.

(6-methyl-3-(pyrimidin-2-yl)pyridin-2-yl)(*(+/-)-exo*-2-((5-(trifluoromethyl)pyridin-2-yl)amino)-7-azabicyclo[2.2.1]heptan-7-yl)methanone (12g)
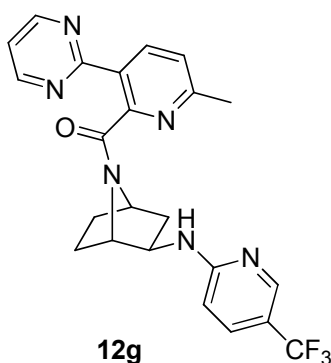
12g

General Procedure D was followed using the 6-methyl-3-(pyrimidin-2-yl)picolinic acid (30 mg, 0.141 mmol), amine **14e** (30 mg, 0.117 mmol), NMM (0.040 mL, 0.364 mmol) and CDMT (32 mg, 0.182 mmol) in dioxane (2 mL). After purification (RediSep Rf Gold AqC18 30g Column, sample dissolved in DMSO+AcOH, eluent additive 0.1% AcOH, eluent: from water/CH$_3$CN 100:0 to 0:100 in gradient) **12g** was obtained as white solid (37 mg; 0.081 mmol; 69.8%).

ANALYSIS

**Formula**: $C_{23}H_{21}F_3N_6O$

Mol. Weight: 454.45 g/mol

¹H NMR (400 MHz, Acetone-d_6) (major rotamer) δ = 8.92 (d, J=4.9 Hz, 2H); 8.26 (m, 2H); 7.53 (dd, J=8.8, 1.9 Hz, 1H); 7.49 (t, J=4.9 Hz, 1H); 7.37 (d, J=8.0 Hz, 1H); 6.45 (d, J=8.8 Hz, 1H); 6.33 (brs, 1H); 4.72 (t, J=4.9 Hz, 1H); 4.26 (m, 1H); 4.18 (d, J=5.3 Hz, 1H); 2.52 (s, 3H); 2.19 (m, 1H); 1.90 – 1.57 (m, 5H).

¹³C-NMR (DEPT) (100 MHz, DMSO-d_6) (major rotamer) δ = 60.79 (CH), 58.20 (CH), 56.36 (CH), 55.16 (CH), 54.45 (CH), 52.42 (CH), 39.87 (CH₂), 38.01 (CH₂), 28.73 (CH₂), 28.47 (CH₂), 25.98 (CH₂), 24.42 (CH₂), 23.80 (2 x CH₃).

MS (ESI+) m/z (%) = 456 (100) [MH]⁺.

(5-methyl-2-(pyrimidin-2-yl)phenyl)((+/-)-exo-2-((5-(trifluoromethyl)pyridin-2-yl)amino)-7-azabicyclo[2.2.1]heptan-7-yl)methanone (12h)

12h
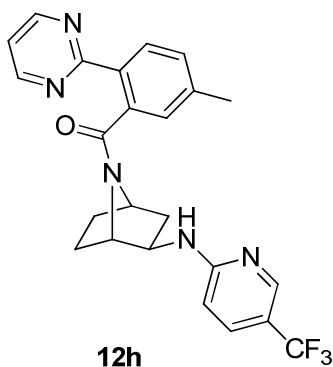
General Procedure D was followed using the 5-methyl-2-(pyrimidin-2-yl)benzoic acid (30.0 mg, 0.140 mmol), amine **14e** (30 mg, 0.117 mmol), NMM (0.040 mL, 0.364 mmol) and CDMT (32 mg, 0.182 mmol) in dioxane (2 mL). After purification (Snap 10g HP-SI Column, sample dissolved in DCM 100%, eluent: from DCM/MeOH 100:0 to 95:5 in gradient) **12h** was obtained as white-yellow solid (47 mg; 0.103 mmol; 88%).

ANALYSIS

Formula: C₂₄H₂₂F₃N₅O

Mol. Weight: 453.46 g/mol

Note: From NMR spectra analysis two signal patterns were observed (about 8:2 ratio in CDCl₃) due to the two rotamers of the molecule. Chemical shifts of the major rotamer are reported.

¹H NMR (400 MHz, CDCl₃) (major rotamer) δ = 8.85 (d, J=4.9 Hz, 2H); 8.24 (s, 1H); 7.87 (d, J=8.5 Hz, 1H); 7.57 (m, 1H); 7.43 – 7.359 (m, 2H); 7.24 (s, 1H); 6.54 (brs, 1H); 4.68 (t, J=4.6 Hz, 1H); 4.21 (m, 1H); 4.02 (d, J=4.9 Hz, 1H); 2.20 (s, 3H); 2.14 (m, 1H); 1.90 – 1.53 (m, 5H).

¹³C-NMR (DEPT) (100 MHz, DMSO-d_6) (major rotamer) δ = 61.45 (CH), 57.94 (CH), 57.05 (CH), 55.08 (CH), 54.13 (CH), 52.11 (CH), 39.70 (CH₂), 37.40 (CH₂), 28.88 (CH₂), 28.42 (CH₂), 25.61 (2 x CH₂), 21.33 (CH₃), 20.79 (CH₃).

MS (ESI+) m/z (%) = 454.2 (100) [MH]$^+$.

(5-chloro-2-(pyrimidin-2-yl)phenyl)((+/-)-*exo*-2-((5-(trifluoromethyl)pyridin-2-yl)amino)-7-azabicyclo[2.2.1]heptan-7-yl)methanone (12i)

12i
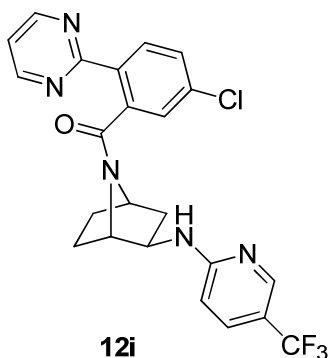
General Procedure D was followed using the 5-chloro-2-(pyrimidin-2-yl)benzoic acid (33 mg, 0.141 mmol), amine **14e** (30 mg, 0.117 mmol), NMM (0.040 mL, 0.364 mmol) and CDMT (32 mg, 0.182 mmol) in dioxane (2 mL). After purification (Snap 10g HP-SI Column, sample dissolved in DCM 100%, eluent: from DCM/MeOH 100:0 to 95:5 in gradient) **12h** was obtained as white-yellow solid (43 mg; purity 95%, 0.086 mmol; 73.9%).

ANALYSIS
Formula: C$_{23}$H$_{19}$ClF$_3$N$_5$O
Mol. Weight: 473.88 g/mol
Note: From NMR spectra analysis two signal patterns were observed (about 75:25 ratio in CDCl$_3$) due to the two rotamers of the molecule. Chemical shifts of the major rotamer are reported.
^{1}H NMR (400 MHz, CDCl$_3$) (major rotamer) δ = 8.85 (d, J=4.9 Hz, 2H); 8.26 (s, 1H); 7.99 (d, J=8.3 Hz, 1H); 7.46 (dd, J=8.4, 2.0 Hz, 1H); 7.34 (m, 2H); 6.01 (brs, 1H); 4.87 (t, J=4.2 Hz, 1H); 4.40 (m, 1H); 4.05 (d, J=3.7 Hz, 1H); 2.23 (m, 1H); 2.20 - 1.50 (m, 5H).
^{13}C-NMR (DEPT) (100 MHz, CDCl$_3$) (major rotamer) δ = 63.55 (CH), 58.46 (CH), 57.67 (CH), 55.06 (CH), 54.88 (CH), 53.16 (CH), 41.58 (CH$_2$), 39.77 (CH$_2$), 29.04 (CH$_2$), 28.04 (CH$_2$), 26.72 (CH$_2$), 25.71 (CH$_2$).
MS (ESI+) m/z (%) = 474 (100) [MH]$^+$.

2.6 Synthesis of (+/-)-endo- and (+/-)-exo-2-azabicyclo[2.2.1]heptan-6-amine (18 and 22), experimental data

(+/-)-2-benzyl-2-azabicyclo[2.2.1]hept-5-ene (15)

15
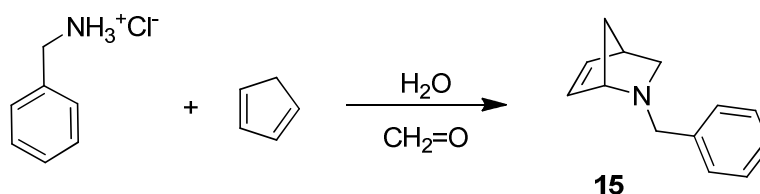
Benzylamine hydrochloride (6.54 g, 45.5 mmol) and formaldehyde 37% Wt in water (4.77 mL, 63.7 mmol) were dissolved in water (25 mL) and the resulting solution was stirred under N_2 for 5 min. Freshly distilled cyclopenta-1,3-diene (7.4 ml, 91 mmol) was then added and the resulting mixture was allowed to stir vigorously for 18 h at room temperature.

Then the reaction mixture was extracted with CyHex/Et$_2$O 1:1 (4x50 mL). The aqueous layer was made basic (pH about 11-12) with NaOH 2M and extracted with Et$_2$O (3x30 mL). The combined organic layers were dried over anhydrous Na$_2$SO$_4$, filtered and concentrated.

Purification: isolera-One Biotage, Snap 340g HP-SI Column, sample dissolved in DCM, eluent: from CyHex/AcOEt 80:20 to 0:100 in gradient.

The containing product fractions were collected and the solvent eliminated under reduced pressure to give **15** as pale yellow oil (7.25g, purity 95%, 37.2 mmol, 82%)

ANALYSIS
Formula: C$_{13}$H$_{15}$N
Mol. Weight: 185.26
^{1}H NMR (400 MHz, CDCl$_3$) δ = 7.39 - 7.29 (m, 4 H); 7.29 - 7.21 (m, 1 H); 6.40 (dd, J=4.9, 3.3 Hz); 6.11 (dd, J=5.7, 1.9 Hz, 1 H); 3.84 (d, J=1.2 Hz, 1 H); 3.60 (d, J=13.2 Hz, 1 H); 3.36 (d, J=13.2 Hz, 1 H); 3.19 (dd, J=8.8, 3.0 Hz, 1 H); 2.95 (brs, 1 H); 1.66 (d, J=8.8 Hz, 1 H); 1.55 (dd, J=8.6, 2.0 Hz, 1 H); 1.43 (dd, J=8.0, 1.5 Hz, 1 H).
^{13}C NMR (DEPT) (100 MHz, CDCl$_3$) δ = 139.93 (C), 136.38 (CH), 130.95 (CH), 128.73 (CH), 128.20 (CH), 126.72 (CH), 64.40 (CH), 59.19 (CH$_2$Ph), 52.60 (CH$_2$), 48.17 (CH$_2$), 43.99 (CH).
MS (ESI+) m/z (%) = 186 (100%) [MH]$^+$.

(+/-)-*exo*-2-benzyl-2-azabicyclo[2.2.1]heptan-6-ol (16)
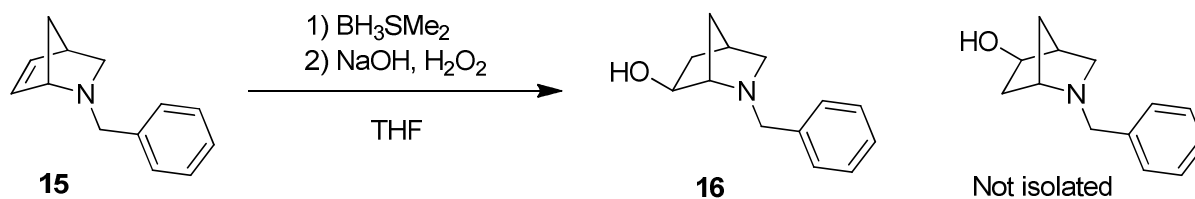
To a stirred solution of **15** (90%) (5.4 g, 26.23 mmol) in dry THF (50 mL), cooled at 0 °C under N_2 atmosphere, borane-dimethylsulfide complex 2M in THF solution (24.29 mL, 48.6 mmol) was added dropwise. The stirring was continued for 4 h at room temperature.

The excess of BH_3 was destroyed by careful addition of a 1:1 mixture of THF-water (15 mL) at 0 °C. Subsequently sodium hydroxide 2N (9.72 mL, 19.43 mmol) was added in one portion and hydrogen peroxide 35% in water (9.57 mL, 109 mmol) dropwise. The resulting mixture was kept at 40 °C for 1.5 h with stirring.

Then, after cooling to room temperature, K_2CO_3 (2.5 g) was added and the THF was removed under reduced pressure. The remaining solution was extracted with DCM (3x 40 mL), and the combined extracts were washed with water (50 mL). The organic extract was dried over anhydrous Na_2SO_4, filtered, and concentrated under reduced pressure.

Purification: Isolera-One Biotage, Snap 340g HP-SI Column, sample dissolved in DCM, eluent: DCM/MeOH/NH_4OH 95:4.5:0.5 isocratic.

The containing product fractions were collected and the solvent was eliminated under reduced pressure to give **16** as clear oil (2.95 g, purity 90%, 13.07 mmol, 50%).

ANALYSIS

Formula: $C_{13}H_{17}NO$

Mol. Weight: 203.28 g/mol
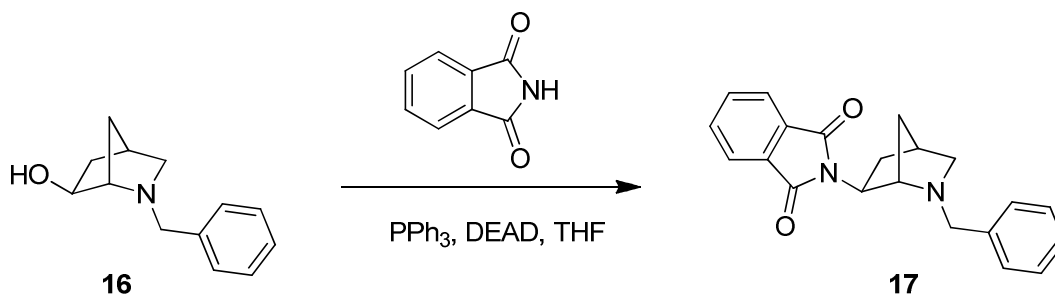
^{1}H NMR (400 MHz, CDCl$_3$) δ = 7.41 - 7.21 (m, 5 H); 4.13 (d, J=6.8 Hz, 1 H); 3.72 (m, 2 H); 3.06 (s, 1 H); 2.53 (dt, J=8.8, 3.0 Hz, 1 H); 2.43 (brs, 1 H); 2.37 (d, J=8.8 Hz, 1 H); 1.87 (dd, J=13.0, 7.1 Hz, 1 H); 1.58 (s, 2 H); 1.49 (brs, 1 H); 1.35 (ddt, J=12.8, 4.5, 2.3, 2.3 Hz, 1 H).

^{13}C NMR (DEPT) (100 MHz, CDCl$_3$) δ = 139.33 (C), 128.65 (CH), 128.29 (CH), 126.97 (CH), 72.12 (CH), 65.84 (CH), 59.45 (CH_2Ph), 58.51 (CH_2), 40.21 (CH_2), 36.50 (CH), 31.17 (CH_2).

MS (ESI+) m/z (%) = 204 (100%) [MH]$^+$.

2-((+/-)-exo-2-benzyl-2-azabicyclo[2.2.1]heptan-6-yl)isoindoline-1,3-dione (17)

To a mixture of **16** (50 mg, 0.246 mmol), phthalimide (57.9 mg, 0.394 mmol) and triphenylphosphine (103 mg, 0.394 mmol) in THF (2 mL), 1,2-ethoxycarbonyl diazene 40% in toluene (0.179 mL, 0.394 mmol) was added under N_2 atmosphere at 0 °C. The reaction mixture was then stirred at room temperature overnight.

The reaction mixture was diluted with Et_2O (15 mL) and the precipitate that formed was filtered off. The filtrate was concentrated under reduced pressure.

Purification: Isolera-One Blotage, Snap HP-SI 10g Column, sample dissolved in DCM, eluent: from CyHex/AcOEt 100:0 to 35:65 in gradient.

The containing product fractions were collected and the solvent was eliminated under reduced pressure to give **17** as white solid (48 mg, purity 95%, 0.14 mmol, 56%)

ANALYSIS

Chemical Formula: $C_{21}H_{20}N_2O_2$

Mol. Weight: 332.40 g/mol

^{1}H NMR (400 MHz, $CDCl_3$) δ = 7.81 (m, 2 H); 7.70 (m, 2 H); 7.42 (m, 2 H); 7.31 (m, 2 H); 7.23 (m, 1 H); 4.66 (ddd, J=8.7, 5.3, 1.1 Hz, 1 H); 3.82 (m, 2 H); 3.38 (s, 1 H) 2.84 (dt, J=8.9, 3.4, 1 H); 2.57 (brs, 1 H); 2.37 (m, 1 H); 2.27 (t, J=9.4, 2 H); 1.89 (ddd, J=11.9, 9.0, 2.1 Hz, 1 H); 1.77 (m, 1 H).

^{13}C NMR (DEPT) (100 MHz, $CDCl_3$) δ = 168.74 (C=O), 134.23 (CH), 133.86 (CH), 131.86 (C), 128.54 (CH), 128.25 (CH), 126.83 (CH), 122.99 (CH), 64.36 (CH), 58.09 (CH_2), 57.72 (CH_2Ph), 51.58 (CH), 37.54 (CH) 35.05 (CH_2) 34.69 (CH_2).

MS (ESI+) m/z (%) = 334.4 (100%) $[MH]^+$.

(+/-)-*exo*-2-benzyl-2-azabicyclo[2.2.1]heptan-6-amine (18)
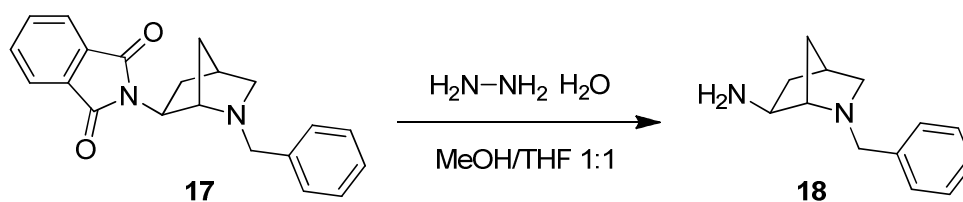
Compound **17** (920 mg, 2.77 mmol) was dissolved in MeOH/THF 1:1 (40 mL). Subsequently hydrazine monohydrate (0.537 mL, 11.07 mmol) was added and the mixture was hated at 65 °C for 2 h.

The formed precipitate was collected by filtration using THF (20 mL), and the filtrate was concentrated under reduced pressure. The residue was treated with NaOH 1M solution (30 mL) and then extracted with DCM (3x30 mL). The organic layers were collected dried over anhydrous Na_2SO_4, filtered, and the solvent was eliminated under reduced pressure to give **18** as white-yellow solid (585 mg, purity 90%, 2.60 mmol, 94%).

ANALYSIS

Formula: $C_{13}H_{18}N_2$

Mol. Weight: 202.30 g/mol

Note: -NH_2 signal was detected only in ^{1}H NMR spectra in DMSO-d_6.

^{1}H NMR (400 MHz, DMSO-d_6) δ = 7.30 (m, 4 H); 7.21 (m, 1 H); 3.66 (d, J=13.7 Hz, 1H); 3.59 (d, J=13.7 Hz, 1H); 3.07 (dd, J=7.6, 3.2 Hz, 1 H); 2.74 (s, 1 H); 2.43 (dt, J=8.6, 3.3 Hz, 1 H); 2.25 (brs, 1 H); 2.12 (d, J=8.8 Hz, 1 H); 1.62 (ddd, J=12.2, 7.6, 2.2 Hz, 1 H); 1.50 (m, 1 H); 1.45 (brs, 2 H); 1.39 (m, 1 H); 0.98 (dq, J=11.9, 3.4 Hz, 1 H).

^{1}H NMR (400 MHz, CDCl$_3$) δ = 7.43 - 7.38 (m, 2 H); 7.36 - 7.31 (m, 2 H); 7.27 - 7.23 (m, 1 H); 3.81 - 3.67 (m, 2 H); 3.35 (m, 1 H); 2.93 (s, 1 H); 2.62 (dt, J=9.1, 3.1 Hz, 1 H); 2.41 (brs, 2 H); 1.87 (ddd, J=12.6, 7.9, 2.0 Hz, 1 H); 1.61 (d, J=10.3 Hz, 1 H); 1.52 (d, J=10.3 Hz, 1 H); 1.11 (dq, J=12.5, 3.4 Hz, 1 H).

^{13}C NMR (DEPT) (100 MHz, CDCl$_3$) δ = 140.17 (C), 128.44 (CH), 128.20 (CH), 126.68 (CH), 67.40 (CH), 59.29 (CH$_2$), 58.50 (CH$_2$), 52.69 (CH), 40.59 (CH$_2$), 37.16 (CH), 31.23 (CH$_2$).

MS (ESI+) m/z (%) = 203 (100%) [MH]$^+$.

(+/-)-exo-*tert*-butyl 6-hydroxy-2-azabicyclo[2.2.1]heptane-2-carboxylate (19)
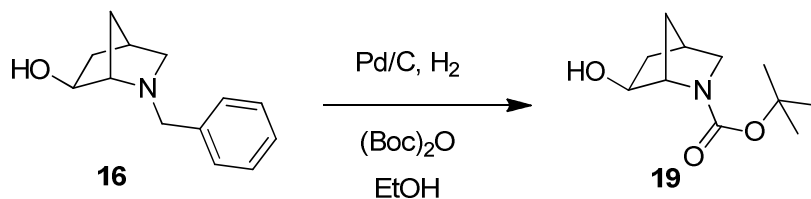
Palladium 10% on activated carbon (0.733 g, 0.689 mmol) was suspended in EtOH (10 mL) and water (2 mL). This mixture was added to a solution of **16** (1.4 g, 6.89 mmol) and di-*tert*-butyl dicarbonate (3.01 g, 13.77 mmol) in EtOH (30 mL). The reaction was conduced in a hydrogenation apparatus. The reaction mixture was subject to four H_2/Vacum cycles. Then the solution was stirred at room temperature under H_2 atmosphere (30 psi) for 1.5 h.

Then the reaction mixture was filtered through a filter septum washing with EtOH (30 mL) and MeOH (5mL). The filtrate was concentrated under reduced pressure to give an oily residue.

Purification: Isolera-One BIotage, Snap HP-SI 100g Column, sample dissolved in DCM, eluent: from CyHex/AcOEt 75:25 to 0:100 in gradient.

The containing product fractions were collected and the solvent was eliminated under reduced pressure to give **19** as white solid (1.28 g, 6.00 mmol, 87%).

ANALYSIS
Formula: $C_{11}H_{19}NO_3$
Mol. Weight: 213.27 g/mol
^{1}H NMR (400 MHz, DMSO-d_6) δ = 4.92 (brs, 1 H); 3.89 (d, J=19.0 Hz, 1 H); 3.68 (brs, 1 H); 3.01 (dd, J=19.1, 3.4 Hz, 1 H); 2.69 (d, J=9.0 Hz, 1 H); 2.43 (brs, 1 H); 1.75 - 1.65 (m, 1 H); 1.65 - 1.57 (m, 1 H); 1.45 - 1.33 (m, 10 H); 1.31 - 1.22 (m, 1 H).
^{13}CNMR (DEPT) (100 MHz, CDCl$_3$) δ = 154.50 (NC=O), 79.38 (C); 72.20 (CH), 60.76 (CH), 51.51 (CH$_2$), 39.40 (CH$_2$), 35.80 (CH), 33.44 (CH$_2$) 28.54 (3 x CH$_3$).
MS (ESI+) m/z (%) = 214 (100%) [MH]$^+$.

(+/-)-*tert*-butyl 6-oxo-2-azabicyclo[2.2.1]heptane-2-carboxylate (20)
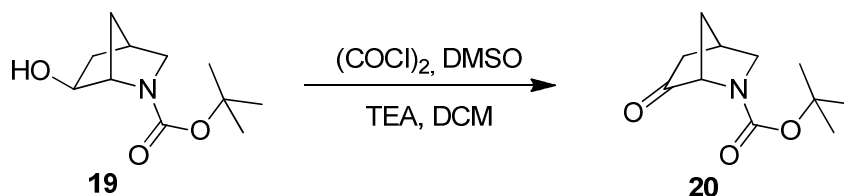
To a stirred solution of oxalyl chloride (0.502 mL, 5.93 mmol) in dry DCM (20 mL), cooled at-78°C, a solution of dimethyl sulfoxide (0.919 mL, 12.94 mmol) in DCM (1 mL) was added dropwise. The mixture was stirred for 10 min, then a solution of **19** (1.15 g, 5.39 mmol) in DCM (10 mL) was added dropwise. The reaction mixture was stirred at -78°C for 3 h, then TEA (2.71 mL, 19.41 mmol) was added and stirring continued for 5min at -78 °C and for 10 min at room temperature. The reaction mixture was then quenched with brine (40 mL), the organic layer was separated and the aqueous phase was extracted with DCM (3x40 mL). The organic layers were collected dried over anhydrous Na_2SO_4, filtered, and the solvent removed under reduced pressure.

Purification: Isolera-One Biotage, Snap HP-SI 50g Column, sample dissolved in DCM, eluent: from DCM/MeOH 100:0 to 95:5 in gradient.

The containing product fractions were collected and the solvent was eliminated under reduced pressure to give **20** as off-white solid (1.70 g, 5.06 mmol, 94%).

ANALYSIS

Note: NMR spectra show some signals splitted by the presence of two rotamers of the molecule. Chemical shifts of both rotamers are reported.

Formula: $C_{11}H_{17}NO_3$

Mol. Weight: 211.26 g/mol

^{1}H NMR (400 MHz, DMSO-d_6) δ = 3.96 (brs, 1 H); 3.31 (d, J=11.3 Hz, 1 H); 3.06 (d, J=9.3 Hz, 1 H); 2.77 (brs, 1 H); 2.23 (dd, J=17.8, 3.5 Hz, 1 H); 1.97 (dd, J=17.9, 3.5 Hz, 1 H); 1.81 (brs, 1 H); 1.74 (d, J=10.7 Hz, 1 H); 1.38 (s, 9 H).

^{13}C NMR (DEPT) (100 MHz, DMSO-d_6) δ = 205.95 (C=O), 154.58 - 153.94 (C=O), 79.59 (C); 61.58 - 61.62 (CH), 50.54 - 50.94 (CH_2), 41.59 (CH_2), 35.69 - 36.20 (CH_2), 34.27 - 34.84 (CH), 28.51 (3 x CH_3).

MS (ESI+) m/z (%) = 156 (100%) [M-56H]$^+$.

Mp: 83.5°C.

(+/-)-endo-tert-butyl 6-(benzylamino)-2-azabicyclo[2.2.1]heptane-2-carboxylate (21)
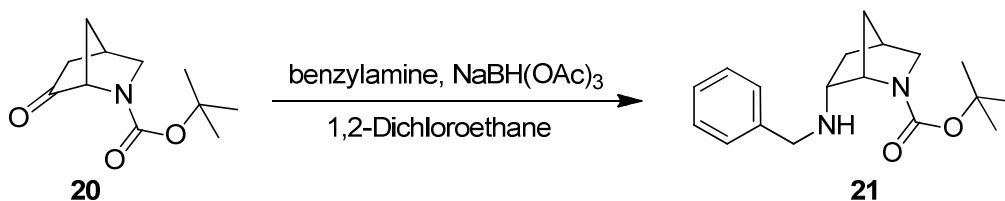
A solution of **20** (980 mg, 4.64 mmol) and benzylamine (0.600 mL, 5.49 mmol) in 1,2-dichloroethane (25 mL) was stirred at room temperature under N_2 atmosphere for 30 min. Then sodium triacetoxyhydroborate (1430 mg, 6.75 mmol) was added and the reaction mixture was stirred at room temperature, under N_2 atmosphere for 1 h.

$NaHCO_3$ sat. sol. (40 mL) was added to the reaction mixture, the organic layer was separated and the aqueous phase was extracted with DCM (3x40 mL). The organic layers were collected, dried over anhydrous Na_2SO_4, filtered, and the solvent was eliminated under reduced pressure.

Purification: Isolera-One Blotage, Snap HP-SI 50g Column, sample dissolved in DCM, eluent: from DCM/MeOH 100:0 to 95:5 in gradient.

The containing product fractions were collected and the solvent was eliminated under reduced pressure to give **21** as off-white solid (1.39 g, purity 95%, 4.35 mmol, 94%).

ANALYSIS

Note: NMR spectra show some signals splitted by the presence of two rotamers of the molecule. Chemical shifts of both rotamers are reported.

**Formula**: $C_{18}H_{26}N_2O_2$

Mol. Weight: 302.41 g/mol

^{1}H NMR (400 MHz, $CDCl_3$) δ = 7.33 (m, 5 H); 4.43 (m, 1 H); 4.01 (m, 1 H); 3.70 (m, 1 H); 3.36 (m, 1 H); 2.98 (m, 1 H); 2.47 (m, 1 H); 2.10 (m, 1 H); 1.68 (m, 1 H); 1.53 (m, 10 H); 0.89 (m, 1 H).

^{13}C NMR (DEPT) (100 MHz, $CDCl_3$) δ = 155.48 - 155.09 (C=O), 140.42 (C), 128.72 (CH), 128.31 (CH), 128.22 (CH), 127.86 (CH), 126.81 (CH), 79.38 - 79.02 (C); 61.45 - 61.13 (CH), 58.12 - 56.80 (CH), 53.63 - 53.15 (CH$_2$), 52.18 - 51.89 (CH$_2$), 37.23 - 36.71 (CH) 36.99 - 36.55 (CH$_2$), 36.38 - 36.30 (CH$_2$), 28.55 (3 x CH$_3$).

MS (ESI+) m/z (%) = 303 (100%) [MH]$^+$.

(+/-)-endo-tert-butyl 6-amino-2-azabicyclo[2.2.1]heptane-2-carboxylate (22)
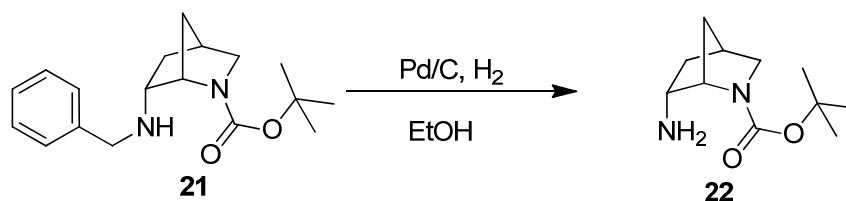
Palladium 10% on activated carbon (0.457 g, 0.430 mmol) was suspended in EtOH (5 mL) and some drops of water. This mixture was added to a solution of **21** (1.30 g, 4.30 mmol) in EtOH (20 mL). The reaction was performed in a hydrogenation apparatus. The reaction mixture was subject to four N_2/Vacum cycles and then to four H_2/Vacum cycles. Then the solution was stirred at room temperature under H_2 atmosphere (1.1 atm) for 4 h.

The reaction mixture was filtered through a filter septum washing with EtOH (20 mL) and MeOH (5 mL). The filtrate was concentrated under reduced pressure to give an oily residue containing trace amount of Pd/C, so it was taken up in EtOH (5 mL), re-filtered through Celite pad washing with further EtOH (5 mL). The filtrate was concentrated under reduced pressure to give **22** as a colorless oil (0.84 g, purity 90%, 3.56 mmol, 83%).

ANALYSIS

Note: NMR spectra show some signals splitted by the presence of two rotamers of the molecule. Chemical shifts of both rotamers are reported.

Formula: $C_{11}H_{20}N_2O_2$

Mol. Weight: 212.29 g/mol

**^{1}H NMR** (400 MHz, CDCl$_3$) δ = 4.04 (m, 1 H); 3.36 (brs, 2 H); 3.01 (m, 1 H); 2.45 (brs, 1 H); 2.11 (dddd, _J_=13.0, 10.6, 4.8, 3.0 Hz, 1 H); 1.64 (m, 2 H); 1.66 - 1.55 (m, 1 H); 1.51 (d, _J_=10.3 Hz, 1 H); 1.47 (s, 9 H); 0.81 (m, 1 H).

^{13}C NMR (DEPT) (100 MHz, CDCl$_3$) δ = 155.57 (C=O), 79.22 (C); 62.15 - 61.19 (CH), 55.37 - 55.19 (CH) 53.69 - 52.99 (CH$_2$), 37.81 - 37.35 (CH$_2$), 37.74 - 37.25 (CH), 36.95 (CH$_2$), 28.55 (3 x CH$_3$).

MS (ESI+) m/z (%) = 213 (100%) [MH]$^+$.

2.7 Synthesis of exo-TYPE III derivatives 23a-b, experimental data

(+/-)-exo-2-benzyl-N-(5-(trifluoromethyl)pyridin-2-yl)-2-azabicyclo[2.2.1]heptan-6-amine (25)
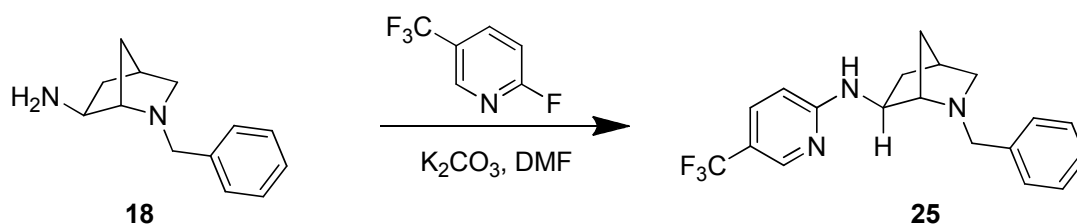
A mixture of **18** (300 mg, 1.483 mmol), 2-fluoro-5-(trifluoromethyl)pyridine (0.190, 1.574 mmol) and K_2CO_3 (360 mg, 2.60 mmol) in DMF (3 mL) was stirred under N_2 atmosphere for 10 min. The reaction mixture was heated at 100 °C for 2.5 h.

The solvent was then evaporated under reduced pressure and the residue was taken up in $NaHCO_3$ sat. sol. (30 mL) and the mixture was extracted with AcOEt (3x30 mL). The organic layers were collected, washed with water (50 mL), dried over anhydrous Na_2SO_4 and filtered. Then the solvent was evaporated under reduced pressure.

Purification: Isolera-One Biotage, Snap 25g HP-SI Column, sample dissolved in DCM, eluent: from CyHex/AcOEt 100:0 to 0:100 in gradient.

The containing product fractions were collected and the solvent was evaporated under reduced pressure to give **25** as white solid (408 mg; purity 95%; 1.116 mmol; 75%).

ANALYSIS

**Formula**: $C_{19}H_{20}F_3N_3$

Mol. Weight: 347.38 g/mol

Rf: 0.29 (CyHex/AcOEt 5:5; SI-TLC)

^{1}H NMR (400 MHz, DMSO-d_6) δ = 8.26 (s, 1 H); 7.57 (dd, J=8.8, 2.1 Hz, 1 H); 7.38 (d, J=7.4 Hz, 2 H); 7.32 (t, J=7.4 Hz, 2 H); 7.22 (t, J=7.1 Hz, 1 H); 7.15 (d, J=6.7 Hz, 1 H); 6.48 (d, J=8.6 Hz, 1 H); 4.13 (brs, 1 H); 3.74 (m, 2 H); 3.05 (s, 1 H); 2.58 (d, J=8.6 Hz, 1 H); 2.38 (brs, 1 H); 2.23 (d, J=8.6 Hz, 1 H); 1.84 (m, 1 H); 1.53 (d, J=9.8 Hz, 1 H); 1.46 (d, J=9.8 Hz, 1 H); 1.39 (d, J=11.7 Hz, 1 H).

^{13}C-NMR (DEPT) (100 MHz, CDCl$_3$) δ = 159.60 (C), 146.09 (q, J= 4.6 Hz, CH), 134.52 (q, J= 3.8 Hz, CH), 128.63 (CH), 128.32 (CH), 127.06 (CH), 124.6 (q, J= 270.7 Hz, CF$_3$), 115.53 (q, J= 33.6 Hz, C), 105.16 (CH), 62.63 (CH), 59.11 (CH$_2$), 58.61 (CH$_2$), 53.51 (CH), 38.82 (CH$_2$), 36.89 (CH), 32.30 (CH$_2$).

MS (ESI+) m/z (%) = 349 (100) [MH]$^+$.

(+/-)-*exo*-N-(5-(trifluoromethyl)pyridin-2-yl)-2-azabicyclo[2.2.1]heptan-6-amine (26)

25

26
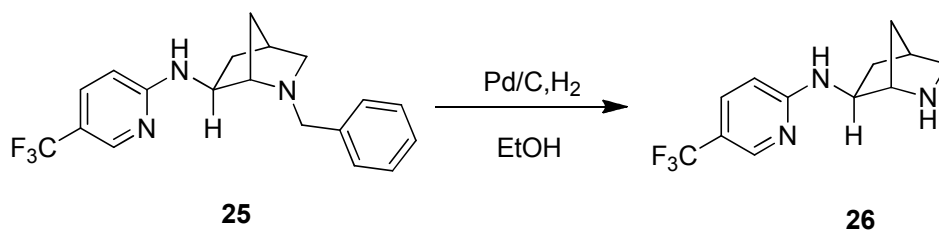
Palladium 10% on activated carbon (107 mg, 0.101 mmol) was dissolved in EtOH (2 mL) and some drops of water. This mixture was added to a solution of **25** (350 mg, 1.008 mmol) in EtOH (4 mL). The reaction was conduced in a hydrogenation apparatus. The reaction mixture was subject to four N_2/Vacum cycles and then four H_2/Vacum cycles. Then the solution was stirred at room temperature under H_2 atmosphere (1 atm) for 1.5 h.

The reaction mixture was then filtered through a filter septum and a Celite pad in order to eliminate the Pd/C. The Pd/C was washed with EtOH (5 mL). The filtrate was concentered under reduced pressure to give **26** as an oily residue (248 mg; 0.935 mmol; 89%)

ANALYSIS

Formula: $C_{12}H_{14}F_3N_3$

Mol. Weight: 257.25 g/mol

Note: in ^{1}HNMR spectrum in CDCl$_3$ the RR'N*H* signal was not observed (probably covered by the water signal at 1.61 ppm).

^{1}H NMR (400 MHz, DMSO-d_6) δ = 8.28 (s, 1 H); 7.61 (dd, *J*=9.3, 2.0 Hz, 1 H); 7.11 (d, *J*=6.8 Hz, 1 H); 6.55 (d, *J*=8.8 Hz, 1 H); 3.76 (brs, 1 H); 3.13 (s, 1 H); 2.66 (dt, *J*=8.8, 2.9 Hz, 1 H); 2.39 (d, *J*=8.8 Hz, 1 H); 2.33 (brs, 1 H); 2.04 (brs, 1 H); 1.79 (ddd, *J*=12.7, 8.3, 2.0 Hz, 1 H); 1.48 (d, *J*=9.23 Hz, 1 H); 1.38 (m, 1 H); 1.30 (d, *J*=9.3 Hz, 1 H).

^{13}C-NMR (DEPT) (100 MHz, CDCl$_3$) δ = 159.43 (C), 146.13 (q, J= 4.7 Hz, CH), 134.52 (q, J= 3.2 Hz, CH), 124.5 (q, J= 268.9 Hz, CF$_3$), 115.72 (q, J= 32.1 Hz, C), 105.84 (CH), 58.61 (CH), 56.28 (CH), 49.96 (CH$_2$), 39.08 (CH$_2$), 35.69 (CH), 34.88 (CH$_2$).

MS (ESI+) m/z (%) = 257 (100) [MH]$^+$.

# General Procedure F: synthesis of *exo*-compounds 23a-b

To a solution of the appropriate carboxylic acid (1.2 eq) in dioxane (1 mL) were added in sequence *N*-methylmorpholine (3 eq) and CDMT (1.5 eq) under N_2 atmosphere and the resultant solution was stirred for 30 min at room temperature. Then was added the amine **26** (1.0 eq) pre-dissolved in dioxane (1 mL) and the mixture was stirred at 100 °C for 1 h.

The solvent was then evaporated under reduced pressure and the residue taken up in AcOEt and washed in sequence with NH_4Cl sat. sol., $NaHCO_3$ sat. sol. and water. Then the organic layer was dried over anhydrous Na_2SO_4, filtered and the solvent was eliminated under reduced pressure.

Purification: Isolera-One Biotage, flash chromatography by HP-SI Column or Reverse Phase Column. The containing product fractions were collected and the solvent eliminated under reduced pressure to give the final compound **23a-b** as *(+/-)-exo*-racemic mixture.

Analysis of proton and carbon NMR spectra reveals for compounds **23a-b** the presence of two rotamers of the molecule in ratio ranging from 7:3 to 6:4. In particular, in proton NMR spectra the major rotamer can be easily detected and described. On the contrary, carbon NMR spectra are complicated by the presence of signals splitted by the presence of C-F coupling and the C_{sp2} carbon atom signals are difficult to distinguish and assign. For these reasons in carbon NMR spectra only the chemical shifts of aliphatic carbons are reported for both rotamers of each compound.

(2-methyl-5-phenylthiazol-4-yl) (+/-)-*exo*-6-((5-(trifluoromethyl)pyridin-2-yl)amino)-2-azabicyclo[2.2.1]heptan-2-carboxylate (23a)
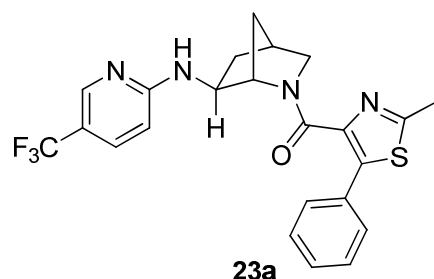
23a

General Procedure E was followed using the 2-methyl-5-phenylthiazole-4-carboxylic acid (44.3 mg, 0.202 mmol), amine **26** (40 mg, 0.155 mmol), NMM (0.050 mL, 0.455 mmol) and CDMT (44 mg, 0.251 mmol) in dioxane (2 mL). After purification (Snap 10g HP-SI Column, sample dissolved in DCM 100%, eluent: from DCM/AcOEt 100:0 to 0:100 in gradient) **23a** was obtained as white solid (54 mg, 0.118 mmol, 76%).

ANALYSIS
Formula: $C_{23}H_{21}F_3N_4OS$
Mol. Weight: 458.50 g/mol
Note: From NMR spectra were observed two signal patterns in about 70:30 ratio due to the two rotamers of the molecule. Chemical shifts of the major roramer are reported.

Rf: 0.35 (DCM/MeOH 95:5; SI-TLC).

^{1}H NMR (400 MHz, DMSO-d_6) (major rotamer) δ = 8.03 (s, 1 H); 7.57 (dd, J=9.0, 2.7 Hz, 1 H); 7.51 - 7.32 (m, 5 H); 7.14 (d, J=5.9 Hz, 1 H); 6.33 (d, J=8.8 Hz, 1 H); 3.90 (s, 1 H); 3.65 (brs, 1 H); 3.30 - 3.24 (m, 1 H); 3.11 (d, J=10.8 Hz, 1 H); 2.68 (s, 3 H); 2.61 (brs, 1 H); 1.89 (dd, J=12.0, 9.0 Hz, 1 H); 1.56 - 1.46 (m, 2 H); 1.32 (d, J=10.3 Hz, 1 H).

^{13}C NMR (DEPT) (100 MHz, CDCl$_3$) (major rotamer) δ = 60.64 (CH), 57.90 (CH), 55.25 (CH), 53.90 (CH), 52.85 (CH$_2$), 51.59(CH$_2$), 38.09(CH$_2$), 37.63(CH$_2$), 36.08 (CH), 35.21 (CH), 34.84(CH$_2$), 33.22(CH$_2$), 19.22(CH$_3$), 19.18(CH$_3$).

MS (ESI+) m/z (%) = 460 (100) [MH]$^+$

(6-methyl-3-phenylpicolin-2-yl) (+/-)-*exo*-6-((5-(trifluoromethyl)pyridin-2-yl)amino)-2-azabicyclo[2.2.1]heptan-2-carboxylate (23b)
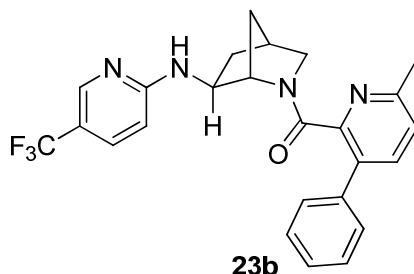
23b

General Procedure E was followed using the 6-methyl-3-phenylpicolinic acid (40 mg, 0.188 mmol), amine **26** (40.2 mg, 0.156 mmol), NMM (0.050 mL, 0.455 mmol) and CDMT (44 mg, 0.251 mmol) in dioxane (2 mL). After purification (Snap 10g HP-SI Column, sample dissolved in DCM 100%, eluent: from DCM/MeOH 100:0 to 95:5 in gradient) **23b** was obtained as white solid (55 mg, 0.122 mmol, 64.8 %).

ANALYSIS

Formula: C$_{25}$H$_{23}$F$_3$N$_4$O

Mol. Weight: 452.47 g/mol

Note: From NMR spectra were observed two signal patterns in about 60:40 ratio due to the two rotamers of the molecule. Chemical shifts of the major roramer are reported.

Rf: 0.32 (DCM/MeOH 95:5; SI-TLC).

^{1}H NMR (400 MHz, CDCl$_3$) (major rotamer) δ = 8.14 (s, 1 H); 7.74 (d, *J*=8.3 Hz, 1 H); 7.81 - 7.30 (m, 7 H); 5.73 (d, *J*=8.8 Hz, 1 H); 4.54 (d, *J*=5.9 Hz, 1 H); 3.62 (brs, 1 H); 3.53 (s, 1 H); 3.25 - 3.16 (m, 2 H); 2.75 (s, 3 H); 2.54 (brs, 1 H); 2.07 (ddd, *J*=13.4, 8.1, 2.4 Hz, 1 H); 1.31 - 1.24 (m, 2 H); 0.75 (d, *J*=10.8 Hz, 1 H).

^{13}C NMR (DEPT) (100 MHz, CDCl$_3$) (major rotamer) δ = 59.94 (CH), 57.37 (CH), 54.81 (CH), 53.69 (CH), 52.25 (CH$_2$), 50.79 (CH$_2$), 37.92 (CH$_2$), 37.47 (CH$_2$), 36.03 (CH), 35.05 (CH), 34.37 (CH$_2$), 33.19 (CH$_2$), 24.22 (CH$_3$), 24.14 (CH$_3$).

MS (ESI+) m/z (%) = 454.2 (100) [MH]$^+$

2.8 Synthesis of endo-TYPE III derivatives 24a-e, experimental data

(+/-)-endo-tert-butyl 6-((5-(trifluoromethyl)pyridin-2-yl)amino)-2-azabicyclo[2.2.1]heptane-2-carboxylate (27)
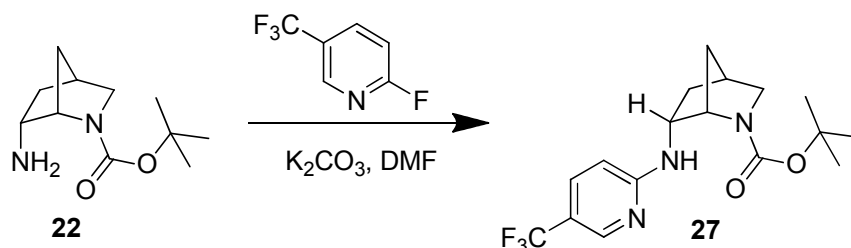
A mixture of **22** (300 mg, 1.272 mmol), 2-fluoro-5-(trifluoromethyl)pyridine (0.190, 1.574 mmol) and K_2CO_3 (360 mg, 2.60 mmol) in DMF (3 mL) was stirred under N_2 atmosphere for 10 min. The reaction mixture was heated at 100 °C for 1.5 h then at 80 °C for 18 h.

The solvent was then evaporated under reduced pressure and the residue taken up in $NaHCO_3$ sat. sol. (30 mL) and the mixture extracted with AcOEt (3x30 mL). The organic layers were collected, washed with water (50 mL), dried over anhydrous Na_2SO_4 and filtered. Then the solvent was evaporated under reduced pressure.

Purification: Isolera-One Biotage, Snap 25g HP-SI Column, sample dissolved in DCM, eluent: from CyHex/AcOEt 100:0 to 50:50 in gradient.

The containing product fractions were collected and the solvent was evaporated under reduced pressure to give **27** as white solid (398 mg; 1.114 mmol; 88%).

ANALYSIS
Formula: $C_{17}H_{22}F_3N_3O_2$
**Mol. Weight**: 357.37g/mol
Rf: 0.43 (CyHex/AcOEt 5:5; SI-TLC)
Note: NMR spectra show some signals splitted by the presence of two rotamers of the molecule. Chemical shifts of both rotamers are reported.
^{1}H NMR (400 MHz, $CDCl_3$) (mixture of rotamers) δ = 8.36 (brs, 1 H); 7.56 (m, 1 H); 6.37 (m, 1 H); 5.41 (brs, 1 H,); 4.43 (brs, 1 H); 4.19 (m, 1 H); 3.48 (m, 1 H); 3.11 (m, 1 H); 2.61 (brs, 1 H); 2.35 (m, 1 H); 1.74 (m, 2 H); 1.56 (m, 9 H); 1.05 (m, 1 H).
^{13}C-NMR (DEPT) (100 MHz, $CDCl_3$) (mixture of rotamers) δ = 160.04 (C), 154.95 (C), 145.83 (CH), 133.98 (CH), 124.59 (q, J=269.1 Hz, CF_3), 115.55 (q, J=35.8 Hz, C), 107.25 (CH), 79.35 (C), 58.58 (CH), 56.08 (CH), 54.92 (CH), 53.69 (CH_2), 52.83 (CH_2), 37.73 (CH), 36.98 (CH), 36.92 (CH_2), 36.72 (CH_2), 36.36 (CH_2), 36.08 (CH_2), 28.42 (3 x CH_3), 28.15 (3 x CH_3).
MS (ESI+) m/z (%) = 358 (100) [MH]⁺.

(+/-)-endo-N-(5-(trifluoromethyl)pyridin-2-yl)-2-azabicyclo[2.2.1]heptan-6-amine (28)
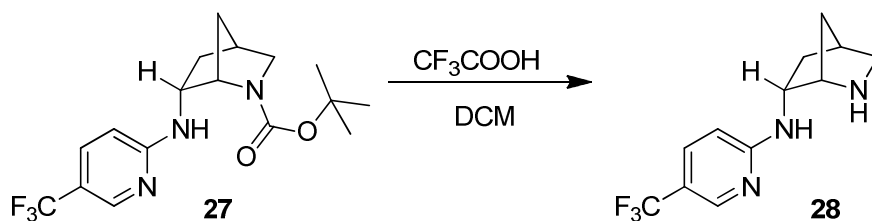
Compound **27** (350 mg, 0.979 mmol) was dissolved in a solution of DCM (Ratio: 4, Volume: 9.00 mL) and TFA (Ratio: 1.000, Volume: 2.25 mL) and then the mixture was stirred at room temperature for 1 h.

The solvent was then evaporated under reduced pressure.

Purification: the residue was taken up in MeOH and loaded on SCX 5g, eluent MeOH then ammonia (2M in MeOH).

The containing product fractions were collected and the solvent was eliminated under reduced pressure to give **28** as white solid (260 mg, 0.979 mmol, quantitative).

ANALYSIS

Formula: $C_{12}H_{14}F_3N_3$

Mol. Weight: 257.25 g/mol

^{1}H NMR (400 MHz, CDCl$_3$) δ = 8.33 (bs, 1 H); 7.54 (m, 1 H); 6.38 (d, *J*=8.8 Hz, 1 H); 6.14 (bs, 1 H); 4.10 - 4.00 (m, 1 H); 3.48 (brs, 1 H); 3.00 (dt, *J*=9.7, 3.2 Hz, 1 H); 2.63 (d, *J*=9.8 Hz, 1 H); 2.47 (brs, 1 H); 2.21 - 2.10 (m, 1 H); 1.68 - 1.63 (m, 1 H); 1.59 - 1.53 (m, 1 H); 0.97 (dt, *J*=12.7, 3.2 Hz, 1 H).

^{13}C-NMR (DEPT) (100 MHz, CDCl$_3$) δ = 160.15 (C), 146.07 (CH), 133.84 (CH), 124.77 (q, J= 269.9 Hz, CF$_3$), 114.75 (q, J=33.2 Hz, C), 107.25 (CH), 58.38 (CH), 52.80 (CH), 51.62 (CH$_2$), 38.46 (CH$_2$), 37.61 (CH), 37.35 (CH$_2$).

MS (ESI+) m/z (%) = 258 (100) [MH]$^+$.

## General Procedure E: synthesis of *endo*-compounds 24a-e

To a solution of the appropriate carboxylic acid (1.0 eq) in dioxane (1 mL) were added in sequence *N*-methylmorpholine (3 eq) and CDMT (1.5 eq) under N_2 atmosphere and the resultant solution was stirred for 30 min at room temperature. Then was added the amine **28** (1.2 eq) pre-dissolved in dioxane (1 mL) and the mixture was stirred at 100 °C for 1 h.

The solvent was then evaporated under reduced pressure and the residue taken up in AcOEt and washed in sequence with NH_4Cl sat. sol., $NaHCO_3$ sat. sol. and water. Then the organic layer was dried over anhydrous Na_2SO_4, filtered and the solvent was eliminated under reduced pressure.

Purification: Isolera-One Biotage, HP-SI Column or Reverse Phase Column.

The containing product fractions were collected and the solvent eliminated under reduced pressure to give the final compound **24a-e** as *(+/-)-endo*-racemic mixture.

(2-methyl-5-phenylthiazol-4-yl) (+/-)-*endo*-6-((5-(trifluoromethyl)pyridin-2-yl)amino)-2-azabicyclo[2.2.1]heptan-2-carboxylate (24a)
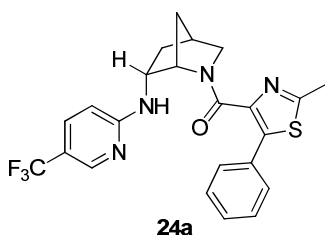
24a

General Procedure E was followed using the 2-methyl-5-phenylthiazole-4-carboxylic acid (44.3 mg, 0.202 mmol), amine **28** (40 mg, 0.155 mmol), NMM (0.050 mL, 0.455 mmol) and CDMT (44 mg, 0.251 mmol) in dioxane (2 mL). After purification (Snap 10g HP-SI Column, sample dissolved in DCM 100%, eluent: from DCM/MeOH 100:0 to 95:5 in gradient) **24a** was obtained as white solid (52.5 mg; 0.115 mmol; 73.6%).

ANALYSIS
Formula: $C_{23}H_{21}F_3N_4OS$
Mol. Weight: 458.50 g/mol
Note: From NMR spectra were observed two signal patterns in about 93:7 ratio due to the two rotamers of the molecule. The signal of 1 C*H* of the 2-azabicyclo[2.2.1]heptan-6-amine is covered by DMSO solvent signal. The chemical shifts of the major rotamer are reported.
^{1}H NMR (400 MHz, DMSO-d_6) (major rotamer) δ = 8.05 (s, 1 H); 7.52 - 7.31 (m, 7 H); 6.36 (d, *J*=8.8 Hz, 1 H); 4.38 (s, 1 H); 3.85 (brs, 1 H); 3.37 - 3.22 (m, 2 H); 2.32 (s, 3 H); 2.07 (m, 1 H); 1.46 (d, *J*=9.8 Hz, 1 H); 1.22 (m, 1 H); 1.16 (m, 1 H).
**^{13}C NMR (DEPT)** (100 MHz, DMSO-d_6) (major rotamer) δ = 163.35 (C), 163.06 (C), 160.40 (C), 145.22 (CH), 144.38 (C), 136.06 (C), 132.57 (CH), 130.79 (C), 129.30 (2 x CH), 128.85 (CH), 128.45 (2

x CH), 128.34 (q, J= 270.7 Hz, CF$_3$), 112.70 (q, J=31.3 Hz, C), 109.42 (CH), 60.09 (CH), 54.54 (CH), 53.13 (CH2), 36.60 (CH$_2$), 36.24 (CH), 33.44 (CH$_2$), 18.73 (CH$_3$).

MS (ESI+) m/z (%) = 460 (100) [MH]$^+$.

(6-methyl-3-phenylpicolin-2-yl) (+/-)-*endo*-6-((5-(trifluoromethyl)pyridin-2-yl)amino)-2-azabicyclo[2.2.1]heptan-2-carboxylate (24b)
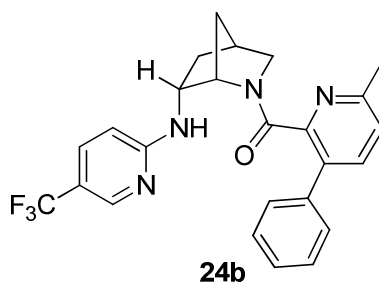
24b

General Procedure E was followed using the 6-methyl-3-phenylpicolinic acid (40 mg, 0.188 mmol), amine **28** (40 mg, 0.155 mmol), NMM (0.050 mL, 0.455 mmol) and CDMT (44 mg, 0.251 mmol) in dioxane (2 mL). After purification (Snap 10g HP-SI Column, sample dissolved in DCM 100%, eluent: from DCM/MeOH 100:0 to 95:5 in gradient) **24b** was obtained as white solid (53 mg; 0.117 mmol; 75%).

ANALYSIS

Formula: C$_{25}$H$_{23}$F$_3$N$_4$O
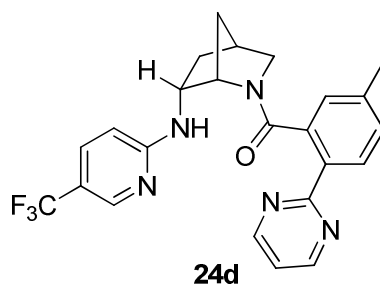
Mol. Weight: 452.47 g/mol

Note: From NMR spectra were observed two signal patterns in about 80:20 ratio due to the two rotamers of the molecule. The chemical shifts of the major rotamer were reported.

^{1}H NMR (400 MHz, DMSO-*d$_6$*) (major rotamer) δ = 7.90 (brs, 1 H); 7.66 (d, J=8.3 Hz, 1 H); 7.57 (dd, J=9.3, 2.4 Hz, 1 H); 7.52 (brs, 1 H); 7.50 - 7.45 (m, 2 H); 7.42 - 7.36 (m, 3 H); 7.09 (d, J=7.8 Hz, 1 H); 6.52 (m, 1 H); 3.81 (brs, 1 H); 3.76 (m, 1 H); 3.14 – 3.05 (m, 2 H); 2.38 (brs, 1 H); 2.11 (s, 3 H); 2.00 (m, 1 H); 1.22 (m, 1 H); 1.12 (d, J=12.7 Hz, 1 H); 0.29 (brs, 1 H).

^{13}C NMR (DEPT) (100 MHz, DMSO-*d$_6$*) (major rotamer) δ = 166.59 (C), 160.50 (C), 156.53 (C), 151.98 (C), 145.30 (CH), 137.81 (C), 137.33 (CH), 133.03 (CH), 130.95 (C), 129.06 (2 x CH), 128.69 (2 x CH), 125.67 (q, J= 269.9 Hz, CF$_3$); 128.23 (CH), 123.38 (CH), 112.53 (q, J= 32.3 Hz, C), 107.43 (CH), 60.13 (CH), 54.12 (CH), 52.29 (CH$_2$), 36.06 (CH), 35.97 (CH$_2$), 33.75 (CH$_2$), 23.56 (CH$_3$).

MS (ESI+) m/z (%) = 454 (100) [MH]$^+$.

(6-methyl-3-(pyrimidin-2-yl)pyridin-2-yl) (+/-)-*endo*-6-((5-(trifluoromethyl)pyridin-2-yl)amino)-2-azabicyclo[2.2.1]heptan-2-carboxylate (24c)

24c
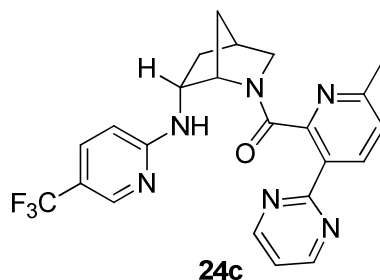
General Procedure E was followed using the 6-methyl-3-(pyrimidin-2-yl)picolinic acid (30 mg, 0.139 mmol), amine **28** (30 mg, 0.117 mmol), NMM (0.040 mL, 0.364 mmol) and CDMT (33 mg, 0.188 mmol) in dioxane (2 mL). After purification (Snap 10g HP-SI Column, sample dissolved in DCM 100%, eluent: from DCM/MeOH 100:0 to 95:5 in gradient) **24c** was obtained as pink solid (18 mg; 0.040 mmol; 34.0%).

ANALYSIS
Formula: $C_{23}H_{21}F_3N_6O$
Mol. Weight: 454.45 g/mol
Note: From NMR spectra were observed two signal patterns in about 90:10 ratio due to the two rotamers of the molecule. The chemical shifts of the major rotamer are reported.
^{1}H NMR (400 MHz, DMSO-d_6) (major rotamer) δ = 8.92 (d, J=4.9 Hz, 2 H); 8.30 (d, J=7.8 Hz, 1 H); 8.05 (brs, 1 H); 7.59 (d, J=8.8 Hz, 2 H); 7.49 (t, J=4.9 Hz, 1 H); 7.26 (d, J=7.8 Hz, 1 H); 6.49 (d, J=7.8 Hz, 1 H); 4.03 (brs, 1 H); 3.95 (brs, 1 H); 3.47 (d, J=9.8 Hz, 1 H); 3.15 (d, *J*=10.23 Hz, 1 H); 2.62 (brs, 1 H); 2.27 (brs, 3 H); 2.19 (brs, 1 H); 1.59 - 1.39 (m, 2 H); 1.18 (d, J=12.7 Hz, 1 H).
^{13}C NMR (DEPT) (100 MHz, DMSO-d_6) (major rotamer) δ = 167.96 (C), 163.30 (C), 159.11 (C), 157.17 (2 x CH), 154.40 (C), 145.19 (CH), 138.65 (CH), 133.78 (CH), 129.60 (C), 127.07 (q, J=275.9, CF$_3$), 123.73 (CH), 119.60 (CH), 114.62 (q, J=33.3 Hz, C), 108.50 (CH), 61.49 (CH), 54.42 (CH), 52.60 (CH$_2$), 37.40 (CH$_2$), 37.01 (CH$_2$), 36.77 (CH), 24.25 (CH$_3$).
MS (ESI+) m/z (%) = 455 (100) [MH]$^+$.

(5-methyl-2-(pyrimidin-2-yl)phenyl) (+/-)-*endo*-6-((5-(trifluoromethyl)pyridin-2-yl)amino)-2-azabicyclo[2.2.1]heptan-2-carboxylate (24d)

24d

General Procedure E was followed using the 5-methyl-2-(pyrimidin-2-yl)benzoic acid (30 mg, 0.140 mmol), amine **28** (30 mg, 0.117 mmol), NMM (0.040 mL, 0.364 mmol) and CDMT (33 mg, 0.188 mmol) in dioxane (2 mL). After purification (Snap 10g HP-SI Column, sample dissolved in DCM 100%, eluent: from DCM/Acetone 100:0 to 5:5 in gradient. Sample was further purified by SCX column) **24d** was obtained as pink solid (16 mg; 0.035 mmol; 30.3%).

ANALYSIS
Formula: $C_{24}H_{22}F_3N_5O$
Mol. Weight: 453.46 g/mol
Note: From NMR spectra were observed two signal patterns in about 90:10 ratio due to the two rotamers of the molecule. The chemical shifts of the major rotamer are reported. The signal of a brideged *CH* was partially covered by DMSO solvent signal.
¹H NMR (400 MHz, DMSO-d_6) (major rotamer) δ = 8.85 (d, J=4.9 Hz, 2 H); 7.97 (brs, 1 H); 7.89 (d, J=7.8 Hz, 1 H); 7.63 (d, J=8.3 Hz, 1 H); 7.56 (d, J=6.8 Hz, 1 H); 7.40 - 7.44 (m, 1 H); 7.08 (d, J=6.8 Hz, 1 H); 6.74 (s, 1 H); 6.66 (brs, 1 H); 4.06 (brs, 1 H); 3.77 (brs, 1 H); 3.39 (dt, J=10.6, 3.0 Hz, 1 H); 3.18 (d, J=10.3 Hz, 1 H); 2.53 - 2.58 (m, 1 H); 2.09 (t, J=11.5 Hz, 1 H); 1.88 (s, 3 H); 1.40 (d, J=9.8 Hz, 1 H); 1.29 - 1.10 (m, 2 H).
¹H NMR (400 MHz, CD₃OD) (major rotamer) δ = 8.83 (d, J=4.9 Hz, 2 H); 8.03 (d, J=7.8 Hz, 1 H); 7.94 (brs, 1 H); 7.59 (dd, J=8.8, 2.4 Hz, 1 H); 7.37 (t, J=4.9 Hz, 1 H); 7.18 - 7.11 (m, 1 H); 6.87 (s, 1 H); 6.68 - 6.48 (m, 1 H); 4.15 - 3.99 (m, 2 H); 3.54 (dt, J=10.8, 3.2 Hz, 1 H); 3.35 (s, 1 H); 2.63 (brs, 1 H); 2.31 - 2.18 (m, 1 H); 1.98 (s, 3 H); 1.55 – 1.42 (m, 1 H); 1.38 - 1.21 (m, 2 H).
¹³C NMR (DEPT) (100 MHz, CD₃OD) (major rotamer) δ = ppm 171.98 (C), 164.17 (C), 160.30 (C), 157.15 (CH), 144.87 (CH), 143.13 (C), 140.29 (C), 136.09 (C), 133.33 (CH), 129.76 (CH), 129.33 (CH), 129.05 (CH), 128.70 (CH), 128.09 (CH), 127.88 (q, J= 269.2 Hz, CF₃), 119.26 (CH), 114.02 (q, J=32.4 Hz, C), 61.37 (CH), 53.82 (CH), 52.64 (CH₂), 36.46 (CH), 35.85 (CH₂), 33.86 (CH₂), 19.70 (CH₃).
MS (ESI+) m/z (%) = 454 (100) [MH]⁺.

(5-chloro-2-(pyrimidin-2-yl)phenyl) (+/-)-*endo*-6-((5-(trifluoromethyl)pyridin-2-yl)amino)-2-azabicyclo[2.2.1]heptan-2-carboxylate (24e)

24e
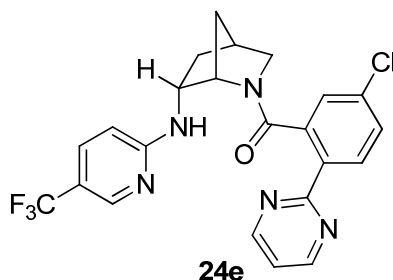
General Procedure E was followed using the 5-chloro-2-(pyrimidin-2-yl)benzoic acid (44 mg, 0.188 mmol), amine **28** (40 mg, 0.155 mmol), NMM (0.050 mL, 0.455 mmol) and CDMT (44 mg, 0.251

mmol) in dioxane (2 mL). After purification (Snap 10g HP-SI Column, sample dissolved in DCM 100%, eluent: from DCM/MeOH 100:0 to 95:5 in gradient) **24e** was obtained as purple solid (29 mg; 0.061 mmol; 39.4%).

ANALYSIS

Formula: $C_{23}H_{19}ClF_3N_5O$

Mol. Weight: 473.88 g/mol

Note: From NMR spectra were observed two signal patterns in about 85:15 ratio due to the two rotamers of the molecule. The chemical shifts of the major rotamer are reported.

^{1}H NMR (400 MHz, DMSO-d_6) (major rotamer) δ = 8.90 (d, *J*=4.9 Hz, 2 H); 7.99 (d, J=8.5 Hz, 1H); 7.95 (m, 1 H); 7.61 (m, 1 H); 7.52 (d, *J*=6.8 Hz, 1 H); 7.48 (t, *J*=4.9 Hz, 1 H); 7.31 (dd, *J*=8.6, 2.2 Hz, 1 H); 6.94 (s, 1 H); 6.56 - 6.69 (m, 1 H); 4.07 (brs, 1 H); 3.73 (brs, 1 H); 3.37 (dt, J=10.4, 2.9 Hz, 1H); 3.23 - 3.16 (m, 1 H); 2.53 (brs, 1 H); 2.09 (m, 1 H); 1.40 (d, *J*=9.8 Hz, 1 H); 1.14 (brs, 2 H).

^{1}H NMR (400 MHz, CD$_3$OD) (major rotamer) δ = 8.86 (d, J=4.9 Hz, 2 H); 8.13 (d, J=8.3 Hz, 1 H); 7.93 (bs, 1 H); 7.56 - 7.63 (m, 1 H); 7.41 (t, J=4.9 Hz, 1 H); 7.31 (dd, J=8.6, 2.2 Hz, 1 H); 7.04 (d, J=2.0 Hz, 1 H); 6.57 (d, J=7.8 Hz, 1 H); 3.88 - 4.12 (m, 2 H); 3.54 (dt, J=10.9, 3.1 Hz, 1 H); 3.36 (bs, 1 H); 2.63 (bs, 1 H); 2.25 (m, 1 H); 1.51 (d, J=9.8 Hz, 1 H); 1.27 (m, 2 H).

^{13}C NMR (DEPT) (100 MHz, CD$_3$OD) (major rotamer) δ = 170.06 (C), 163.24 (C), 160.14 (C), 157.31 (2 x CH) 144.88 (CH), 137.61 (C), 135.87 (C), 133.83 (CH), 133.49 (C), 130.59 (CH), 128.77 (CH), 128.38 (CH), 127.56 (C), 124.82 (q; J= 269.7; CF$_3$), 119.71 (CH), 114.44 (q, J= 32.8 Hz; C), 108.27 (CH), 61.30 (CH), 53.90 (CH), 52.76 (CH$_2$), 36.37 (CH), 35.84 (CH$_2$), 33.64 (CH$_2$).

MS (ESI+) m/z (%) = 474 (100) [MH]$^+$.

Chapter 3. Computational chemistry

3.1. Drug-like Properties Evaluation

The drug-like properties of a molecule or of a set of molecules, considered for pharmaceutical purposes (drugs), are qualitative indications that describe how "drug-like" a substance is with respect to several parameters and these properties can be extrapolated from the molecular structure.[1] Nevertheless, it should be noted that the drug-like properties are referred only to the bioavailability of a drug-candidate and not to its biological properties.

A smart method to evaluate the drug-like properties of a compound is to apply specific and rational "rules" based on a set of guidelines and able to predict, from the structural properties of a molecule, the probability of being well absorbed after oral administration. These guidelines are not absolute, nor are they intended to give severe cut-off values, however they are often quite efficacious.

In the design of the new *TYPE II* and *TYPE III* scaffolds derivatives and in particular in the rationale evaluation of the best substitution patterns for the two nitrogen atoms embedded in the core structures, we apply the so-called "*Lipinski rules*" (*Lipinski et al.*).[2] These rules are an assets of values deduced from the analysis and classification of the key physiochemical properties of a series of drug-like compounds taken from the literature.

The Lipinski rules were originally studied and employed at Pfizer Inc. in the US for some years and after their publication in 1997 become largely used by the medicinal chemists community. In the drug discovery fields, the impact of these rules was very significant. The Lipinsky rules are also known as the "*rule of 5*" because the proposed values for each of the parameters are all near to 5 or to a multiple of 5. The intended purpose of the "*rule of 5*" is to analyze specific physicochemical properties of compounds, in order to predict their absorption or permeation. In particular, good absorption or permeation are more likely when a drug-like compound possesses:

- less than 5 H-bond donors (sum of all OHs and NHs);
- has a molecular weight (MW) < 500;
- the Log P is between 2 and 5 (octanol/water partition coefficient);
- less than 10 H-bond acceptors (sum of all Ns and Os);
- rotable bonds < 8;
- compounds that are substrates for biological transporters and natural compounds are exceptions to the rule.

The Lipinsky rules were extrapolated by the structural properties of compounds that passed the phase I clinical trials and moved on to phase II studies. Phase I clinical trials entail human administration of the drug candidate in order to define the pharmacokinetic profile and the toxicity. When a compound moves on Phase II studies it means that sufficient adsorption in humans and low toxicity were observed and consequently it is liable for further investments for his

---

[1] E. H. Kerns, L. Di in "Drug-like Properties: Concepts, Structure Design and Methods", Elsevier Ltd, **2008**.

[2] a) C. A. Lipinski, F. Lombardo, B. W. Dominy, P. J. Feeney *Adv. Drug Del. Rev.* **1997**, *23*, 3-25; b) C. A. Lipinski, F. Lombardo, B. W. Dominy, P. J. Feeney *Adv. Drug Del. Rev.* **2001**, *46*, 3-26.

development. More than 2200 molecules were analyzed in order to extrapolate and build up the general rules of drug likeness. Validation of the Lipinsky rules demonstrated that the 90% of the compounds possessing molecular property values that fall within the guidelines show sufficient absorption after oral dosing.

The rules were building up on the basis of robust physicochemical evaluations:

- Hydrogen bonds increase solubility in water of a compound and they must be broken in order to permit lipid bilayer membrane permeation. Thus, a high number of hydrogen bonds decrease the partition from the aqueous phase into the lipid bilayer membrane decreasing the membrane permeation by passive diffusion.
- Molecular weight (MW) is related to the dimension of the molecule. Increasing MW reduces the compound concentration at the surface of the intestinal epithelium, thus reducing absorption. Increasing size also inhibits passive diffusion through the tightly packed aliphatic side chains of the bilayer membrane.
- Increasing Log P also decreases aqueous solubility and reduces absorption.
- Finally, membrane transporters can either enhance or reduce compound absorption by either active uptake transport or efflux, respectively. Thus, transporters can have a strong impact on increasing or decreasing absorption and molecules that are substrates for membrane transporters represent an exception to the *rule of 5* Natural products are another important exception to the *rule of 5*. In this case natural evolution leads to the optimization of these compounds in terms of active transport, developing conformationally and configurationally useful features for passive transport.

However, when a drug-like compound is recognized, often the lead optimization procedure (achievement of a drug candidate) requires structural modifications that increase both molecular weight and lipophilicity. So, the activity improvement can decrease the drug-like properties of a compound. These drawbacks can be overcome introducing the concept of lead-like molecules.[3] A lead-like molecule possesses less severe requirements with respect to a drug-like compound. In particular:

- less than 3 H-bond donors (sum of all OHs and NHs);
- has a molecular weight (MW) < 300;
- the Log P is between 1 and 3 (octanol/water partition coefficient);
- less than 3 H-bond acceptors (sum of all Ns and Os);
- rotable bonds < 3.
- compounds that are substrates for biological transporters and natural compounds are exceptions to the rule.

Thus, when a lead-like compound is identified, the lead optimization is less difficult because the introduction of hydrophobic groups to increase potency has a little effect on MW and logP as

---

[3] M.S. Lajiness, M. Vieth, J. Erickson *Curr. Opin. Drug Discovery Dev.* **2004**, *7*, 470-477.

definited by the rule of 5 and compounds can become larger and more lipophilic without loss of their drug-like properties.

It should pointed out that, from biological point of view, a drug-like and a lead-like compound can show diverse level of activity towards the selected target, nM *vs* mM activity, because a lead-like compound is open to wider margin of improvement with respect to a drug-like compound on the basis of reported rules.

Moreover, over the last years, these descriptors have been modified and improved to obtain indication on the physiochemical features required for compound targeting particular human body district. For example, the polar surface area of a molecule (PSA) expressed in squared Å, is stated as the surface occupied by all polar atoms (mainly oxygen and nitrogen and their hydrogens) and indicates the ability of a molecule to permeate cell membranes.[4] Molecules with a polar surface area higher than 140 squared Å have the tendency to be scarce in permeating cell membranes.

In this PhD project, we focused our attention on the search for new antagonist of the orexinic receptors that are mainly located in the Central Nervous System (CNS). As a consequence, particular physiochemical features are required for the potential orexin antagonists for the blood-brain barrier (BBB) permeation. In fact, the commercial CNS drugs have fewer hydrogen bond donors, higher Log P, lower PSA (polar surface area), and fewer rotatable bonds than the corresponding non-CNS drugs.[5] Pardrige proposed a set of physiochemical BBB rules for molecules with potential effects on CNS.[6] In particular, he postulated that a molecule should have:

- Total H-bonds < 8–10;
- MW < 400-500;
- No acid groups.

More restrictive features were also proposed suggesting that the H-bond donors must be < 2 and H-bond acceptors < 6. This is in agreement with general consideration that H-bond donors are more limiting than H-bond acceptors. Moreover, molecules able to penetrate the BBB (and thus act on receptors in the central nervous system) normally have a PSA of 60-70 squared Å.[7]

All these features are useful for evaluating BBB permeability of a class of compounds prior to their synthesis and can suggest which structural modifications provide better BBB permeation.

These considerations led us to perform an *In Silico* filtering phase for the evaluation of the physiochemical properties (*ChemBioDrow Ultra - 12.0 - Cambridgesoft*) of the two series of compounds we planned to synthesize as antagonists for the orexinic receptors.

Actually, we choose to evaluate the molecular weight (MW), the log P, the total polar surface area (tPSA) and the total H-bonds (HBA + HBD).

[4] P. Ertl *Molecular Drug Properties*, R. Mannhold (ed.), Wiley-VCH, **2007**, 111-126.

[5] K. M. M. Doan, J. E. Humphreys, L. O. Webster, S. A. Wring, L. J. Shampine, C. J. Serabjit-Singh, C. J. *J. Pharm. Exp. Th.* **2002**, *303*, 1029-1037.

[6] a) W: M. Pardridge *Adv. Drug Del. Rev.* **1995**, *15*, 5-36; b) W. M. Pardridge *J. Neurochem.* **1998**, *70*, 1781-1792; c) W. M. Pardridge *Drug Discovery Today* **2007**, *12*, 54-61.

[7] a) D. E. Clark *Drug Discovery Today* **2003**, *8*, 927-933; b) M. Lobell, L. Molnar, G. M. Keseru *J. Pharm. Sci.* **2003**, *92*, 360-370.
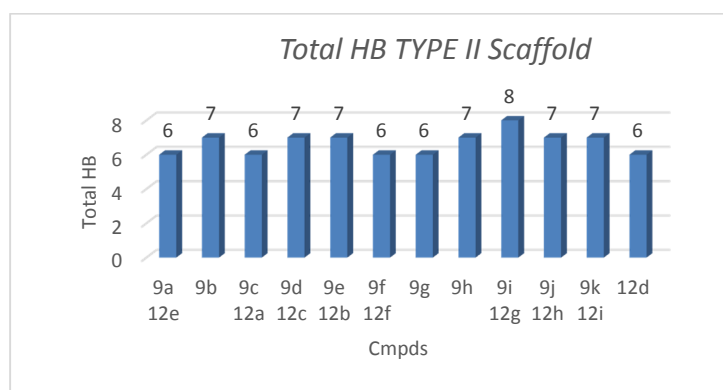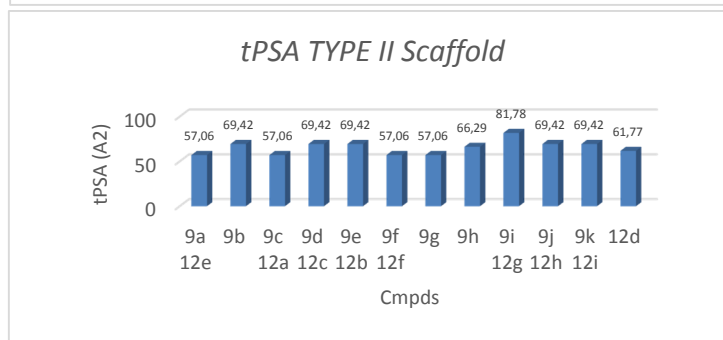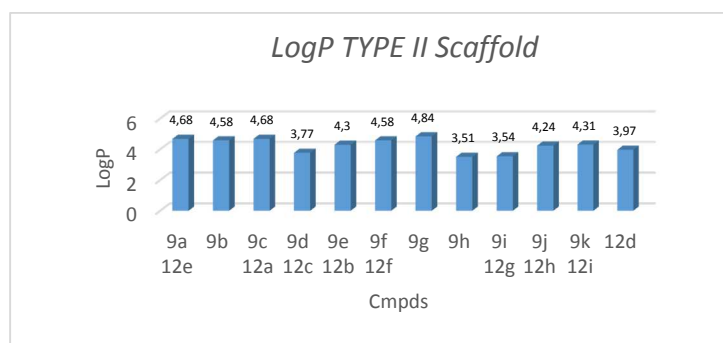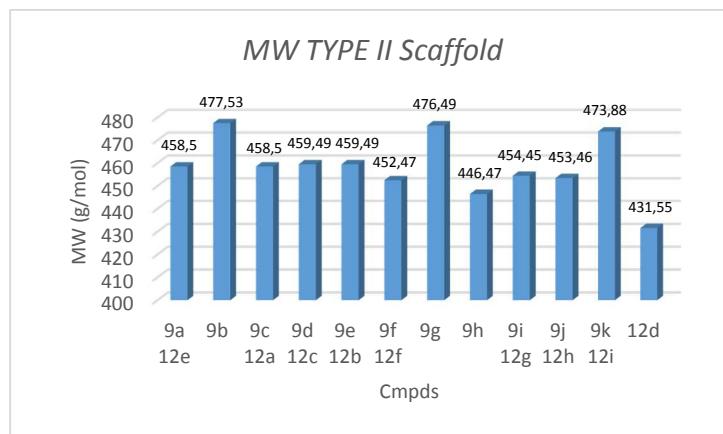
*TYPE II Scaffold derivatives **9a-k** and **12a-i***

The first parameter evaluated in the final 20 *endo/exo TYPE II* compounds (**9a-k** and **12a-i**) was the molecular weight. In general, the molecular weights of the designed molecules were above the flag level of 500 g/mol proposed by Lipinski and Partrige.[2,6]

The LogP parameter, calculated with the *ChemBioDrow Ultra* software, was evaluated to obtain an indication about the lipophilic nature of the final compounds obtained. The LogP values are under the reported value of 5 reported by Lipinski ranging from the 3.51 of compound **9h** to 4.84 of compound **9g**. The peculiar feature of compound **9h** is the presence of the cyclopropylmethoxy group that displaces the phenyl or the pyrimidin-2-yl rings present in the other derivatives. While the compound **9g** contains an additional fluorine atom in the 2-methyl-5-phenylthiazol-4-yl group. The tPSA (expressed as Å^2) values are comprised between 57.06 (compounds **9f**, **9g** and **12f**) and 81.78 (compounds **9i** and **12g**). These latter compounds contain the 6-methyl-3-(pyrimidin-2-yl)pyridin-2-yl group that increase the tPSA over the reference values proposed by Clark and Lobell.[7]

Finally, the total number of H-bonds (HBD+HBA) present in the structure of the final compounds was evaluated. The total number of H-bonds of the *TYPE II* derivatives ranging between 6 and 7, only the compounds **9i** and **12g** present 8 H-bonds in the structure in agreement with the requirements reported by Partrige.[6]

The collected data TYPE II derivatives **9a-k** and **12a-i** are reported in Figure 1.

MW TYPE II Scaffold

LogP TYPE II Scaffold

tPSA TYPE II Scaffold

Total HB TYPE II Scaffold

Figure 1. Drug-like properties evaluated for the *endo/exo TYPE II* scaffold derivatives **9a-k** and **12a-i** : 1) molecular weight (MW); 2) Log P; 3) total polar surface area (tPSA); 4) total H-bonds (HBA + HBD).

*TYPE III Scaffold derivatives **23a-b** and **24a-e***

The functionalization employed for the design of the 7 *endo/exo TYPE III* scaffold derivatives (**23a-b** and **24a-e**) are selected moieties already used for the *TYPE II* final compounds, so the evaluated drug-like properties are quite similar, Figure 2.

The molecular weights ranged from 458.50 g/mol of compounds **23a** and **24a** to 473.88 g/mol of compound **24e** that contain the trifluoromethyl)pyridin-2-yl moiety and the 5-chloro-2-(pyrimidin-2-yl)phenyl group as substituents.

Also in this case, the LogP values are under the value of 5 of Lipinski and ranging from the 3.59 of compound **24c** to 4.73 of compounds **23a** and **24a**. The compounds **24c** contain the 6-methyl-3-(pyrimidin-2-yl)pyridin-2-yl group that lowers the LogP value and consequently increase the tPSA value (81.78), that is the higher of the *TYPE III* series. Compound **24c** also shows the higher number of total H-bonds (8) with respect to the other compounds that contain 6 or 7 total H-bonds.
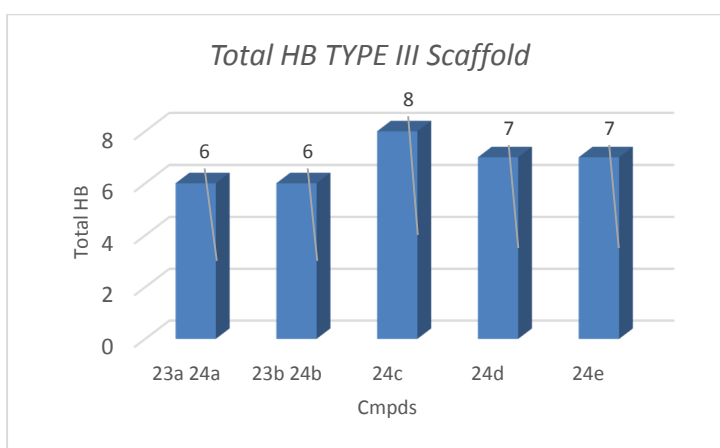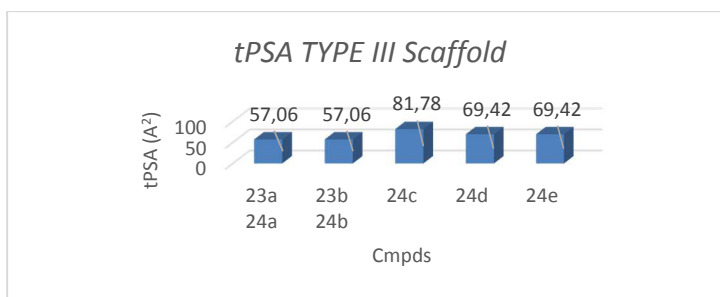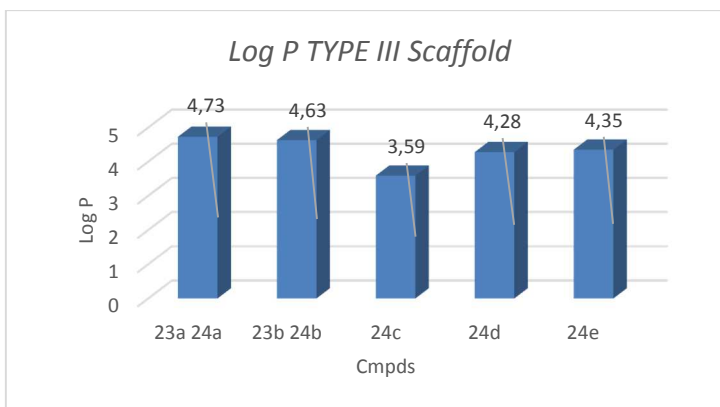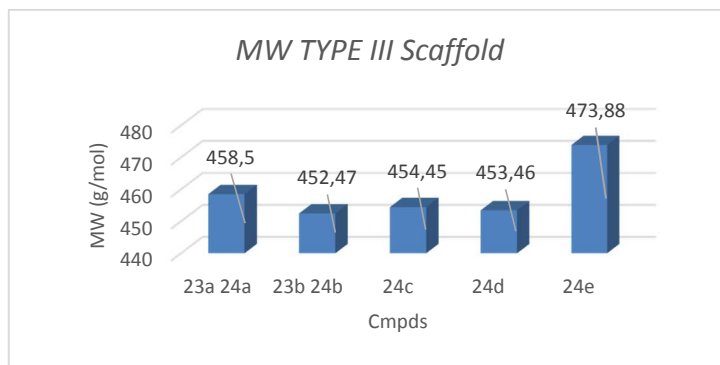
Figure 2. Drug-like properties evaluated for the *endo/exo TYPE III* scaffold derivatives **23a-b** and **24a-e**: 1) molecular weight (MW); 2) Log P; 3) total polar surface area (tPSA); 4) total H-bonds (HBA + HBD).

3.2 Pharmacophore Model Hypothesis

3.2.1 Introduction

In this part of the PhD work we focused our attention on the key structural features and key residues of OX receptors involved in the synthesized antagonists binding. In principle, these studies can be performed in different ways. For example, molecular modelling and docking are useful methods to explore the preferred orientation of small molecules to their target ligands (receptors) when they form a stable complex. In particular, docking techniques are often used to predict the binding orientation of small molecules, such as drug candidates, to the protein target in order to predict their affinity and activity. Therefore, docking techniques play a central role in the rational design of drugs. To perform a docking screen, it is mandatory to define the 3D structure of the protein/receptor of interest and this can be done using biophysical techniques such as X-ray crystallography or NMR spectroscopy. Unfortunately, the 3D structures of both OX1 and OX2 receptors are not available in the literature. Recently, some research groups attempted to address this lack by constructing the *homology models* of OX1 and OX2 receptors by using the available high-resolution crystal structures of correlated class *GPCRs-A* (in particular the dopamine-3 receptor and the β2-adrenergic receptor).[1] This *Homology models* were then used to conduct studies of *Molecular Dynamics* and *Docking*. Unfortunately, this kind of approach cannot be applied in our project because the *homology models* of OX1 and OX2 receptors constructed by Heifetz and Gotter are not available to the scientific community. Moreover, we evaluated that the re-construction of the homology model of OX1 and OX2 receptors would be to much expensive and onerous in terms of resources and time. Therefore, the computational study undertaken as a part of this PhD project was devoted to identify a *Pharmacophoric Model* able to indicate compounds with potential biological activity toward the orexin receptors. The software used to perform this *In Silico* study was *MOE 2010.10 (Chemical Computing Group)*.[2]

The scope of the pharmacophore modelling procedure is the determination of the chemical features and their mutual spatial arrangements, necessary for the binding of a ligand to its receptor and consequently for the drug activity of the ligand. Pharmacophore models can be build up from the known structural data of ligand-protein complexes, starting from the analysis of known ligands (when receptor information are not available) or from the receptor structure (when ligands are not available).

The pharmacophore model obtained can be subsequently used for the virtual screening of compounds libraries, in order to individuate potentially active molecules.

---

[1] (a) A. Heifetz, G. B. Morris, P. C. Biggin, et al. *Biochemistry*, **2012**, 51, 3178-3197. (b) A. L. Gotter, A. L. Webber, P. J. Coleman, J. J. Renger, C. Winrow *Pharmacological Review*, **2012**, 64, 398-420.

[2] *Molecular Operating Environment (MOE)*; Chemical Computing Group Inc., 1010 Sherbooke St. West, Suite #910, Montreal, QC, Canada, H3A 2R7.

Already in 1909, Paul Ehrlich coined the term *Pharmacohore* in order to indicate "a molecular framework that carries (*phoros*) the essential features responsible for a drug's (*pharmacon*) biological activity".[3]

More recently, the IUPAC (IUPAC 1998) gave a more precise definition: "A pharmacophore is an ensemble of steric and electronic features that is necessary to ensure the optimal supramolecular interactions with a specific biological target and to trigger (or block) its biological response".[4]

With the term supramolecular are indicated the non-covalent interactions and consequently key pharmacophoric features include ionized areas (positively and negatively), hydrogen bond donors and acceptors, hydrophobic areas (**Figure1**). A pharmacophore feature is referred to a particular property and is not tied to a specific chemical moiety. Indeed, the same property may be shared from diverse chemical groups that consequently can be represented by the same feature.
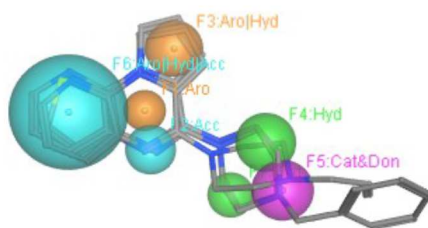
Figure 1. Representative Pharmacophoric features for a set of aligned molecules. Picture taken from the MOE 2010.10 contents.

The *Pharmacophore modelling* procedure consists in the generation of a pharmacophore hypothesis for the binding interactions in a particular active site.

In MOE program, the representation of a theorised pharmacophore is called a *pharmacophore query* and consists is a set of *query features* that are generally created from ligand *annotation points*. Annotation points are indicators in space that spot the location and the nature of atoms and functional groups that are biologically important (aromatic centres, charged groups, hydrogen donors and acceptors, projected positions of possible interaction partners).

For a ligand, the annotation points correspond to the potential location of the pharmacohore query features. The annotation points that are chosen for the pharmacophore building are converted in query features (addition of non-zero radius parameter for the variation of the pharmacophore query's geometry).

---

[3] P. Ehrlich *Ber. Dtsch. Chem. Ges.* **1909***, 42,* 17–47.

[4] C. G. Wermuth, C. R. Ganellin, P. Lindberg, L. A. Mitscher; Glossary of Terms Used in Medicinal Chemistry (IUPAC Recommendations 1998); *Pure & Appl.Chem.* **1998***, 199870:5,* 1129-1143.

The pharmacophore query generated can be subsequently employed for the virtual screening of compound libraries and can also be used to filter conformer databases, for example for the biologically active conformations identification.

The study performed for the individuation of a pharmacopore model for the orexin receptors and subsequent TYPE II and TYPE III derivatives evaluation can be summarized in the following items: flexible alignment of known active molecules, pharmacophore query generation, pharmacophore validation and *TYPE II/TYPE III* scaffold derivatives testing.

3.2.2 Flexible alignment

Flexible Alignment is an application for flexibly aligning small molecules (Labute 2001).[5] The method employs as input a collection of small molecules and computes a collection of alignments. To each alignment a score is given that quantifies the quality of the alignment in terms of both internal strain and overlap of molecular features. Flexible Alignment is a stochastic search procedure that simultaneously searches the conformation space of a collection of molecules and the space of alignments of those molecules. The scoring of alignments is based upon a Gaussian density representation of features.

As in our case, when atomic-level details of the structures of pharmaceutically relevant receptors are not available, the 3D alignment (or superposition) of putative ligands can be used to deduce structural requirements for biological activity.

For the Flexible Alignment procedure, we employed a set of selective orexin receptor 2 antagonists (*SORAs 2*). We choose to use the *SORAs 2* because these compounds are present in a greater number and greater chemical diversity in literature with respect to *SORAs 1*.

However, the pharmacophore model subsequently obtained on the basis of *SORAs 2* alignment, may be able to individuate also the *DORAs* (dual orexin receptor antagonists) molecules.

Thus, we select 5 arrays of *SORAs 2*, each containing six different molecules, that were superimposed and aligned. As an example, in table1 is reported the array_1 of *SORAs 2* employed in the Flexible Alignment procedure.
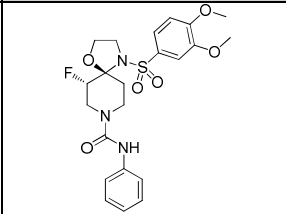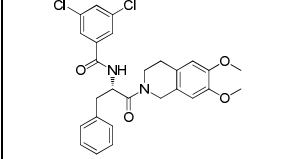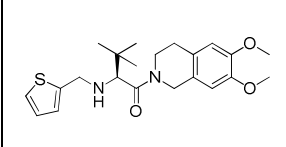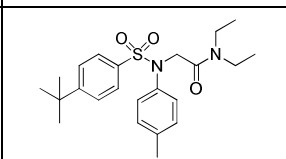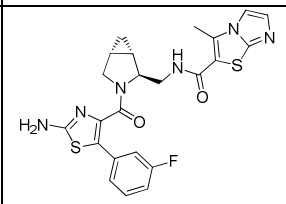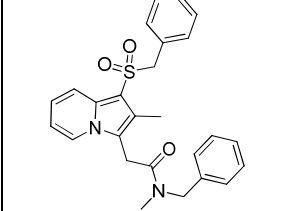
For the molecules compared in the same array the same biological data values (*Ki*, *fKi* or IC_{50}) were available in the literature. For example, for the array_1 of 6 molecules reported in Table 1, the IC_{50} values are known.

---

[5] P. Labute, C. Williams, M. Feher, E. Sourial, J. M. Schmidt; Flexible Alignment of Small Molecules; *J. Med. Chem.* **2001**, *44*, 1483-1490.

Table 1. IC_{50} = IC50 determined by FLIPR assay.

Entry	Compound Structure	OX1 Activity IC_{50} (nM)	OX2 Activity IC_{50} (nM)	Reference
1		1500	3,3	*Bioorg. Med. Chem. Lett.* **2011**, 21, 6409-6413
2		2300	30	*J. Med. Chem.* **2009**, *52*, 891-903
3		1130	25	*J. Med. Chem.* **2009**, *52*, 891-903
4		>10000	5	*J. Med. Chem.* **2009**, *52*, 891-903
5		7023	12	*ChemMedChem* **2010**, *5*, 1197-1214 WO2009016560A2
6		3784	1	WO2011138266A1

Before the alignment, the *SORAs 2* molecules were minimized in their energy and an appropriate force field was selected: for the small molecules alignment, the *MMFF94* force field was employed. The alignments obtained for an arrays of molecules were sorted and selected on the bases of the subsequent parameters:

• *U* parameter. The average strain energy of the molecules in the alignment in kcal/mol. This is calculated as the sum of the individual force field potential energies (possibly with solvent model) divided by the number of molecules.

• **F** parameter. The similarity measure of the configuration. F is the negative value of the P-density overlap function (P= probability). Lower values indicate greater similarity.

• **S** parameter. The grand alignment score. This is simply the sum of the U and the F columns. Lower values are intended to indicate better alignments.

Typically, the top scoring few alignments should be investigated. The best alignment obtained for the array_1 is depicted in Figure 1, and its *U*, *F* and *S* parameters are:

U *parameter*: 90.3672 Kcal/ml;

F *parameter*: -165.8883;

S *parameter*: -75.5211.
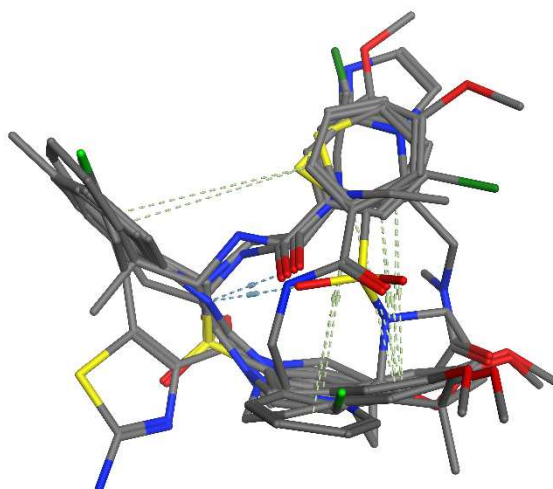
Figure 1. Representation of the best alignment obtained for the array_1 of SORAs OX2 described in Table 1.

Also the other 4 arrays of *SORAs 2* considered in this study were aligned giving rise to *U*, *F* and *S* parameters quite similar to those reported for the first array and were subsequently employed in Pharmacophore Query procedure.

3.2.3 Pharmacophore query

The purpose of the Pharmacophore Query Editor in MOE is to create a query consisting of a set of constraints on the location and type of ligand annotations which can then be used to search and filter a database of molecules in their deepest energy conformations.

Thus, the best alignments obtained for each of the 5 arrays of molecules in the flexible alignment phase, were employed to build up five Pharmacophoric models. In each identified pharmacophore common features were identified, in particular:

• 2 Aromatic features (Aro);

• 1 hydrophobic or Aromatic feature (Hyd/Aro);

• 1 hydrogen bond acceptor feature (Acc);

• 1 hydrogen bond acceptor projection feature (Acc2); *Projected* annotations are typically located along implicit lone pair or implicit hydrogen directions and are used to annotate the location of possible hydrogen bond. This means that in this area of the receptor active site there may be a donor of H-bond.

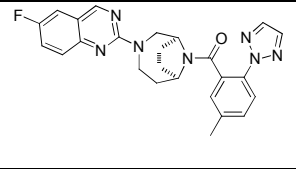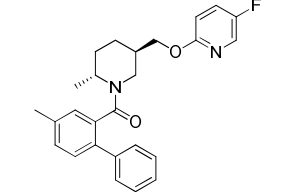The 5 features individuated using the array_1 are shown in Figure 2 as spheres within the 6 molecules of the array_1*.*
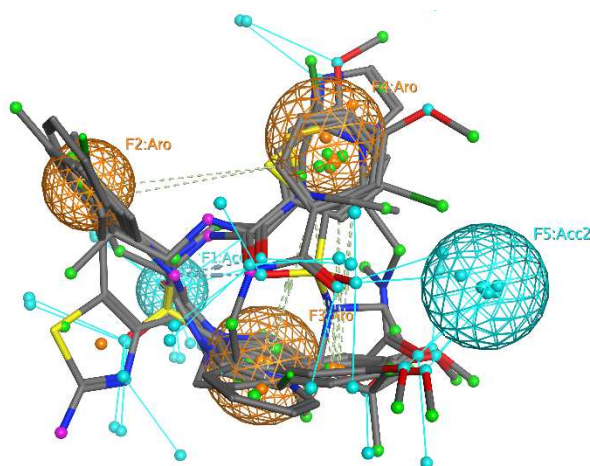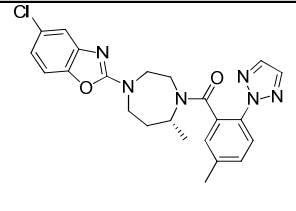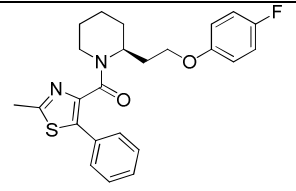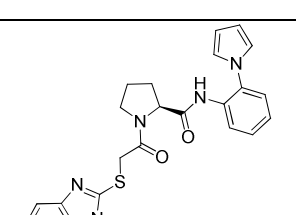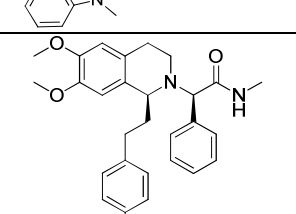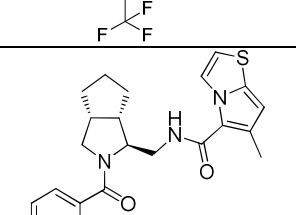

Figure 2. Representation of the 5 features individuated with the pharmacophore query procedure and the aligned molecules of the array_1.
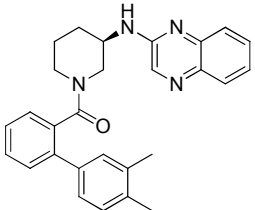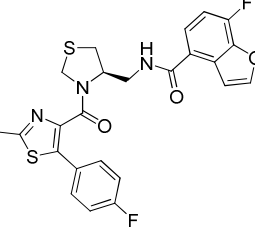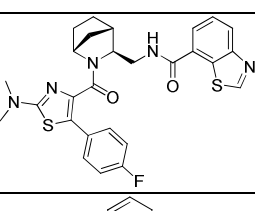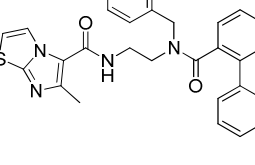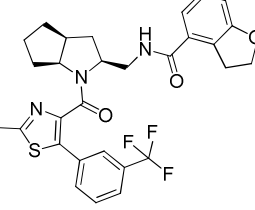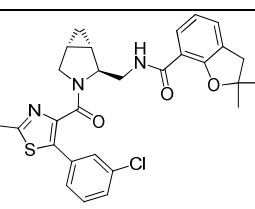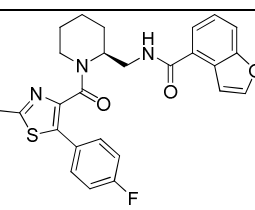
The radius (in angstroms) of each spherical volume of the feature specifies both the radius of the displayed sphere and the maximum permitted distance between the feature and a matched ligand annotation point.
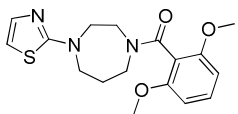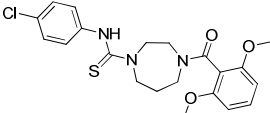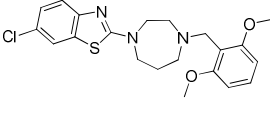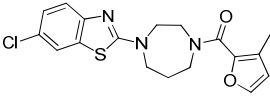
3.2.4 Pharmacophore validation
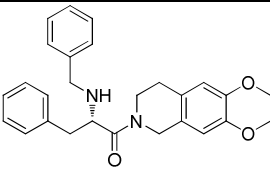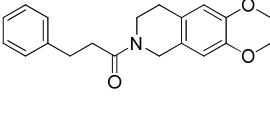
All the obtained Pharmacophore Models were validated with an array of 14 potent *DORAs* (*Ki*, *fKi* and IC$_{50}$ values under 50 nM for both the orexin receptors) selected from 133 *DORAs* taken from literature and an array of 6 non-active molecules. The structure and relative data of selected *DORAs* and inactive molecules are reported in Table 2 and Table 3 respectively.

Table 2. *Ki*= binding constant. *fK*i= functional *Ki* determined by FLIPR assay. IC$_{50}$ = IC50 determined by FLIPR assay.

Entry	Compound Structure	OX1 Activity (nM)			OX2 Activity (nM)			Reference
		Ki	fKi	IC$_{50}$	Ki	fKi	IC$_{50}$	
23		0,55	#	50	0,35	#	56	J. Med. Chem. 2010, 53, 5320–5332
30		0.6	#	98	0.4	#	136	Bioorg. Med. Chem. Lett. 20 (2010) 4201–4205
50		0,71	#	48	0,08	#	58	WO2008147518A1 ChemMedChem 2012, 7, 415 – 424
70		0,06	#	#	1,0	#	#	ChemMedChem 2012, 7, 415 – 424
83		9	22	#	0,3	2	#	J. Med. Chem. 2009, 52, 891 – 903
95		#	#	13	#	#	8	J. Med. Chem. 2009, 52, 891 – 903
106		#	#	16	#	#	21	ChemMedChem 2010, 5, 1197 - 1214 WO2009004584A1

	Structure							Reference
109		#	#	13	#	#	11	ChemMedChem 2010, 5, 1197 - 1214 WO2009133522A1
114		#	#	2	#	#	1	ChemMedChem 2010, 5, 1197 - 1214 WO2008117241A2
118		#	#	12	#	#	14	ChemMedChem 2010, 5, 1197 - 1214 WO2009104155A1
120		#	#	5,7	#	#	5,8	ChemMedChem 2010, 5, 1197 - 1214 WO2009022311A2
127		#	#	11	#	#	12	ChemMedChem 2010, 5, 1197 - 1214 WO2009016564A2
130		#	#	21	#	#	9	ChemMedChem 2010, 5, 1197 - 1214 WO2009016560A2
133		0,32	#	#	0,40	#	#	Biorg. Med. Chem. Lett. 21 (2011) 5562 - 5567

Table 3. *Ki*= binding constant. *fKi*= functional *Ki* determined by FLIPR assay. IC$_{50}$ = IC50 determined by FLIPR assay.

Entry	Compound Structure	OX1 Activity (nM)			OX2 Activivity (nM)			Reference
		Ki	fKi	IC$_{50}$	Ki	fKi	IC$_{50}$	
01		15000	#	15000	8800	#	10000	CemMedChem 2009, 4, 1069 - 1074
02		880	#	15000	4100	#	10000	CemMedChem 2009, 4, 1069 - 1074
03		15000	#	15000	3200	#	6100	CemMedChem 2009, 4, 1069 - 1074
04		11000	#	10000	1070	#	8700	CemMedChem 2009, 4, 1069 - 1074
05		#	#	>10000	#	#	>10000	J. Med. Chem. 2009, 52, 891 – 903
06		#	#	>10000	#	#	>10000	J. Med. Chem. 2009, 52, 891 – 903

For the *DORAs* and the non-active molecules a database of their normalized and energetically allowed conformers was generated. These conformers were "introduced and fitted" in the proposed *Pharmacphoric Models*.

The pharmacophore model build up on the array_01 alignment emerged as the best in the discrimination among the *DORAs* and the inactive molecules. It was able to identify all the active molecules and only one molecule considered inactive (but showing *Ki* OX1 = 880 nM and *Ki* OX2 = 4100 nM). The other 5 inactive compounds don't fit with the pharmacophore model.

The relative MOE molecular database, generated after the pharmacophore validation process, is reported in Figure 3.

	mol	rmsd	mseq	row	hitmap	cmpd	Ox1 Activity	Ox2 Activity
1		0.6538	1	59	35 65 64 6	DORA Ox1-Ox2 entry 23	Ki= 0.55 nM	Ki= 0.35 nM
2		0.7909	2	74	29 68 67 6	DORA Ox1-Ox2 entry 30	Ki= 0.6 nM	Ki= 0.4 nM
3		0.8470	3	102	19 66 67 6	DORA Ox1-Ox2 entry 50	Ki=0.71 nM	Ki= 0.08 nM
4		0.6720	4	122	18 64 63 5	DORA Ox1-Ox2 entry 70	Ki= 0.06 nM	Ki= 1.0 nM
5		0.9245	5	202	16 65 66 5	DORA Ox1-Ox2 entry 83	Ki= 9 nM	Ki= 0.3 nM
6		0.7641	6	906	64 81 80 7	DORA Ox1-Ox2 entry 95	IC50= 13 nM	IC50= 8 nM
7		1.0540	7	954	21 74 75 7	DORA Ox1-Ox2 entry 106	IC50= 16 nM	IC50= 21 nM
8		0.9788	8	1024	26 71 69 6	DORA Ox1-Ox2 entry 109	IC50= 13 nM	IC50= 11 nM
9		0.6173	9	1045	29 64 62 5	DORA Ox1-Ox2 entry 114	IC50= 2 nM	IC50= 1 nM
10		0.6939	10	1104	27 74 75 6	DORA Ox1-Ox2 entry 118	IC50= 12 nM	IC50= 14 nM
11		0.7133	11	1263	27 72 71 6	DORA Ox1-Ox2 entry 120	IC50= 5.7 nM	IC50= 5.8 nM
12		0.6724	12	2124	52 78 77 7	DORA Ox1-Ox2 entry 127	IC50= 11 nM	IC50= 12 nM
13		0.6146	13	2458	46 78 77 6	DORA Ox1-Ox2 entry 130	IC50= 21 nM	IC50= 9 nM
14		0.6916	14	2479	44 69 67 6	DORA Ox1-Ox2 entry 133	Ki= 0.32 nM	Ki= 0.40 nM
15		0.6357	15	2825	40 62 61 5	Inactive Compounds entry 02	Ki: 880 nM	Ki: 4100 nM

15 entries, 0 selected, all visible. 8 fields, 0 selected, all visible.

Figure 3. MOE molecular database generated after the validation of the pharmacophore model based on array_01 alignment. The compounds that match in the pharmacophore query are reported in the database. For each compound, only the conformation with lower ***rmsd*** parameter is displayed. ***mol*** (molecule): conformation found in the input databases possibly rotated and translated to match the pharmacophore query. ***rmsd***: root of the mean square distance between the query features and their matching ligand annotation points. ***mseq*** (sequence): molecule sequence number. ***row***: the entry number of the matched conformation in the searched input database. ***hitmap***: a numerical representation of the mapping between the query features and their matching ligand annotation points. All annotation points are distinguished, regardless of their symmetry. For each feature of the query, the field stores the index of the matched ligand annotation point or 0 if the feature is not matched.

The others four pharmacophoric models obtained in the pharmacophore query step resulted less prone to distinguish between active and inactive molecules. In particular, they were able to recognize all the active compounds together with two or more inactive molecules.

The *Validated Pharmacophoric Model* is shown in Figure 4 and the distances (in angstroms) among the different features are reported.
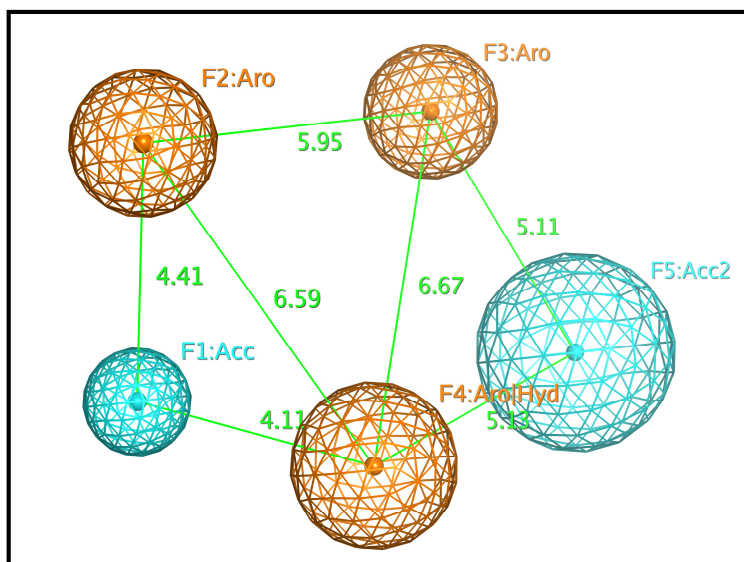
Figure 4. Validated Pharmacophore model arising from the array_1 alignment. The pharmacophore features are shown as spherical volumes and the distances in angstroms (in green) are reported. **Aro**: aromatic feature; **Hyd/Aro**: hydrophobic or aromatic feature; **Acc**: hydrogen bond acceptor feature; **Acc2**: hydrogen bond acceptor projection feature.

### 3.2.5 TYPE II and TYPE III derivative analysis

TYPE II Scaffold

After the *Pharmacophore Validation* step we test all possible four stereoisomers of the designed *TYPE II* scaffold derivatives: the two enantiomers of the *endo* compounds **9** and the two enantiomers of *exo* compounds **12**. As for the validation step also in this case a conformers database for the tested molecules was first generated. The derivatives showed as example are compounds *endo*-**9a** and *exo*-**12e**. For this two compounds both the enantiomers were analyzed and indicated as *enant1* and *enant2*, Figure 5. The first remark emerged was the different arrangement in the pharmacophore of the *endo-TYPE II* and *exo-TYPE II* derivatives. At a first glance it appears that the two enantiomers of the *exo*-**12e** derivative fit better than the two enantiomers of the *endo*-**9a** in the features described in the *Pharmacophoric Model*. Moreover, the great importance of *NCCN*-containing bicyclic core for the fitting with the Hydrophilic/Aromatic feature is well recognized.

In addiction, both the enantiomers ***endo*-9a** seem direct the 2-methyl-5-phenylthiazole-4-carbonyl substituent (B-C moiety) in a not-allowed zone of the orexin receptors, leaving the shape tolerated for the correct fitting.

Finally, an accurate analysis of the behavior of the two enantiomers **12e**_*enant1* and **12e**_*enant2* clearly shows that the 2-methyl-5-phenylthiazole-4-carbonyl substituent accommodate in diverse manner with the hydrogen acceptor feature. Consequently, the two enantiomer assume diverse spatial assessment that confer only to one enantiomer (*enant1* or *enant2*) the spatial requirements to accommodate in the binding site of both the orexin receptors (see Chapter 4).
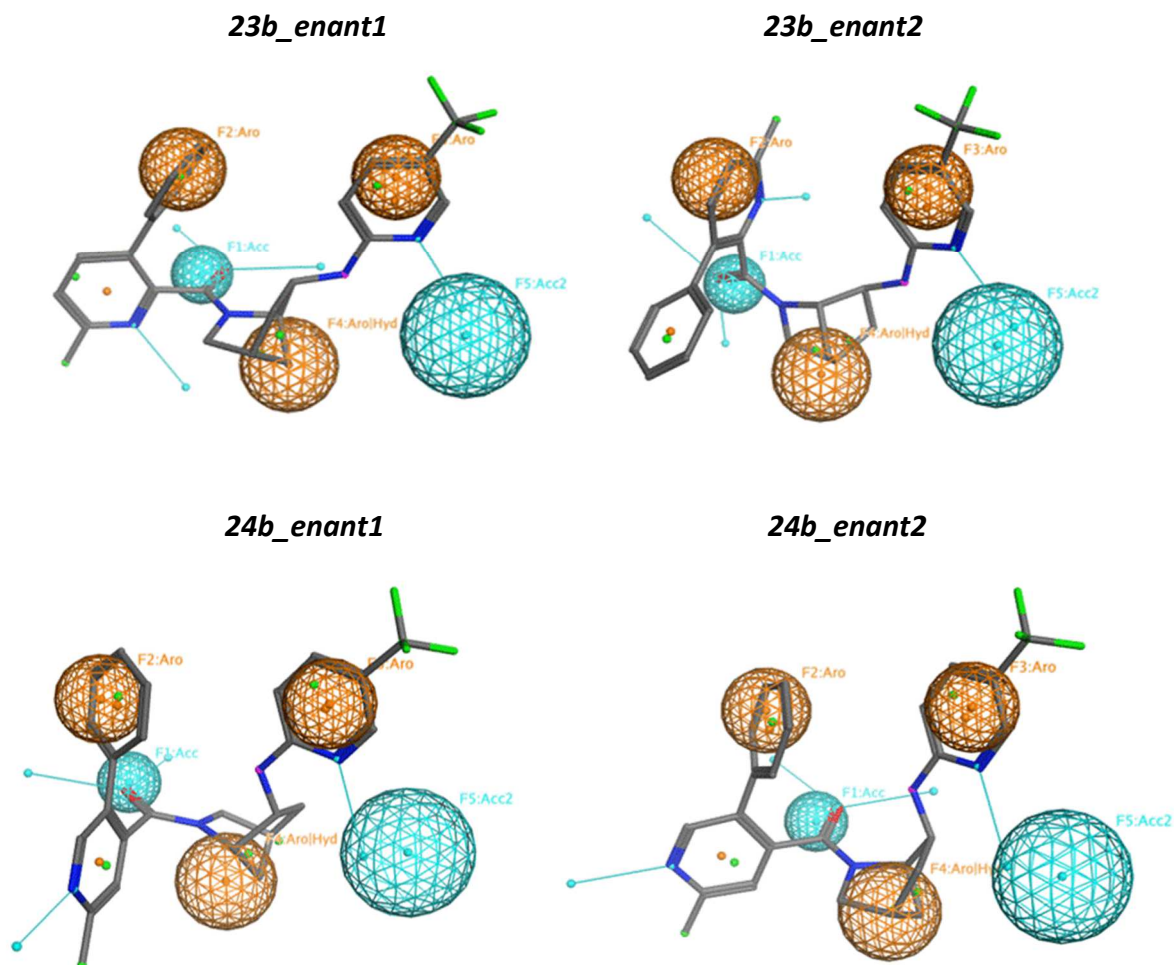
9a_enant1   **9a_enant2**

12e_enant1   **12e_enant2**
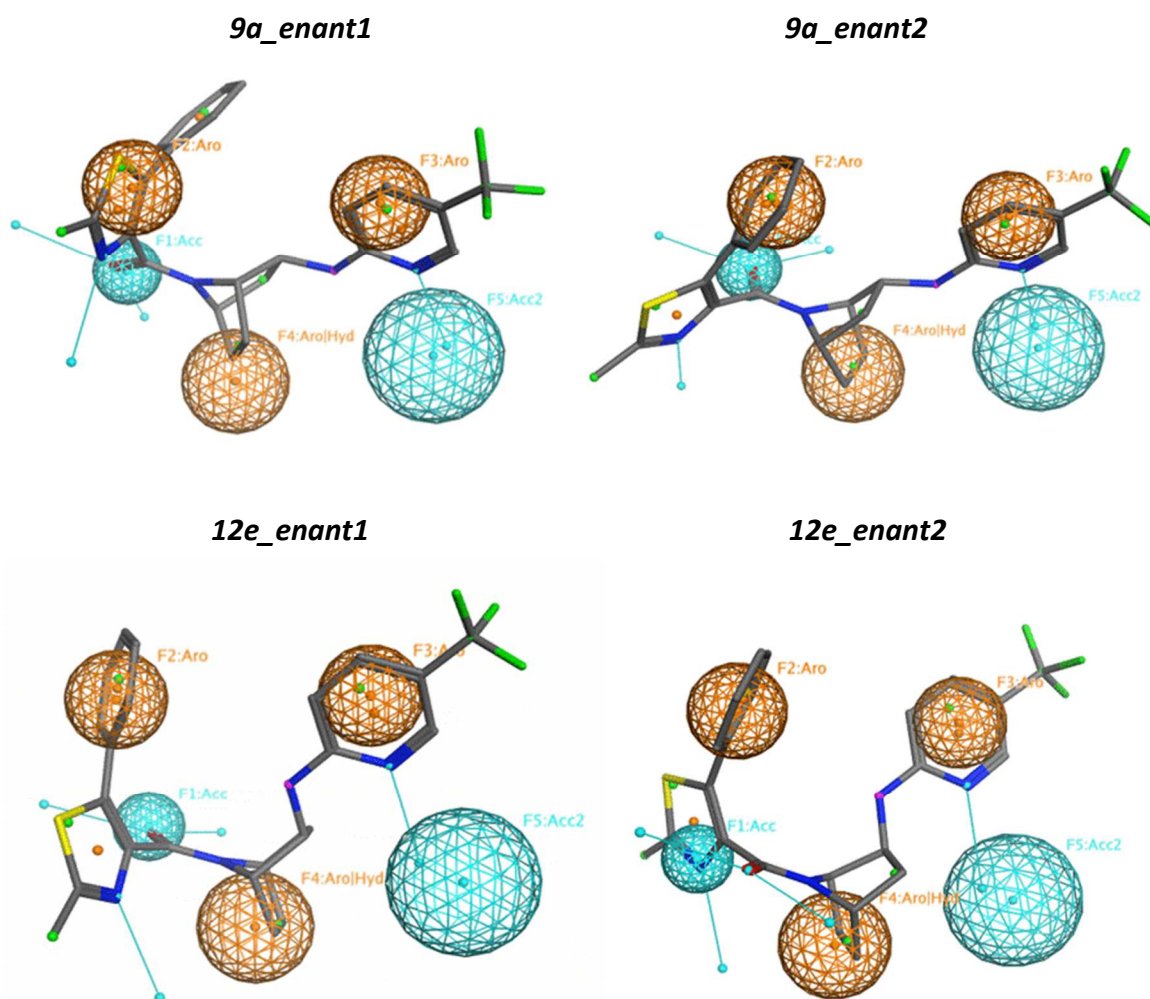
Figure 5. Pharmacophore model matching representation for compounds **9a** and **12e** (*TYPE II* scaffold). For the two compounds, both the enantiomers (*enant1* and *enant2*) were assayed in the model. The conformers with best *rmsd* (root of the mean square distance between the query features and their matching ligand annotation points) parameter are reported.

TYPE III Scaffold

The procedure was identical to that used for *TYPE II* scaffolds and the examples reported in Figure 6 are *endo*-**24b** beside compound *exo*-**23b**. Also in this case, both the enantiomers were analyzed and labeled as *enant1* and *enant2.* First, a conformer database of the selected derivatives was generated. In this case, the obtained results indicate that the two enantiomers of the *endo*-**24b** derivative fit better than the two enantiomers of the *exo*-**23b** in the features described in the *Pharmacophoric Model*.

Also in this case, the two enantiomers of compound **24b** (**24b**_*enant1* and **24b**_*enant2*) direct in different manner the bi-aromatic moiety connected by amide bond to the *NCCN* motif, in this case the 6-methyl-3-phenylpyridin-2-yl substituent. It seems that 6-methylpyridin-2-yl group assessment in a postulated pocket is important for the interaction in the active site of the

receptor. Consequently, only one of the two enantiomers properly interact with the orexin receptor.

23b_enant1   **23b_enant2**

24b_enant1   **24b_enant2**

Figure 6. Pharmacophore model matching representation for compounds **23b** and **24b** (*TYPE III* scaffold). For the two compounds, both the enantiomers (*enant1* and *enant2*) were assayed in the model. The conformers with best *rmsd* (root of the mean square distance between the query features and their matching ligand annotation points) parameter are reported.

It is worth to note that the information achieved by computational methods are in perfect agreement with the biological data obtained and described in the Chapter 4.

Chapter 4. Biological activity evaluation

4.1. Biological functional activity evaluation

4.1.1. Materials and Methods

To evaluate the biological functional activity toward the orexin receptors, the *TYPE II* and *TYPE III* scaffolds derivatives were assayed into *CHO* (Chinese Hamster Ovary) cell line and *HEK-293* (Human Embryonic Kidney) cell line engineered to overexpress, respectively, the human orexin 1 receptor and the human orexin 2 receptor, Table 1.[1]

Table 1. In Vitro pharmacology: cellular receptor functional assay.

Assay Receptors	Source	Stimulus	Incubation	Measured Component	Detection Method
OX1 (*h*) (antagonist effect)	Human recombinant (CHO cells)	orexin-A (3nM)	RT	intracellular [Ca^{2+}]	Fluorimetry
OX2 (*h*) (antagonist effect)	Human recombinant (HEK-293 cells)	orexin-B (10nM)	RT	intracellular [Ca^{2+}]	Fluorimetry

Orexin receptors activity was studied by using a FLIPR (Fluorometric Imaging Plate Reader) assay.[2] The FLIPR protocol consists in a calcium flux measurement for functional determination of orexin antagonism. While endogenous orexin peptides induce an intracellular [Ca^{2+}] increasing, a substance with an antagonist activity towards the OX1R/OX2R decreases the calcium flux.

The samples were dissolved in DMSO as solvent to give a stock solution of 1E-02M. For *In Vitro* pharmacology assays, depending on the assay volume and solvent tolerance, the stock solutions were diluted to [100x], [333x] or [1000x] in 100% solvent, then added directly or further diluted to [10x] or [5x] in H_2O or assay buffer before addition to the assay vial (final solvent concentration was kept constant).

The results are expressed as percent of control agonist response:

$$\frac{\text{measured response}}{\text{control response}} * 100$$

and as percent inhibition of control antagonist response:

$$100 - \left(\frac{\text{measured response}}{\text{control response}} * 100 \right)$$

obtained in the presence of the tested compounds.

[1] a) D. Smart et al. *Brit. J. Pharmacol*. **2001**, *132*, 1179-1182; b) S. Ammoun et al. *J. Pharmacol. Exp. Ther*. **2003**, *305*, 507-514.

[2] E. Sullivan, E. M. Tucker and I. L. Dale *Methods in Molecular Biology* **1999**, *114* (II), 125-133.

The IC$_{50}$ values (concentration causing a half-maximal inhibition of the control agonist response) were determined by non-linear regression analysis of the concentration-response curves generated with mean replicate (two times) values using Hill equation curve fitting:

$$Y = D + \left[\frac{A-D}{1+(C/C_{50})^{nH}} \right]$$

where Y= response, A= left asymptote of the curve, D= right asymptote of the curve, C= compound concentration, C$_{50}$= EC$_{50}$ or IC$_{50}$ and nH= slope factor.

For the antagonists, the binding constant (Kb, espressed in nM) were calculated using the modified Cheng-Prusoff equation:

$$K_B = \frac{IC_{50}}{1+(A/EC_{50A})}$$

where A = concentration of reference agonist in the assay, and EC$_{50A}$ = EC$_{50}$ value of the reference agonist.

Results showing an inhibition higher than 50% are considered to represent significant effects of the tested compounds. 50% is the most common cut-off value for further investigation (determination of IC$_{50}$ values from concentration-response curves). Results showing a stimulation or an inhibition between 25% and 50% are indicative of weak to moderate effects (in some assays, they may be confirmed by further testing as they are within a range where more inter-experimental variability can occur).

Results showing a stimulation or an inhibition lower than 25% are not considered significant and mostly attributable to variability of the signal around the control level.

In each experiment and if applicable, the respective reference compound was tested concurrently with the test compounds, and the data were compared with historical values determined.

The reference compound adopted for the antagonist effect toward the human OX1R was the *SORA 1* SB-334867, and the reference compound for the OX2 antagonist effect was JNJ-10397049. The structure of the two reference compounds are reported in Figure 1.
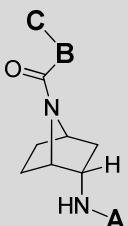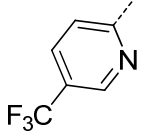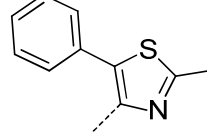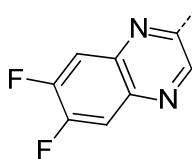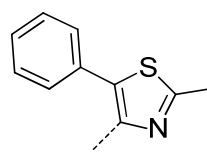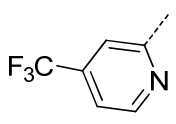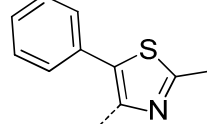

SB-334867   JNJ-10397049
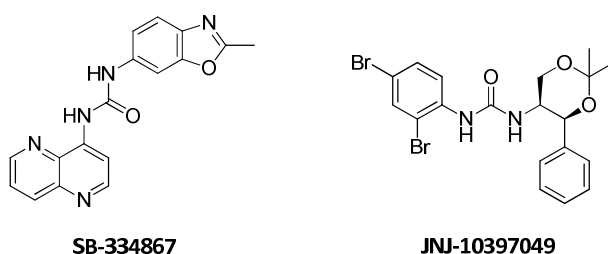
Figure 1. Structures of the reference compounds in the FLIPR assay. SB-334867 was employed for the OX1 antagonist effect, while JNJ-10397049 for the OX2 antagonist effect.
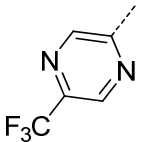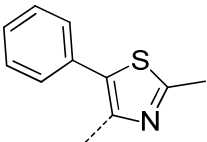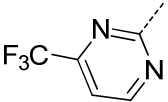
4.1.2. TYPE II Scaffold Derivatives 9a-k and 12a-i
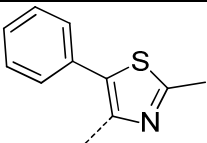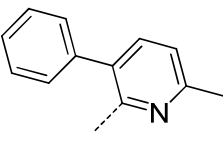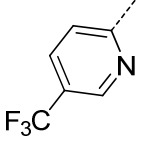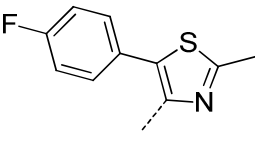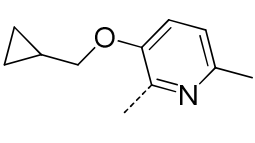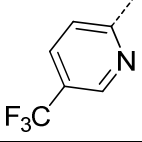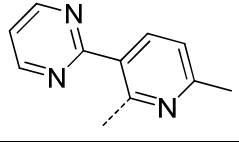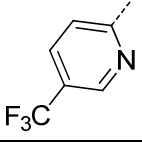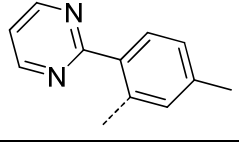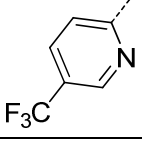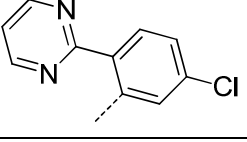
The rational exploration (substitution pattern at the two nitrogen atoms of the bicyclic core) of the *TYPEII* scaffold started with the employment of heterocycles which respond to the bioisosterism rules, as the bioisosteric replacement approach of cyclic systems plays an important role in drug design. Also, we employed *"analogy approaches"* by implementing ring contractions or expansions and *"conjunctive approaches"*, based on the creation or addition of further rings.[3] This rationale resulted in the construction of two small libraries of compounds, namely the *(+/-)-endo-TYPE II* derivatives **9a-k** and the *(+/-)-exo-TYPE II* derivatives **12a-i**.

The *in vitro* biological data (binding constant, *Kb*) of compounds **9a-k** are reported in Table 2. From this evaluation it emerged that all the 11 *(+/-)-endo* derivatives tested showed no antagonism toward both the orexin receptors at the tested concentration. Only the compound **9j** showed a weak signal of activity at the concentrations tested (Kb>1000 nM) toward OX1 receptor.

Table 2. Functional *Kb* at OX1 and OX2 receptors (*FLIPR* assay) for the *TYPE II* scaffold derivatives. The *Kb* data were determined from the IC_{50}. The IC_{50} values were extrapolated from a 5 points curves (1, 3, 10, 100, 1000 nM). **N.C.:** IC_{50} value not calculable. Concentration-response curve shows less than 25% effect at the highest tested concentration. **> 1000**: concentration-response curve shows an effect lower than 50 % but higher than 25% at the highest tested concentration.

(+/-)-*endo*-TYPE II derivatives **9a-k**				
Entry	Cmpd	A	B-C	OX1R activity (Kb nM)	OX2R activity (Kb nM)
1	**9a**			N.C.	N.C.
2	**9b**			N.C.	N.C.
3	**9c**			N.C.	N.C.

[3] C. G. Wermuth in "The Practice of Medicinal Chemistry 3rd ed.", Elsevier Ltd **2008**, Cap. 15-16

4	**9d**	pyrazine, F₃C-substituted	5-phenyl-2-methylthiazol-4-yl	N.C.	N.C.
5	**9e**	pyrimidine, F₃C-substituted, 2-methyl	5-phenyl-2-methylthiazol-4-yl	N.C.	N.C.
6	**9f**	F₃C-pyridin-2-yl	3-phenyl-6-methylpyridin-2-yl	N.C.	N.C.
7	**9g**	F₃C-pyridin-2-yl	5-(4-fluorophenyl)-2-methylthiazol-4-yl	N.C.	N.C.
8	**9h**	F₃C-pyridin-2-yl	3-(cyclopropylmethoxy)-6-methylpyridin-2-yl	N.C.	N.C.
9	**9i**	F₃C-pyridin-2-yl	2-(pyrimidin-2-yl)-6-methylpyridin-3-yl	N.C.	N.C.
10	**9j**	F₃C-pyridin-2-yl	2-(pyrimidin-2-yl)-4-methylphenyl	>1000	N.C.
11	**9k**	F₃C-pyridin-2-yl	2-(pyrimidin-2-yl)-4-chlorophenyl	N.C.	N.C.

The in vitro biological data (binding constant, *Kb*) of compounds **12a-i** are reported in Table 3. In this case, all compounds tested (with an exception) showed nanomolar antagonist activity towards both OX1R and OX2R and thus the obtained biological results are discussed in detail.

These results underline how the *exo*-stereochemistry is a mandatory requirement to achieve active compounds for this class of bicyclic derivatives. The *exo*-conformation give the spatial assessment necessary to accommodate in the binding site in both OXR1 and OXR2.

First was investigated the aromatic/heteroaromatic substitution (A-ring) directly connected to the exocyclic nitrogen atom of the *NCCN* motif (entries 1-5), maintaining as B-C moiety the 2-methyl-5-phenylthiazole-4-carbonyl substituent. For this cluster of tested derivatives, it emerged that compound **12e** (entry 5), that employed as A substituent the 5-(trifluoromethyl)pyridin-2-yl group is the most active compound of the series toward both the orexin receptors, even if the OX1R antagonism is major (KbOX1=4.7 nM; KbOX2=21 nM). The shift of the CF₃ group from position 5- to position 4- in the pyridineyl ring (entry 1; compound **12a**) lead to a small loss in activity towards the OX1R, resulting in an equipotent compound towards both the orexin receptors. Compound

12b (entry 2) contains a 4-(trifluoromethyl)pyrimidin-2-yl substituent and the introduction of a second nitrogen atom on the A-ring lead to a one order of magnitude loss in activity (KbOX1=150 nM; KbOX2=100 nM) toward both the OXRs, but the compound showed even major activity towards the OX2R. From the analysis of data relative to the compounds **12a** and **12b** emerged that the 4-CF$_3$ substitution on six-membered heteroaromatic ring lead to an increasing of antagonistic activity on OX2R respect the OX1R. Compound **12c** presents the 5-(trifluoromethyl)pyrazin-2-yl substituent (entry 3), that confer major polarity to the molecule. The compound presents a slightly loss in activity respect the compound **12e**, whit major antagonism towards OX1R.

Compound **12d** (entry 4) presents some structural features useful to understand the importance of the appropriate substitution pattern. In fact, the A-ring in **12d** is a 2-phenylacetamidic moiety instead of a heteroaromatic substituent bioisoster of the carboxylic group (all the six membered rings contain a nitrogen atom at position 2 respect the carbon linked to the *NCCN* motif). This variation has been done because in literature are present some examples of orexin receptor antagonists in which the core scaffold bears two amide functions. The 2-phenylacetamidic group was also chosen as probe in order to obtain spatial and electronic informations of the binding site of the orexin receptors. From *In Vitro* evaluation emerged that the compound **12d** gave only a weak signal of activity towards the OX1R, while shown no antagonism towards the OX2R (KbOX > 1000 nM; KbOX2 = N.C.). These results underline that the bis-amide substitution for the *TYPE II* scaffold are not accepted by the OXRs binding sites.

Subsequently, the moiety B-C was investigated synthesizing further four compounds (entries 6-9).

The 5-(trifluoromethyl)pyridin-2-yl group, that confer to the compound **12e** high activity towards both the OXRs, was preserved as A-ring in the entire series.

The first modification was performed on ring B: the 2-methylthiazole ring was replaced with the 2-methylpyridine ring in order to confer diverse electronic features (substitution of the S atom with two C atoms) and spatial arrangement to the phenyl ring used as **C**-ring (entry 6). As a result, the antagonist activity of compound **12f** is quite similar to **12e** activity (KbOX1 = 6.9 nM; KbOX2 = 12 nM).
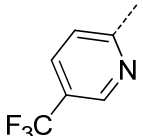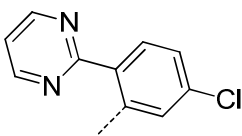
Subsequently, we amplified the polarity of the C-ring with the introduction of the pyrimidin-2-yl group. Compound **12g** (entry 7) presented the 6-methyl-3-(pyrimidin-2-yl)pyridin-2-yl substituent as B-C moiety, that conferred to the molecule a lowering in the LogP value to 3.54 (the lowest in the panel; see Computational Approach chapter) and an increased tPSA (81.78 Å^2, that is the highest value in the panel). From the biological evaluation, this modification lead for **12g** to a loss of one order of magnitude in activity respect to the reference compound **12f (**KbOX = 64 nM; KbOX2 = 130 nM).

Further 2 compounds with the B-C moiety elaboration were finally synthetized. Compounds **12h** and **12i** are substituted with a 5-methyl-2-(pyrimidin-2-yl)phenyl and with a 5-chloro-2-(pyrimidin-2-yl)phenyl group, respectively (entries 8 and 9). They contain again the pyrimidin-2-yl group as C-ring, but we introduced modification in the ring B in order to mitigate the global polarity of the molecules. Respect to compound **12g**, this modification produced an improvement in activity towards the OX1R, while the antagonist effects for the OX2R were quite similar.

From this analysis emerged that increasing the polarity in the C-ring results in a lower antagonist activity, mainly for the OX2R.

Table 3. Functional K_b at OX1 and OX2 receptors (*FLIPR* assay) for the *exo-TYPE II* scaffold derivatives. The K_b data were determined from the IC$_{50}$. The IC$_{50}$ values were extrapolated from a 6 point curves (3, 10, 30, 100, 300, 1000 nM). **N.C.:** IC$_{50}$ value not calculable. Concentration-response curve shows less than 25% effect at the highest tested concentration. **> 1000**: concentration-response curve shows an effect lower than 50 % but higher than 25% at the highest tested concentration.

		*(+/-)-exo-TYPE II derivatives **12a-i***			

Entry	Cmpd	A	B-C	OX1R activity (Kb nM)	OX2R activity (Kb nM)
1	**12a**			35	28
2	**12b**			150	100
3	**12c**			9.2	43
4	**12d**			>1000	N.C.
5	**12e**			4.7	21
	*(+)-*12e**			5.1	14
	*(-)-*12e**			190	>1000
6	**12f**			6.9	12
7	**12g**			64	130
8	**12h**			20	92

9	**12i**	F₃C-pyridine structure	pyrimidine-chlorophenyl structure	28	140
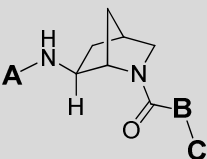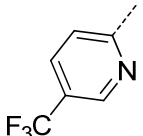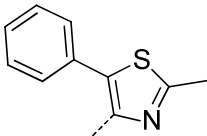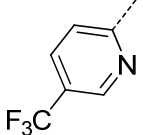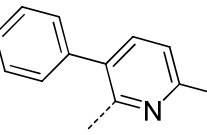
From this panel, compound **12e** emerged as the most powerful antagonist toward both the orexin receptors (entry 5), and was selected for further evaluations. In order to study the stereospecificity of its interaction and to determine the eutomer (i.e. the active enantiomer) compound **12e** was subjected to chiral HPLC separation. As reported in Table 3, only the enantiomer *(+)-***12e** maintains a low nanomolar antagonist activity (KbOX1 = 5.1 nM; KbOX2 = 14 nM), while the second enantiomer *(-)-***12e** showed lower activity (KbOX1 = 150 nM; KbOX2 > 1000 nM).

4.1.3. TYPE III Scaffold Derivatives 23a-b and 24a-e

The indications emerged from the *TYPE II* exploration were used to design proper and targeted functionalization of both nitrogen atoms of the *TYPE III* scaffold. This rationale resulted in the construction of two small libraries of compounds, namely the *(+/-)-exo-TYPE III* derivatives **23a-b** and the *(+/-)-endo-TYPE III* derivatives **24a-e**.

The *TYPE III* scaffold *In Vitro* biological data (always expressed as *Kb*) of compounds **23a-b** and compound **24a-e** are reported in Table 4 and Table 5, respectively. From the data analysis it emerged that, at a variance from the *TYPE II* series, the *exo*-conformation for the *TYPE III* scaffold gives inactive compounds towards both the orexin receptors at the concentration tested (compounds **23a** and **23b**), Table 4.

Table 4. Functional K_b at OX1 and OX2 receptors (*FLIPR* assay). The K_b data were determined from the IC_{50}. The IC_{50} values were extrapolated from a 6 point curves (3, 10, 30, 100, 300, 1000 nM) for the exo-*TYPE II* derivatives. **N.C.:** IC_{50} value not calculable. Concentration-response curve shows less than 25% effect at the highest validated testing concentration.

Entry	Cmpd	A	B-C	OX1R activity (Kb nM)	OX2R activity (Kb nM)
		(+/-)-exo-TYPE III derivatives **23a-b**			
1	**23a**	F₃C-pyridine structure	phenyl-methylthiazole structure	N.C.	N.C.
2	**23b**	F₃C-pyridine structure	phenyl-methylpyridine structure	N.C.	N.C.

139

On the contrary, all compounds **24a-e** with *endo*-stereochemistry are all active towards the orexin receptors at nanomolar concentrations. Generally, these compounds are more active on the OX1R. The *Kb* values of the *endo-TYPE III* scaffold derivatives **24a-e** are listed in Table 5.

In this panel of compounds, the exploration was focused on the B-C moiety, while A-ring was fixed as the 5-(trifluoromethyl)pyridin-2-yl ring.

First, in compound **24a** (entry 1) the 2-methyl-5-phenylthiazole-4-carbonyl substituent was employed as B-C ring. For the *endo-TYPE III* scaffold, this substitution gave OX1R antagonism at low nanomolar level, but shown a *Kb* value for the OX2R > 100nM (KbOX1 = 9.8 nM; KbOX2 = 150 nM). Instead, compound **24b** contains as B-C ring the 6-methyl-3-phenylpyridin-2-yl substituent (the 2-methylthiazole ring of **24a** was replaced with the 2-methylpyridine). This modification retains the antagonist OX1R activity at low nanomolar level, while produced a marked gain of activity towards the OX2R (KbOX1 = 8.1 nM; KbOX2 = 30 nM).

This improvement in the OX2R antagonism probably is due to the diverse spatial assessment of the phenyl group in the B-C moiety in compound **24b**.

Finally, also in this exploration, the B-C moiety was modified in order to vary the polarity of the final compounds (entries 3-5).

Compounds **24c**, **24d** and **24e** present in the B-C moiety a pyrimidin-2-yl group as C-ring. For these three molecules the *Kb* values for the OX1R were retained under the 20nM concentration, while significant lost in the OX1R antagonism was observed.

From this data it emerged that the OX1R binding site is more sensitive to the structural modifications (even punctual) of the B-C moiety. In particular, as already observed for *TYPE II* series, it seemed that the introduction of polarity in the C-ring lead to a marked decrease in activity toward the OX2R.

Table 5. Functional K_b at OX1 and OX2 receptors (*FLIPR* assay). The K_b data were determined from the IC$_{50}$. The IC$_{50}$ values were extrapolated from a 6 point curves (3, 10, 30, 100, 300, 1000 nM) for the exo-*TYPE II* derivatives. **N.C.:** IC$_{50}$ value not calculable. Concentration-response curve shows less than 25% effect at the highest validated testing concentration.

Entry	Cmpd	A	B-C	OX1R activity (Kb nM)	OX2R activity (Kb nM)
		*(+/-)-exo-TYPE III derivatives **24a-e***			
1	**24a**			9.8	150
2	**24b**			8.1	30
	*(+)-**24b***			5.6	16
	*(-)-**24b***			N.C.	N.C.
3	**24c**			12	170
4	**24d**			8.8	250
5	**24e**			6.7	100

Compound **24b**, which is the most active antagonist in this panel, was subjected to chiral HPLC separation for the enantiomer resolution. Also in this case only one of the enantiomer [*(+)*-**24b**] preserves antagonist activity at nanomolar level (KbOX1 = 5.6 nM; KbOX2 = 16 nM).

4.2. Drug Metabolism Pharmacokinetic Evaluation.

The two compounds *(+)-12e* and *(+)-24b* were selected for further investigation in order to obtain a complete biological characterization, in particular they were assessed in a *Cytochrome-P450* inhibition test and in an *In Vivo* murine model to obtain their pharmacokinetic profiles.

4.2.1 Drug to drug Interaction

Several different enzyme families catalyse the reactions of phase I metabolism. The most important are the *monooxygenases*, which include the *Cytochrome-P450* (CYP) family and the flavine monooxygenase (FMO) family. The CYP family consists of over 400 isozymes. In mammals, they are present in liver, lung, kidney, intestine, brain, and skin. The different amino acid sequences in the isozymes structure confer different binding affinity for different compound classes. The rate of the metabolism reaction is the result of the affinity of the substrate (for example a drug) for a particular CYP enzyme whereas the site of reaction is normally related to the proximity with the heme group of CYP.[1]

When two of more drugs are co-administered, and one drug inhibits at a specific isoenzyme the metabolism of a second drug, drug to drug interactions (DDI) can occur. These interactions can lead to toxic effects, affecting the rate of clearance of the second drug. In other words, DDI is the interference of one drug with the normal metabolic or pharmacokinetic behavior of a co-administered drug.

Normally DDI occurs by competition at a specific metabolizing enzyme, involved in ADME processes. A major DDI concern is cytochrome P450 inhibition. CYP inhibition has caused withdrawal from clinical use or restricted use of some major drugs. CYP inhibition has become an important concern with the Food and Drug Administration (FDA) and at pharmaceutical companies, because of its effects on clearance and half-life.

The CYP inhibition is assessed for biological active compounds in the early stages of the discovery project.

Many CYP isozymes have been discovered, and their individual contributions to drug metabolism understood. The major isozymes present in human liver are shown in Figure 1. Among the major isozymes there are the 3A family (28% of total CYP protein) and the 2C family (18%).

---

[1] E. H. Kerns, L. Di in "Drug-like Properties: Concepts, Structure Design and Methods", Elsevier Ltd, **2008**.
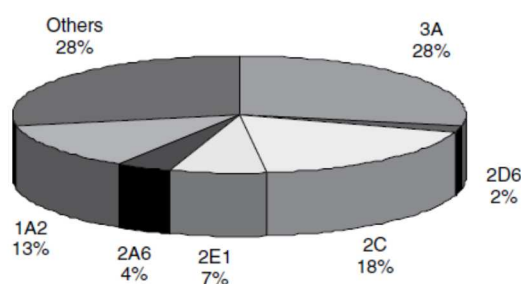
Figure 1. CYP isoforms in human liver microsomes and their relative abundances.[2] Picture taken from "Drug-like Properties: Concepts, Structure Design and Methods", Elsevier Ltd, **2008**.

Often a drug is metabolized by more than one CYP isozyme. However, different CYP isozymes tend to metabolize specific class of substrates (drugs) with different structural features, Table 1. Insights on the structural characteristics that permit the binding and the likely sites of oxidation are useful in the enhancing the metabolic stability of designed molecules.

Table 1. Characteristics of isozyme substrates. Table revised from "Drug-like Properties: Concepts, Structure Design and Methods", Elsevier Ltd, **2008**.

CYP	Range of Log P	Other characteristics	Typical substrate
3A4	0.97 to 7.54	Large molecules	Nifedipine
2D6	0.75 to 5.04	Basic (Ionized)	Propranolol
2C9	0.89 to 5.18	Acidic (Nonionized)	Naproxen
1A2	0.08 to 3.61	Planar amines/amides	Caffeine

Among the CYP isozymes, the P450 3A4 catalyzes the metabolic clearance of a large number of clinically used drugs, and a number of adverse drug-drug interactions reflect the inhibition or induction of the enzyme. CYP 3A4 exhibits a relatively large substrate-binding site that is consistent with its capacity to oxidize bulky substrates such as statins, cyclosporin, taxanes, and macrolide antibiotics.[3] The structure of the human microsomal CYP 3A4 is reported in Figure 2.

---

[2] S. E. Clarke and B. C. Jones (Eds.) in "Human cytochromes P450 and their role in metabolism-based drug-drug interactions", New York: Marcel Dekker, **2002**.

[3] J.K. Yano, M. R. Wester, G. A. Schoch, K. J. Griffin, C. D. Stout, E. F. Johnson, "The Structure of Human Microsomal Cytochrome P450 3A4 Determined by X-ray Crystallography to 2.05-A Resolution" *J.Biol.Chem*. **2004**, *279*, 38091-38094.
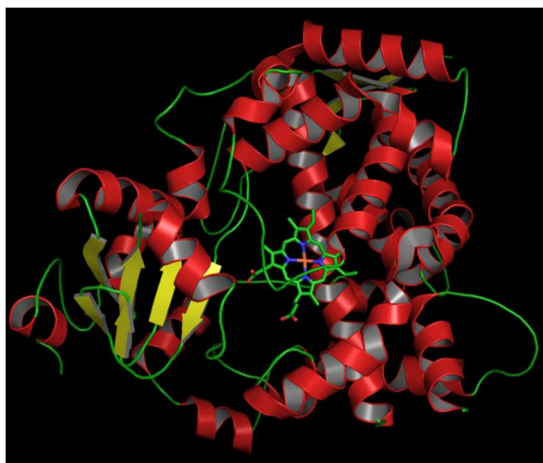
Figure 2. Representation of the human microsomal CYP 3A4. Elaboration of the PDB file 1TQN. The proteic structure was shown as cartoon (α-helices in red and β-sheets in yellow), the heme group is shown as sticks. Source: J.K. Yano, M. R. Wester, G. A. Schoch, K. J. Griffin, C. D. Stout, E. F. Johnson, "The Structure of Human Microsomal Cytochrome P450 3A4 Determined by X-ray Crystallography to 2.05-A Resolution" *J.Biol.Chem*. **2004**, *279*, 38091-38094.

DRUG TO DRUG INTERACTION EVALUATION FOR (+)-12e AND (+)-24b

The drug to drug interaction (DDI) potentials of the derivatives *(+)*-**12e** and *(+)*-**24b** were verified in a Cytochrome P450 inhibition test on the major isoforms: 1A2, 2C9, 2C19, 2D6 and 3A4. In order to obtain the diverse CYP isoforms was employed the cDNA (complementary DNA) protocol. The cDNA-expressed human Cyp450 enzymes provide a reproducible, consistent source of single enzymes for many types of studies. In particular, the cDNA-expressed enzymes are used to study the Cyp450 form-selective inhibition by drugs or drug candidates. This analysis is accomplished through the study of the inhibition of the metabolism of a model substrate by the drug or drug candidate.[4]

The two compounds *(+)*-**12e** and *(+)*-**24b** were assayed at the concentration of 3 μM. The results obtained and the *Suvorexant* DDI data (taken as reference) are reported in Table 2.

Table 2. *Cyp P450* inhibition test (*cDNA*). Samples tested at 3 μM concentration. The data indicate the perceptual of activity reduction of the CYP isoforms due to the compounds assayed. *Suvorexant* used as reference and the relative data were taken from literature. **NI**: non - inhibited.

Cmpd	Cyp P450 Inhibition @3μM
Suvorexant	1A2 NI; 2C9 40%; 2C19 60%; 2D6 NI; 3A4 65%
(+)-**12e**	1A2 NI; 2C9 NI; 2C19 33%; 2D6 NI; 3A4 66%
(+)-**24b**	1A2 NI; 2C9 13%; 2C19 NI; 2D6 NI; 3A4 9%

[4] C. L. Crespi, B. W. Penman *Advances in Pharmacology* **1997**, *43*, 171-188.

The compound *(+)-12e* DDI profile involve the 2C19, and 3A4 isoforms (33% and 66% of inhibition respectively) while the compound *(+)-24b* present a better DDI profile: only the 2C9 and 3A4 isoforms are slightly involved (inhibition under 15%).

In the complex, no-significant DDI liabilities were observed for both the compounds evaluated in the CYP inhibition test.

4.2.2 In Vivo Phrmachokinetic Profiles of Compounds (+)-12b and (+)-24b

The pharmacokinetic profiles of compounds *(+)-12e* and *(+)-24b* were studied in rats by administration of 1mg/kg IV and PO. Each pharmacokinetic profile was conduce on groups of 3 rats (weight of each rat about 250 mg). The animals were monitored for 24h. The two compounds *(+)-12e* and *(+)-24b* were detected with a chiral HPLC method developed for the enantiomer resolution (see Chemistry section).

For the compound *(+)-12e*, the clearance is moderately high, being equal to the total hepatic blood flow (875 mL/h; 105% Qh). This data seems to indicate a high hepatic metabolism and a minor contribution of extra-hepatic elimination (compounds extensively eliminated by the kidneys would have a percent of Qh around 300%). The volume of distribution Vz is high (2506 mL) indicating broad distribution in tissues. The oral bioavailability (16%) is very close to that reported for *Suvorexant* (19%) and demonstrates an incomplete but rapid (as showed by the value of Tmax of 30min) adsorption in rats. The Cmax value (39.5 ng/mL) represents the 6.4% of the maximal concentration measured after IV administration. From Cmax value obtained after 1mg/kg PO administration (i.e. approximately 100nM), emerged that this dose could be a fully pharmacologically active dose, considering the *Kb* values of *(+)-12e* (KbOX1 = 5.1 nM; KbOX2 = 14 nM). The pharmacokinetic curve and the relative data for the compound *(+)-12e* are reported in Figure 3.
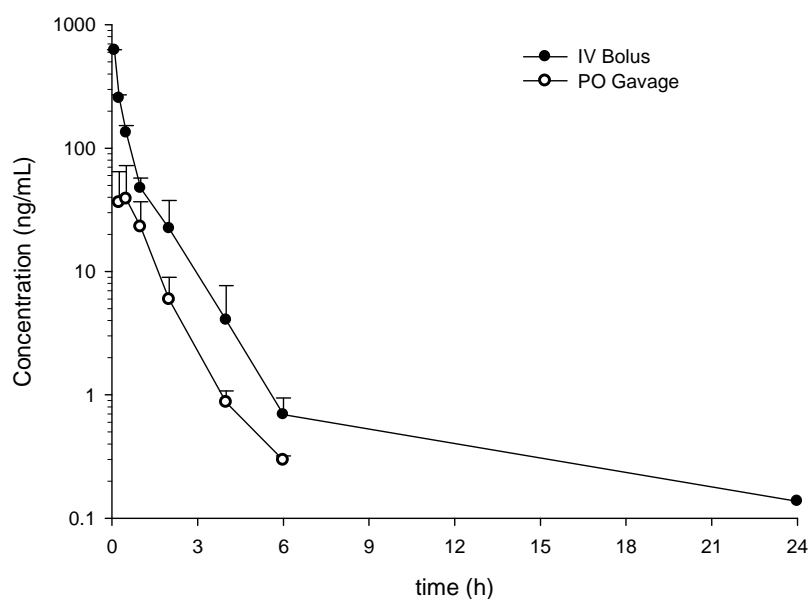
Species	Route	Dose (mg/kg)	CLp (mL/h)	Vz (mL)	AUC 0-t (ng.h/mL)	AUC inf (ng.h/mL)	F%	Cmax (ng/mL)	Tmax (h)	Tlast (h)
Rat	IV	1.0	875.6 (105 % Qh)	2506 (15 TBW)	277.7	278.5				24
Rat	PO	1.0			47.6	48.0	16	39.5	0.5	6

*Figure 3.*Pharmacokinetic profile of compound *(+)-*12e. *CLp:* plasmatic clearance. *Qh*: hepatic blood flow rate. *Vz:* volume of distribution. *TBW*: total body water. *AUC:* area under the curve. *F%:* Bioavailability.

Compound *(+)-*24b has similar even if slightly worse pharmacokinetic profile, Figure 4. It presents higher clearance (1160 mL/h; 140% Qh) and lower bioavailability (9%). Also in this case the Vz is high. The Cmax value (14.4 ng/mL) was reached 30min after the oral administration that represents the 2.8% of the maximal concentration measured after IV administration. The pharmacokinetic curve and the relative data of the compound *(+)-*24b are reported in Figure 4.
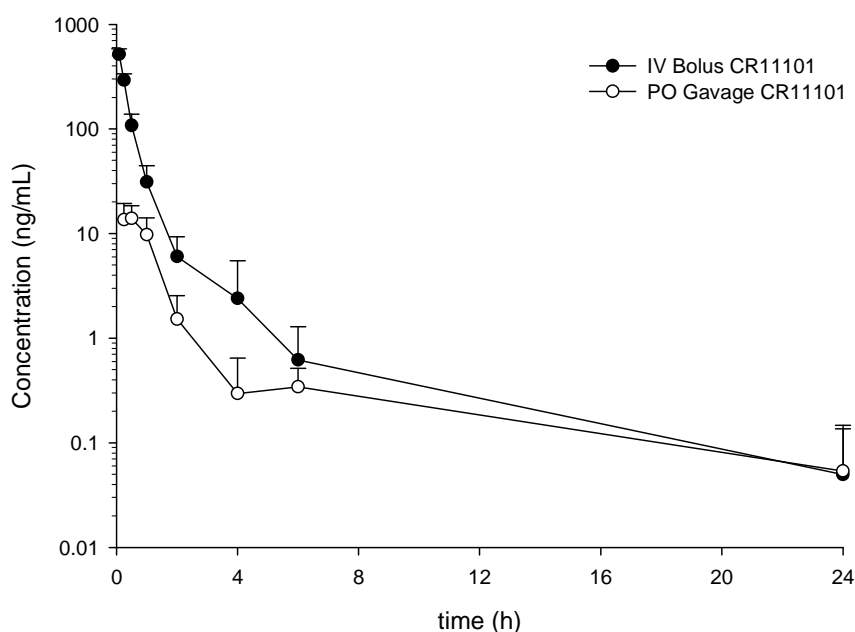
Species	Route	Dose (mg/kg)	CLp (mL/h)	Vz (mL)	AUC 0-t (ng.h/mL)	AUC inf (ng.h/mL)	F%	Cmax (ng/mL)	tmax (h)	tlast (h)
Rat	IV	1.0	1160 (140 % Qh)	2984 (17.9 TBW)	221	222				24
Rat	PO	1.0			19.5	20.9	9	14.4	0.5	24

Figure 4. Pharmacokinetic profile of compound *(+)-***24b***. **CLp:*** plasmatic clearance. ***Qh***: hepatic blood flow rate. ***Vz:*** volume of distribution. ***TBW***: total body water. ***AUC:*** area under the curve. ***F%:*** Bioavailability.

Brain penetration (that is the exposure of compound to the therapeutic target in the brain) is a major barrier for some compound series that are designed and developed for brain diseases.[1]

The blood-brain barrier (BBB) permeation is a major factor in brain penetration of a substance, and it is the sum of multiple mechanisms at the BBB. In addition, brain distribution mechanisms (for example protein binding, metabolism) also affect brain penetration of drugs.

In Vivo pharmacokinetic methods for the distribution determination of compound between plasma and brain (e.g., brain to plasma ratio [B/P]) are widely used.

The brain penetration of the two lead compounds *(+)-***12e*** and *(+)-***24b*** was determined by an *In Vivo* method.

The experiment was conducted in rats groups (3 rats) by IV administration of 1mg/Kg. The animals were sacrificed after 1h from the treatment: both compounds assayed were formulated in 5% DMSO in phosphate buffer pH 7 (150mM) with 0.1% Tween 80 and 5% Cremophor EL.

The two compounds *(+)-***12e*** and *(+)-***24b*** were detected with a chiral HPLC method developed for the enantiomers resolution (see Chapter 2). The data relative of the *In Vivo* brain penetration test for the two lead compounds are reported in Table 1.

Table 1. Brain penetration data relative to compound *(+)*-**12e** and compound *(+)*-**24b**.

Species	Cmpd	Analytical method	Route	Dose (mg/kg)	time (h)	Mean Brain conc (ng/g)	Mean Plasma conc (ng/mL)	Brain/Plasma
Rat	*(+)*-**12e**	Chiral	IV	1.0	1	86.1	49.9	**1.7**

Species	Cmpd	Analytical method	Route	Dose (mg/kg)	time (h)	Mean Brain conc (ng/g)	Mean Plasma conc (ng/mL)	Brain/Plasma
Rat	*(+)*-**24b**	Chiral	IV	1.0	1	25.78	33.9	**0.76**

Compound *(+)*-**12e** shows a B/P ratio of 1.7, while for compound *(+)*-**24b** B/P is 0.76. Compound *(+)*-**12e** provides best brain penetration, but in complex both compounds show a very good B/P ratio justifying their development as hypnotic drugs.

Chapter 5. Summary and conclusions

5.1. Summary and Conclusions

• *TYPE II scaffold.*

The *TYPE II* scaffold was obtained in both *exo-* and *endo-* conformation and it was subsequently functionalized with proper substituents. From the biological activity evaluation it emerged that the derivatives with the *exo*-configuration were active at nanomolar level towards both OX1R and OX2R.

• *TYPE III scaffold.*

Also the *TYPE III* scaffold was obtained in the *exo-* and *endo*-stereochemistry. After a targeted exploration with selected functionalization, the *endo-TYPE III* scaffold derivatives showed nanomolar activity for both the orexin receptors.

• *In Silico Study.*

As integrant part of this Ph.D. project, a computational analysis of the designed final compounds was performed. Initially were evaluated the physiochemical properties of designed *TYPE II* and *TYPE III* scaffolds analogues. Subsequently the designed molecules were assessed in a *Pharmacophore Model* previously identified and validated.

The observation obtained from the Pharmacophore Model were subsequently confirmed by the biological data obtained.

• *Drug Metabolism Pharmacokinetic Evaluation.*

The lead compounds *(+)-12e* and *(+)-24b* were assessed in a *Cytochrome-P450* inhibition test and in an *In Vivo* murine model to obtain their pharmacokinetic profiles.

In conclusion, compounds *(+)-12e* and *(+)-24b* are promising *DORAs* comparable to *Suvorexant* in their in vitro and pharmacokinetic profiles and will be evaluated in further pharmacological tests to assess their potential as new treatment for insomnia (i.e. analysis of sleep in rats and/or marmosets).